

**Identification and
Characterisation of the
Enzymes Involved in the
Biosynthetic Pathway of
Tartaric Acid in *Vitis
vinifera***

By

Crista Ann Burbidge

B. Science (Hons)

Flinders University

School of Biological Sciences

Faculty of Science and Engineering

July, 2011

Table of Contents

Summary	5
Declaration	7
Acknowledgments	8
Abbreviations	9
Chapter 1: Introduction	11
1.1 General Introduction.....	12
1.2 Tartaric Acid and Higher Plants.....	14
1.3 Grapevine Development, Solute Localisation and Transport.....	17
1.4 Tartaric Acid Biosynthetic Pathway's in Higher Plants.....	20
1.4.1 The Asc-Inclusive C4/C5 Cleavage Pathway of Vitaceae.....	20
1.4.2 The Asc-Inclusive C2/C3 Cleavage Pathway of Geraniaceae.....	24
1.4.3 The Asc-Noninclusive, Glucose Precursor Pathway of Leguminosae.....	27
1.5 Enzymes of the Biosynthetic Tartaric Acid Pathway's in Vitaceae.....	31
1.5.1 Step (1a) L-Ascorbic Acid → 2-Keto-L-Gulonic Acid.....	33
1.5.2 Step (1b) D-Glucose → D-Gluconic Acid.....	33
1.5.3 Step (2a) 2-Keto-L-Gulonic Acid → L-Idonic Acid.....	33
1.5.4 Step (2b) D-Gluconic Acid → 5-Keto-D-Gluconic Acid.....	34
1.5.5 Step (3) L-Idonic Acid → 5-Keto-D-Gluconic Acid.....	34
1.5.6 Step (4) 5-Keto-D-Gluconic Acid → Tartaric Acid Semialdehyde.....	35
1.5.7 Step (5) Tartaric Acid Semialdehyde → L-Tartaric Acid.....	36
1.6 Tartaric Acid Enzymes of Bacterial Origin.....	36
1.7 Dissimilation of Tartaric Acid.....	45
1.8 Environmental Factors.....	50
1.9 Conclusions and Aims.....	52
Chapter 2: Materials and Methods	54
2.1 Chemicals.....	55
2.2 Plant Material.....	55
2.3 Sampling.....	55
2.4 Seasonal Data Analysis.....	56
2.4.1 °Brix and Fresh Weight.....	56
2.4.2 Organic Acid extraction and High-Performance Liquid Chromatography Analysis.....	56
2.4.2.1 Organic Acid Extraction.....	56
2.4.2.2 High Performance Liquid Chromatography.....	57
2.5 RNA Extraction.....	58
2.6 cDNA Synthesis via Reverse Transcription.....	59
2.7 Gene Expression Analysis via Quantitative Real Time Polymerase Chain Reaction.....	59
2.8 Genomic DNA Extraction from Young Leaf Tissue.....	61
2.9 Enzyme Extraction from Berry Tissue.....	61

2.10 Bioinformatics	62
2.11 Polymerase Chain Reaction.....	63
2.11.1 Nucleic Acid Sequencing	66
2.12 Construction of Candidate Cassette for Protein Expression	66
2.12.1 Restriction Digest of Template.....	66
2.12.2 Ligation of Candidate Open Reading Frame into Vector.....	66
2.12.2.1 pDRIVE Vector.....	66
2.12.2.2 pET-14b Vector.....	67
2.12.3 Transformation of Vector + Cassette into <i>E. coli</i>	67
2.13 Competent Cells for DNA Cloning and Protein Expression.....	67
2.14 Culture Media for Cell Growth and Protein Expression	68
2.15 Expression, Extraction and Purification of Recombinant Protein.....	69
2.15.1 Extraction of Soluble Recombinant Protein	69
2.15.1.1 Standard Extraction	69
2.15.1.2 Cell Lysis and Extraction of Soluble Proteins using BugBuster™	70
2.15.2 Protein Purification via Immobilized Metal Affinity Chromatography	70
2.15.3 Confirmation of Protein Purity via Sodium Dodecyl Sulphate	
Polyacrylamide Gel Electrophoresis	71
2.16 Kinetic Parameters of Enzyme Activity.....	71
2.17 Calculation of Enzyme Activity.....	72
2.18 Liquid Chromatography Mass Spectrometry	72

Chapter 3: Identification and Bioinformatic Analysis of Candidate Genes Encoding Enzymes Involved in Tartaric Acid Biosynthesis 73

3.1 Introduction	74
3.2 Results	76
3.2.1 Identification and Bioinformatic Analysis of Candidate Genes Involved in Tartaric Acid Biosynthesis.....	76
3.3 Discussion	92

Chapter 4: Cloning, Heterologous Expression and Analysis of Candidate Tartaric Acid Biosynthetic Enzymes 97

4.1 Introduction	98
4.2 Results	100
4.2.1 Cloning of Putative <i>Vitis vinifera</i> Tartaric Acid Biosynthetic Genes into an Expression Vector	100
4.2.2 Heterologous Expression and Purification of Recombinant <i>Vitis vinifera</i> Proteins in <i>Escherichia coli</i>	101
4.2.3 Determination of the Kinetic Parameters of Enzyme Activity.....	109
4.2.4 Optimal pH of Enzyme Activity	110
4.2.5 Favourable pH of TC59682 Catalytic Activity	111
4.2.6 Activity of Recombinant TC59682 Protein Against 2-keto-L-gulonate	113
4.2.7 Coenzyme Affinity of TC59682.....	115
4.2.8 Optimal Temperature of TC59682 Activity.....	119
4.2.9 Substrate Range of Putative Recombinantly Expressed <i>Vitis vinifera</i> Enzymes	120

4.2.10 Identification of Product Obtained from Candidate TC59682's Primary Reaction.....	124
4.3 Discussion	128
Chapter 5: Characterisation of Various Physiological and Molecular Parameters of Tartaric Acid Biosynthesis in <i>Vitis vinifera</i> cv Shiraz over the 2007/2008 Season	139
5.1 Introduction	140
5.2 Results	141
5.2.1 Fresh Weight and °Brix.....	141
5.2.2 Organic Acids Accumulation	143
5.2.3 Gene Expression Analysis utilising Qualitative Real Time PCR.....	144
5.2.4 Enzyme Extractions.....	150
5.3 Discussion	155
Chapter 6: Using Complementation Strategies to Characterise Candidates Genes Encoding Putative Members of Tartaric Acid Biosynthetic Pathway	164
6.1 Introduction	165
6.2 Results	170
6.2.1 Complementation Studies using Mutant <i>Escherichia coli</i> Strains Growing on Various Carbon Sources.....	170
6.2.2 Identification of Putative Tartaric Acid Biosynthetic Enzymes in Members of the Vitaceae Family.	175
6.2.3 Gene Expression Analysis utilising Qualitative Real Time PCR in RNAi Thompson Seedless Lines	180
6.3 Discussion	185
Chapter 7: Discussion and Future Work	190
7.1 Introduction	191
7.2 Future Research.....	192
7.3 Conclusion.....	195
Appendix	197
A.1 Analysis of the RNAi L-IdnDH knockdown Thompson Seedless Lines	198
Bibliography	203

Summary

Vitis vinifera cv Shiraz is a member of Vitaceae, one of three higher plant families in which tartaric acid (TA) accumulates to significant levels. The accumulation of TA in *V. vinifera* berry tissue is crucial for commercial wine making, preventing discolouration and spoilage due to bacterial contamination. In *V. vinifera*, TA is biosynthesised via two pathway's, the primary-ascorbate and secondary-glucose precursor pathway's. Little is known regarding the enzymes responsible for the biosynthesis of TA with L-idonate dehydrogenase (L-idonate-5-dehydrogenase) the only enzyme identified in the primary-ascorbate precursor pathway. The results presented in this study describe a bioinformatic approach to the identification of putative candidates for a 2-keto-D-gluconate reductase (possessing 2-keto-L-gulonate reductase activity) and gluconate 5-dehydrogenase suggested as being responsible for the catalysis of the second steps of the primary-ascorbate and secondary-glucose precursor pathway's respectively. *In vitro* biochemical characterisation of recombinantly expressed proteins in conjunction with *in vivo* molecular analysis was performed to support the candidates inclusion in the respective pathway's.

Comparative analysis of the *V. vinifera* genome with enzymes identified as catalysing identical reactions in bacteria identified three candidate 2-keto-D-gluconate reductases, *TC61548*, *TC59682* and *TC55752* and three candidate gluconate 5-dehydrogenases, *TC52437*, *TC58004* and *TC55097* (Gene Indices: Grape database).

All candidate genes were identified in immature berry cDNA except *TC52437*, therefore *TC52437* was not pursued further. No active recombinant protein was obtained for candidates *TC61548*, *TC58004* and *TC55097*. Kinetic analyses were performed on purified samples of the recombinant *TC59682* and *TC55752* protein. Optimal activity of recombinant *TC59682* was observed at 35°C, pH 7.5. Activity studies indicated the primary substrate of *TC59682* to be 2-keto-L-gulonate (2KGA) with a K_m of 4.67mM. The K_m for NADH was also determined as 0.77mM. A two-step assay utilising the highly-specific L-idonate dehydrogenase indicates L-idonate is a product of this reaction. The reversibility of *TC59682* was confirmed against L-

idonate in the presence of NAD^+ , at a rate 37-fold lower than the forward direction under identical conditions. Activity was also observed against ascorbate, the pathway precursor, 8.9-fold lower than that observed against 2KGA. Activity increased against all tested substrates in the presence of coenzyme NADP(H) as compared to NAD(H). Candidate TC55752 showed activity against 2KGA and ascorbate, 7.13-fold lower and 1.82 fold higher than TC59682 in the presence of coenzyme NADPH respectively.

QRT-PCR analysis of the candidate genes expression was conducted in developing *V. vinifera* cv Shiraz berries over the 2007-2008 season. The expression pattern of TC59682 strongly coincided with the biosynthesis of TA over development. TC55752's expression pattern does not indicate involvement in TA biosynthesis. Expression patterns of TC61548, TC58004 and TC55097 suggest these candidates are not involved in TA biosynthesis

Activity of extracted soluble enzymes from a subset of the sampled Shiraz berries showed an increase in activity against 2KGA over development suggesting, as recently shown with L-idonate dehydrogenase, the presence of the enzyme late in berry development.

The results presented in this study suggest TC59682 has a role in the primary TA biosynthetic pathway. Based upon primary substrate activity TC59682 will be annotated as a 2-keto-L-gulonate reductase.

Declaration

I certify that this thesis does not incorporate without acknowledgment any material previously submitted for a degree or diploma in any university; and that to the best of my knowledge and belief it does not contain any material previously published or written by another person except where due reference is made in the text.

Crista Burbidge

Acknowledgments

I wish to acknowledge my supervisors and co-supervisors Associate Professor Kathleen Soole, Dr Christopher Ford and Dr Matthew Hayes for their encouragement, advice and guidance throughout my PhD and for their critical review of this manuscript. I thank Kathleen for giving me the opportunity to undertake this research, Christopher for welcoming me into your lab and Matthew for your constant interest in my research.

To fellow PhD students Crystal Sweetman, Vivek Vijayraghavan, Vanessa Melino, Kerry Dungey, Cyd Yonker and other members of the Flinders and Waite campuses, thank you for all the invaluable advice you have given me both in the laboratory, tea room and over a cold beverage. For all their support and help keeping me focused or distracted, whichever the occasion called for. A special thank you to Crystal, whose advice and support got me through the most frustrating times of my research.

I wish to acknowledge my Mother Karen, Father Paul and Brother Neil for their constant reassurance, love and support in making this journey possible. For keeping my head above the water and always answering the phone, I would not be me without you.

Abbreviations

2KGA	2-keto-L-gulonate
2KGR	2-ketogluconate reductase
5KGA	5-Keto-D-Gluconic Acid
AGRF	Australian Genome Research Facility
AKR	aldo-keto reductase
ANK	Ankyrin
Asc	Ascorbic acid
ATP	Adenosine triphosphate
BLAST	Basic Local Alignment Search Tools
BME	β -mercaptoethanol
BSA	Bovine Serum Albumin
CAU	Corrected Area Units
cDNA	complementary DNA
DEDTC	diethyldithiocarbamate trihydrate
DHA	Dehydroascorbate
DMSO	dimethyl sulfoxide
DNA	deoxyribonucleic acid
DTT	Dithiothreitol
EDTA	ethylenediaminetetraacetic acid
EST	Expressed Sequence Tags
FAM	Fluorescein
FLC	full length clone
FW	fresh weight
G5Dh	gluconate-5 dehydrogenase
GA	D-gluconic acid
GC-MS	Gas chromatography–mass spectrometry
gDNA	Genomic DNA
GFP	Green Fluorescent Protein
HEPES	4-(2-Hydroxyethyl)piperazine-1-ethanesulfonic acid
HPLC	High Performance Liquid Chromatography
IA	L-idonic acid
IMAC	immobilized metal affinity chromatography
IPTG	Isopropylthiogalactoside
KCN	potassium cyanide
kDa	kilodalton
KEGG	Kyoto Encyclopedia of Genes and Genomes
LB	Luria-Bertani
LC-MS	Liquid chromatography–mass spectrometry
L-IdnDH	L-idonate dehydrogenase
LN	liquid nitrogen
MA	Malic acid
MDH	Malate dehydrogenase
MEB	Modified Elution Buffer
mETC	mitochondrial electron transport chain

mRNA	Messenger RNA
MS	mass spectrometry
MSB	Modified Sonication Buffer
MWB	Modified Wash Buffer
MWL	Molecular weight ladder
NAD ⁺	Nicotinamide adenine dinucleotide
NADH	Nicotinamide adenine dinucleotide, reduced
NADP ⁺	Nicotinamide adenine dinucleotide phosphate
NADPH	Nicotinamide adenine dinucleotide phosphate, reduced
NCBI	National Centre for Biotechnology Information
NoC	no coenzyme
NoE	no enzyme
NoS	no substrate
nt	Nucleotide
OA	Organic Acid
OG	octyl gallate
ORF	open reading frame
OxA	oxalic acid
PCR	Polymerase Chain Reactions
PEB	protein extraction buffer substituted for purified enzyme
PEG	polyethylene glycol
PI	isoelectric point
PMSF	phenylmethanesulfonyl fluoride
PVDF	Polyvinylidene Difluoride
PVP	Polyvinylpyrrolidone
PVPP	Poly(vinylpyrrolidone)
QRT-PCR	Quantitative Real Time Polymerase Chain Reaction
RE	Restriction enzymes
RNA	Ribonucleic acid
RNAi	RNA interference
SARDI	South Australian Research and Development Institute
SDS-PAGE	Sodium Dodecyl Sulphate Polyacrylamide Gel Electrophoresis
TA	Tartaric acid
TB	Terrific Broth
TC	tentative consensus sequence
TCEP	<i>tris</i> (2-carboxyethyl)phosphine
TEMED	N,N,N',N'-Tetramethylethylenediamine
ThA	L-threonic acid
TrB	Transformation Buffer
TSAD	tartaric semialdehyde dehydrogenase
Ubq	Ubiquitin
WT	wild type

Chapter 1:

Introduction

1.1 General Introduction

Tartaric (TA) and malic (MA) acids account for 69-90% of the total acid in the grape berry (Kliewer, 1966, Lamikanra *et al.*, 1995). In the developing pre-véraison berry, where véraison is denoted by the acquisition of berry colour and the onset of hexose accumulation, TA levels rapidly increase, peaking approximately 50-70 days post-anthesis (flowering), and remain constant thereafter (Saito and Kasai, 1968, Saito and Kasai, 1978). The catabolism of Ascorbic acid (Asc), a ubiquitous antioxidant vital to cellular function, to TA, a seemingly inert organic acid, is a curious process in developing berries. Although currently there is no evidence linking TA with the wider metabolic activities of the cell, it is essential in wine production. The addition of TA to wine must raises titratable acidity (the sum of the volatile and non-volatile acids present) lowering the pH, preventing discolouration and spoilage due to microorganisms (Cirami, 1973, Es-Safi *et al.*, 2000, Toit *et al.*, 2006, Zoecklein *et al.*, 1995). TA is a naturally occurring non-volatile acid in table grapes that is not degraded by the wine making process and which remains essentially inert to microbial metabolism, rendering it the prime candidate for use in pH adjustment (Zoecklein *et al.*, 1995). The grapevine is Australia's seventh largest economically important agricultural commodity, responsible for the production of food stuffs including table grapes, sultanas, juice and wine (Australian Bureau of Statistics, 2010). TA is also important in the palatability of wine, with the content and composition of organic acids in conjunction with the sugars present greatly affecting the organoleptic quality of grape cultivars (Liu *et al.*, 2007, Plane *et al.*, 1980).

Examination of TA levels among higher plants identified significant levels of TA across the Vitaceae, Geraniaceae and Leguminosae families only (Stafford, 1959, Vickery and Palmer, 1954). Work throughout the second half of the 20th century focused on the elucidation of the biosynthetic pathway's of TA across these families, identifying three pathway's of TA production based on the identified precursor. L-Asc has been identified as the precursor of two of these pathway's (Asc-inclusive pathway, defined by cleavage at either the C4/C5 or the C2/C3 of a six-carbon

intermediate compound), with D-glucose the precursor of the third (Asc-noninclusive pathway). L-Asc is a ubiquitous constituent in the growth cycle of all active plant tissues (Bánhegyi and Loewus, 2004). This biologically crucial organic acid has multiple roles including the maintenance of the cell's redox balance and antioxidant protection against reactive oxygen species (Smirnoff, 2000). The ability for the plant cell system to readily convert an acid, whose presence within the system is fundamental, to an acid of arguably less priority and functional benefits is a curious occurrence.

Identification of the intermediate compounds of TA biosynthesis has enabled researchers to focus on the identification of enzymes responsible for the catalysis of these pathway's. Through candidate selection, DeBolt *et al.* (2006) identified L-idonate dehydrogenase, the first known enzyme involved in TA biosynthesis. Activity studies showed that this enzyme is responsible for the conversion of L-idonate to 5-keto-L-idonic acid (also known as 5-keto D-gluconic acid), which is believed to be step 3 in the Asc-inclusive C4/C5 pathway in *V. vinifera*. L-Idonate dehydrogenase will be denoted L-idonate dehydrogenase 1 (L-IdnDH.1) throughout this study to distinguish it from a putative homolog identified based on sequence similarity also investigated as part of this project.

The development of DNA sequencing technologies has enabled the mapping of the *V. vinifera* genome using Expressed Sequence Tags (EST) and Contigs (Assembled EST's, Iandolo *et al.*, 2004, The French–Italian Public Consortium for Grapevine Genome Characterization, 2007, Troggio *et al.*, 2007, Velasco *et al.*, 2007). *V. vinifera* is a non-novel species for molecular work with the seasonality of fruit tissue a limiting factor. The public availability of the *V. vinifera* genome enables identification of putative enzymes based upon protein architecture and sequence similarity to enzymes capable of performing these reactions as described in other organisms. This introduction will review the literature pertaining to the biosynthesis of TA in relation to the biochemical and viticultural aspects of its accumulation, focusing on tartaric acid in the fruit tissue of the Vitaceae member *Vitis vinifera*.

1.2 Tartaric Acid and Higher Plants

L-Tartaric acid (or L-threarate) exists as the four carbon dicarboxylic acid (2R, 3R) 2,3-dihydroxybutanedioic acid with three structural isomers (see Figure 1.1): *meso*, *levo* and *dextro*, based on their optical activity (Pasteur, 1860).

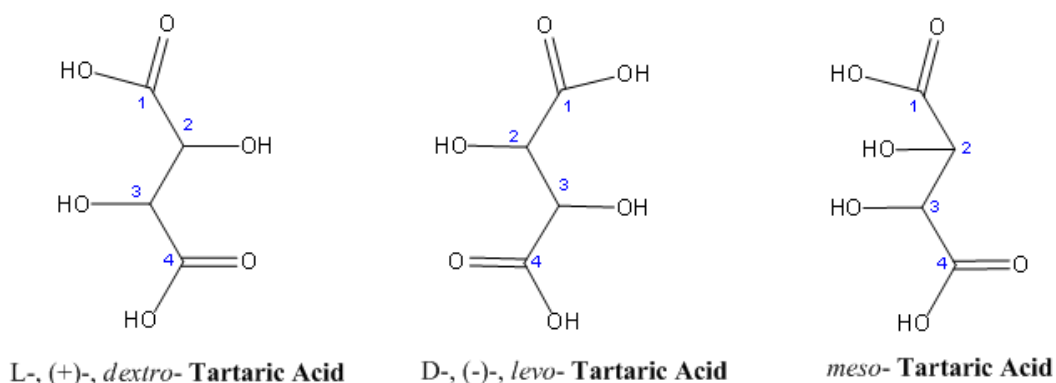


Figure 1.1: The three isomers of TA as identified by Pasteur (1860). All forms are found in nature, in addition to racemic acid, an optically inactive form comprising equal parts of *dextro* and *levo*. The common annotations of each isomer are also included.

Each stereoisomeric form of TA has been identified in higher plants including: *dextro*-TA, Vitaceae and Geraniaceae (Stafford, 1959, 1961); *levo*-TA, *Bauhinia* (Rabate and Gourevitch, 1938); *meso*-TA, spinach (Tadera and Mitstda, 1971). The stereoisomeric form of *dextro*-TA is the metabolic product of both the Asc-inclusive and Asc-noninclusive pathway's (Wagner *et al.*, 1975). Although some strains of bacteria are known to utilise *levo*-TA as a carbon source (Rode and Giffhorn, 1983), only the metabolic origin of *dextro*-TA has been investigated (Wagner *et al.*, 1975).

Research into TA has received little attention compared to the more common malic, ascorbic and citric acids. These acids are known substrates utilised in primary cellular

processes including metabolism in the citric acid cycle (citric, Lance and Rustin, 1984, malic, Schulze *et al.*, 2002), and as an antioxidant in cellular defences (Asc, reviewed by Foyer, 2004). To date, there is no evidence suggesting TA has a role in primary cellular function. Of the plant kingdom, the Vitaceae, Geraniaceae and Leguminosae are the only families known to accumulate tartrate in significant levels (Figure 1.2). Although these families have been identified as significant TA accumulators, variation in the level of TA accumulation is large with non-TA accumulating members identified within each family (Figure 1.2). It is important to note that the model plant species *Arabidopsis thaliana* is a non-TA accumulating system, rendering modern molecular techniques inapplicable. Chaïb *et al* (2010) have recently developed a microvine grape model system that promises to enable rapid genetic studies.

Species	Family	$\mu\text{moles/g FW}$ Leaf tissue	$\mu\text{moles /g FW}$ Berry tissue
<i>Vitis vinifera</i>	Vitaceae	182	85.3*
<i>Bauhinia malabarica</i>	Leguminosae	154	
<i>Vitis labruscana</i>	Vitaceae	121	
<i>Vitis riparia</i>	Vitaceae		117.9*
<i>Vitis acerifolia</i>	Vitaceae		112.6*
<i>Vitis bloodworthiana</i>	Vitaceae		109.9
<i>Vitis amerenensis</i>	Vitaceae		79.3*
<i>Vitis californica</i>	Vitaceae	79	64.0*
<i>Vitis jaquomontii</i>	Vitaceae		75.3*
<i>Vitis champinii</i>	Vitaceae		63.3*
<i>Parthenocissus tricuspidata</i>	Vitaceae	57	
<i>Parthenocissus quinquefolia</i>	Vitaceae	54	
<i>Parthenocissus henryana</i>	Vitaceae		53.3*
<i>Pelargonium hortorum</i>	Geraniaceae	29	
<i>Phaseolus vulgaris</i> cv Wakaba	Leguminosae	6.6*	
<i>Coleus blumei</i>	Labiatae	6	
<i>Ampelopsis brevipedunculata</i>	Vitaceae		4.0*
<i>Tropaeolum majus</i>	Tropaeolaceae	0.5-5.0	
<i>Rosa sp.</i>	Rosaceae	0.5-5.0	
<i>Magnolia soulangeana</i>	Magnoliaceae	0.5-5.0	
<i>Glycine max</i>	Leguminosae	0.5-5.0	
<i>Phaseolus limensis</i>	Leguminosae	0.5-5.0	
<i>Pisum sativum</i>	Leguminosae	0.5-5.0	
<i>Zea mays</i>	Gramineae	0.5-5.0	
<i>Erodium cicutarium</i>	Geraniaceae	0.5-5.0	
<i>Geranium viscosissimum</i>	Geraniaceae	0.5-5.0	
<i>Ricinus communis</i>	Euphorbiaceae	0.5-5.0	
<i>Oxalis corniculata</i>	Oxalidaceae	0-0.5	
<i>Medicago sativa</i>	Leguminosae	0-0.5	
<i>Trifolium pratense</i>	Leguminosae	0-0.5	
<i>Aesculus hippocastanum</i>	Hippocastanaceae	0-0.5	
<i>Hordeum vulgare</i>	Gramineae	0-0.5	
<i>Geranium richardsonii</i>	Geraniaceae	0-0.5	
<i>Chrysanthemum sp.</i>	Compositae	0-0.5	
<i>Beta vulgaris</i>	Chenopodiaceae	0-0.5	
<i>Phaseolus vulgaris</i> cv Morocco	Leguminosae	0	
<i>Ampelopsis aconitifolia</i>	Vitaceae		0
<i>Arabidopsis thaliana</i>	Brassicaceae	0	

Figure 1.2: Composite table of tartaric acid levels in various Angiosperms. The highest tartrate accumulators belong to the higher plant families Vitaceae, Geraniaceae and Leguminosae. Data collected from DeBolt (2006), Melino (unpublished) and Stafford (1959). *values have been converted to $\mu\text{moles /g FW}$ from the published mg/g FW value

1.3 Grapevine Development, Solute Localisation and Transport

Maturation of a grapevine is a process which, from seed to bearing fruit can take up to 3 years. With this extended generation time it is not feasible to use the grapevine for genetic manipulation studies. The development of the microvine system enables forward and reverse genetic studies in a shorter time frame (Chaïb *et al.*, 2010). The development of this system stems from a mutation of the *Vvgail* allele conferring dwarf stature, short generation time and continuous flowering. The system enables the use of modern molecular techniques; however, subsequent effects due to the alteration of *Vvgail* should be considered. The growth of the grape berry is biphasic (see Figure 1.3, Skene and Hale, 1971) comprising of two periods of rapid cell growth. The former denoted 'berry formation', the latter 'berry ripening' are intersected by a lag phase in which cell division is minimal (Coombe and Iland, 2004, Skene and Hale, 1971). The first phase occurs immediately post-anthesis and is characterised by the accumulation of malic and tartaric acids (Ruffner and Hawker, 1977). The second period of rapid growth, denoted 'berry ripening', is characterised by the onset of hexose accumulation (rise in °Brix), the metabolism of malate and the enlargement of the berry tissue due to water intake. This intake of water dilutes the *concentration* of tartrate leading to the speculation of tartrate metabolism (see section 1.7). The initiation of the second phase is termed véraison, observed visually by the acquisition of colour (in red fruit varieties) and softening of the berry tissue.

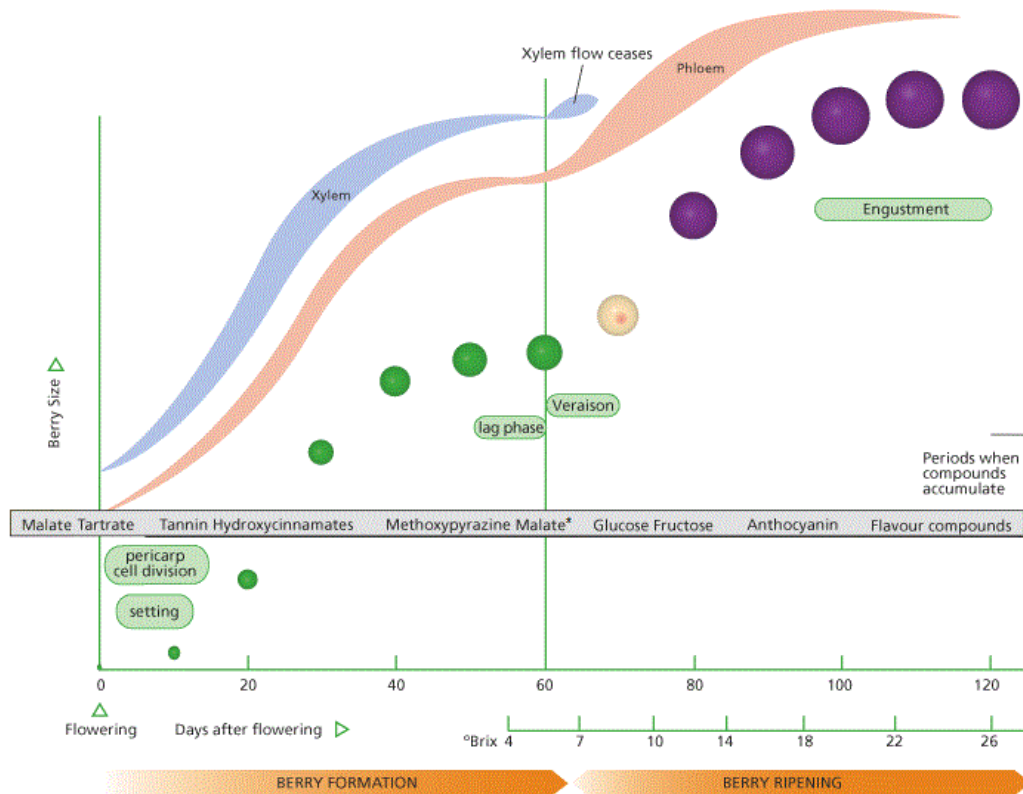


Figure 1.3: Diagrammatic representation of grape berry development over a single season. The accumulation of major solutes and the levels of °Brix, berry size and inflow through the xylem and phloem are also shown across development. Malate* indicates the metabolism of malate not the accumulation. Picture modified from Coombe and Iland (2004).

Metabolically speaking, there is a continual turnover of solutes within the plant system (Beever, 1969). Tartrate accumulation is exclusive to the developmental stage of berry formation, where synthesis is associated with rapid cell division (Kliwer and Nassar, 1966). This rapid division of cells may be essential for TA biosynthesis with cultured berry tissue lacking TA accumulation (Skene and Hale, 1971). Although accumulation of TA is most pronounced in the berry (Saito and Loewus, 1989b), evidence that the berry itself was a site of TA biosynthesis was the subject of much conjecture. Early research suggested TA was synthesised in leaf tissue then

translocated into the ripening berry (Stafford and Loewus, 1958). Young leaves are capable of synthesising TA, with rapid formation during initial growth stages (first 4 weeks of growth) and a gradual cessation as maturation proceeds (Kliewer and Nassar, 1966, Williams and Loewus, 1978). With leaf growth occurring prior to cap-fall, the synthesis and translocation of TA within the set developmental period is probable (Stafford and Loewus, 1958). Translocation of TA from the leaf to berry, if operational, may be a regulatory process (Hardy, 1968, Williams and Loewus, 1978). Evidence implicating berries as an important site of TA synthesis came from feeding $^{14}\text{CO}_2$ to an adjacent leaf prior to girdling the stem above and below an immature berry cluster, eliminating solute transport via the phloem and isolating the cluster via the removal of all leaf tissue (Hale, 1962). Hale (1962) observed 62-73% of radioactivity incorporated into MA with 15% into TA. This was further supported in *V. labruscana* B Delaware berries by Saito and Kasai (1968) who observed 30% incorporation of fed $^{14}\text{CO}_2$ into TA. These results indicate TA biosynthesis occurs in both leaf and fruit tissue.

At a cellular level, the vacuole is the storage organelle of TA (Terrier and Romieu, 2001) with synthesis occurring in the cytoplasm. The localisation of Asc, the precursor of TA via the primary C4/C5 pathway, in the cytoplasm (Pignocchi *et al.*, 2003) supports this hypothesis. Transport of TA across the tonoplast is suggested to occur via a malate transporter with affinity for both organic acids (Terrier *et al.*, 1998). Transporters AtDT and AtALMT9 have been identified as responsible for the transport of MA across the tonoplast in *Arabidopsis thaliana* (Emmerlich *et al.*, 2003, Hurth *et al.*, 2005, Kovermann *et al.*, 2007). To date, 4 ALMT9-like proteins have been identified in *V. vinifera* (Patel, 2008, Rongala, 2008). Expression patterns of *VvALMT9:1-4* correlated with the synthesis and metabolism of MA over development with evidence suggesting *VvALMT9:1*, *VvALMT9:2* and *VvALMT9:4* are localised to the tonoplast membrane when expressed exogenously in onion epidermal cells (Patel, 2008, Rongala, 2008). The affinity of these transporters to TA has yet to be investigated. Wen *et al* (2010) determined that L-IdnDH.1 is localised predominantly in the cytoplasm of immature berries whereas mature berry tissue showed localisation to the cytoplasm and vacuole, further supporting the cytoplasm as the site of TA

biosynthesis. The detection of L-IdnDH.1 in the vacuole of mature berry tissue is very interesting as it lacks a signal peptide targeting the vacuole. Autophagic transport may be relocating L-IdnDH.1 to the vacuole indicating the catabolism of excess protein by vacuolar proteases.

1.4 Tartaric Acid Biosynthetic Pathway's in Higher Plants

The predominant pathway of TA biosynthesis differs in each of the three TA-accumulating higher plant families. TA biosynthesis predominantly occurs via an Asc-inclusive C4/C5 cleavage pathway in Vitaceae (Figure 1.4), whereas Geraniaceae operates an Asc-inclusive C2/C3 cleavage pathway (Figure 1.5). TA biosynthesis in Leguminosae does not involve Asc with D-glucose the precursor of the predominate pathway (Figure 1.6). Evidence also indicates these families operate one or more of these pathway's as a secondary minor pathway. The application of radiotracer studies accelerated the identification of the compounds involved in TA biosynthesis. Although, as the realisation of multiple biosynthetic pathway's within one family had yet to become apparent, confusion as to the sequence of each pathway persisted.

1.4.1 The Asc-Inclusive C4/C5 Cleavage Pathway of Vitaceae

Early suggestions that L-Asc was the precursor to TA were derived from data suggesting the C4/C5 of Asc corresponded to the C2/C3 of TA (Hough and Jones, 1956). However, addition of labelled [6-¹⁴C]Asc to excised grape leaves showed insignificant levels of recovered label in TA (Loewus and Stafford, 1958), suggesting that L-Asc was not the immediate precursor of TA. Research then focused on various hexoses and their derivatives as the precursor (see section 1.4.3). The breakthrough came when, utilising [1-¹⁴C]Asc rather than [6-¹⁴C]Asc, Saito and Kasai (1969) recovered 72% of the radioactive label administered to immature *V. labruscana* cv Delaware berries in C1 of TA. Further analysis of the labelled TA molecule showed the radiolabel was restricted to the carboxyl groups. Additional investigations using [1-¹⁴C]Asc in other Vitaceae members including *V. labrusca* berries, *Parthenocissus*

inserta leaves (Wagner and Loewus, 1974) and *Parthenocissus quinquefolia* leaves (Helsper *et al.*, 1981) confirmed the incorporation of label into the L-(+)-isomer of TA (Wagner *et al.*, 1975). Williams and Loewus (1978) fed *Vitis labrusca* leaves [4-¹⁴C]Asc and recovered 80% of the label in TA. Interestingly, analysis of the radiolabel in TA resulting from [1-¹⁴C]Asc and [4-¹⁴C]Asc incorporation showed the label location corresponded to the C1 and C4 carbons respectively indicating the C1-C4 carbons of Asc are conserved as the C1-C4 carbon skeleton of TA (Williams and Loewus, 1978).

To determine the intermediates of the C4/C5 pathway (Figure 1.4), Saito and Kasai (1982) administered iodoacetic acid to slices of immature berries of *V. labrusca* which had been vacuum infiltrated with [1-¹⁴C]Asc. This resulted in the identification of three metabolic products based on the ¹⁴C incorporation, L-idonic acid (L-idonate), L-idono- γ -lactone and 2-keto-L-idonic acid (Saito and Kasai, 1982). When labelled L-idonic acid and 2-keto-L-idonic acid (2-keto-L-gulonic acid, 2KGA) were fed to grape berries, TA and an unknown acidic compound accumulated. This acidic compound was later confirmed to be 5-keto-L-idonic acid (5-keto-D-gluconic acid, 5KGA). Malipiero *et al* (1987) investigated the kinetics of TA synthesis from this pathway indicating a consecutive formation of intermediates 2KGA, L-idonic acid and 5KGA in developing *Vitis* leaves (Figure 1.4). This kinetic data led Malipiero *et al* (1987) to suggest the oxidation of L-idonate as the regulatory enzymatic reaction of the pathway.

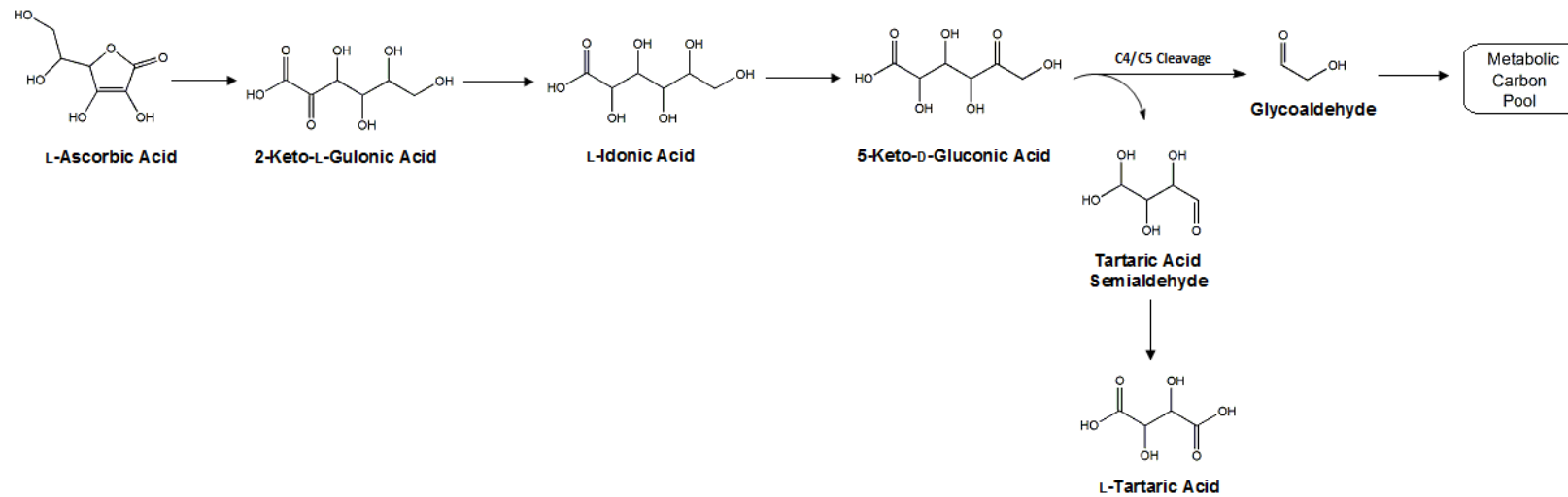


Figure 1.4: The Asc-inclusive C4/C5 cleavage pathway TA biosynthesis. Identified as the primary pathway in Vitaceae. Image modified from Loewus (1999).

The cleavage at C4/C5 of 5KGA before its conversion to TA was established based on separate feeding experiments using 5KGA individually labelled at atoms C1 and C6 (Saito and Kasai, 1982, 1984, Wagner *et al.*, 1975). Labelled TA arising from feeding *V. labrusca* cv Delaware berries with 1-¹⁴C and not 6-¹⁴C labelled 5KGA indicated a C4/C5 cleavage of 5KGA. The detection of substance-X (later identified to be glycoaldehyde) supported this hypothesis (Saito and Loewus, 1989a). Analysis of the fate of glycoaldehyde with [6-¹⁴C]Asc showed ¹⁴C distribution in glucose consistent with the C2 fragment recycled back into the carbon/triose pool (Loewus and Stafford, 1958, Wagner and Loewus, 1974). Investigations feeding L-[4-¹⁴C]threotetruronate to *V. labrusca* cv Delaware leaves identified threotetruronate (tartaric acid semialdehyde) as the 4-carbon product resultant from the C4/C5 cleavage of 5KGA (Saito, 1992). To investigate the presence of this pathway in Geraniaceae, 2-keto-L-[U-¹⁴C]idonic acid, L-[U-¹⁴C]idonic acid, 5-keto-D-[1-¹⁴C]gluconic acid and 5-keto-D-[6-¹⁴C]gluconic acid were fed to detached *Pelargonium* leaves (Saito *et al.*, 1984). Although each compound underwent partial metabolism they did not contribute to the pool of TA.

In a review of Asc biosynthesis and catabolism, Hancock and Viola (2005) proposed dehydroascorbate (DHA) as an intermediate in TA biosynthesis. In this model, Asc is oxidised to DHA, which is further hydrolysed to TA. The data to support this hypothesis was derived from the work of Saito and Kasai (1984). Radiolabelled dehydro-[1-¹⁴C]Asc, when fed to grapevine leaf apices, resulted in the incorporation of ¹⁴C into 2KGA, IA and ultimately TA in a similar pattern to that obtained through feeding with radiolabelled [1-¹⁴C]Asc. The conversion of DHA to Asc is a widely observed component of the oxidation-reduction cycle of Asc metabolism in many cells (Foyer, 2004) and no evidence stating DHA was not converted to Asc before further metabolism to TA was provided. Melino *et al* (2009b) found *V. vinifera* cv Shiraz leaf tissue accumulates higher quantities of Asc and subsequently a higher Asc to DHA ratio than berries throughout development. This suggests the incorporation of radiolabel in TA may be a result of DHA recycling. Investigations in berry tissue are required before the inclusion of DHA in this pathway.

Recent investigations into the regulation of genes involved in the biosynthesis and metabolism of Asc in *V. vinifera* cv Shiraz berries have shown no pre-emptive up-regulation of Asc biosynthetic genes pre-TA accumulation (Melino, 2009, Melino *et al.*, 2009a). Melino *et al* (2009a) showed that in early berry development the metabolism of Asc to products TA and oxalate more active than Asc recycling whereas in late berry development Asc recycling was dominant. Melino *et al* (2009a) suggest TA biosynthesis is a gradual process with the synthesised Asc in immature berries predominantly catabolised, and predominantly recycled in mature berries without a significant change in genetic regulation.

Since the suggestion of Asc as a precursor in 1956, the grapevine has been the primary plant species used to determine the Asc-inclusive C4/C5 pathway. Values of 70% and 80% incorporation of label in TA from intermediates of this pathway clearly implicate it as the primary pathway in *V. vinifera*. Unfortunately, much of the data pertaining to the elucidation of this pathway is the result of work conducted upon excised leaf tissue, and not fruit. The results of Melino *et al* (2009a) investigation based on the use of radiolabel substrates has reasserted this TA biosynthetic pathway in grape berry tissue.

1.4.2 The Asc-Inclusive C2/C3 Cleavage Pathway of Geraniaceae

The presence of a C2/C3 cleavage of Asc to form oxalic acid (OxA) and L-threonic acid (ThA, which is further oxidised to yield TA, Figure 1.5) was first detected by Herbert *et al* (1933). Investigations into the stereochemical backbone of Asc showed correspondence between C4/C5 of Asc and C2/C3 of TA. This suggested the C3-C6 of Asc produced the resultant TA molecule via a C2/C3 cleavage (Hough and Jones, 1956). Confirmation came from radiolabel studies utilising labelled [6-¹⁴C]Asc fed to detached leaves of *Pelargonium crispum* L. cv Prince Rupert (Wagner and Loewus, 1973). Significant label was recovered in TA exclusively in the carboxyl carbon corresponding to the C3-C6 of Asc (Loewus *et al.*, 1975, Wagner and Loewus, 1973). Studies utilising [1, 6-¹⁴C] Asc in geranium leaves recovered ¹⁴C labelled OxA, ThA

and TA, confirming the pathway's presence in Geraniaceae (Helsper and Loewus, 1982). Earlier work testing the pathway's operation in Vitaceae was however unsuccessful: Loewus and Stafford (1958) fed [6-¹⁴C]Asc to a detached grape leaf and found no significant incorporation into TA. Thus TA production via the Asc-inclusive C2/C3 cleavage pathway was deemed non-operational in Vitaceae instigating further research into Asc-inclusive C4/C5 pathway (see section 1.4.1).

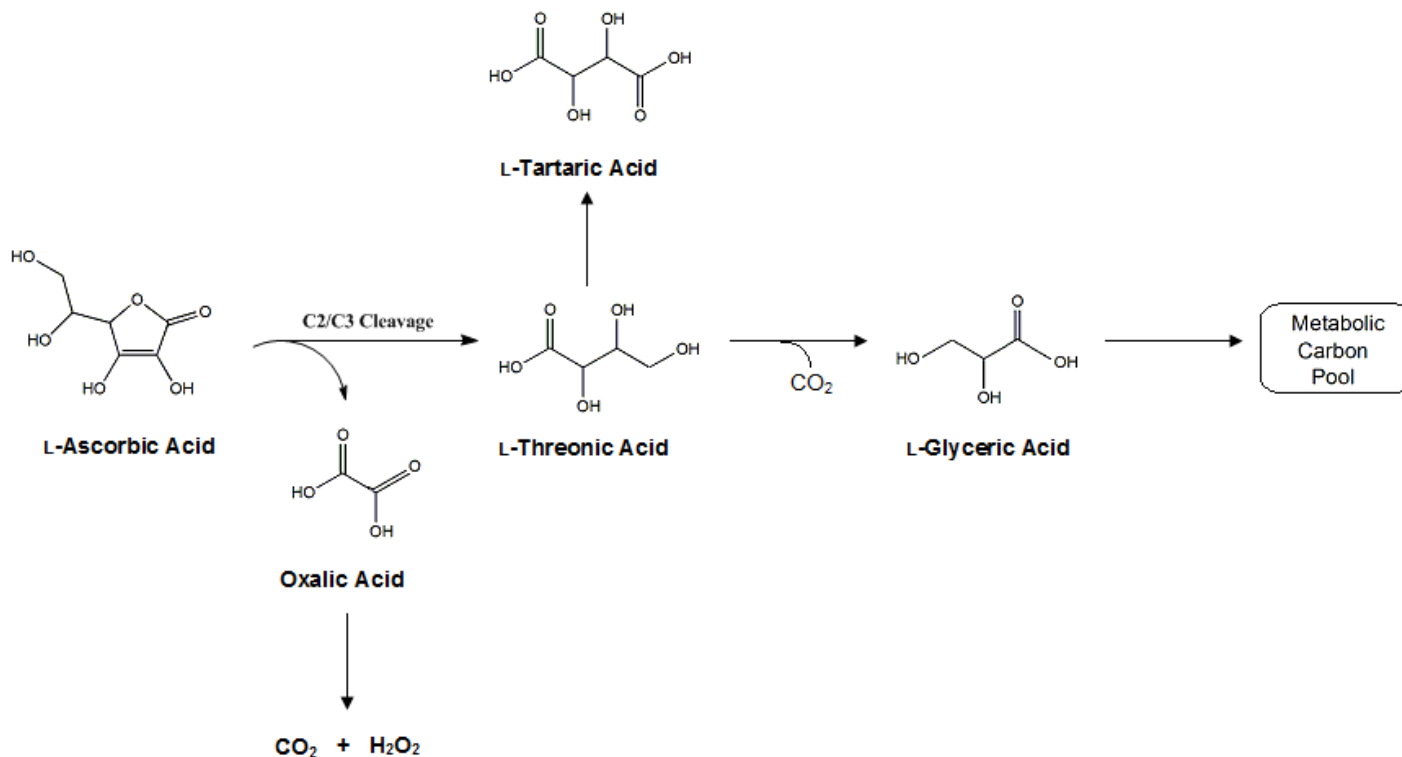


Figure 1.5: The Asc-inclusive C2/C3 cleavage pathway of TA biosynthesis. Identified as the primary pathway in Geraniaceae for TA production. Oxalate-accumulating species also operate this pathway, although TA production is rare. Image modified from Loewus (1999).

Those species of higher plants identified as oxalate accumulators are also known to operate this pathway (Figure 1.5); however, TA production in these species is rare. In these species, threonic acid is commonly metabolised to glyceric acid which is recycled back into the metabolic carbon pool (Nuss and Loewus, 1978, Yang and Loewus, 1975). Green and Fry (2005) fed L-[1-¹⁴C]ascorbate to *Rosa* cell-suspension cultures showing the pathway operates extracellularly via several novel intermediates including the previously unidentified 4-*O*-oxalyl-L-threonate. Green and Fry (2005) also suggest a non-enzymatic operation of the pathway with multiple steps having the capacity to generate peroxide, triggering oxidative bursts.

1.4.3 The Asc-Noninclusive, Glucose Precursor Pathway of Leguminosae

Numerous studies early in the literature suggested glucose as a candidate for precursor to TA synthesis in plants (Hardy, 1968, Loewus and Stafford, 1958, Maroc-Gyr, 1965, Saito and Kasai, 1969, 1984, Saito and Loewus, 1989a, b, c, Stafford and Loewus, 1958, Wagner *et al.*, 1975). In grapevines, Ribéreau-Gayon (1968, as cited by Saito and Kasai, 1984) first suggested a pathway of TA synthesis exploiting glucose suggesting the C1-C4 carbon backbone of the glucose molecule provides the carbon skeleton of TA via cleavage of 5-keto-D-gluconate, an intermediate common to both the glucose and Asc-inclusive C4/C5 pathway. Labelling behaviour resultant from D-[1-¹⁴C]glucose in *Pelargonium* leaves suggested the presence of a hexonic acid located between D-glucose and 5-keto-D-gluconate (Saito *et al.*, 1984, Figure 1.6). Saito *et al* (1984) reasoned the unidentified hexonic acid was D-gluconic acid based on several facts: (1) its use as a precursor to 5-keto-D-gluconate in microorganisms; (2) its efficiency as a TA precursor over sucrose in grapes, and (3) its chemical structure in comparison to the other chemical constituents of the pathway. The identification of the hexose as 5KGA, as well as this pathway's primary operation in Leguminosae, was later confirmed in *Phaseolus vulgaris* (Saito and Loewus, 1989c).

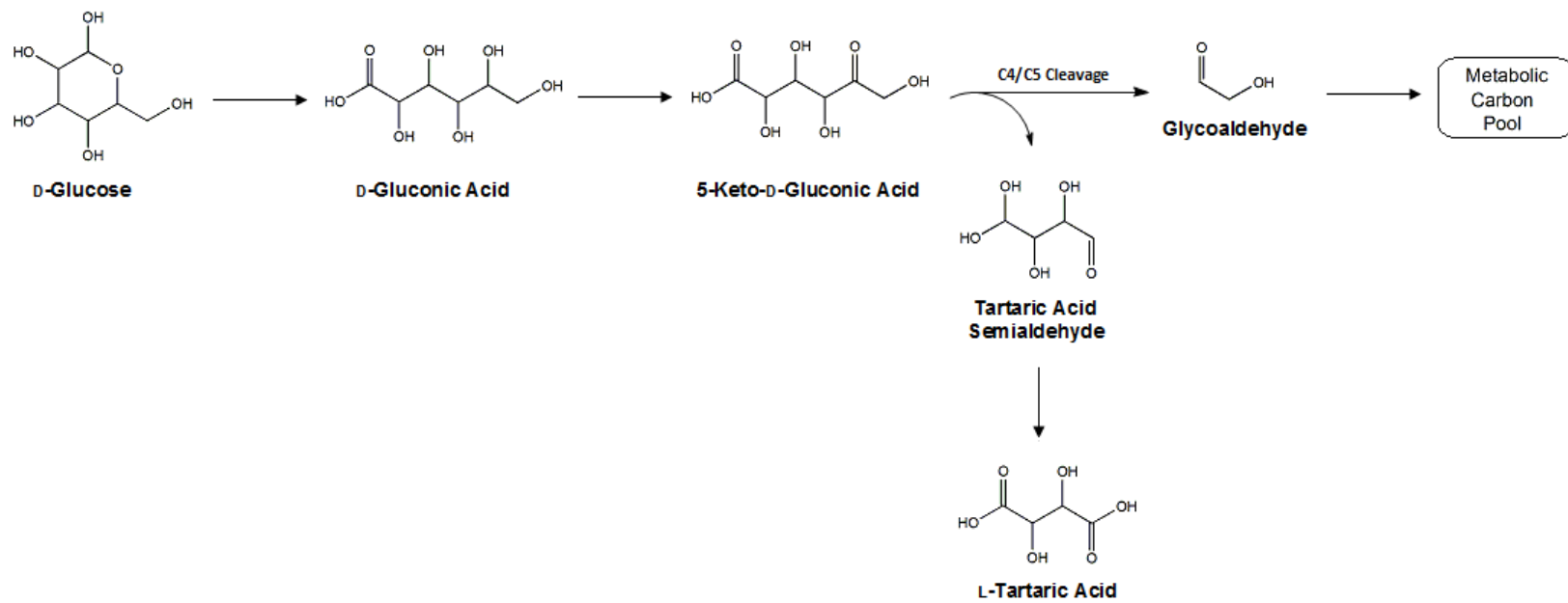


Figure 1.6: Asc-noninclusive, glucose precursor pathway of TA biosynthesis. Identified as the primary pathway in Leguminosae and a secondary pathway in Vitaceae. Image modified from Loewus (1999).

To confirm the presence of the glucose precursor pathway in Vitaceous plants, Saito and Loewus (1989b) used [2-¹⁴C, 3-³H]glucose and compared the ratios of ³H to ¹⁴C in TA and glucosyl residues in order to determine the significance of the pathway's contribution to TA synthesis. The expectation was that due to oxidation at C3 prior to Asc formation, TA synthesised by the Asc pathway would not contain ³H. Similarly, TA formed via the glucose pathway should retain ³H with the difference reflected in the ³H to ¹⁴C ratios in TA and cell wall-derived glucosyl units. Berries of *Vitis labrusca* cv Delaware, and leaves of *Parthenocissus quinquefolia* (Virginia Creeper, a member of the Vitaceae) were studied. Analysis of the proportion of radiolabel recovered in TA suggested that in *V. labrusca*, 85-91% of TA was formed by the C4/C5 pathway, while in *P. quinquefolia* 98% of TA was formed in this way. Values were slightly lower when these treatments were conducted on dark-growing plants. These data suggested that the Asc-non-inclusive pathway is responsible for a minor portion of TA synthesis in Vitaceae (Saito and Loewus, 1989b).

In 1994, Saito published data suggesting the glucose precursor pathway in Vitaceae operates in a different manner. Saito (1994) fed labelled [1-¹⁴C]GA to grape leaves in the dark detecting a significant evolution of ¹⁴CO₂. Saito (1994) suggests this result can be explained by the breakdown of GA to 6-phosphogluconic acid, an intermediate of the pentose phosphate pathway, before following the steps described in the Asc-inclusive C4/C5 pathway downstream of 2-keto-L-gulonic acid (Figure 1.7). This is also supported by the accumulation of ³H into TA in [3-³H]GA fed tissue. Saito (1994) then suggests the conversion of GA to 5KGA is negligible contradicting his previous findings. Subsequent to publication, this work has been referenced twice in review articles (Hancock and Viola, 2005, Loewus, 1999) in relation to Asc biosynthesis and catabolism in plants. Both review articles do not draw upon this alternative sequencing of the secondary pathway, presenting the pathway sequence as shown in Figure 1.6. Due to this, the research conducted herein refers to the accepted TA secondary biosynthetic pathway model (Figure 1.6)

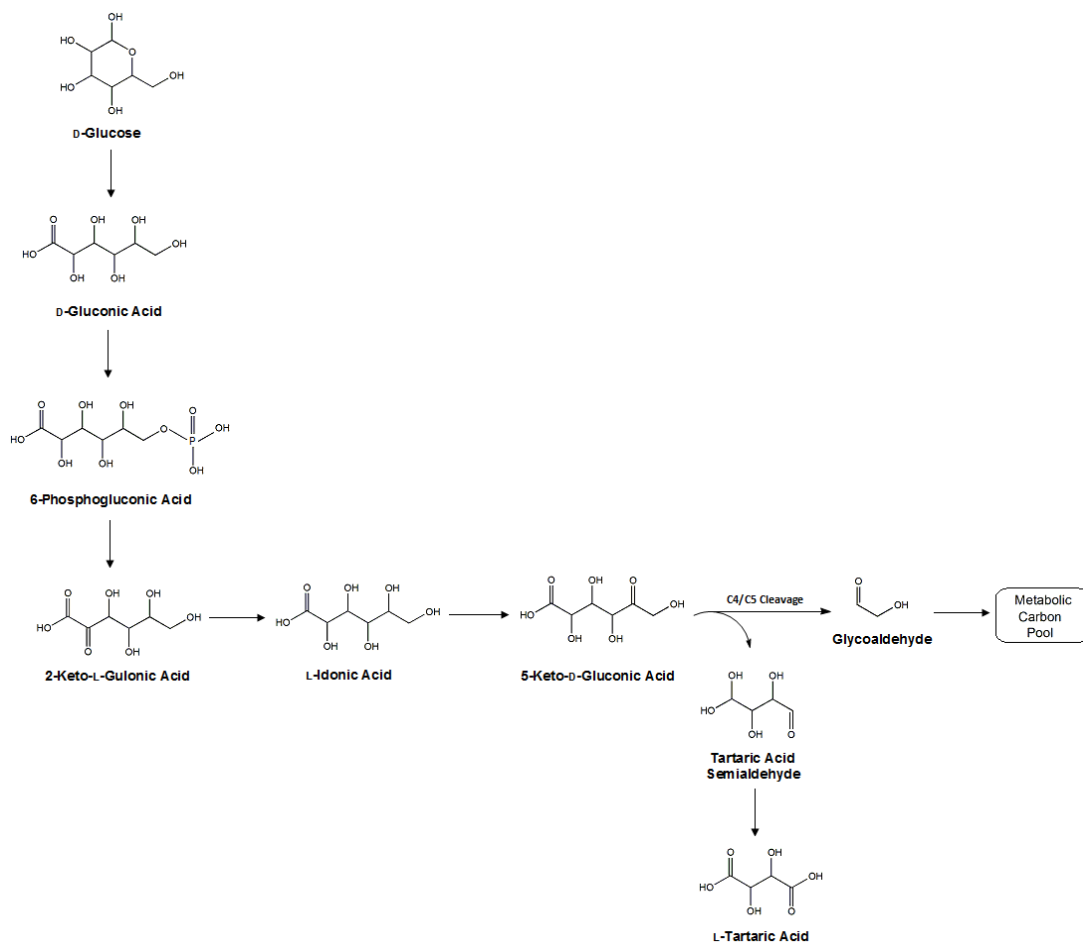


Figure 1.7: Alternative sequence of the glucose precursor pathway of TA biosynthesis in Vitaceae. This alternative sequence incorporates 6-phosphogluconic acid and the Asc-inclusive C4/C5 pathway downstream of 2-keto-L-gulonic acid.

1.5 Enzymes of the Biosynthetic Tartaric Acid Pathway's in Vitaceae

In Vitaceae, two pathway's have been identified capable of synthesising TA: a secondary Asc-noninclusive pathway and a primary Asc-inclusive pathway C4/C5 cleavage pathway. The secondary pathway, whose initial metabolic compound is glucose, generates 5KGA which undergoes further metabolism to TA following the same steps as the Asc-inclusive pathway (Figure 1.8). This suggests the enzymes responsible for the metabolism of 5KGA and ultimately the synthesis of TA are common to both pathway's. Evidence supporting the enzymatic control of TA biosynthesis came from the addition of iodoacetic acid, a potent enzyme inhibitor, to immature berry slices (Saito and Kasai, 1982). Saito and Kasai (1982) showed this addition to immature berry slices inhibited the production of TA.

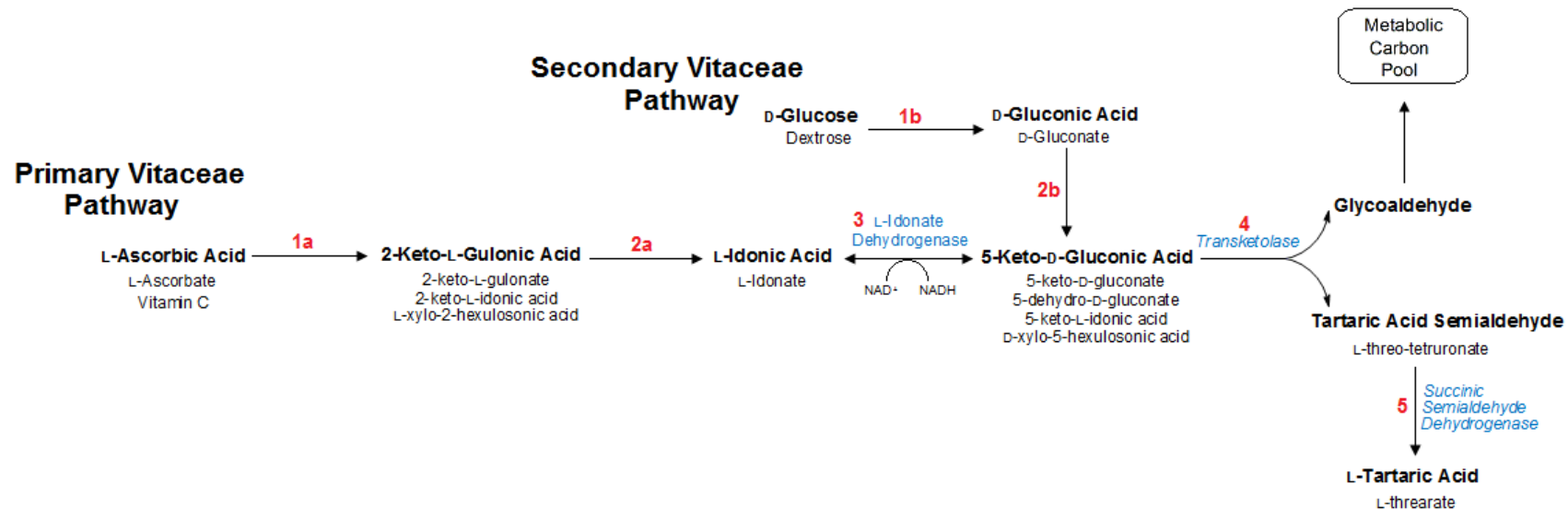


Figure 1.8: Summary of the primary (Asc-C4/C5) and secondary (glucose) pathway's of TA synthesis identified in Vitaceae. The intermediate compounds and their common synonyms are listed. Known enzymes are shown in blue. It should be noted that transketolase and succinic semialdehyde dehydrogenase have been suggested but their role has yet to be confirmed. Composite pathway derived from those shown in Loewus (1999). The steps of the pathway labelled in red correspond to section 1.5.

1.5.1 Step (1a) L-Ascorbic Acid → 2-Keto-L-Gulonic Acid

In spite of the multiple TA biosynthetic pathways present in *V. vinifera*, only the L-(+)-isomer is formed (Wagner *et al.*, 1975). This highly stereospecific process would not be expected unless under enzymatic control (Saito and Kasai, 1978) specific to the reductive reaction of the Asc-ene-diol group (Saito and Kasai, 1982).

1.5.2 Step (1b) D-Glucose → D-Gluconic Acid

Research into the enzymatic control of this reaction in plant tissue has yet to be conducted. The production of D-gluconic acid is not a common fate for D-glucose in plant tissue. Based on the identified reaction of product and substrate in this step, glucose oxidase (β -D-glucose:O₂ oxidoreductase) is a plausible candidate. Glucose oxidase (EC 1.1.3.4) is responsible for the conversion of D-glucose to H₂O₂ and D-glucono-1,5-lactone, which spontaneously hydrolyses to D-gluconic acid in the presence of oxygen and catalase (Anastassiadis *et al.*, 2003). This catalysis is used commercially in the removal of residual sugars or the prevention of oxidative deterioration in food stuffs such as beer, wine and mayonnaise (Walon, 1969). Currently, D-glucono-1,5-lactone has not been identified within this reaction. A BLASTn of the cDNA sequence of glucose oxidase (GenBank accession J05242) from *Aspergillus niger* against the grape gene indices database did not identify candidates within the *V. vinifera* genome.

1.5.3 Step (2a) 2-Keto-L-Gulonic Acid → L-Idonic Acid

The retention of the L-isomer specificity of 2KGA and its conversion to L-idonic acid is also believed to be under enzymatic control (Saito and Kasai, 1984). Early evidence suggests an oxido-reductase responsible for the catalytic activity observed. Whilst examining gene expression libraries DeBolt (2006) identified a set of candidate genes based on expression and protein homology. Amongst this set, 4 genes encoding oxido-reductase proteins were identified. *In planta* activity of these proteins has yet to be determined.

1.5.4 Step (2b) D-Gluconic Acid → 5-Keto-D-Gluconic Acid

The apparent uniqueness of the second enzymatic step of the secondary glucose precursor pathway in *V. vinifera* has resulted in no investigations into the enzymatic control of this step. In bacteria, this interconversion precedes substrate entry into the Entner-Doudoroff and pentose phosphate pathway's (reviewed by Peekhaus and Conway, 1998). The bacterial enzyme identified as performing this reversible reaction in *Gluconobacter oxydans* is gluconate 5-dehydrogenase (Klasen *et al.*, 1995, Merfort *et al.*, 2006a, Prust *et al.*, 2005). Identification of this enzyme in *V. vinifera* has yet to occur.

1.5.5 Step (3) L-Idonic Acid → 5-Keto-D-Gluconic Acid

L-Idonate dehydrogenase (denoted L-idonate dehydrogenase 1 in this study, DeBolt, 2006) is the first enzyme positively identified in the Asc-inclusive C4/C5 pathway in *V. vinifera*. Malipiero *et al* (1987) showed the cessation of TA biosynthesis in mature leaves occurred at the oxidation of L-idonic acid, which subsequently accumulated indicating this as the 'rate limiting' step of the C4/C5 pathway. Through examination of gene expression libraries corresponding to the developmental stages of the berry in which TA synthesis is the highest, the candidate L-idonate dehydrogenase 1 (L-IdnDH.1) was identified. Analysis of *L-IdnDH.1* showed high levels of expression in the green immature berry, ceasing 14 weeks post-flowering. This expression pattern coincided with the period of TA synthesis, indicating specificity of the enzyme to the TA pathway and not general metabolism. This expression pattern has been confirmed in *V. vinifera* cv Cabernet Sauvignon, cv Shiraz, cv Semillon, and cv Syrah (DeBolt, 2006, Melino, 2009, Wen *et al.*, 2010). Not surprisingly, L-IdnDH.1 showed homology to several plant sorbitol dehydrogenases and low homology to an L-IdnDH.1 from *E. coli*. Characterisation of the recombinant protein *in vivo* showed catalytic activity specific to the metabolism of L-idonate (DeBolt, 2006, DeBolt *et al.*, 2006). Recent studies utilising an L-IdnDH.1 specific antibody have detected the

presence of L-IdnDH.1 in mature berry tissue when *L-IdnDH.1* expression has ceased (Wen *et al.*, 2010). This may be due to an extended half life of the L-IdnDH.1 protein.

DeBolt *et al* (2006) also identified a natural mutant, Vitaceae species *Ampelopsis aconitifolia* which lacked TA accumulation during berry development. Nevertheless, *A. aconitifolia* was found to have a higher than mean quantity of Asc indicating the presence of the precursor pathway. The absence of *L-IdnDH.1* was indicated using specific primers probed against the *A. aconitifolia* genome (DeBolt *et al.*, 2006). L- idonic acid did not accumulate in this species, and exogenous addition of 5-keto-D- gluconic acid did not result in TA accumulation, suggesting the Asc-C4/C5 TA biosynthetic pathway is absent in *A. aconitifolia* (DeBolt, 2006).

Analysis of the grapevine EST database has identified a possible homologue to *L-IdnDH.1*, *L-IdnDH.2* (Hayes, DeBolt, Cook and Ford, manuscript in preparation). *L-IdnDH.2* was identified due to a 70% nucleic acid and 77.59% amino acid identity. Expression and purification of soluble recombinant L-IdnDH.2 protein has been successfully achieved. Preliminary characterisation of the recombinant protein *in vivo* has yet to occur.

1.5.6 Step (4) 5-Keto-D-Gluconic Acid → Tartaric Acid Semialdehyde

Enzymatic activity in relation to the C4/C5 cleavage of 5-Keto-D-Gluconic Acid (5KGA), resulting in TA formation was initially disputed by Saito and Kasai (1984) due to the substrate's ability to undergo oxidative cleavage to TA under both acidic and alkaline conditions. Radiolabel studies based on the number of atoms incorporated into TA via H₂¹⁸O and ¹⁸O indicate a hydrolase responsible for this conversion (Saito *et al.*, 1997). Work by Salusjärvi *et al* (2004) in *Gluconobacter suboxydans* suggest a transketolase may be responsible for the catalytic activity during this step in the bacterium. Examination of gene expression libraries by DeBolt (2006) identified two transcripts with shared homology to plant transketolases. *In vitro* assays to confirm the role of these candidates are required.

1.5.7 Step (5) Tartaric Acid Semialdehyde → L-Tartaric Acid

Preliminary evidence has suggested succinic semialdehyde dehydrogenase as responsible for the conversion of TA semialdehyde to TA (Salusjärvi *et al.*, 2004, Zimmermann, 2005). A candidate, provisional name tartaric semialdehyde dehydrogenase (TSAD) was identified by DeBolt (2006) based on differential expression of the candidate during early berry development. The amino acid sequence of TSAD showed 99.4% and 98.9% similarity to the domain architecture of the aldehyde dehydrogenase family and the NAD⁺-dependent aldehyde dehydrogenase domains respectively, key components of the aldehyde dehydrogenase class of enzymes. A conceptual translation of the transcript shows close similarity to succinic semialdehyde dehydrogenase, further supporting the candidate's role in the pathway (DeBolt, 2006).

1.6 Tartaric Acid Enzymes of Bacterial Origin

Microorganisms including *E. coli* (Yum *et al.*, 1998a), *Pseudomonas* spp. (La Rivière, 1956, Lockwood and Nelson, 1951), *Gluconobacter* spp. (Chandrashekar *et al.*, 1999, Koichi *et al.*, 1971) and *Acetobacter* spp. (Kamlet, 1943) are capable of producing, metabolising, or performing many of the identified catalytic steps of TA biosynthesis. Kotera *et al.* (1972) first suggested a comparison between the reactions of both plant and bacterial enzymes. Across these microorganisms (*E. coli*, *Gluconobacter*, *Acetobacter*, *Pseudomonas*), a number of enzymes have been identified to catalyse reactions identical to those responsible for TA biosynthesis in plants (Figure 1.9). As shown in Figure 1.9, the steps common to TA biosynthesis in *V. vinifera* feed major metabolic pathway's including glycolysis, Entner-Doudoroff and pentose phosphate pathway's. Although TA is produced by the aforementioned microorganisms, the method of production occurs via the excretion of a TA intermediate during fermentation (Chandrashekar *et al.*, 1999, Kamlet, 1943, Yamada *et al.*, 1971) and not an enzymatic process (Klasen *et al.*, 1992a). *Gluconobacter* has been shown to biosynthesise 5KGA from glucose, which is then converted to TA

extracellularly through an oxidising catalysis with vanadate in the culture medium and not a bacterial process (Klasen *et al.*, 1992a). Although the later stages of TA production are different, the upstream reactions mirror that of TA biosynthesis in *V. vinifera* enabling the utilisation of these enzymes in this study.

Figure 1.9: Composite bacterial pathway constructed from the data obtained from the EcoCyc database (<http://ecocyc.org/>) (Keseler, 2005). Compounds listed in red are those common to the primary Asc-C4/C5 and secondary glucose precursor pathway's with enzymes listed in blue. The coloured squares indicate the bacterial metabolic pathway the substrate is associated with: yellow: glycolysis, purple: Entner-Doudoroff pathway, green: ketogluconate metabolism, orange: pentose phosphate pathway.

Of interest in this study are the enzymes 2-ketogluconate reductase and gluconate-5 dehydrogenase. These enzymes are described as responsible for the catalysis of reactions identical to step 2a of the primary Asc-C4/C5 and step 2b of the secondary glucose pathway respectively (Figure 1.8). Unfortunately, the nomenclature of these enzymes is inconsistent throughout the literature (Table 1.1). For this study, the enzymes will be referred to by the name assigned in the *E. coli* system, 2-ketogluconate reductase (2KGR) and gluconate-5 dehydrogenase (G5Dh).

Table 1.1: Summary of the enzymes investigated in this study. Each enzyme is grouped by the enzymatic name it is referred to throughout this study. Synonyms for each enzyme are listed including their designated EC classification number. Data compiled from the Brenda database (<http://www.brenda-enzymes.org/>)

Enzyme Name	L-Idonate Dehydrogenase 1	2-Ketogluconate Reductase	Gluconate 5-Dehydrogenase
EC Classification	1.1.1.128	1.1.1.215	1.1.1.69
Synonyms	L-idonate 2-dehydrogenase L-idonate:NADP+ 2-oxidoreductase 5-keto-D-gluconate 2-reductase 5-ketogluconate 2-reductase 5-ketogluconate 5-reductase (L-idonate-forming) 5-ketoglucono-ido- reductase 5KGR L-IdnDH	D-gluconate:NADP+ oxidoreductase 2-keto-D-gluconate reductase 2-keto-D-gluconate-yielding D-gluconate dehydrogenase 2-ketoaldonate reductase 2KGA reductase gluconate 2-dehydrogenase 2KGR 2KR FAD-GADH GADH	5-keto D-gluconate reductase 5-keto-D-gluconate 5-reductase 5-ketogluconate 5-reductase 5-ketogluconate reductase gluconate 5-dehydrogenase gluconate:NADP 5-oxidoreductase pyrroloquinoline quinone-dependent

2-Ketogluconate reductase (2KGR) has been identified across a variety of bacterial systems with an affinity to a broad range of substrates (Adachi *et al.*, 1978). The reactions attributed to 2KGR activity across these systems are summarised in Table 1.2. This broad substrate specificity led to the suggestion 2KGR is responsible for the regeneration of NADP⁺ for the pentose phosphate pathway in acetic acid bacteria (Adachi *et al.*, 1979). 2KGR has successfully been crystallised from *Gluconobacter liquefaciens* (Chiyonobu *et al.*, 1975a) and *Acetobacter ascendens* (Adachi *et al.*, 1978) although the structure has yet to be resolved. 2KGR activity is localised to the cytosol (Adachi *et al.*, 1978), the proposed site of TA biosynthesis in *V. vinifera*.

Table 1.2: Summary of the reactions performed by 2-ketogluconate reductase across various systems. The intermediates identified in the respective pathway's of *V. vinifera* are listed in blue (Asc-C4/C5 pathway) and red (secondary glucose pathway) with those common to both in purple and those not known to be involved in either of the pathway's in black. The reversibility of each enzyme in relation to the organism the enzyme was identified is listed, untested indicates the reversibility of the enzyme was not determined. Data compiled from Yum *et al* (1998a, 1998b), Pitt and Mosley (1985), Adachi *et al* (1978), Ameyama and Adachi (1982b), Chiyonobu *et al* (1976), Toyama *et al* (2007), and Saichana *et al* (2007).

Reaction	Reversible	Organism
2-keto-L-gulonate + NADPH → L-idonate + NADP ⁺	Untested	<i>Brevibacterium ketosoreductum</i> <i>Escherichia coli</i>
	Yes	<i>Acetobacter ascendens</i> <i>Acetobacter rancens</i> <i>Gluconobacter liquefaciens</i> <i>Gluconobacter oxydans subsp. suboxydans</i>
L-idonate + NADP ⁺ → 2-keto-L-idonate + NADPH	Untested	<i>Acetobacter ascendens</i> <i>Acetobacter rancens</i> <i>Gluconobacter liquefaciens</i> <i>Gluconobacter oxydans subsp. suboxydans</i>
5-keto-D-gluconate + NADPH → D-gluconate + NADP ⁺	Untested	<i>Acetobacter ascendens</i> <i>Acetobacter rancens</i> <i>Gluconobacter liquefaciens</i> <i>Gluconobacter oxydans subsp. suboxydans</i>
2,5-diketo-D-gluconate + NADPH → 5-keto-D-gluconate + NADP ⁺	Untested	<i>Escherichia coli</i>
	No	<i>Brevibacterium ketosoreductum</i>
2-dehydro-D-gluconate + NADPH → D-gluconate + NADP ⁺	Untested	<i>Brevibacterium ketosoreductum</i> <i>Escherichia coli</i> <i>Penicillium notatum</i>
	Yes	<i>Acetobacter ascendens</i> <i>Acetobacter rancens</i> <i>Gluconobacter liquefaciens</i> <i>Gluconobacter oxydans subsp. suboxydans</i>
D-gluconate + NADP ⁺ → 2-dehydro-D-gluconate + NADPH	Untested	<i>Gluconobacter frateurii</i> <i>Gluconobacter oxydans</i>
acetaldehyde + NADPH → ethanol + NADP ⁺	Untested	<i>Acetobacter rancens</i>
D-galactonate + NADP ⁺ → 2-keto-D-galactonate + NADPH	Yes	<i>Acetobacter ascendens</i> <i>Acetobacter rancens</i> <i>Gluconobacter liquefaciens</i> <i>Gluconobacter oxydans subsp. suboxydans</i>
D-xylonate + NADPH → 2-keto-D-xylonate + NADP ⁺	Untested	<i>Acetobacter rancens</i> <i>Gluconobacter liquefaciens</i> <i>Gluconobacter oxydans subsp. suboxydans</i>
glyoxylate + NADPH → glycolate + NADP ⁺	Untested	<i>Acetobacter rancens</i>
hydroxypyruvate + NADPH → 2,3-dihydroxypropanoate + NADP ⁺	Untested	<i>Acetobacter rancens</i>
pyruvate + NADPH → lactate + NADP ⁺	Untested	<i>Acetobacter rancens</i>

Gluconate-5 dehydrogenase (G5Dh) has also been identified across a variety of bacterial systems with an affinity to a broad range of substrates (summarised in Table 1.3) with the exclusive utilisation of NAD(P)H (Ameyama *et al.*, 1974, Klasen *et al.*, 1992b). Two G5Dh enzymes have been identified based on localisation and primary substrate affinity. The G5Dh responsible for the generation of 5KGA from GA is localised to the cytosol, the proposed site of TA biosynthesis in *V. vinifera* (De Ley and Stouthamer, 1959). The cellular function of G5Dh in microorganisms is suggested to be the production of various ketogluconates as extracellular carbon sources (Shinagawa *et al.*, 1978). Purified G5Dh is highly unstable unless substrate-bound suggesting the requirement of high turnover of protein to maintain a carbon source (Ameyama and Adachi, 1982a). Various strains of *Gluconobacter* have been engineered via the over-expression of G5Dh in the commercial production of L-TA to increase the yield of 5KGA (Elfari *et al.*, 2005, Herrmann *et al.*, 2004). 5KGA is then excreted into the culture medium where the vandate-dependent catalysis of 5KGA to TA under optimised fermentation conditions occurs (Klasen *et al.*, 1992a).

Table 1.3: Summary of the reactions performed by gluconate 5-dehydrogenase across various systems. The intermediates identified in the respective pathway's of *V. vinifera* are listed in blue (Asc-C4/C5 pathway) and red (secondary glucose pathway) with those common to both in purple and those not known to be involved in either of the pathway's in black. The reversibility of each enzyme in relation to the organism the enzyme was identified is listed. Untested indicates the reversibility of the enzyme was not determined. * indicates experimental data was determined using a recombinant enzyme. PND indicates the product of the reaction was not determined. Data compiled from Pitt and Mosley (1985), Saichana *et al* (2007), Ameyama *et al* (1974), De Ley (1966), Adachi *et al* (1979), Ameyama and Adachi (1982a), Klasen *et al* (1992b), Chiyonobu *et al* (1975b), Merfort *et al* (2006a, 2006b) and Elfari *et al* (2005).

Reaction	Reversible	Organism
$\text{D-gluconate} + \text{NAD(P)}^+ \rightarrow \text{5-dehydro-D-gluconate} + \text{NAD(P)H} + \text{H}^+$	Untested	<i>Acetobacter aceti</i> <i>Acetobacter ascendens</i> <i>Acetobacter aurantium</i> <i>Acetobacter kuetzingianus</i> <i>Acetobacter orleanensis</i> <i>Acetobacter pasteurianus</i> <i>Acetobacter rancens</i> <i>Acetobacter xylinum</i> <i>Gluconobacter albidus</i> <i>Gluconobacter cerinus</i> <i>Gluconobacter dioxyaceticus</i> <i>Gluconobacter gluconicus</i> <i>Gluconobacter melanogenus</i> <i>Gluconobacter oxydans subsp. suboxydans</i> <i>Gluconobacter roseus</i>
	Yes	<i>Gluconobacter liquefaciens</i> <i>Gluconobacter oxydans</i>
$\text{5-keto D-gluconate} + \text{NADPH} \rightarrow \text{D-gluconate} + \text{NADP}^+$	Untested	* <i>Gluconobacter oxydans</i>
$\text{5-dehydro-D-gluconate} + \text{NADPH} \rightarrow \text{D-gluconate} + \text{NADP}^+$	Untested	<i>Escherichia coli</i> <i>Gluconobacter oxydans subsp. suboxydans</i> <i>Klebsiella sp.</i> <i>Penicillium notatum</i>
	Yes	<i>Gluconobacter liquefaciens</i> <i>Gluconobacter oxydans</i>
$\text{5-dehydro-D-fructose} + \text{NADPH} \rightarrow \text{D-fructose} + \text{NADP}^+$	Untested	<i>Gluconobacter liquefaciens</i>
$\text{D-fructose} + \text{NADPH} \rightarrow \text{5-dehydro-D-fructose} + \text{NADP}^+$	Untested	<i>Gluconobacter liquefaciens</i> <i>Gluconobacter oxydans</i>
$\text{D-glucono-delta-lactone} + \text{NADP}^+ \rightarrow \text{PND}$	Untested	<i>Gluconobacter liquefaciens</i>
$\text{sorbitol} + \text{NAD}^+ \rightarrow \text{PND} + \text{NADH}$	Untested	<i>Gluconobacter oxydans</i>

Although both 2KGR and G5Dh have shown broad-range substrate specificity, the localisation in the cytosol and the observed affinity towards the substrates 2KGA and GA respectively suggests these enzymes may be responsible for TA biosynthesis in *V. vinifera*. Developmental studies indicate TA synthesis is active in young immature berries (Kliwer, 1964). This provides a defined developmental window in which expression of enzymes specific to TA synthesis is expected. However, should the enzymes be responsible for the regeneration of NAD(P)H or ketogluconate as a carbon source, the expression patterns may cover multiple stages of berry development.

1.7 Dissimilation of Tartaric Acid

To date, TA has no known role in cellular metabolism in higher plants. The suggestion of TA metabolism in *V. vinifera* arose from early investigations detecting a decrease in TA concentration post-véraison. TA accumulation occurs in immature berry tissue (see section 1.3) plateauing as berries undergo véraison (Hale, 1968). Post-véraison berries undergo various developmental changes including an increase in fresh weight due to water intake (Coombe, 1976). Calculation of TA on a per berry basis shows the amount (mg) of TA remains relatively constant during maturation. The detected decrease in TA is attributed to a dilution not a dissimilation (Ruffner *et al.*, 1983).

The use of radiolabelled substrates was again employed to investigate the dissimilation in ripening berries with L-(+)-tartaric acid-[1,4-¹⁴C] fed to detached berries via the peduncle and the respired ¹⁴CO₂ calculated (Saito and Kasai, 1968). Saito and Kasai (1968) found the ratio of radioactivity between the fed L-(+)-tartaric acid-[1,4-¹⁴C] and that recovered as ¹⁴CO₂ was constant throughout ripening suggesting TA was metabolised. Further support was given by Hardy (1968) who also fed L-(+)-tartaric acid-[1,4-¹⁴C] to excised immature berries via the pedicel. Hardy (1968) detected trace amounts of ¹⁴C in glycolic and malic acids; however, this was less than 1% of the extracted ¹⁴C after 24 hours. Interestingly, Hardy (1968) then

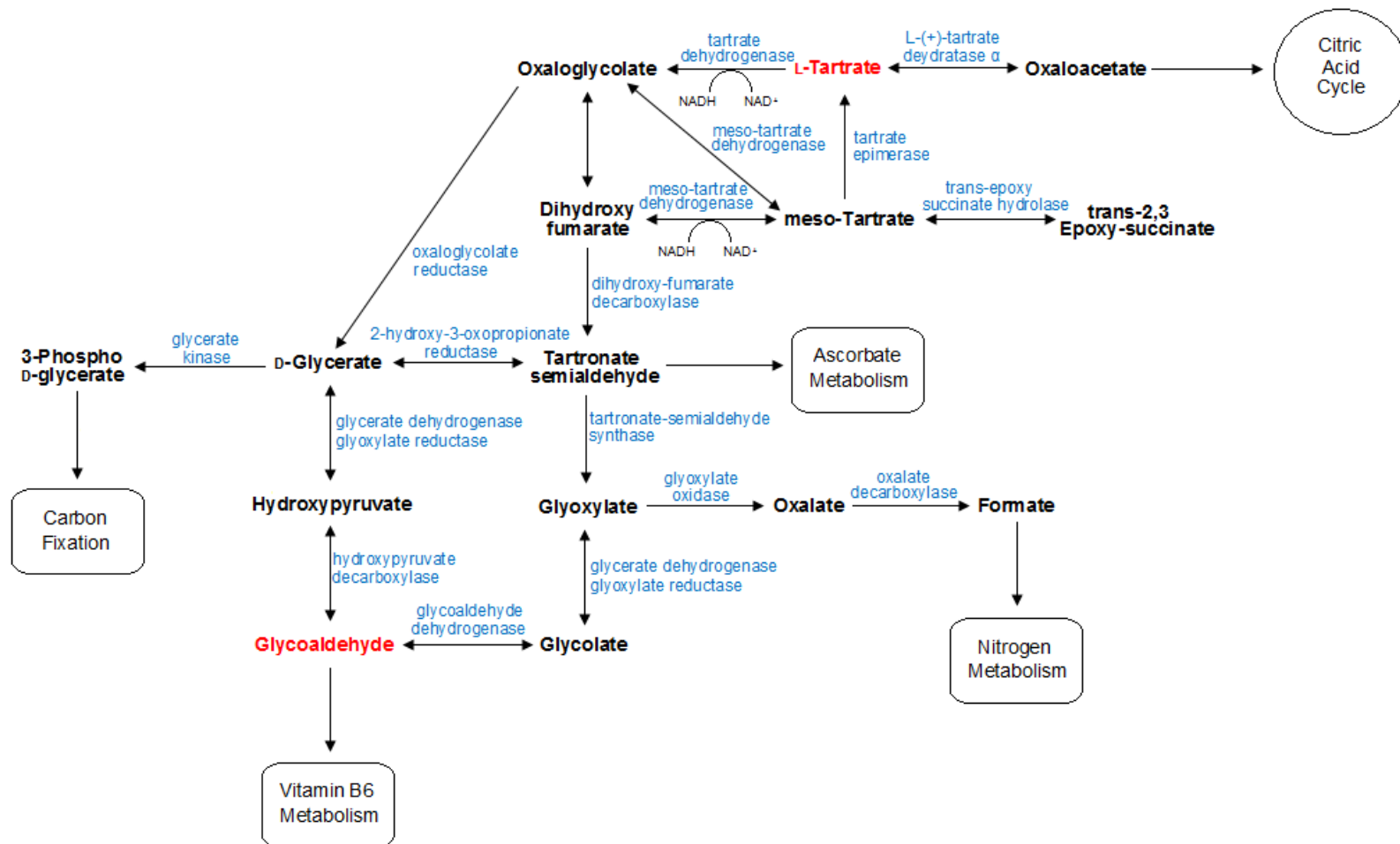
goes on to state that TA does not undergo degradation, although previously stating it did within the same paper. Takimoto *et al* (1976) repeated Saito and Kasai's (1968) experiment utilising L-(+)-tartrate[U-¹⁴C]. Takimoto *et al* (1976) calculated the ratio of ¹⁴CO₂ evolution producing results consistent with the previous work. Takimoto *et al* (1976) then went on to identify monoethyl-tartrate and malate as the products in which the radioactive ¹⁴C resided. Hrazdina *et al* (1984) extracted and measured the g TA/100g FW over development from 3 weeks post-fruit set to harvest in de Chaunac berry tissue. Hrazdina *et al* (1984) reported a rapid metabolism of TA over this period denoted by two sharp declines in g/100g berry levels intersected by a period of TA synthesis in which levels rose. No explanation for either of the observed rise or fall of TA levels is offered by Hrazdina *et al*; however, the steady overall decline of TA correlates with the steady increase of berry weight (g) upon maturation. Each case of TA dissimulation utilising radiolabel studies used excised berry clusters. Additional factors induced by removal of the cluster from the vine must also be considered, including the possibility of TA utilisation as a carbon source.

Saito and Kasai (1968) reported the TA synthesised early in grape development was readily converted to its salt form, tartrate, before equilibrating approximately 100 days post-flowering. Degradation systems, if present, are thought to be inactive against the inert salt (Saito and Kasai, 1968, Vickery and Palmer, 1954). Inhibition of enzymatic degradation due to the formation of the L-isomer (Lewis and Neelakanthan, 1959) and the storage of TA in the vacuole preventing cytoplasmic enzymes degrading the compound have also been postulated. This does not explain the negligible quantities of dissimulation products detected. Saito and Kasai (1968) proposed the constant level of TA was maintained by the synthesis and degradation of the acid working in equilibrium. TA biosynthesis is associated with the rapid growth of young berries and has yet to be detected in mature berries (Ruffner, 1982). *L-IdnDH.1*, the first enzyme confirmed to be involved in TA biosynthesis, is only expressed in young immature berries (DeBolt *et al.*, 2006, Melino *et al.*, 2009a). The *L-IdnDH.1* protein has been detected in mature berry tissue when *L-IdnDH.1*

expression is not detected (Wen *et al.*, 2010) supporting the possibility of TA biosynthesis late in berry development.

In addition to possessing enzymes capable of catalysing steps of the TA biosynthetic pathway (see section 1.6) microorganisms are capable of metabolising TA as a carbon source (Figure 1.10). The ability to dehydrate TA to oxaloacetate and glycerate has been identified in various species including *Pseudomonas* (Furuyoshi *et al.*, 1987, Hurlbert and Jakoby, 1965, Kohn and Jakoby, 1968, Kohn *et al.*, 1968, Shilo, 1957, Shilo and Stanier, 1957), *Rhodopseudomonas* (Ebbighausen and Giffhorn, 1984, Giffhorn and Kuhn, 1983, Rode and Giffhorn, 1982), *Rhodotorula* (Dagley and Trudgill, 1963, Ebbighausen and Giffhorn, 1984, Fernández and Ruíz-Amil, 1965) and *E. coli* (Kim *et al.*, 2007, Kim and Uden, 2007). As shown in Figure 1.10 the metabolism of tartrate feeds major metabolic pathway's including carbon fixation, the citric acid cycle and ascorbate metabolism, the primary precursor for TA biosynthesis in *V. vinifera*. It is also worth noting that it is the L-isomer of TA that is metabolised, although D-tartrate metabolism in *E. coli* has been identified (Kim *et al.*, 2007). To date, the enzymes directly responsible for the metabolism of TA have not been identified in *V. vinifera*.

Figure 1.10: Composite bacterial pathway constructed from the data obtained from the KEGG database (<http://www.genome.jp/kegg/>) (Kanehisa and Goto, 2000). Compounds listed in red are those common to the primary Asc-C4/C5 and secondary glucose precursor pathway's with enzymes listed in blue.



Crouzet and Otten (1995) identified four intact open reading frames present in the *Agrobacterium vitis* genome encoding enzymes capable of degrading TA. The grapevine is the natural host of the tumourigenic bacterium whose specificity to the L(+)-isomer leads to the suggestion of a symbiotic relationship. The utilisation of L-TA by *A. vitis* however, appears to be negligible with no decrease in TA or benefit to the vine reported.

1.8 Environmental Factors

The quality and respective ratios of organic acids within a grape berry has a significant impact on the organoleptic properties of the resultant wine (Liu *et al.*, 2007). Environmental factors such as region, irrigation, temperature and light intensity are known to influence acid levels during berry development (Amerine, 1956, Buttrose *et al.*, 1971, Cirami, 1973, Kliewer, 1964, Kliewer and Schultz, 1964). Careful consideration of these factors in relation to the grape cultivar is required to ensure the quality of wine variety produced.

Early investigations into the influence of light exposure by artificial shading in *V. vinifera* cv Sauvignon blanc resulted in delayed maturation of berry tissue and a 13% increase in MA levels. TA remained consistent across treatments (Kliewer *et al.*, 1967). Additional studies incorporating the application of light treatments consistently altered levels of MA, leaving TA levels without significant alteration (Dokoozlian and Kliewer, 1996, Kliewer and Lider, 1968, Stafford and Loewus, 1958, Wagner and Loewus, 1974) suggesting only MA levels are influenced by light exposure. Recent research investigating the effect of light exposure on individual acids throughout berry development has shown TA levels significantly lower in shaded berries throughout all stages of development (DeBolt *et al.*, 2008). DeBolt *et al* (2008) encased attached berry bunches of *V. vinifera* cv Shiraz BVRC12 in boxes reducing ambient light without affecting temperature conditions. DeBolt *et al* (2008) determined light exclusion significantly reduced berry weight and TA accumulation at all stages of development with pre-véraison accumulation of MA slower yet peaking higher than the control lines. Melino *et al* (2011), utilising the same technique, showed significant decreases in berry

weight, Asc and TA accumulation. No alteration in MA accumulation pre-véraison was observed; however, post-véraison MA metabolism was altered. Melino *et al* (2011) also investigated the effect of light exposure on the regulation of respective Asc-synthetic and catabolic enzymes over berry development. Melino *et al* (2011) determined 4 biosynthetic Asc genes are responsive to light exposure, limited to a defined pre-véraison stage. Asc recycling genes were determined to be light dependent; however, *L-IdnDH.1*, the only identified TA biosynthetic enzyme showed no light regulation. TA synthesis has been associated with rapid cell division (Skene and Hale, 1971) therefore the decrease in TA observed may be associated with the decreased growth of berry tissue.

Temperature also influences organic acid accumulation with initial investigations suggesting low temperature stimulates formation whereas high temperature triggers metabolism through increased respiration (Peynaud and Maurié, 1958). Low temperature has been shown to increase acid levels in berry tissue with varieties grown in low temperate environments shown to accumulate 2-3 fold higher MA and TA levels than those in higher temperate conditions (Kliewer, 1968, 1971). The relationship between low temperature and high acid levels is not consistent among trials involving opposing temperature treatment across consecutive seasons (Kliewer, 1964).

The elucidation of the effects associated with light and temperature on berry development are complicated by the suggestion of diurnal regulation of enzymatic activity specific to organic acid accumulation (Takimoto *et al.*, 1976). Immature grape berries show levels of principal organic acids 10% higher during the day supporting diurnal regulation (Kriedemann, 1968). Diurnal regulation of TA synthesis was investigated via the determination of radiolabel incorporation in TA under both light and dark conditions. Saito and Loewus (1989b) fed radiolabelled [2-¹⁴C, 3-³H]glucose to leaves of *Parthenocissus quinquefolia* and detected 85-98% of labelled TA arose via the Asc pathway in the light, yet only 68-74% from the same pathway in the dark. Similar results in relation to light influencing the quantity of incorporated radiolabel were also observed by Stafford and Loewus (1958) in excised *V. vinifera* cv Mission leaves and Takimoto *et al* (1976) in *V. labruscana* cv Delaware berries suggesting Vitaceae may alternate pathway usage

based upon light- or dark-cycle conditions. Diurnal regulation of organic acid-associated enzymatic activity is supported by recent investigations into temperature regulation of the biosynthetic and catabolic enzymes of MA. Sweetman (2011) showed the effect of temperature on MA related genes was dependent upon the diurnal cycle the treatment was applied, supporting the function of phosphoenolpyruvate carboxylase and NAD-malic enzyme in temperature-responsive malate synthesis and catabolism, respectively.

1.9 Conclusions and Aims

Grapes are globally the second most cultivated fruit with to 65.4×10^6 tonnes produced in 2005 (Liu *et al.*, 2007). Economically, TA is a vital component with levels determining the suitability of grapes for use in winemaking (DeBolt *et al.*, 2007). As well as affecting the organoleptic properties of the wine, it is also important in preventing spoilage and oxidative damage during processing.

The synthesis and accumulation of TA in the developing berry is still poorly understood in spite of its importance to the industry (Coombe, 1992). TA accumulation is not present in any model plant species adding to the complexity of research into this acid. The confirmation of L-IdnDH.1 as a functional component of TA biosynthesis has increased the understanding of the process, but the identification of enzymes responsible for the other intermediate conversions within the pathway is yet to occur. The identification of a natural L-IdnDH.1 mutant, the ornamental variety *A. aconitifolia* and its resultant lack of tartrate accumulation also warrants further investigation.

The specific aims of this study include:

- Identify, clone, and determine kinetic parameters of recombinant candidate enzymes pertaining to both the primary and secondary tartaric acid biosynthetic pathway's
- Determine the accumulation of tartaric acid in grape berries over a developmental season to enable correlation of *in situ* parameters

- Determine the transcriptional patterns of candidate tartaric acid biosynthetic genes and subsequent protein activity *in situ* over development and correlate this with the predetermined accumulation of tartaric acid
- Determine the prevalence of the identified genes in various table and ornamental grape cultivars
- Provide *in vivo* evidence supporting the candidate genes' inclusion in tartaric acid biosynthesis

Chapter 2:

Materials and Methods

2.1 Chemicals

All chemicals and reagents used were of analytical or molecular grade and supplied by Sigma-Aldrich (USA), Bio-Rad (USA), Amresco (USA), Fluka (USA), Merck (Germany) or Roche (Germany) as required.

2.2 Plant Material

The cultivars *Vitis vinifera* cv Shiraz (clone BVRC12 on Schwarzmann rootstock), Pinot Noir (own roots), Riesling (own roots) and Cabernet sauvignon (own roots) were sampled from the University of Adelaide Coombe vineyard, Waite Campus, Urrbrae, South Australia (elevation 123m, latitude 34°58'S).

The species *Ampelopsis aconitifolia* (own roots), *A. brevipedunculata* (Accession G875018) and *Parthenocissus henryana* (Accession G831859) were sampled from the Adelaide Botanic Gardens, South Australia (elevation 180m, latitude 34°53'S).

Construction of transgenic *V. vinifera* cv Thompson Seedless L-idonate dehydrogenase knockdown vines (Hayes, DeBolt, Cook and Ford, manuscript in preparation) was performed by The Ralph M. Parsons Foundation, Plant Transformation Facility at the University of California.

2.3 Sampling

A randomized complete block design was employed to ensure statistical viability of the sample set for the developmental series of the cultivar *V. vinifera* cv Shiraz. 4 replicates repeated across 5 rows located in similar regions of the vineyard were selected and pooled resulting in 5 individual vines constituting 1 replicate. The order of these replicates within the rows was randomly assigned, reducing the effect of vineyard variability.

Individual berry bunches which had reached the developmental stage of 50% cap-fall across all replicates were tagged. At each time-point across development, berries were removed from randomly selected bunches and pooled. The pooling of

multiple vines enabled sampling without affecting the carbohydrate sink-source ratio within each vine. These berries were immediately snap-frozen and stored at -70°C until required.

The fruit sampled for this project was also used by Melino (2009) and Sweetman (2011) in their respective projects.

2.4 Seasonal Data Analysis

2.4.1 °Brix and Fresh Weight

A random selection of berries from the pooled samples (10 berries at pre-véraison and 40 at post-véraison time-points) were selected and allowed to thaw at room temperature. Any excess water due to condensation was removed and the sample weighed. Fresh weight/berry was calculated using the following calculation:

$$\text{Fresh Weight (g/berry)} = \text{Total weight (g) of } n \text{ berries} / n$$

The berries were placed in a resealable plastic bag and crushed by hand. Cellular debris was allowed to settle and a sample of the extracted juice taken. The sample (approximately 60µL) was placed on the detection platform of a self-calibrating ARAGO hand refractometer, and the °Brix value read. Distilled H₂O was used as a reference solvent.

2.4.2 Organic Acid extraction and High-Performance Liquid Chromatography Analysis

2.4.2.1 Organic Acid Extraction

0.5g of whole berry tissue was ground under liquid nitrogen (LN) in a mortar and pestle, transferred to a LN cooled 10mL centrifuge tube and resuspended in cooled 3% (w/v) *meta*-phosphoric acid-1mM ethylenediaminetetraacetic acid (EDTA) to a final volume of 5mL. The tubes were wrapped in aluminium foil to prevent degradation of the organic acids (namely Asc) by ultraviolet light. The homogenate was then centrifuged at 2200x *g* for 10 min at 4°C. 2mL of the resultant supernatant (supernatant 1) was transferred into a fresh tube. The pellet was resuspended in the remaining supernatant and mixed on a rotating wheel at

room temperature for 2 hours. The tube was centrifuged as previously described and the supernatant (supernatant 2) removed. Supernatants 1 and 2 were individually filtered through a 0.45 micron PVDF filter (Millex HV, Adela Scientific, Australia) into a pre-cooled 2mL centrifuge tube with a 300 μ L (A1) and 200 μ L (E1) aliquot for supernatant 1, and a single 200 μ L (E2) aliquot for supernatant 2 taken. 150 μ L of 0.8M Trizma-HCl pH 9- 2.5mM *tris*(2-carboxyethyl)phosphine (TCEP) was added to sample A1 to a final pH of 6.0 (TCEP is a reducing agent used to reduce all the Asc in the sample to enable total Asc to be determined). The sample was covered and incubated at room temperature for 20 minutes then reacidified with 5 μ L of 8.7M *ortho*-phosphoric acid to pH 2.5. 0.2mL of the sample was then transferred to a fresh 2mL centrifuge tube (E3).

2.4.2.2 High Performance Liquid Chromatography

Organic acids from each extract were separated on an Agilent 1100 series High Performance Liquid Chromatography (HPLC) (Agilent Technologies, USA) equipped with a photodiode array detector set to signals 210 nm for OxA, TA and MA, and 245 nm for Asc. 5 μ L of each extract was individually injected into a 150 x 4.6mm Synergi Fusion column (Phenomenex, Australia) fitted with a guard cartridge of the same material maintained at 30°C. A gradient elution at 1 mL/min was employed with the mobile phases: eluent A: 25 mM KH₂PO₄-0.1 mM EDTA (pH 2.5); eluent B: methanol. The incremental decrease of eluent A from 100 to 90% coincided with the incremental increase of eluent B from 0 to 10% over a 10 minute period. This gradient was reversed so that at the final run time of 20 minutes, the column was re-equilibrated to 100% eluent A and 0% eluent B. The data was analysed using Chemstation for LC 3D systems software (Agilent Technologies, USA). Concentrations of soluble TA, MA and Asc were determined from extract E1; total Asc was determined from extract E3; and OxA was determined from extract E2. Dehydroascorbic acid was determined by subtracting the calculated concentration of Asc (extract E1) from the total Asc concentration (extract E3).

The techniques of extraction and analysis of organic acid have subsequently been published by Melino (2009).

2.5 RNA Extraction

Total RNA was extracted from berry tissue using the sodium-perchlorate method described by Rezaian and Krake (1987), modified by Davies and Robinson (1996) with additional modifications as detailed below.

2g of berry tissue was ground under LN and transferred to a cooled 50mL sterile disposable centrifuge tube containing 10 volumes of RNA Extraction Buffer (5M sodium perchlorate, 0.2M Tris pH 8.3, 2% (w/v) polyethylene glycol 8000 (PEG), 1% (w/v) sodium dodecyl sulphate (SDS), 8.5% (w/v) insoluble Polyvinylpyrrolidone (PVP), 1% (v/v) β -mercaptoethanol (BME)). The homogenate was inverted 3 times to mix and incubated at room temperature for 30 minutes on a platform mixer at low speed. The homogenate was passed through a 10mL syringe containing a sterile filter (consisting of a pinch of glasswool, wrapped in Miracloth and autoclaved) sitting in a sterile 50mL centrifuge tube by centrifugation at 100x g at 4°C for 10 minutes. The eluate was resuspended in 30mL of cold (-20°C) 100% ethanol by inversion and stored overnight at -20°C to allow nucleic acid precipitation. The suspension was centrifuged at 2,500x g for 20 minutes at 4°C. The pellet was air-dried for 5 minutes before resuspension in 10mL of cold (-20°C) 70% (v/v) ethanol. Homogenate was centrifuged at 1,250x g for 5 minutes at 4°C and the resultant pellet air-dried. The dried pellet then underwent RNA purification using the RNeasy Mini kit (Qiagen, Australia) and DNase treatment using SUPERase-In (Ambion, Europe) according to the manufacturer's instructions.

RNA quality was assessed by visual observation of intact ribosomal bands after treatment with a denaturing formaldehyde dye following gel electrophoresis. In addition, spectrophotometric parameters were recorded, and for the RNA to be acceptable for further use, a 260/280nm ratio >2.0 and 260/230nm ratio >1.4 was required. RNA that did not meet these conditions were re-precipitated as per Davies and Robinson (1996).

2.6 cDNA Synthesis via Reverse Transcription

RNA extracted from berry tissue was reverse transcribed using SuperScript[®] III Reverse Transcriptase and Oligo(dT)₂₀ primer (Invitrogen, USA). The standard cycle consisted of 65°C for 5 minutes, ice for 1 minute, 50°C for 50 minutes, 85°C for 5 minutes. The sample was additionally treated with 2 units RNase H (Invitrogen, USA) at 37°C for 20 minutes. The process was conducted in a Bio-Rad MyCycler thermocycler (Bio-Rad, USA).

2.7 Gene Expression Analysis via Quantitative Real Time Polymerase Chain Reaction

The Quantitative Real Time Polymerase Chain Reaction (QRT-PCR) reactions were conducted on a fee-basis by the South Australian Research and Development Institute (SARDI). Data analysis was conducted as part of the thesis work and is described in Chapters 5 and 6.

QRT-PCR was performed using an ABI HT7900 Fast Real Time PCR System with results analysed using Sequence Detection System version 2.3 software (Applied Biosystems, USA). QRT-PCR was conducted utilising the Universal Probe Library (Roche, Germany) in conjunction with gene specific primers (Table 2.1). The probes are labelled at the 5' end with fluorescein (FAM) and at the 3' end with a dark quencher dye. The sample reaction contained 0.9µM (final) primer, 0.2pmol (final) probe, 50ng (final) cDNA and 1x FastStart Universal Probe Master Mix to a final volume of 16µL.

The cycling conditions used were: 95°C for 10 minutes, 95°C for 15 seconds, 57°C for 1 minute. Steps 2-3 were cycled 45 times. Quantification was achieved via a standard curve of known concentration samples (1, 10⁻², 10⁻⁴, 10⁻⁵, 10⁻⁶, 10⁻⁷, 10⁻⁸, 10⁻⁹ femtomole). Normalisation was performed using reference genes Ankyrin (ANK) and Ubiquitin (Ubq).

Table 2.1: Gene specific primer/probe combinations for use in QRT-PCR against berry-derived template cDNA. Primers were designed via the Universal Probe Library Assay Design Centre: ProbeFinder version 2.45 database (www.rocche-applied-science.com) and ordered through GeneWorks Pty Ltd (Australia). L-IdnDH.1 and L-IdnDH.2 primers designed by MA Hayes (personal communication) and reference primers Ankyrin and Ubiquitin were designed by Sweetman (2011). All primers are non-degenerate.

	Target Gene	Forward Primer 5'→3'	Reverse Primer 5'→3'	Probe	Amplicon Length (nt)	Intron Spanning
Reference	Ankyrin	GGTTATGGCAGGAAGGAGTG	GGTGTCTTGCCATCCATGTT	120	83	Yes
	Ubiquitin	GTGGCCACAGCAACCAGT	GCAACCTCCAATCCAGTCAT	143	64	Yes
Candidate	TC58004	GGACGTATCGATGCTTTGCT	GAGTATTATTCATTCTCCTCAGA	82	91	Yes
	TC55097	CTATGTATGGAGTGACAAAAACAGC	TGTCTGGGCCCATCTCAG	117	72	Yes
	TC61548	GATCGTGGTACCTCACATTGC	CCAATGTAGCCATTCCTTCG	38	62	Yes
	TC59682	GACAAGATCGATTTGGTGAGG	CATCCGGAGTGTTCGTAACC	133	61	No
	TC55752	CCAAGCTATGACCCCTCATATT	CCTTCACTCCAGCTGCGTAT	157	71	Yes
	L-IdnDH.1	GAAGTTTTTTGGATCTCCTCCACCCAA	GCATGGATGCCGACACTGAGC	12	141	Yes
	L-IdnDH.2	TGGCAAAGTTTGTCTCGTGGGGA	CATATCGGCCATGTGTTCTTGAC	18	121	Yes

2.8 Genomic DNA Extraction from Young Leaf Tissue

Genomic DNA (gDNA) was extracted from young leaf tissue of grapevine species *V. vinifera* cv Pinot Noir, *A. aconitifolia*, *A. brevipedunculata* and *P. henryana* as described in Kim *et al.* (1997). Additional gDNA samples were obtained from Dr Tricia Franks (University of Adelaide, *V. vinifera* cv Chardonnay and Riesling).

0.25g of young leaf material was ground under LN in a 1.5mL centrifuge tube with 5µL of 1% (v/v) BME. 300µL of Extraction Buffer (25mM EDTA, 200mM Tris-HCl pH 8.0, 250mM NaCl, 0.5% (w/v) SDS) was added, mixed by vortex and incubated at room temperature for 1 hour. 6% (w/v final) soluble PVP-10 and 0.5 volumes of 7.5M ammonium acetate were added and the sample incubated on ice for 30 minutes. The homogenate was centrifuged at 10,000x g for 10 minutes at 4°C and the supernatant transferred to a fresh tube. The gDNA was precipitated via the addition of 1 volume of chilled (-20°C) isopropanol and incubated at -20°C for 30 minutes. The sample was centrifuged as previously described, the supernatant discarded and the gDNA pellet vacuum dried. The pellet was resuspended in 500µL of TE Buffer (10mM Tris, 0.1mM EDTA, pH adjust to 8.0 with HCl and autoclave). The extract was treated with 2µL of 1mg/ml RNase A (Sigma-Aldrich, USA) and incubated at 37°C for 15 minutes. One volume of chloroform:isoamyl alcohol (24:1) was added, inverted to mix and the extract centrifuged at 10,000x g for 5 minutes at 4°C. The upper layer of supernatant was transferred to a fresh 1.5mL centrifuge tube and 1 volume chilled isopropanol added. The extract was incubated at 20°C for 10 minutes and centrifuged at 10,000x g for 10 minutes at 4°C. The supernatant was discarded and the pellet washed with 100µL 80% ethanol and vacuum dried. The pellet was resuspended in 30µL TE and quantified spectrophotometrically at 260nm with quality ascertained from 260/280nm ratios.

2.9 Enzyme Extraction from Berry Tissue

Enzymes were extracted from ground berry tissue as described in Sweetman (2011).

1g of berry tissue was ground under LN and transferred to a pre-cooled 50mL centrifuge tube. Extraction Buffer (0.5M Tris-HCl pH 8.5, 10mM EDTA, 5mM dithiothreitol (DTT), 6.2mM L-cysteine hydrochloride, 7mM sodium diethyldithiocarbamate trihydrate (DEDTC), 1mM phenylmethanesulfonyl fluoride (PMSF), 1mM 4-aminobenzamidine dihydrochloride, 2% (w/v) PVPP, 8% (w/v) PEG-4000) was added to a final volume of 12mL. The pH of each extracts was checked to ensure remained higher than 7.0, and adjusted as required. Extracts were incubated at 4°C for 15 minutes with occasional mixing. Extracts were centrifuged at 1,000x g for 2 minutes at 4°C. The supernatant was transferred to a fresh tube and 65% final PEG-4000 added and mixed on a shaking platform on medium speed at 4°C for 60 minutes until all PEG-4000 dissolved. Extracts were centrifuged at 30,000x g for 15 minutes at 4°C and pellet resuspended in 500µL of Resuspension Buffer (5mM Tris-HCl pH 7.0, 10mM EDTA, 5mM DTT, 1mM PMSF, 1mM 4-aminobenzamidine dihydrochloride, 3% (v/v) Triton X-100), adjusted to a final volume of 2mL. The activity of the extracted enzymes was immediately assayed as described in section 2.16.

0.5mM potassium cyanide (KCN) and 0.5µM octyl gallate (OG) were added to the assay buffer to inhibit the activity of enzymes involved in cellular respiration. KCN inhibits cytochrome oxidase (Baker *et al.*, 1987) and OG inhibits alternative oxidase (Albury *et al.*, 1996) of the electron transport/respiratory chain.

2.10 Bioinformatics

The grapevine genome sequences for *V. vinifera* cv Pinot Noir (Troggio *et al.*, 2007, Velasco *et al.*, 2007) and the Pinot Noir derived PN40024 (The French–Italian Public Consortium for Grapevine Genome Characterization, 2007) were accessed using The Gene Index Project: Gene Indices: Grape database on the Computation Biology and Functional Genomics Laboratory website (www.compbio.dfci.harvard.edu/tgi). The aforementioned database was also utilised for EST library analysis. Basic Local Alignment Search Tools (BLAST; Altschul *et al.*, 1990) including BLASTn, BLASTx and tBLASTn were performed using the National Centre for Biotechnology Information (NCBI) database (www.ncbi.nlm.nih.gov). Protein domain and motif analysis was performed using InterProScan (www.ebi.ac.uk/tools/interproscan) and the Centre

for Biological Sequence Analysis: CBS Prediction Servers (www.cbs.dtu.dk/serives). Sequence identities were determined using COBALT (Papadopoulos and Agarwala, 2007) alignments analysed using GeneDoc software version 2.7.000 (Nicholas and Nicholas, 1997).

2.11 Polymerase Chain Reaction

All Polymerase Chain Reactions (PCR) were conducted in a Bio-Rad MyCycler thermocycler (Bio-Rad, USA). Volumes of PCR reactions varied from 20 μ L-50 μ L in 0.2mL clear flat-cap tubes (Adelab, Australia). Bioline (Australia) reagents were used unless otherwise stated.

A standard PCR reaction (20 μ l) contained: 1x PCR Buffer, 1 unit Taq DNA Polymerase, 0.25mM dNTP, 0.3mM forward and reverse primers (GeneWorks, Australia), 2mM MgCl₂, varying concentration of template DNA and HPLC molecular grade water (Sigma-Aldrich, USA). Standard (Mango Taq, GoTaq Flexi, (Promega, USA)) and Hi-fidelity (Platinum Taq (Invitrogen)) Taq DNA polymerase were used throughout this project.

The standard PCR cycle consisted of: 94°C for 2 minutes, 35 cycles of the following temperature programme: 94°C for 30 seconds, 60°C for 30 seconds, 72°C for 1 minute, with a final extension step of 72°C for 4 minutes. PCR reactions were visualised by gel electrophoresis. Optimisation occurred with respect to the following parameters: the annealing temperature of the primer pair (T_{anneal}), MgCl₂ concentration, primer concentration and number of cycles with both standard and Hi-fidelity Taq DNA polymerase, to ensure amplification of a single PCR product without primer dimerisation.

All primers (Table 2.2) used were supplied by GeneWorks Pty Ltd (Australia) with the exception of the pDRIVE sequencing primer M13 purchased from QIAGEN (Australia) and the pET sequencing primer T7r purchased from Novagen (Germany). The melting temperature, T_m , for each primer was calculated using the oligonucleotide properties calculator OligoCalc (<http://www.basic.northwestern.edu/biotools/oligocalc.html>).

Agarose gel electrophoresis was performed essentially as described by Sambrook (1989).

Standard gel electrophoresis was performed using 1-1.5% (w/v) analytical grade agarose in 1x TAE buffer (40mM Tris, 1mM EDTA pH 8, 0.1% (v/v) glacial acetic acid). Loaded samples were mixed with DNA loading buffer (Promega) as required.

Staining of DNA was achieved using a 0.01% (v/v) ethidium bromide soak (15 minutes following electrophoresis), or by the use of 0.005% (v/v) GelRed nucleic acid stain (Biotium, USA) added to the molten agarose before gel casting. Visualisation of the stained gels was achieved under ultra violet light on a Fusion SL-3500.wl gel image system utilising Fusion version 15.11 software (Fisher Biotech, USA).

Table 2.2: Primers used in the amplification of a full length clone (FLC) from cDNA and fragment from gDNA (G) templates for each candidate gene grouped in relation to the homologue of interest. Restriction sites NdeI (Forward primer) and BamHI (Reverse primer) were incorporated in the primers as indicated in bold and ordered through GeneWorks Pty Ltd (Australia). pDRIVE sequencing primers were purchased from QIAGEN (Australia) and pET sequencing primer T7r purchased from Novagen (Germany). All primers are non-degenerate.

Candidate		Forward Primer 5'→3'	Reverse Primer 5'→3'	Amplicon (nt)
2 Ketogluconate Reductase				
TC55752	FLC	CTACATATGATGGCGATGATGAAGCGAGTTGCTGAG	CCAGGATCCTTACTGGTACTGGCTGCTAGTTGGCC	1150
	G	AAAGCACATTCCCGACCTCCATGTTCTCATATCTACCCC	GGGAAGCATCACATCAACATCCTCTTCAAACCTTGCTCC	487
TC61548	FLC	CTACATATGATGGCTGTTGGATAACAATGTTGA	CCAGGATCCTTAGATGAAAAGCCAGTGTGAACAAGATGG	994
	G	GTTTGCCTGTTTCAAAGCTATGAGCAGGAGGGG	FLC Primer	132
TC59682	FLC	CTACATATGACCAGCGAAGTCCCCAAAGATATCGGA	CCAGGATCCTTAAACCACTGGAGTTAACAGTGGTTGTTTCAG	1055
	G	FLC Primer	CCTCACAAATCGATCTTGTCCAACCCAACGC	369
Gluconate 5 Dehydrogenase				
TC58004	FLC	CTACATATGGGTCGCGAACCACCTCGA	CCAGGATCCTTACATGATGAATAACCCAAGAAAACC	893
	G	FLC Primer	CTCTAATGCCCGCATTATTTAGCAAAGCATCGATACGTC	292
TC55097	FLC	CTACATATGATGGAGAAGATCGGAAAGAGATTTCAAGGG	CCAGGATCCCTAGAGTCTAGAAGGTATTCCACCAGC	760
	G	AGAAGGACATTGAGGATAAACTCTACTCAACAGGCTTGG	FLC Primer	149
TC52437	FLC	CTACATATGATGGCTCAGACATGTGGGTTTCAGC	CCAGGATCCCTAGAACAGGTTTGGCTCAAAAACC	876
L-Idonate Dehydrogenase				
L-IdnDH.1	G	ATGGGGAAAGGAGGCAACTCTGAGG	CCCAGAGAAGGGAGAATGTAGGGTTG	125
L-IdnDH.2	G	GTTGTGCATCCTGCAGATCTATGCTTTAAACTG	CGGTAATCGTCTACATCCACAATGACAATTCTG	230
Vector Sequencing				
pET-14b	T7r		CCCTATAGTGAGTCGTATTA	
	T7r_upR		TCATGAGCCCGAAGTGG	
pDRIVE	M13	GTAAAACGACGGCCAGT	AACAGCTATGACCATG	

2.11.1 Nucleic Acid Sequencing

Sequencing of templates was performed by the Australian Genome Research Facility (AGRF).

Purified DNA samples were supplied according to AGRF requirements. Double stranded plasmids were supplied at between 600-1500ng with 9.6pmol of appropriate primer. PCR products were supplied as recommended by length (bp) of template with 9.6pmol of appropriate primer. The cycling conditions used to determine sequence information include: 96°C for two minutes, 96°C for ten seconds, 50°C for five seconds, 60°C for four minutes. Steps 2-4 were cycled thirty times. Primers used are listed in Table 2.2.

2.12 Construction of Candidate Cassette for Protein Expression

PCR products were purified using the Wizard[®] SV minipreps DNA Purification System (Promega, USA) as per the manufacturer's centrifugation protocol.

2.12.1 Restriction Digest of Template

Restriction digests were performed over a range of volumes from 10µL-50µL. Restriction enzymes (RE) used (NdeI and BamHI) were supplied from New England Biolabs (USA) and used in conjunction with the compatible buffer. Concentrations of 1 unit/µg DNA of RE were used in 10x RE buffer. A 10x volume of 1mg/ml Bovine Serum Albumin (BSA) was also added to each digest reaction which was conducted at 37°C for 3 hours. Digest was confirmed via 1% agarose gel electrophoresis.

2.12.2 Ligation of Candidate Open Reading Frame into Vector

2.12.2.1 pDRIVE Vector

Template DNA was ligated into the pDRIVE (Qiagen, Australia) vector using the PCR Cloning Kit (Qiagen, Australia) as per manufacturer's instructions.

25ng of pDRIVE cloning vector, 2µL purified PCR product and 1x ligation master mix were added to a flat-top PCR tube and incubated at 16°C for 2 hours. Ligation mixture was then used for transformation of *E. coli*.

2.12.2.2 pET-14b Vector

100-200ng of purified restriction digested PCR product, 50ng digested pET-14b vector (Novagen, Germany), 1x T4 DNA ligase (New England Biolabs, USA) and 1x ligation buffer were added to a 0.2mL flap-top tube and incubated overnight at 16°C. Mixture was incubated at 65°C for 10 minutes to inactivate the ligase. Ligation mixture was then used for transformation of *E. coli*.

2.12.3 Transformation of Vector + Cassette into *E. coli*

E. coli strain DH5α (Sigma-Aldrich, USA) was used for cloning and BI21 (DE3) pLysS-T1^R (Sigma-Aldrich, USA) used for protein expression.

5µL of ligation mixture was added directly into the centre of a 50µL sample of the desired competent cell line and incubated on ice for 5 minutes. The mixture was then incubated in a water bath for 45 seconds at 42°C, 250µL of pre-warmed SOC Media (solution 1 (autoclave); 2% (w/v) tryptone, 0.5% (w/v) yeast extract, 10mM NaCl, 2.5mM KCl. Solution 2 (filter); 10mM MgCl₂, 10mM MgSO₄, 20mM D-glucose. Combine solutions once cooled) added and incubated at 37°C for 1 hour shaking at 225 rpm. Culture was then transferred to Luria-Bertani (LB) agar plates (with antibiotics as required) and incubated overnight at 37°C. Colonies were selected and PCR screened for positive transformants.

50µM isopropylthiogalactoside (IPTG) and 80µg/mL X-Gal were added to LB agar plates for blue-white screening of positive transformants incorporating pDRIVE + cassette.

2.13 Competent Cells for DNA Cloning and Protein Expression

E. coli strains DH5α and BI21 (DE3) pLysS-T1^R (Sigma-Aldrich, USA) were made chemically competent as described in Inoue *et al.* (1990).

250mL of SOB Media (2% (w/v) bacto tryptone, 0.5% (w/v) yeast extract, 10mM NaCl, autoclaved; 2.5mM KCl, 10mM MgCl₂, 10mM MgSO₄, filtered) was inoculated with a culture of the desired cell line grown overnight in LB Media (1% (w/v) bacto tryptone, 0.5% (w/v) yeast extract, 0.5% (w/v) NaCl, autoclaved). The culture was incubated on a shaking platform at 18°C until optical density at 600nm reached 0.6-0.7. The culture was transferred to a 300mL centrifuge bottle, incubated on ice for 10 minutes and centrifuged at 2500x g for 10 minutes at 4°C. The cells were resuspended in 80mL of Transformation Buffer (TrB; 10mM Pipes, 15mM CaCl₂, 250mM KCl, 55mM MnCl₂, pH to 6.7 with KOH, filter sterilised and cooled in -20°C) and incubated on ice for 10 minutes. Homogenate was centrifuged at 2500x g for 10 minutes at 4°C and pellet resuspended in 20mL of TrB. 7% (v/v final) of dimethyl sulfoxide (DMSO) was added and the solution incubated on ice for 10 minutes. The solution was dispensed into pre-cooled 1.5mL centrifuge tubes, snap frozen in LN and stored at -70°C.

2.14 Culture Media for Cell Growth and Protein Expression

Bacterial Strains were grown in sterile LB Media (1% (w/v) bacto tryptone, 0.5% (w/v) yeast extract, 0.5% (w/v) NaCl, autoclaved). 1.5% bacto agar was added as required.

Growth studies were conducted in M9 minimal media (2mM MgSO₄, 0.1mM CaCl₂, 20% (v/v) M9 salts [64g/L Na₂HPO₄·7H₂O, 15g/L KH₂PO₄, 2.5g/L NaCl, 5g/L NH₄Cl]) 0.4% (v/v final) carbon source was added as required.

Protein expression was conducted in sterile Terrific Broth (TB; solution 1 (900ml); 4ml glycerol, 12g bacto tryptone, 24g bacto yeast extract. Solution 2 (100ml); 0.17M KH₂PO₄, 0.72M K₂HPO₄·3H₂O. Autoclave solutions separately, combine once cooled.

Antibiotics were added as required including ampicillin (sodium salt; 100µg/mL), chloramphenicol (34µg/mL), and kanamycin (sulphate; 15µg/mL).

2.15 Expression, Extraction and Purification of Recombinant Protein

1L of TB (with antibiotics as appropriate) was inoculated with 1mL of an overnight culture of *E. coli* BL21 pLysS cells transformed with the recombinant construct and incubated on a shaking platform at 180 rpm at 37°C until the optical density at 600nm reached 0.6-0.7. Isopropylthiogalactoside (IPTG; 0.1-0.4mM final) was added to the culture to induce protein expression. The culture was continuously shaken at 180 rpm on a platform shaker at a constant temperature (18-37°C) for the duration found optimal (3-48 hours). Cells were harvested by centrifugation at 3000x g for 5 minutes at 4°C and the pellet stored at -70°C until required.

1mL samples of pre- and post-induction cell culture were transferred to a 1.5mL centrifuge tube and centrifuged at max speed for 5 minutes. The pellet was then dried and stored at -20°C until required.

2.15.1 Extraction of Soluble Recombinant Protein

2.15.1.1 Standard Extraction

Pelleted cell culture was thawed on ice and resuspended in 4mL/g wet cell paste Modified Sonication Buffer (MSB; 20mM Tris-HCl pH 8.0, 500mM NaCl, 10% (v/v) glycerol, 0.5% (v/v) Tween 20, 3mM imidazole, 1mM BME). The cell paste was then freeze/thawed via immersion in LN for 30 seconds and room temperature water until thawed, repeated 4 times. 1/10 volume of reconstituted complete mini EDTA-free cocktail protease inhibitor (Roche, Germany) and a level microspatula of DNase 1 (Sigma-Aldrich, USA) was added and tubes inverted. The cell paste was then drawn up and expelled through a polyethylene syringe fitted with a 20 gauge needle to ensure cell lysis, repeated 10 times. Tubes were then spun on a rotating wheel mixer for 30 minutes at 4°C, the centrifuged at 10,000x g for 30 minutes at 4°C. The supernatant (soluble fraction) was aliquoted into 1.5mL centrifuge tubes and stored at -70°C until required. The pellet (insoluble fraction) was transferred into a 1.5mL centrifuge tube and stored at -20°C.

2.15.1.2 Cell Lysis and Extraction of Soluble Proteins using BugBuster™

Pelleted cell culture was thawed on ice and resuspended in 5mL/g wet cell paste BugBuster™ Master Mix (Novagen, Germany). 1/10 volume reconstituted complete mini EDTA-free cocktail protease inhibitor (Roche, Germany) was added and the homogenate spun on a rotating wheel mixer at a slow setting for 20 minutes at room temperature. Tubes were centrifuged at 16,000x *g* for 20 minutes at 4°C. The supernatant (soluble fraction) was aliquoted into 1.5mL centrifuge tubes and stored at -70°C until required. The pellet (insoluble fraction) was transferred into a 1.5mL centrifuge tube and stored at -20°C.

2.15.2 Protein Purification via Immobilized Metal Affinity Chromatography

Bulk protein was purified at room temperature using a Bio-Rad Biologic LP system fitted with a Bio-Rad Biofrac Fraction Collector. A 10 x 100mm glass Pharmacia Biotech (USA) was packed with 9mL of cobalt-based TALON (Clontech, USA) resin. Flow-rate was a constant 1mL/minute. Resin was equilibrated in 5 bed volumes MSB. The soluble fraction was then passed through the column. A minimum of 10 bed volumes of Modified Wash Buffer (MWB; 20mM Tris-HCl pH 8.0, 500mM NaCl, 10% (v/v) glycerol, 0.5% (v/v) Tween20, 10mM imidazole, 1mM BME) was then passed through the column removing any unbound proteins. The wash phase was monitored spectrophotometrically using LP Data View Software v1.03 to ensure all unbound proteins had been removed. Bound proteins were then eluted using Modified Elution Buffer (MEB; 20mM Tris-HCl pH 8.0, 500mM NaCl, 10% (v/v) glycerol, 0.5% (v/v) Tween20, 200mM imidazole, 1mM BME) and collected in 1-2mL fractions.

A plastic mini gravity-fed column (Bio-Rad, USA) was also used to test purification at 4°C following the same protocol.

2.15.3 Confirmation of Protein Purity via Sodium Dodecyl Sulphate Polyacrylamide Gel Electrophoresis

Sodium Dodecyl Sulphate Polyacrylamide Gel Electrophoresis (SDS-PAGE) gels consisted of 3mL of 5% Stacking Gel (5% (v/v) T Acrylamide:bis-acrylamide, 0.125M Tris-HCl pH 8.8, 0.1% (w/v) SDS, 0.05% ammonium persulphate, 0.03% N,N,N',N'-Tetramethylethylenediamine (TEMED)) atop 6mL of 12% Resolving Gel (12% (v/v) T Acrylamide:bis-acrylamide, 0.75M tris-HCl pH 8.8, 0.1% (w/v) SDS, 0.05% ammonium persulphate, 0.03% TEMED).

5 μ L of Sample buffer (100mM DTT, 2% (w/v) SDS, 8% (v/v) glycerol, 60mM tris-HCl pH 6.8, 0.1% (w/v) bromophenol blue) was mixed with 20 μ L of each purified fraction and boiled for 5 minutes. Sample was then loaded into a SDS-PAGE Bio-Rad apparatus, using SDS-PAGE Running Buffer (50mM Tris, 150mM Glycine, 0.1% (w/v) SDS) as per manufacturer's instructions and run at 180 volts for 45 minutes. Gels were removed and immersed in 50mL of Coomassie Blue stain (40% (v/v) ethanol, 7% glacial acetic acid, 0.1% (w/v) Coomassie Blue R250) and heated on high using a Sharp Carousel microwave for 50 seconds. Excess Coomassie Blue stain was then removed at the gel immersed in 50mL of Coomassie Blue destain (20% (v/v) ethanol, 7% (v/v) glacial acetic acid) and heated as previously described. The gel was then incubated overnight on a platform mixer at low speed with fresh Coomassie Blue destain as required until all Coomassie Blue removed.

Proteins were visualised using Fusion SL-3500.wl gel image system utilising Fusion version 15.11 software (Fisher Biotech, USA). Proteins were quantified as required using a NanoDrop ND-1000 spectrophotometer (Thermo Scientific, USA).

2.16 Kinetic Parameters of Enzyme Activity

Enzyme activity was monitored at 340nm using a FLUOstar Omega spectrophotometer (with pathlength correction activated) with Omega software version 1.02 (BMG Labtech, Germany) for oxidation or reduction of the coenzyme NAD(P)H. Various conditions including temperature, buffer pH, substrate and coenzyme concentration (mM) were tested. The pH range tested was

covered by multiple buffers to ensure changes in activity were due to pH and not interaction with the solutes of the differing buffers.

A bulk reagent mix comprising purified enzyme (0.1-10 μ g), buffer (40-100mM), coenzyme, 1.7mM MgCl (as required), to a total reaction volume of 200 μ L, was dispensed into a 96 well flat-bottom UV plate (Costar, USA) in triplicate and equilibrated to the assay running temperature for 5-15 minutes. The desired substrate was added to each well to ensure activity was substrate dependent. The reaction was monitored for 40 minutes with absorbance readings taken every 60-90 seconds. Negative controls used included no enzyme (NoE), no substrate (NoS), no coenzyme (NoC), protein extraction buffer substituted for purified enzyme (PEB), plus a positive control of malic dehydrogenase (Sigma-Aldrich, USA).

Data was analysed using MARS Data Analysis Software and GraphPad Prism version 5.03.

2.17 Calculation of Enzyme Activity

The initial rate of enzyme activity was calculated using a modified Beer-Lambert formula;

$$\left[\left(\frac{\text{Slope}}{\text{Extinction Coefficient} * \text{Pathlength}} \right) \times 1000 \right] \times \frac{\text{Dilution Factor}}{\text{mg/mL Protein}} = \mu\text{moles/min/mg protein}$$

The molar extinction coefficient of NAD(P)H used was 6200 M⁻¹ cm⁻¹ at 340nm.

2.18 Liquid Chromatography Mass Spectrometry

The identification of compounds produced by enzymatic reactions was performed by Flinders Analytical (Flinders University, Australia) using a Waters 2695 HPLC with dual wavelength UV detection coupled to a triple quadrupole mass spectrometer (<http://www.flinders.edu.au/research/flinders-laboratories/flinders-analytical/>).

Chapter 3:

Identification and Bioinformatic Analysis of Candidate Genes Encoding Enzymes Involved in Tartaric Acid Biosynthesis

3.1 Introduction

Model plant systems used for high-throughput analysis include *Arabidopsis thaliana*, maize (*Zea mays*) and rice (*Oryza sativa*), species with small genomes, rapid generation times and ease of cultivation in controlled environments. Unfortunately the grapevine, a globally significant horticultural crop, does not meet these requirements. Physiological constraints including vineyard space requirements, an annual reproductive cycle and long generation time limit the use of the grapevine in genetic studies (Chaïb *et al.*, 2010). The successful mapping of the *V. vinifera* genome using Expressed Sequence Tags (EST) and Contigs (Assembled EST's) is enabling researchers to overcome this problem (Iandolino *et al.*, 2004, The French–Italian Public Consortium for Grapevine Genome Characterization, 2007, Troggio *et al.*, 2007, Velasco *et al.*, 2007). The grapevine is Australia's seventh largest economically important agricultural commodity, responsible for the production of food-stuffs including table grapes, sultanas, juice and wine (Australian Bureau of Statistics, 2010). With many parts of the world experiencing changing climates and water deficiencies, interest in the mechanism of fruit development and stress response is increasing. Although much of the genome still requires annotation, the public accessibility of data in databases such as NCBI (www.ncbi.nlm.nih.gov) and Grape Indices (www.compbio.dfci.harvard.edu/tgi) is enabling the identification of genes involved in grapevine development, metabolism and water stress. Bioinformatics enables the identification of putative homologue proteins based on characteristics previously identified in other systems. Additional work is then required to confirm the protein's function within the system of interest. This chapter describes the use of such tools in the identification of candidate proteins for the inclusion in the primary Asc-precursor and secondary glucose-precursor TA biosynthetic pathway's.

As previously discussed in Chapter 1 (section 1.6) bacteria possess enzymes capable of catalysing reactions comparative to those of the TA biosynthetic pathway. Extensive work has been conducted into these reactions in their bacterial systems, knowledge which can be applied to other systems via bioinformatics. Unfortunately, the nomenclature of these enzymes is inconsistent throughout the

literature (Table 1.1). Of interest in this study are the enzymes 2-ketogluconate reductase (2KGR) and gluconate-5 dehydrogenase (G5Dh). These enzymes are described as responsible for the catalysis of 2-keto-L-gulonic acid (2KGA) → L-idonic acid (IA) and D-gluconic acid (GA) → 5-keto-D-gluconic acid (5KGA) respectively. 2KGR and G5Dh have also been identified as responsible for the catalysis of additional reactions with slight variance in the specific product or substrate involved (Table 1.2. and 1.3 respectively). Recently a G5Dh in *Gluconobacter oxydans* (Merfort *et al.*, 2006a) and a 2KGR in *Escherichia coli* (Yum *et al.*, 1998a) have been identified. These enzymes catalyse reactions within their respective systems identical to those described in TA biosynthesis. Enzymatic characterisation of 2KGR in *E. coli* confirmed its catalytic activity in the reduction of 2KGA to IA (Yum *et al.*, 1998a), whereas the accumulation of downstream products in over-expression lines of *G. oxydans* confirmed G5Dh catalysis of GA to 5KGA (Merfort *et al.*, 2006a).

This chapter will focus on the identification of putative homologues of the identified bacterial enzymes in *V. vinifera*. 2KGR and G5Dh have yet to be identified in plant tissue. Comparative analysis with bacterial enzymes has been used to identify genes of interest based upon sequence similarity to the bacterial gene of confirmed enzymatic activity. The PLEX database (<http://www.plexdb.org>) facilitates the comparative analysis of gene expression across multiple plant species and large-scale data sets (Wise *et al.*, 2007). The PLEX database compiles gene expression data from a multitude of microarray experiments from plant systems including Arabidopsis, barley, citrus, cotton, grape, maize, Medicago, poplar, rice, soybean, sugarcane, tomato, wheat (Wise *et al.*, 2007). Microarray data has been used primarily in the identification and expression analysis of candidate genes in previous studies in *V. vinifera* (Cramer *et al.*, 2007, DeBolt, 2006, Deluc *et al.*, 2007, Grimplet *et al.*, 2007, Lund *et al.*, 2008, Pilati *et al.*, 2007). Although not utilised as the primary source of candidate identification in this study, QRT-PCR of a developmental grape series has been used to support the role of the identified candidates' involvement in the TA biosynthetic pathway (Chapter 5). Sequencing of the grape transcriptome (Goes da Silva *et al.*, 2005, Iandolino *et al.*, 2004, Terrier *et al.*, 2001) has enabled deeper investigations into the genetic workings of *V. vinifera*. The isolation of

tissue specific transcripts provides direct evidence for their inclusion in tissue specific processes. Unfortunately, current library descriptors include ‘immature’, ‘pre-véraison’, or ‘green hard berries’. A complete developmental series at defined timepoints over development would be highly beneficial in the identification of TA biosynthetic genes. As yet this is not available, therefore a structured sampling process and analysis focusing on the individual genes of interest is required to gain a complete understanding of the role of the candidate genes over berry development.

3.2 Results

3.2.1 Identification and Bioinformatic Analysis of Candidate Genes

Involved in Tartaric Acid Biosynthesis

Investigations into the reactions of the TA biosynthetic pathway identified enzymes of bacterial origin responsible for catalysing identical reactions within their native system. In this study, enzymes responsible for steps 2a and 2b (Figure 1.8) of the primary and secondary TA biosynthetic pathway were investigated. The enzymes capable of performing step 2a of the primary-Asc precursor pathway are denoted 2-ketogluconate reductases (2KGR). The enzymes identified as capable of catalysing step 2b of the secondary glucose-precursor pathway are denoted gluconate-5 dehydrogenases (G5Dh). One protein corresponding to each desired activity was identified in *Escherichia coli* (Blattner *et al.*, 1997, Sofia *et al.*, 1994) and *Gluconobacter oxydans* (Klasen *et al.*, 1995, Prust *et al.*, 2005) respectively (Figure 3.1). The identification of the *E. coli* 2KGR (NCBI Accession P37666) resulted from the purification of the gene product from region 80.1 min (gene *yiaE*) on the *E. coli* chromosome. Kinetic analysis showed the enzyme capable of catalysing multiple reactions including the reduction of 2KGA to IA. Further support was provided with the deletion of this gene resulting in the loss of 2KGR activity (Yum *et al.*, 1998a). The activity of G5Dh from *G. oxydans* (NCBI Accession P50199) was confirmed through the accumulation of products in over-expression lines (Merfort *et al.*, 2006a, Merfort *et al.*, 2006b).

- A) MKPSVILYKALPDDLLQRLQEHFTVHQVANLSPQTVEQNAAIFAEAEGLLSNENVNAAAL
LEKMPKLRATSTISVGYDNFDVDALTARKILLMHTPTVLTETVADTLMALVLTARRVVE
VAERVKAGEWTASIGPDWYGTDVHKKTLGIVGMGRIGMALAQRAHFNFNPILYNARRH
HKEAEERFNARYCDLDTLLQESDFVCLILPLTDETHHLFGAEQFAKMKSSAIFINAGRGPVV
DENALIAALQKGEIHAAGLDVFEQEPLSVDSPLLSMANVVAVPHIGSATHETRYGMAACA
VDNLIDALQGKVEKNCVNPVAD
- B) MSHPDLFSLSGARALVTGASRGIGLTLAKGLARYGAEVVLNGRNAESLDSAQSGFEAEGL
KASTAVFDVTDQDAVIDGVAAIERDMGPIDILINNAGIQRRAPLEEF SRKDWDDL MSTNVN
AVFFVGQAVARHMIPRGRGKIVNICSVQSELARPGIAPYTATKGA VKNLTKGMATDWGRH
GLQINGLAPGYFATEMTERLVADEEFTDWLCKRTPAGRWGQVEELVGA AVFLSSRASSFV
NGQVLMVDGGITVSL

Figure 3.1: Deduced amino acid sequences of the identified bacterial enzymes A) 2-ketogluconate reductase (NCBI Accession P37666) from *Escherichia coli*. B) Gluconate 5-dehydrogenase from *Gluconobacter oxydans* (NCBI Accession P50199).

A tBLASTn search (Gish and States, 1993) was performed against the Gene Index Project: Gene Indices: Grape database on the Computation Biology and Functional Genomics Laboratory website (www.compbio.dfci.harvard.edu/tgi) using P37666 of *E. coli* and P50199 of *G. oxydans* to identify homologues in the *V. vinifera* genome. 9 TC (tentative consensus sequence, aligned EST's forming a putative gene) sequences were identified within the grapevine genome in relation to P37666 (Table 3.1) and 18 TC sequences in relation to P50199 (Table 3.2). The libraries from which the EST sequences were identified were also recorded to aid in the identification of an enzyme involved in the TA biosynthetic pathway. Three candidate homologues for each enzyme were selected based upon selection criteria including: tBLASTn rank, EST library location, % similarity to bacterial enzyme (Tables 3.1 and 3.2) and the possession of conserved residues, family signatures and cofactor binding domains (Tables 3.3 and 3.4).

Table 3.1: Results of a tBLASTn search of *E. coli* P37666 against the *V. vinifera* genome. The libraries the EST's were identified in are summarised with the 'Other' category representing petiole, stem, root, flower and leaf tissue. The shaded sequences indicate those selected for further analysis (see Chapter 4) based upon selected criteria including: EST library location and the presence of catalytic/binding domains and conserved residues (Table 3.3). Percent identity calculated at the amino acid level.

Contig	Preliminary Annotation	EST Libraries		E Value	Identity (%)
		Berry	Other		
TC59682	Hydroxyphenylpyruvate	5	8	3.0e-35	37
TC61548	Hydroxypyruvate reductase	5	1	1.3e-29	33
TC66090	Oxidoreductase (<i>A. thaliana</i>)	2	2	1.2e-25	29
TC57226	Hydroxypyruvate reductase	2	9	1.6e-23	19
TC55752	Formate dehydrogenase	24	15	1.1e-22	28
TC70223	Oxidoreductase (<i>A. thaliana</i>)	2		4.8e-22	32
TC65273	Oxidoreductase (<i>A. thaliana</i>)	7	2	4.9e-22	32
TC54577	Hydroxypyruvate reductase	2		4.9e-14	39
TC70044	Hydroxypyruvate reductase	2	13	8.6e-08	35

Table 3.2: Results of a tBLASTn of *G. oxydans* P50199 against the *V. vinifera* genome. The libraries the EST's were identified in are summarised with the 'Other' category representing petiole, stem, root, flower and leaf tissue. The shaded sequences indicate those selected for further analysis (see Chapter 4) based upon selected criteria including: EST library location and the presence of catalytic/binding domains and conserved residues (Table 3.4). Percent identity calculated at the amino acid level.

Contig	Preliminary Annotation	EST Libraries		E Value	Identity %
		Berry	Other		
TC55106	3-oxoacyl-[acyl-carrier-protein] reductase	2	7	6.4e-36	22
TC53716	Oxidoreductase (<i>A. thaliana</i>)	7	6	4.1e-34	25
TC52437	Oxidoreductase (<i>A. thaliana</i>)	7	33	1.8e-33	27
TC64853	Oxidoreductase (<i>A. thaliana</i>)		2	3.8e-33	26
TC68844	Oxidoreductase (<i>A. thaliana</i>)		2	1.3e-31	29
TC58159	Oxidoreductase (<i>A. thaliana</i>)	3	2	1.0e-30	23
TC68502	3-oxoacyl-[acyl-carrier-protein] reductase	1	1	3.7e-28	32
TC55665	Oxidoreductase (<i>A. thaliana</i>)	1	2	1.5e-26	29
TC65709	Short-chain dehydrogenase/reductase	2	6	2.4e-24	28
TC55097	Short-chain alcohol dehydrogenase		5	7.5e-24	28
TC70734	Oxidoreductase (<i>A. thaliana</i>)	2		5.6e-23	29
TC58004	Dehydrogenase-like protein	43	1	7.3e-23	26
TC57281	Peroxisomal 2,4-dienoyl-CoA reductase	11	6	1.1e-22	22
TC66370	Oxidoreductase (<i>A. thaliana</i>)		2	2.7e-22	26
TC56205	Peroxisomal 2,4-dienoyl-CoA reductase	8	6	1.0e-18	23
TC53841	Short-chain alcohol dehydrogenase	19	2	1.2e-18	28
TC51869	Oxidoreductase (<i>A. thaliana</i>)	3		8.9e-18	22
TC54798	CPRD12 protein	7	1	2.7e-17	27

TA biosynthesis has been identified within berry tissue during the first phase of berry development denoted 'berry formation' (Saito and Kasai, 1968, Saito and Kasai, 1978). Therefore, the putative genes of interest are those identified in berry EST libraries. Table 3.1 summarises the *V. vinifera* homologues for 2KGR. TC59682 and TC61548 were shown to be the most similar to P37666 based on the tBLASTn ranking. Although preliminary annotation indicates TC55752 as a formate dehydrogenase, it has the highest number of EST's identified in berry libraries. Table 3.2 summarises the *V. vinifera* homologues for G5Dh. TC58004 has the highest number of EST's identified within berry EST libraries, yet it is ranked twelfth similar to P50199 based on the tBLASTn ranking. TC52437 is ranked third similar yet the majority of the putative genes EST's are located in

libraries other than berry. In both selections of *V. vinifera* candidate homologues additional analysis was required to select probable enzymes for further analysis.

Sequence analysis was conducted to identify signatures suggestive of each of the putative enzyme's catalytic activity and family in which it resides (Table 3.3 and Table 3.4). Reaction 2a of the Asc-precursor pathway involves the reduction of 2-keto-L-gulonate to L-idonate (Figure 1.8). This process is enzymatic and indicates a coenzyme such as NAD(P)H is required. The presence of a binding and/or catalytic region would be indicative of an enzyme capable of catalysing the reaction. Recognition of the presence of integrated domains (a structurally conserved feature related to protein activity sourced from multiple databases), family (diagnostic feature found in or related to regions indicative of a certain family of proteins) and conserved sites (a region of sequence identified to be highly conserved across a protein family) within the sequence was integral in the candidate selection process (Mulder and Apweiler, 2008).

Table 3.3: Summary of the integrated domains identified within *E. coli* P37666 and the *V. vinifera* homologues. Identification was conducted using the web-based program InterProScan (www.ebi.ac.uk/tools/interproscan). No family or conserved site signatures were identified in the amino acid sequences. The shaded sequences indicate those selected for further analysis (see Chapter 4) based upon selected criteria including: EST library location and the presence of catalytic/binding domains and conserved residues.

Name	Signature	P37666	TC59682	TC61548	TC66090	TC57226	TC55752	TC70223	TC65273	TC54577	TC70044
NAD(P)-Binding	G3DSA:3.40.50.720	Y	Y	Y			Y				
D-Isomer Specific 2-Hydroxyacid Dehydrogenase, Catalytic	2 Hacid Dh	Y	Y	Y	Y		Y	Y			Y
D-Isomer Specific 2-Hydroxyacid Dehydrogenase, NAD-Binding	2 Hacid Dh C	Y	Y	Y	Y	Y	Y	Y	Y	Y	Y
	D 2 Hydroxyacid Dh 1		Y	Y		Y	Y				Y
	D 2 Hydroxyacid Dh 2	Y					Y				
	D 2 Hydroxyacid Dh 3	Y					Y				

V. vinifera candidates TC59682, TC61548 and TC55752 show the presence of multiple signatures of NAD(P) binding domains congruent with the *E. coli* P37666 2KGR protein. The signature of a catalytic domain was also detected in these contigs. The domains detected are comparable to the *E. coli* P37666 sequence, suggesting the ability to catalyse a coenzyme dependent reaction. These candidates were therefore selected for *in vitro* activity analysis (see Chapter 4).

Reaction 2b of the secondary glucose-precursor pathway involves the oxidation of D-gluconic acid to 5-keto-D-gluconic acid (Figure 1.8). This enzymatic process indicates a coenzyme such as NAD(P)⁺ is required. Again, the presence of a binding and/or catalytic region would be indicative of an enzyme capable of catalysing this reaction.

Table 3.4: Summary of integrated family, domain and conserved site signatures within *G. oxydans* P50199 and the *V. vinifera* homologues. Identification was conducted using the web-based program InterProScan (www.ebi.ac.uk/tools/interproscan). The shaded sequences indicate those selected for further analysis (see Chapter 4) based upon selected criteria including: EST library location and the presence of catalytic/binding domains and conserved residues.

Name		Signature	P50199	TC55106	TC53716	TC52437	TC64853	TC68844	TC58159	TC68502	TC55665	TC65709	TC55097	TC70734	TC58004	TC57281	TC66370	TC56205	TC53841	TC51869	TC54798	
Family	Short Chain Dehydrogenase/Reductase SDR	SDR Family	Y	Y	Y	Y	Y	Y		Y	Y	Y	Y	Y	Y	Y		Y	Y		Y	
		Short Chain Dehydrogenase/Reductase Family Member	Y	Y	Y	Y	Y	Y	Y	Y	Y	Y	Y	Y	Y	Y	Y	Y	Y	Y	Y	Y
		ADH-Short	Y	Y	Y	Y	Y	Y	Y	Y	Y	Y	Y	Y	Y	Y	Y	Y	Y	Y		Y
		Glucose/Ribitol Dehydrogenase	GDHRDH	Y	Y	Y	Y	Y			Y	Y	Y	Y	Y	Y	Y	Y	Y	Y	Y	Y
		3-Oxoacyl-(Acyl Carrier Protein) Reductase	3-oxoacyl-[acyl-carrier-protein] reductase		Y						Y											
Domain	NAD(P)-Binding Domain	G3DSA:3.40.50.720	Y	Y	Y	Y	Y	Y	Y	Y	Y	Y	Y	Y	Y	Y	Y	Y	Y	Y	Y	
Conserved Site	Short-Chain Dehydrogenase/Reductase	ADH Short	Y	Y	Y	Y	Y	Y		Y	Y		Y		Y		Y		Y		Y	

Family signatures, coenzyme binding and conserved sites were identified (Zdobnov and Apweiler, 2001) based on the amino acid sequence of the contig (Table 3.4). Due to the high number of candidates identified from the *V. vinifera* genome (Table 3.2), candidates were selected based upon the presence of conserved sites and NAD(P) binding signatures, and the libraries from which the EST's were identified. Although TC55097 EST's were identified exclusively in other EST libraries, signatures congruent with the *G. oxydans* G5Dh protein were identified in this contig suggesting that the encoded protein has the capacity to catalyse the reaction. Therefore, the contigs selected for *in vitro* activity analysis (see Chapter 4) were TC52437, TC55097 and TC58004.

The nucleic and amino acid sequences of the selected contigs, *V. vinifera* TC59682, TC61548 and TC55752 for 2KGR and *V. vinifera* TC52437, TC55097 and TC58004 for G5Dh are listed in Figures 3.2 and 3.3 respectively. These sequences were obtained from the Gene Index Project: Gene Indices: Grape database and used for all bioinformatic analysis described within this section.

Figure 3.2: Nucleic (A) and amino (B) acid sequence of candidate proteins for a 2-ketogluconate reductase involved in the primary Asc-precursor pathway in *V. vinifera*. Blue and red bases indicate the start and stop codons of the open reading frame respectively. * denotes intron positions identified via the Spidey mRNA-genomic alignment program (www.ncbi.nlm.nih.gov/IEB/Research/Ostell/Spidey).

TC61548 **A** **ATGGCTGTTGGATACAACAATGTTGATGTGAATGCTGCTAATAAGTACGGTGTGCTGTTGG**
GAACACTCCA*GGAGTACTTACAGAGACTACAGCAGAGCTAGCAGCCTCACTTCTTATGGCA
GCTGCTCGAAGAATAGTTGAAGCAGACGAGTTTATGAGGGCAGGCTTATACAGCAGGATGGC
TTCTCATCT*GTTTGGGGAAATTTGCTCAGAGGACAGACTGTTGGTGTGATTGGAGCAGGT
CGTATTGGATCTGCGTATGCTAGAAATGATG*GTAGAAGGGTTCAAATGAACCTGATTTACT
ATGATCTGTACCAAGCCACACGCTGGAGAAGTTTGTACAG*CTTATGGTTCAGTTCCCTGAA
AGCCAGTGGTGAACAACCACTGACCTGGAAAAGAGCTGCAAGTATGGATGAGGTGCTCCGA
GAGGCTGATCTT*ATTAGTCTCCATCCAGTATTGGATAAGACCCTTATCATCTAGTCAACAA
GGAAAAGGCTCTCAATGATGAAGAAG*GAAGCGATCCTTATAAACTGCAGCAGAGGGCCTGT
GATTGATGAAGTAGCTTTGGTGGCACATCTGAAAGAGAACCCCATGTTTCCGAGTTGGACTTG
ATGTCTTTGAG*GATGAACCTTACATGAAACCTGGTCTTGTCTGAAATGAAGAACCGATCGT
GGTACCTCACATTGCTTCTGCTTCCAAG*TGGACTCGCGAAGGAATGGGTACATTGGCTGCT
TGAATGTCCTG*GGAAAGATCAAAGGATACCCAATTTGGCATGATCCAATAAGGTTGAACC
ATTCTCAACGAGAATCCCTGCCCCAGCTGCATCTCCAAGTATAGTCAATGCAAAAAGCCT
TAG*GTTTGCTGTTTCAAAGCTATGAGCAGGAGGGGTTGAA

B **MAVGYNNVDVNAANKYGVAVGNTPGVLTETTAELAASLSMAAARRIVEDEFMRAGLYDGW**
LPHLFVGNLLRGQTVGVIGRIGSAYARMMVEGFKMNLIIYDLYQATRLKFTVAYGQFLKA
SGEQPVTKRAASMDEVLRADLISLHPVLDKTTYHLVNERLSMMKKEAILINCSRGPVIDEV
ALVAHLKENPMFRVGLDVFEDEPYMKPGLAEMKNAIVPHIASASKWTREGMATLAALNVLG
KIKGYPIWHDPNKVEPLNENSLPPAASPSIVNAKALGLPVSKLU

TC59682 **A** **ACCAGCGAAGTCCCCAAGATATCGGACGGCTCATCCGCCACCCTACCCGCCGCTGC**
CCCACCTCCGTGCGCGCCGAGTGTATAGTGCCTTTCACAAAGCGAAACATGGAAAGCA
TCGGGGTACTGTTGACTTGGCCAAATGAACCCATACCTGGAACAGGAACTGGACAAGCGCTTC
AAGCTCTCCGCTTCTGGGACTTTCCAAGCGCCAACGATCTTTTCAGGGAGCATTCAAATTC
GATCCGAGCTGTGGTTGGAAACTFCTTTCATCGCGCCGACGCCAGATGATCGGAGCGTTCG
CCAAGATGGAGATTGTGTCGAGTTTCAGCGTTGGGTTGGACAAGATCGATTGGTGAGGTGC
AAGGAGAAGGGAATTAGGTTACGAACACTCCGGATGTGCTGACGGAGGACGTGGCGGACT
TGGCACTGCTTTGATTTTGGCGACTCTGAGACGTATTGTGAAAGTATCGTATGTGAGG
AGTGGGTCGTGGAAGAAAGGGGATTTC AAGTTGACTACCAAG*TTCACTGGAAAATCAGTTG
GCATTATAGGTTGGGTAGGATTGGCTCAGCAATTGCCAAGAGAGCCGAGGATTTAGCTG
TCCAATTAGTTACCATCCAGAACAGAGAAACCAGGACAAACTCAAGTACTATCCTAGT
GTCGTTGAATTGGCCTCCAACCTGTCAAATCCTGGTTGTTGCTTGGCGGTTAACACCAGAAAC
CCGCCACATCATCAACCGTGAAGTCAATGC ACTGGGTC A AAGGGTGTGGTTCATCAACA
TCGGAAGGGGATTACATGTGGATGAACCTGAGCTTGTATCCGCACTGGTTGAAGGCCGTTG
GGAGGTGCTGGACTTGATGTGTTGAAAAATGAGCCTAATGTACTGAAAGAGCTGTTAGCAAT
GGACAATGTAGTCCTTTTGCTCATGTTGGAAGCGGAACCGTGGAAACCCGGAAAGACATG
GCTGACCTGGTACTTGGAAACTTAGAGGCTCACTTTCTGAACAAACCCTGTTAACTCCAGT
GGTTTAA

B **TSEVPKDIGRLIRPTVTAALPPCAAEICIVRLSQSETMESIGVLLTCPMPNYPLEQLDKRFLFRF**
WDFPSANDLFRHSNSIRAVVNSFIGADAQMIEALPKMEIVSSPSVGLDKIDLVRCKEKRIVTN
TPDVLTEDVADLALALILATLRRICESDRYVRSWSWKKGDFKLTTKFTGKSVGIIGLRIGSIAIK
RAEGFSPISYHSRTEKPGTNYKYYPVVELASNCQILVVACALTPETRIHINREVINALGPKGVVI
NIGRGLHVDEPELVSAIVEGRLLGGALDVFENEPNVPEELLAMDNVLLPHVGSQTVETRKDM
ADLVLGNLEAHFLNKPLTPVVU

TC55752 **A** **ATGGCGATGATGAAGCGAGTTGCTGAGTCTGCGGTTAGGGCTTTTGTCTGGGTTCTACTTC**
CGGGGCTCTTACCAGGCACCTCCAT*GCTTCAGCTGGCAGCAAAAAGATTGTTGGGGTGT
TACAAGCCAAATGAATATGCTGCCATGAATCCCAACTTTGTGGGCTGTGTTGAGGGAGCCTT
GGGCATTGAGATTGGTTGGAAATCACAAGGGCACAGTACATAGTTACTGATGACAAAAGAA
GGACCAGATTGTG*AACTTGAAAAGCACATCCCGACTCCATGTTCTCATATCTACCCCTT
CCACCTGCCTACGTAACAGCAGAGAGGATCAAGAAGGCCAAAAATCTACAACCTTCTGCTT
ACAGCTGGAATTGGATCTGATCATATTGATTTGAAGGCAGCTGCTGCTGCTGGGCTAACAGT
TGCTGAGGTCACTGGAAGCAACGTAGTGTCTGTTGCAAGAAGATGAGCTCATGAGAATCCTCA
TTCTGTCCGGAATTTCTGCTGGACACCATCAGGTTATTAGTGGGGAGTGGAAATGTTGCA
GGTATTGCTTACAGAGCTTATGATCTTGAAGGCAAGACAGTGGGAACTGTTGGGGCTGGAC
GTATTGGTAGGCTTTTGTCCAGCGATTGAAGCCTTTCAACTGTAATCTCCTCATCATGATC
GGATTAATAATGGACCCAGAATTGGAGAATCAGATAGGAGCAAAGTTGAAGAGGATGTTGA
TGTGATGCTTCCCAAATGTGACATAATTGTCATCAACATGCCTCTTACTGAAAAACAAA* A
GGAAATGTTCAACAAAGAGAGGATTGCAAAGTTGAAAAGGGAGTTCTAATTGTTAACAATG
CTCGAGGAGCAATCATGGATACACAAGCTGTTGCCGATGCATGCTCCAGTGGGCATATTGCA
G*GTTACAGTGGGGATGTTGGTATCCACAGCCAGCCCCAAAGGACCATCCATGGCGGTACA
TGCCAAACCAAGCTATGACCCCTCATATTCTGGCACCACCATTGATGCACAG*TTGGGATA
CGCAGCTGGAGTGAAGGACATGCTAGACAGGTAAGGAGAAAGACTTTCCGGCACAA
CATTACATCGTCAAGGAGGGCAACTAGCAAGCCAGTACCAGTAA

B **MAMMKRVAESA VRALFALGSTSGALTRHLHASAGSKKIVGVFYKANEY AAMNPNFVGCVEGAL**
GIRDWLESQGHQYIVTDDKEGPDCELEKHIPDLHLVLISTPFHPAYVTAERIKKAKNLQLLLTAGIG
SDHIDLKAAAAGLTVAEVTGSNVVSAEDELMLRILIVRNFLPGHHQVISGEWNVAGIAYRAY
DLEKTVGTGAGRIGRLLQLRKPFCNLLYHDRIKMDPELENQIGAKFEEDVDVMLPKCDIIV
INMPLTEKTKGMFNKERIAKLLKQVGLIVNARGAIMDTQAVADACSSGHIAGSYGDVWYYPQPA
PKDHPWRYMNPQAMTPHISGTTIDAQLRYAAGVKDMLDRYFKGEDFPAQHYIVKEGQLASQY
QU

TC52437 **A** **ATG**GGCTCAGACATGTGGGTTTCAGCTCTGGAGATAGTAGATGGTCTCTCAAGGGAATGACTGCTCTTGTAACTGGTGGAACTAAAGGAATTGGGCATGCAATTGTGGAGGAAGCTGGCTGGATTAGGAGCAACCATACACCGTGTCTCGAAAAGAAACCGAGCTCAATGAATGCTTAAAGGATTGGAAAGCTAAAGGTTTTGGAGTGTAGTGGTTCAGTGTGTGATGTATCCTCTCGGGGCCAAAGGGAGAAGCTAATGGAGACTGTGTCTCTGTGTCAATGGGAAGCTGAATATCCTTGTCAACAACGCTGCTATTGTTATTCAGAAACCAACAGTAGAGGTCACGGCAGAAGAGTTCTCAA CAATCATGGCCATAAAATTTGAAATCTGTGTATCATCTGTCCAACTCGCACACCCCTTTTA AAGGCATCAGGAGCGGAAGCATTGTGTTTCATCTCTCTGTGGCAGGGTGTAGTGTCACTCA AGTATCTGTCTGCTTATTCAGCGACCAAGGAGCAATGAATCAACTTACAAGAATTTGGC ATGCGAGTGGGCGGAAGATAAATATTAGAAGTAATGCAGTTGCTCCTTGGTACATCAAAACT CCGATGGTGGATCAGATGCTCAGTAACAAAACCTTTCTGGAAGGGGTGATAAATCGAGCT CCACTTCGCCGTGTGGGAGATCCGAAGGAGGTGTCATCTTTGGTGGCATTCTCTGTCTAC CAGCATCATCTTACATTACTGGACAGACTATTTGTGTGATGGTGGCGTACTGTTAATGG TTTTGAGCCAAACCTGTTC**TAG**

B **MAQ**TCGFSSGDSRWSLKGMTALVTGGTKGIGHAIVEELAGLGIHTCSRKETELNECKLDW KAKGFGVSGSVCVSSRAQREKLMETVSSVFNGKLNILVNNAAIVIQKPTVEVTEEFSTIMAI NFEVSYHLSQLAHPLLKASGAGSIVFISSVAGVSLKYLAYSATKGMNQLTKNLACEWAED NIRSNAVAPWYIKTPMVDQMLSNKTFLEGVINRAPLRRVGDPPREVSSLVAFLLCPASSYITGQTI CVDGGVTVNGFEPNLF**U**

TC58004 **A** **ATG**GTCACCGGCGCTTCTCGGGTCTCGGCAGCGAGTTCTGCCTCAACCTCGCCAAAGCCG GCTGCAAGATCGTGGCGGCCCGCCCGAGTTGACCGACTCAAGTCTCTCTGCGACGAGAT CAACAACCTCACCCTCGAACCTTCTCCAAACGCTGATCCGCTCTCCGAGCCGTAGCA GTCGAACTTGACGTCAACAGCGATGGCTCCTCAATCGGCGCCTCCGTTCAAGAGGCTTGGG AGGCCTTTGGACGTATCGATGCTTTGTCTAAATAATCGGGACATTAGAG*GCAATGTGAAC TCTCTCTGGATATATCTGAGGAGGAATGAATAAATACTCTGAAGACAACTTGACGGGATC ATGTTTGGTGTCAAAAATATGTCGGTATGCGCATGAGGGATGCCAAGAATGGAGGATCAAT CATCAATATTTCTCCATTGCTGCTCTTAATCGGGGACAGTTACCTGAGGAGATGATG TGTCTTCAAGTCAGGCTTGAGCGCCATGACAAAAG*GTAATGGCTCTGGAATTGGGGCAT ACAATATTAGAGCGAATGCAATAGCACCTGGACTATTCAAATCAGAGATAACTTCGGGCCT TATGCAAAAAGACTGGCTCAACACTGTGGCTCAGAGAACATGCCCTATGCGGACCTTTGGA ACATCGGACCCTGCATTGACATCCCTGGTGGGATACTTGATTATGATTCTTACGATAACAT ATCAGGTAACATTTTCATTGTCGATGCAAGGTGCAACCTGCGGGGTGCCCAATTTCTCTT CCTTT**TGA**

B **MVT**GASSGLGSEFCLNLAKAGCKIVAAARRVDRKSLCDEINNLTHSNLPPNADPLRAVAVE LDVTSDGSSIGASVQKAWAFAFRIDALLNNAIRGNVNSPLDISSEEWNNLTKNLNLTGWSLVS KYVGMRRMDAKNGSIISSIAALNRQLPGGVAYVSSKSGLSAMTKVMALELGAYNIRAN AIAPGLFKSEITSGLMQKDWLNTVAQRTCPMRTFGTSDPALTSLVRYLIHDSRYISGNIFIVDA GATLPGVPIFSSLU

TC55097 **A** **ATG**GAGAAGATCGGAAAAGAGATTTCAAGGGAAGGTGGCGATCGTGACGGCGTCTACTCAG GGTATCGGCTTCAGCATTGCAGAGCGGCTGGGCTTGGAGGGCGCCTCGGTTGTACTCTCGT CTCGCAAGCAG*ACAATGTAGATGAGGCAGTTAAAAAGCTCAAAGCTCAAGGAATTGAA GCGATGGGCGTGGTTTGTATGTGTCCAATGCCAACATAGGAAGAATCTGATTGAAAAG ACGGTTACAG*AAATACGGAGCAATAGATGTGGTTGTGTCCTGCTGCAACCCATCT GTTGATCCTACGCTGGAACACGAGAATCGGTTCTAGACAAGCTATGGGAAATCAACGTC AAATCTTCTATACTCATTCTACAG*GAGGCAGCTCCTCACTTGAGAAAGGGTTCGTGGTTG TCCTAATTTCTCTATTGCGGGTATCAGCCACAGTCTTCCATGCTATGATGAGTGACA AAAACAGCCCTTCTTGGGCTTACCAAG*GCCCTTGCAGCTGAGATGGGCCAGACACTCGT GTAATTTGTGTTGCGCCTGGTTTTGTACCAACACACTTTGCCGAATTCCTCAGCAAAAATG CTGAGATT*AAGAAGGACATTGAGGATAAAACTTACTCAACAGGCTTGAACACCAAG GATATGGCTGCAGCCACGGCCTTCTGGCTTCCGACGATGCTTCTATATCACTGGAGAGA CGCTGGTGTGGCTGGTGAATACCTTCTAGACTCT**TAG**

B **MEK**IGKRFQGVAVTASTQIGFSAERLGLGASVVLSSRKQNNVDEAVKKLKAQGIEAMG VVCHVSNAQHRKNLIEKTVQKYGAIDVVVSNAAAANPSVDPTLETRESVLDKLEWVNVKSSILIL QEAAPHLRKGSSVLLISSIAGYQPSSMSMYGVTKTALLGLTKALAAEMDPDRVNCVAPGFV PTHFAEFLTKNAEIKKIDIEDKTLNRLGTTKDMAAATAFLASDDASYITGETLVVAGGIPSR**LU**

Figure 3.3: Nucleic (A) and amino (B) acid sequence of candidate proteins for a gluconate 5-dehydrogenase involved in the secondary glucose-precursor pathway in *V. vinifera*. Blue and red bases indicate the start and stop codons of the open reading frame respectively. *denotes intron positions identified via the Spidey mRNA-genomic alignment program

(www.ncbi.nlm.nih.gov/IEB/Research/Ostell/Spidey).

A COBALT alignment (Papadopoulos and Agarwala, 2007) of the amino acid sequences of the bacterial candidates against the respective *V. vinifera* homologue sequences was performed to identify regions of homology and to determine percent identity across the sequences.

Alignment of the candidates for step 2a of the primary Asc-precursor pathway (Figure 3.4) shows multiple conserved residues; however, homology over large sections of consecutive amino acids is not present. Identity over the open reading frame (ORF) of TC59682, TC61548 and TC55752 as compared to P37666 was calculated as 34.7%, 31.5% and 21.3% respectively.

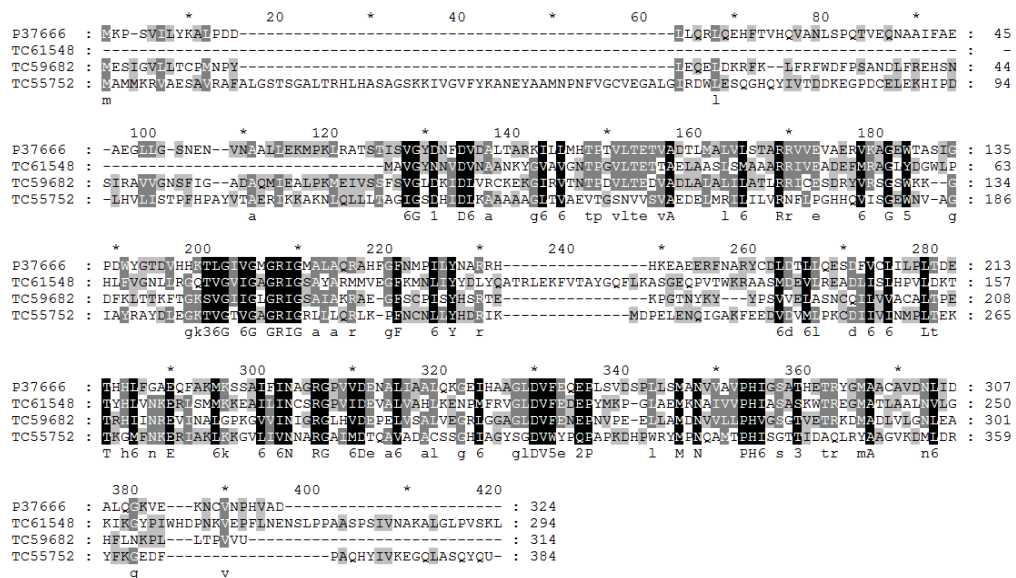


Figure 3.4: COBALT alignment of the *E. coli* 2KGR P37666 and putative *V. vinifera* homologues TC61548, TC59682 and TC55752

Alignment of the candidates for step 2b of the secondary glucose-precursor pathway (Figure 3.5) shows a similar pattern to the previous alignment with homology over large sections of consecutive amino acids not present. Identity over the ORF of TC52437, TC58004 and TC55097 as compared to P50199 was calculated as 30.7%, 26.2% and 28.3% respectively.

```

P50199 : M-----*-----20-----*-----40-----*-----60-----*-----80-----
TC52437 : MAQTCGFSSGDSRWSLKMTALVTGCTKIGIHAIVEPLAGLCAITHTCSRRETEFLNECLKDKRKC-----FGVS : 70
TC58004 : M-----*-----20-----*-----40-----*-----60-----*-----80-----
TC55097 : MEKIGK-----RFQCKVALVFASTQCIGICPSIAERLGLGCSVLLSRKQNNVDEAVKRLKQC-----HEEM : 62
M g a VTg 3 G6G La Ga 6v R 6 a g a

P50199 : TAVFVVDQDAVIDGAAATERDMGSDILINNACTQ--RRAPLIEEFSRKDWDIDVSTNNNAVTFVGCVAVAREMI-PRGR : 139
TC52437 : GSTCIVSSRAQREKLEETVSSVENGRINILVNNALIV--CKKTVETVAFE-ESTINAINFESVYHISLAHPLIR-ASGA : 147
TC58004 : AVELDVTSIDGSSIGASVQKAWAFAFRIDILLNNACTIRGNVNSPI-DISEPEWINTIKTNTGSLVSKYVGMRRMDAKNG : 139
TC55097 : GVVCHVSNACHRKNLEKTVQKM-GAIDVVSNAAANPSPDPTI--ETRESVLRLWEIINVKSSILILFAAPPLR---KG : 137
v dV3 G 61 66nNA i p1 3 e N 6 q 6

P50199 : GKIVNICSQSEIAR--EGTALVDPKFGAVKMLTRGMATDNGRHGQINGLAPGYEAFEMTERVAEETDWCRRH-FA : 217
TC52437 : GSIVFISSVAGVVSLL--KYLSPYSAFKGSAAMNQLTRNLCEWAPEDNIRSNVAVAPWIKRTEVDQMLSNKTFLEGVINRA-PI : 225
TC58004 : GSTIINISSTALNRGQLEGGVYVSSKSGLISAMTRVMALGLCAYNIRANAIAAPLERSETSGILM-QKDWLNTVACRIPCPI : 219
TC55097 : SSVVHISSTLGYQPC--SSVSNYGVKIKTLLGLTRALAAKMPDITRVNCAVAPGVVPHFAEELITRKAIEIKKDIPEKII-IL : 214
gs66 IsS6a Y 3K a6 6TK 6A e g r N 6APg 3 6 6 4t p

P50199 : GRNGQVEE-IVGAAVFTSSRASSFVNGCVLMVDGGITVSL----- : 256
TC52437 : RRVGDPKE-VSSLVAFCLPASSYINGQLICVDGCVTVNGFEPNLFU--- : 271
TC58004 : RTRGTSDPALTSLVRYLIHDSRYVIGNIFIVVACATIPGVP--IFSSLU : 267
TC55097 : NRICTKD-MAAATAFTASDDASYINGEELVAGCIPSRLU----- : 254
r G 6 5L ss56 G VdgG t

```

Figure 3.5: COBALT alignment of the *G. oxydans* G5Dh P50199 and putative *V. vinifera* homologues TC52437, TC58004 and TC55097. The conserved bases pertaining to a functionally significant region are boxed in yellow.

The highly conserved Y-x-x-x-K preceded by a serine residue is believed to be functionally significant. This conserved polar region is believed to define a secondary structure important in protein-substrate interactions (Klasen *et al.*, 1995, Persson *et al.*, 1991, Reid *et al.*, 2003). Although TC55097 was not identified in any berry EST libraries, it possesses the conserved residues of a G5Dh.

The amino acid sequence of each enzyme was further analysed using web-based BLAST interfaces to predict protein characteristics based upon compiled experimental data. The sites used include: PepStats (<http://www.ebi.ac.uk/tools/emboss/pepinfo>) basic information based upon the individual amino acid residues; Prosite (<http://expasy.org/prosite>) predicts tertiary structure and function of the protein based on patterns/profiles specific to protein families and domains (de Castro *et al.*, 2006); and the Centre for Biological Sequence Analysis protein annotation services (www.cbs.dtu.dk/services) NetPhos, identification of generic phosphorylation sites suggesting regulation of enzymatic activity (Blom *et al.*, 1999); TargetP, subcellular localisation of

proteins based on the presence of signal peptides (Emanuelsson *et al.*, 2000); TMHMM, presence of transmembrane helices indicating membrane bound (Krogh *et al.*, 2001); NetNES identification of leucine-rich nuclear export signals (la Cour *et al.*, 2004). These sites enabled the prediction of general protein characteristics aiding in candidate selection and subsequent analysis of enzymatic activity (P37666 and P50199 were not analysed for certain descriptors as the database protocols pertain to Eukaryotic sequences).

Comparison of *E. coli* 2KGR P37666 and putative *V. vinifera* 2KGRs TC61548, TC59682 and TC55752 show similarities across all proteins (Table 3.5). No transmembrane helices were detected in any of the candidate proteins indicating they are not membrane bound; however, TC59682 was identified as possessing a leucine-rich nuclear export signal suggesting its transport across the nuclear envelope. TC55752 is the largest of the proteins and the only protein predicted to encode a mitochondrial targeting peptide. Multiple serine, threonine and tyrosine residues were predicted as phosphorylation sites within each candidate sequence. This suggests the proteins may be post-transcriptionally regulated.

Comparison of *G. oxydans* G5Dh P50199 and putative *V. vinifera* G5Dh's TC52437, TC58004 and TC55097 (Table 3.5) showed similar results to the previous comparison with a high degree of commonality across the proteins observed. No transmembrane helices were detected in any of the candidate proteins indicating they are not membrane bound; however, TC52437 was identified as possessing a leucine-rich nuclear export signal suggesting its transport across the nuclear envelope. TC58004 was predicted to encode a chloroplast transit peptide, the only protein identified as encoding a targeting peptide. A similar number of phosphorylated sites was predicted across the *V. vinifera* proteins with multiple serine, threonine and tyrosine residues predicted as phosphorylation sites suggesting post-transcriptional regulation.

Table 3.5: Summary of the bacterial enzyme sequences and their respective *V. vinifera* homologues. Properties are predicted based on the amino acid sequence analysed via web-based protocols. NP indicates the descriptor not predicted. *Other indicates the sequence does not encode a chloroplast transit, mitochondrial targeting or signal peptide targeting it to the chloroplast, mitochondria or secretory pathway respectively. N/A indicates analysis not performed.

	P37666 <i>E. coli</i>	TC61548 <i>V. vinifera</i>	TC59682 <i>V. vinifera</i>	TC55752 <i>V. vinifera</i>	P50199 <i>G. oxydans</i>	TC52437 <i>V. vinifera</i>	TC58004 <i>V. vinifera</i>	TC55097 <i>V. vinifera</i>
Molecular Weight (kDa)	35.39	36.41	38.27	42.08	27.25	28.83	28.14	26.89
Number of Residues (AA)	324	331	351	383	256	270	266	253
Charge	- 6.0	+ 3.0	- 1.0	+ 6.0	- 2.5	+ 3.0	+ 5.0	+ 6.0
Isoelectric Point (IP)	5.68	7.23	6.26	7.42	5.37	7.75	8.91	9.38
Nuclear Export Signals (Residues)	N/A	NP	L:147, A:148 L:149, I:150 L:151, L:154	NP	N/A	L:243	NP	NP
Subcellular Localisation	N/A	<i>Other*</i>	<i>Other*</i>	Mitochondria	N/A	<i>Other*</i>	Chloroplast	<i>Other*</i>
Phosphorylation Sites								
– Serine	N/A	4	6	2	N/A	9	10	6
– Threonine		3	4	3		2	3	3
– Tyrosine		4	2	2		1	2	2

3.3 Discussion

Bacterial species such as *Escherichia coli* and *Gluconobacter oxydans* possess enzymes capable of catalysing steps 2a and 2b of the TA biosynthetic pathway respectively (Merfort *et al.*, 2006a, Yum *et al.*, 1998a). Putative homologues were identified in *V. vinifera* based on the similarity of the deduced amino acid sequence to the respective bacterial enzyme. Additional characterisation of these homologues at a sequence level was conducted to investigate the probability of their involvement in the TA biosynthetic pathway. The presence of functional domains and family signatures suggesting enzymatic activity of the candidates was also tested and positive outcomes used to further add weight to candidate identity. The libraries from which the EST sequences forming the candidate's open reading frame were identified in were also considered. TA biosynthesis takes place within berry tissue during the berry formation phase of development (Saito and Kasai, 1968, Saito and Kasai, 1978). Contigs of interest therefore are those identified in berry EST libraries. Of the EST's constituting candidate TC61548, 83% were identified within berry tissue. Saito and Kasai (1984) suggested an oxidoreductase as responsible for catalysis of step 2a of the primary Asc-precursor pathway. Although this is a broad class of enzymes, preliminary annotation of contig TC70223 suggests it to be an oxidoreductase identified exclusively in berry EST libraries (Table 3.1). Fedorova *et al* (2002) applied the Audic and Claverie (1997) statistical approach to gene expression to validate experimentally obtained digital Northern data in *Medicago truncatula*. Calculations indicated a TC sequence must be composed of greater than 4 ESTs for its expression to be considered greater than basal level, a finding supported by experimental data (Fedorova *et al.*, 2002). TC70223 does not meet the minimum EST requirement, suggesting the expression of this transcript in berry tissue is low. Candidates TC70734 and TC51869 for step 2b of the secondary glucose-precursor pathway are found exclusively in berry EST libraries; however, they also do not meet the minimum EST requirement (Table 3.2). Therefore, additional experimentation is required to validate these gene products. The reliability of the data presented in these EST libraries is complicated by factors including the potential cross-hybridization of

closely related sequences and the depth at which the individual libraries have been sequenced. This can produce false positives or TC sequences composed of low-number ESTs. Without a defined timeframe of berry age, the tissue analysed in these libraries may not include a representative sample of TA biosynthetic tissue.

Although TC55097 EST's were not identified in any berry libraries the presence of conserved residues and motif analysis indicates it appropriate for further investigation. In bacterial systems the enzymes involved in this pathway have multiple substrate-specificity. If this also applies to higher plant systems, the same enzyme capable of catalysing the reactions of TA production in young berry tissue may also possess the ability to catalyse other reactions in late berry tissue. TC55097's tentative annotation of a formate dehydrogenase is also a curiosity that led to its inclusion for *in vitro* activity analysis.

Analysis of the amino acid sequence of each candidate was also conducted to enable identification of integrated domains, family signatures and conserved sites. Both step 2a and 2b of the TA biosynthetic pathway require the oxidation or reduction of the substrate, suggesting a coenzyme such as NAD(P)H is required. The presence of binding and/or catalytic domains of this coenzyme within the amino acid sequence is indicative of a protein capable of catalysing this reaction. 2KGR candidates TC61548, TC59682 and TC55752 (Table 3.3) and G5Dh candidates TC52437, TC55097 and TC58004 (Table 3.4) meet this requirement. 2KGR belongs to the aldo-keto reductase (AKR) enzyme superfamily. The AKR superfamily consists of 114 members over 14 families identified in both Eukaryotic and Prokaryotic systems (Hyndman *et al.*, 2003). The members of this family constitute a diverse group of cytosolic NAD(P)H-dependent oxidoreductases approximately 300 amino acids in length (Jeudy *et al.*, 2006). Collectively, the AKR superfamily members are associated with the detoxification of a broad range of substrates (Grimshaw, 1992). All identified AKR members possess a conserved catalytic tetrad comprising of a D, Y, K and H residue. This catalytic tetrad corresponds to residues D:47, Y:52, K:77 and H:108 in the aldo-keto reductase AKR4C9 from *A. thaliana* (Simpson *et al.*,

2009b). The *viaE* gene product (NCBI Accession P37666) in *E. coli* is denoted a 2-ketogluconate reductase, an AKR family member; however, COBALT analysis of the sequence compared with AKR4C8, AKR4C9 and AKR4C10 from *Arabidopsis thaliana* does not align with the conserved catalytic tetrad (data not shown). A COBALT alignment of the *V. vinifera* candidates with the *E. coli* reductase showed conserved regions (Figure 3.4); however, these did not align with the catalytic tetrad of the *A. thaliana* AKR (data not shown). This may explain why analysis with InterProScan did not detect any family signatures within the amino acid sequence (Table 3.4). The *viaE* gene product was denoted a 2KGR as a result of activity and knockdown studies and a 69.4% identity with a 2KGR from *Erwinia herbicola* (Yum *et al.*, 1998a). Identification of the residues pertaining to the conserved catalytic tetrad was not performed. The catalytic region of the *E. coli* reductase and the candidate *V. vinifera* 2KGR may be present spanning a broader or narrower region of the protein sequence as compared to the *A. thaliana* 2KGR. Structural studies of may be required to identify this region, confirming the enzymes as AKR family members.

The selected *V. vinifera* candidates for each step were compared to the bacterial enzyme to determine homology and the level of identity across the sequences. The percent identity across the 2KGR and G5Dh candidates was similar, indicative of a comparison of genes from distantly related systems. Persson *et al* (1991) analysed sequence characteristics across the short chain dehydrogenase family and found residue identities between members to be typically 25%, with glycine identified as the most conserved residue across the family. This is also evident within the *V. vinifera* alignments (Figure 3.5). Each *V. vinifera* G5Dh candidate possessed the highly conserved polar region Y-x-x-x-K preceded by a serine residue believed to be important in protein-substrate interactions (Klasen *et al.*, 1995, Persson *et al.*, 1991, Reid *et al.*, 2003). Although *TC55097* was not identified in any berry EST libraries, it possesses the conserved residues of a G5Dh. The grape berry library was generated using a 'reliability filter' applied to the sequencing runs performed. EST's were included if identified in more than 1 of the 4 sequencing runs performed. Of the signatures detected, 3.2% were not considered reliable (Iandolino *et al.*, 2008). The

absence of *TC55097* from berry libraries may be due to the lack of detection in the sequencing runs. The plant expression database (<http://www.plexdb.org>) is a gene expression database comprising of microarray data from various experiments involving plant and plant pathogens. A gene with 99.3% identity to *TC55097* was identified on the *V. vinifera* 16K microarray in Cabernet Sauvignon berry specific tissue differentiation and long term water and salt stress experiments. The tissue differentiation experiment detected expression in skin, seed and pulp indicating *TC55097* is present in berry tissue.

The current hypothesis of the site of TA and MA biosynthesis is the cytoplasm, before the acids are transported into the vacuole and stored. MA is transported back to the cytoplasm and respired or used for biosynthesis; TA however, remains in the vacuole and is not degraded. MA transporters *AttDT* and *AtALMT9* have been identified in *A. thaliana* responsible for MA transport across the tonoplast (Emmerlich *et al.*, 2003, Hurth *et al.*, 2005, Kovermann *et al.*, 2007). MA and TA are dicarboxylic acids with high structural similarity and it is hypothesised both acids are transported using the same transporter. Studies by Emmerlich *et al* (2003) investigating *AttDT* support this hypothesis. To date, 4 ALMT9-like proteins have been identified in *V. vinifera* (Patel, 2008, Rongala, 2008) with localisation and expression patterns supporting their role in MA transport. The affinity of these transporters to TA has yet to be investigated. *TC55752* was identified as containing a mitochondrial targeting peptide sequence and *TC58004* contained a chloroplast transit peptide sequence (Table 3.5). The presence of these targeting signals does not support the hypothesis that TA biosynthesis occurs completely in the cytoplasm. It should be noted however, that these web-based protocols are predictions based upon model data. Recently Wen *et al* (2010) detected L-IdnDH.1 in the vacuole of mature berry without possession of a signal targeting sequence. Multiple residues across all candidates of both 2KGR and G5Dh were predicted to undergo phosphorylation indicating a potential role in regulating enzymatic activity (Lindsley and Rutter, 2006). Post-translational phosphorylation and ubiquitination has been suggested to occur to the *V. vinifera* gibberellin signal pathway regulator *GAI1*

(<http://www.uniprot.org/uniprot/Q8S4W7>) with ubiquitination triggering degradation of the protein, thus post-translational regulation is not without precedent in *V. vinifera*.

Based upon the analysis conducted at the amino acid level, putative candidates TC52437, TC55097 and TC58004 for a *V. vinifera* G5Dh and putative candidates TC61548, TC59682 and TC55752 for a *V. vinifera* 2KGR were selected for *in vitro* kinetic analysis (see Chapter 4) and *in vivo* activity over development (see Chapter 5).

Chapter 4:

Cloning, Heterologous Expression and Analysis of Candidate Tartaric Acid Biosynthetic Enzymes

4.1 Introduction

The predominant pathway of tartaric acid (TA) biosynthesis in *V. vinifera* is the Asc-inclusive C4/C5 cleavage pathway (Figure 1.4). This pathway accounts for 85-91% of TA production (Saito and Loewus, 1989b) with a secondary pathway involving the cleavage of D-glucose contributing a minor portion to the TA pool (Figure 1.6). Work throughout the second half of the 20th century focused on the elucidation of these biosynthetic pathway's; however, the associated enzymes have received little attention. To date, L-idonate dehydrogenase 1 (L-IdnDH.1) is the only known enzyme involved in the primary-Asc TA biosynthetic pathway (DeBolt, 2006, DeBolt *et al.*, 2006). Activity studies showed L-IdnDH.1 is responsible for catalysing the reversible conversion of L-idonate to 5-keto-L-idonic acid (also known as 5-keto D-gluconic acid). Substrate analysis indicates L-IdnDH.1 is highly specific to these substrates, with no detectable activity observed against alternative substrates (DeBolt, 2006, DeBolt *et al.*, 2006). Investigations into the kinetics of the primary-Asc pathway led Malipiero *et al* (1987) to suggest this reaction as the regulatory enzymatic reaction of the pathway.

The focus of this study is the identification of additional enzymes involved in tartaric acid biosynthesis, namely the identification of enzymes responsible for the catalysis of steps 2a of the primary-Asc and 2b of the secondary glucose pathway (Figure 1.8).

Step 2a of the primary-Asc pathway is proposed to involve the conversion of 2-keto-L-gulonic acid (2KGA) to L-idonic acid, which is subsequently converted to 5-keto-D-gluconic acid (5KGA) by L-IdnDH.1 (DeBolt *et al.*, 2006, Saito and Kasai, 1982). *Escherichia coli* possesses the enzyme 2-ketogluconate reductase (2KGR) capable of catalysing the described reaction (Blattner *et al.*, 1997, Sofia *et al.*, 1994, Yum *et al.*, 1998a). The identification and cloning of three putative candidates for 2KGR, TC61548, TC59682 and TC55752, from the *V. vinifera* genome was described in Chapter 3.

Step 2b of the secondary glucose pathway involves the conversion of D-gluconate to 5-keto-D-gluconic acid (5KGA). Investigations into the secondary pathway are limited, focusing only on the intermediate compounds and not the enzymes involved. The bacterium *Gluconobacter oxydans* possesses a gluconate-5 dehydrogenase (G5Dh) capable of catalysing the described reaction (Klasen *et al.*, 1995, Merfort *et al.*, 2006a, Prust *et al.*, 2005). The identification and cloning of three putative candidate G5Dh, TC58004, TC55097 and TC52437 from the *V. vinifera* genome was described in Chapter 3.

The work in this chapter describes the cloning, heterologous expression and kinetic analysis of each respective candidate. Investigations into the presence of each candidate in berry cDNA and kinetic parameters of the recombinant protein *in vitro* including temperature, pH, substrate range and coenzyme affinity are described.

Kinetic analysis is essential in the understanding of an enzymes mechanism and its interaction within the biological system in question (Cornish-Bowden, 2001, Schnell and Maini, 2003). Heterologous expression is a standard technique used in the characterisation of proteins enabling the inexpensive large-scale production of the desired protein in an alternative, well characterised cell line such as *Saccharomyces cerevisiae* or *E. coli* (Joubert *et al.*, 2010, Novy *et al.*, 1995). Heterologous expression enables the production of soluble protein in shorter time periods than the native cell line. The pET vector system, within the *E. coli* host cell line has been specifically engineered for the cloning and expression of recombinant proteins, a technique which proved successful for the characterisation of L-IdnDH.1 (DeBolt, 2006, DeBolt *et al.*, 2006, Novagen, 2006). During investigations into *L-IdnDH.1*, a transcript with approximately 70% nucleic acid identity with *L-IdnDH.1* was identified in grapevine EST databases. This transcript, informally called *L-IdnDH.2*, shares 83% identity with L-IdnDH.1 at the amino acid level suggesting it may be a homologue of *L-IdnDH.1* (Hayes, DeBolt, Cook and Ford, manuscript in preparation). The function of this enzyme has not been determined; therefore characterisation of purified recombinant L-IdnDH.2 (supplied by Dr MA Hayes, University of Adelaide) was also investigated in this chapter.

4.2 Results

4.2.1 Cloning of Putative *Vitis vinifera* Tartaric Acid Biosynthetic Genes into an Expression Vector

Genes *TC61548*, *TC59682* and *TC55752* are suggested to encode a 2-ketogluconate reductase (2KGR) possibly involved in the primary-Asc TA biosynthetic pathway (identification described in Chapter 3). *TC58004*, *TC55097* and *TC52437* are suggested to encode a gluconate 5-dehydrogenase (G5Dh) possibly in the secondary TA biosynthetic pathway (identification described in Chapter 3). Gene specific primers were designed based upon the published sequences obtained from the Gene Indices: Grape database (www.compbio.dfc.harvard.edu/tgi) and the presence of these genes within pre-véraison berry tissue investigated. Pre-véraison berry cDNA (obtained from material prepared by Vanessa Melino, University of Adelaide) was used as the template of each candidate open reading frame in *V. vinifera* cv Shiraz. The PCR products generated were ligated into the cloning vector pDRIVE (Qiagen, Australia) as described in Section 2.12. Confirmation of the amplified nucleic acid sequence was obtained through sequencing of the construct as described in Section 2.11.1. All genes suggested to encode 2KGR were identified in pre-véraison *V. vinifera* cv Shiraz berry cDNA. Of the candidates suggested to encode G5Dh, *TC58004* and *TC55097* were successfully amplified from pre-véraison berry cDNA. The expected open reading frame of *TC52437* could not be amplified from pre-véraison berry cDNA. Conceptual translation of the obtained sequence generated multiple stop codons throughout the putative protein sequence (data not shown). Modifications to the *TC52437* specific primer sets did not result in the expected protein sequence; therefore, this candidate was not pursued further.

Upon confirmation of the expected open reading frame, each candidate genes' open reading frame was digested and ligated into the expression vector pET-14b as described in Section 2.12.2.1. Confirmation of the insertion of each candidate open

reading frame into the expression vector pET-14b was obtained through sequencing of the vector as described in Section 2.11.1.

4.2.2 Heterologous Expression and Purification of Recombinant *Vitis vinifera* Proteins in *Escherichia coli*

Conditions of isopropylthiogalactoside induced expression of candidate genes were optimised to enable efficient heterologous expression of soluble protein (see Section 2.15). Purification of the heterologously expressed protein was performed using immobilized metal affinity chromatography (IMAC, see Section 2.15.2) with a cobalt-based resin and visualised using sodium dodecyl sulphate polyacrylamide gel electrophoresis (SDS-PAGE, see Section 2.15.3).

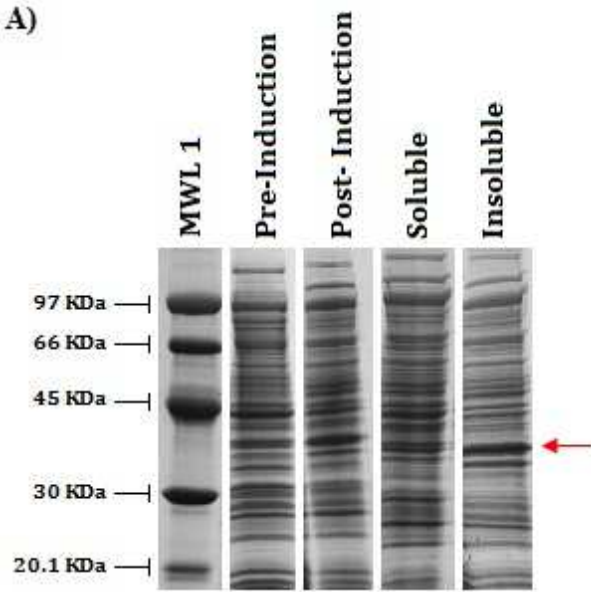
Expression of the protein encoded by *TC61548* was tested under multiple conditions as described in Section 2.15. Computational analysis indicates the protein encoded by *TC61548* is 36.4 kDa (Table 3.5). Standard extraction from induced cell culture (Section 2.9.1) did not result in purified soluble protein of the expected size (data not shown). Crude extracts of a post-induction whole cell sample showed an increase in protein at the expected size (Figure 4.1 A) suggesting expression of the protein encoded by *TC61548* was successful. Crude extracts of the insoluble fraction obtained during purification also showed an increase in protein at the expected size (Figure 4.1 A) suggesting the *TC61548* protein remained in the insoluble fraction. Comparison of crude extracts of the pre-induction and soluble fractions showed no visual increase in protein at the expected size (Figure 4.1 A).

Due to the apparent insoluble nature of the *TC61548* protein, a high detergent buffer was used as described in Section 2.15.1.2. No soluble protein was extracted under these conditions (Figure 4.1 B) suggesting the *TC61548* protein may be hydrophobic. This is supported by computational analysis which shows 33.8% of the amino acid residues of the protein encoded by *TC61548* are hydrophobic. The *TC61548* protein may have been expressed within the *E. coli* pET-14b system and not purified due to

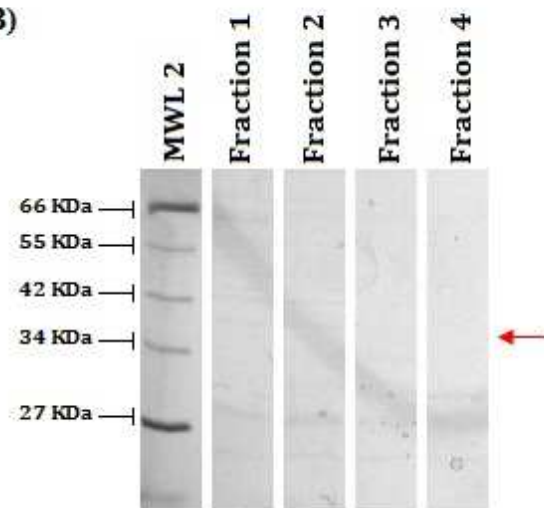
storage in the inclusion bodies. Additional purification would be required to support this.

Figure 4.1: Heterologous expression of the protein encoded by TC61548 separated on an SDS-PAGE gel stained with Coomassie Blue and visualised under white light. A 20 μ L aliquot of each fraction was loaded. Red arrow indicates the expected size (36 kDa) of the TC61548 protein. A) Crude extracts of the respective fractions, protein of expected size detected in the insoluble fraction. MWL 1 – Molecular weight ladder LMW (GE Healthcare, USA). B) IMAC purified elution fractions, soluble protein was not obtained. Protein extracted using the high detergent buffer BugBusterTM. MWL 2 – Molecular weight ladder, broad range (New England Biolabs, USA). Note: The lanes of the SDS-PAGE gel have been separated in the above image to enable clear definition of each fraction. Image A and B are the result of a single experimental run

A)



B)



Computational analysis indicates the protein encoded by *TC59682*, the second candidate for step 2a of the Primary-Asc precursor TA biosynthetic pathway, is 38.2 kDa (Table 3.5). Expression of the protein encoded by *TC59682* under induction conditions described in Section 2.15 resulted in no soluble protein of the expected size (data not shown). The induction temperature was reduced and duration extended to slow the expression of the protein encoded by *TC59682*, increasing solubility (Tolia and Joshua-Tor, 2006). Induction conditions of 16°C for 24 hours were tested without success; however, when the induction duration was extended to 48 hours, soluble protein of the expected size was purified (Figure 4.2). Additional protein was also present in the eluted fractions, as indicated by bands present on the SDS-PAGE gel (Figure 4.2). Extended wash periods prior to elution and purification at 4°C did not eliminate the additional bands observed (data not shown).

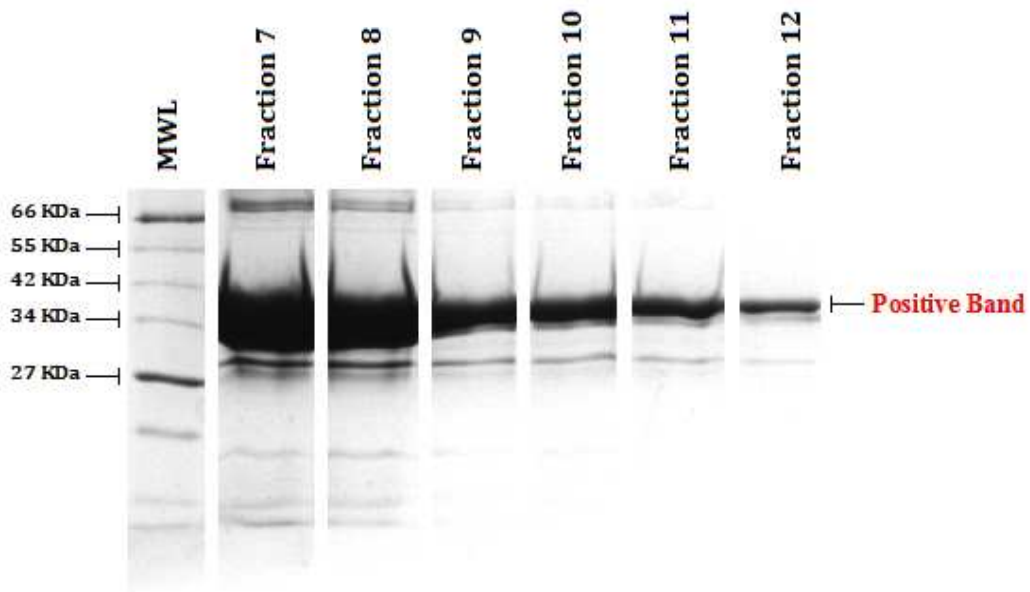


Figure 4.2: Heterologous expression of the protein encoded by TC59682 separated on an SDS-PAGE gel stained with Coomassie Blue and visualised under white light. A 20 μ L aliquot of each IMAC purified elution fraction was loaded. Soluble protein of the expected size (38 kDa) was obtained as indicated on the gel. Fraction 7 was used in all kinetic analysis (Section 4.2.3). MWL – Molecular weight ladder, broad range (New England Biolabs, USA). Note: The lanes of the SDS-PAGE gel have been separated in the above image to enable clear definition of each fraction. The above image is the result of a single experimental run.

Expression of the protein encoded by *TC55752* was characteristically similar to those observed for *TC61548*. Expression of the protein encoded by *TC55752* was analysed under the induction conditions described in Section 2.15. Crude extracts of a post-induction sample indicate expression was successful with an increase in protein at the predicted size of 42 kDa (Table 3.5) observed. However, soluble protein was not successfully purified (data not shown). An increase in protein at the expected size was observed in the insoluble fraction (data not shown). A reduction in induction temperature was performed to aid in solubility of the *TC61548* protein; however, soluble protein was unable to be purified (data not shown) using techniques described in Section 2.15.1.1. Soluble protein of the

expected size (Figure 4.3) was successfully purified utilising the high-detergent extraction buffer BugBuster™ (see Section 2.15.1.2). This low-yield TC55752 protein was purified from a 100mL batch culture expression system. An increase in the culture volume resulted in a decrease in purified soluble protein (data not shown) suggesting a decrease in the stability of the protein.

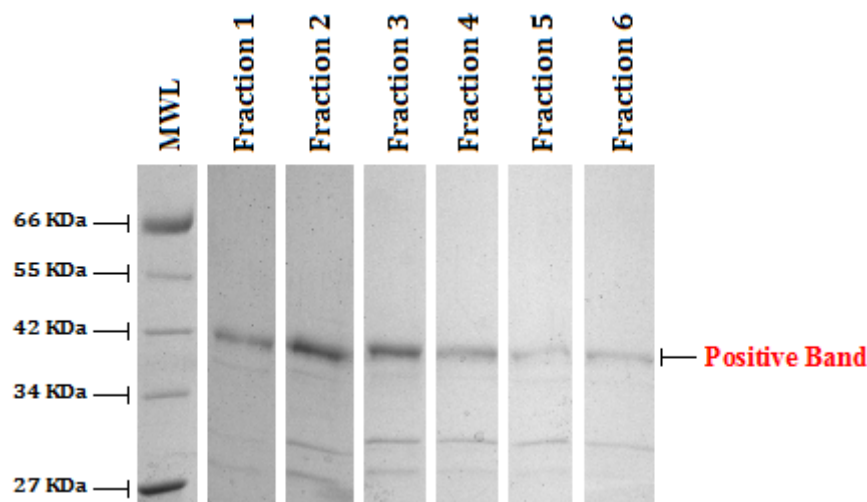


Figure 4.3: Heterologous expression of the protein encoded by TC55752 separated on an SDS-PAGE gel stained with Coomassie Blue and visualised under white light. A 20 μ L aliquot of each IMAC purified elution fraction was loaded. Soluble protein of the expected size (42 kDa) was obtained as indicated on the gel. Fraction 1 was used in all kinetic analysis (Section 4.2.3). MWL – Molecular weight ladder, broad range (New England Biolabs, USA). Note: The lanes of the SDS-PAGE gel have been separated in the above image to enable clear definition of each fraction. The above image is the result of a single experimental run.

Computational analysis indicates the protein encoded by *TC58004* is 28.1 kDa (Table 3.5). Expression of the protein encoded by *TC58004* under induction conditions described in Section 2.15 resulted in no purified soluble protein of the expected size (data not shown). A decrease in the induction temperature resulted

in the successful purification of soluble protein (Figure 4.4). Scale-up of the batch-culture did not increase the yield of TC58004 (data not shown).

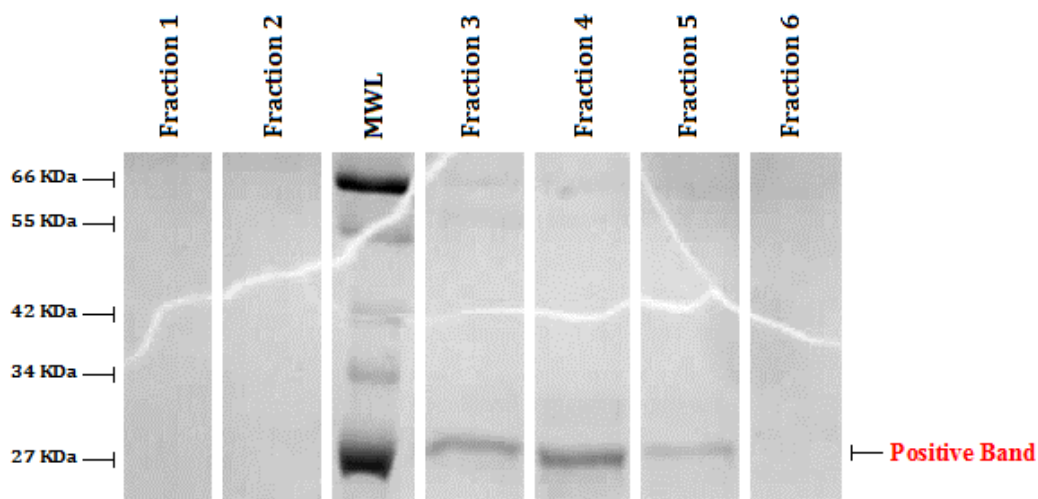


Figure 4.4: Heterologous expression of the protein encoded by TC58004 separated on an SDS-PAGE gel stained with Coomassie Blue and visualised under white light. A 20 μ L aliquot of each IMAC purified elution fraction was loaded. Soluble protein of the expected size (28 kDa) was obtained as indicated on the gel. Fraction 4 was used in all kinetic analysis (Section 4.2.3). MWL – Molecular weight ladder, broad range (New England Biolabs, USA). Note: The gel fragmented during visualisation procedures. The lanes of the SDS-PAGE gel have been separated in the above image to enable clear definition of each fraction. The above image is the result of a single experimental run.

Computational analysis indicates the second candidate for the secondary glucose pathway, *TC55097*, encodes a protein of 26.8 kDa (Table 3.5). Crude extracts of the expression of the protein encoded by *TC55097* under conditions described in Section 2.15 showed an increase in protein at the expected size in the insoluble fraction. A decrease of induction temperature resulted in a substantial increase in yield of soluble protein. Up-scale of the batch-culture volume under these conditions was successful with a high-yield of soluble TC55097 protein purified (Figure 4.5).



Figure 4.5: Heterologous expression of the protein encoded by TC55097 separated on an SDS-PAGE gel stained with Coomassie Blue and visualised under white light. A 20 μ L aliquot of each IMAC purified elution fraction was loaded. Soluble protein of the expected size (26 kDa) was obtained as indicated on the gel. Fraction 3 was used in all kinetic analysis (Section 4.2.3). MWL – Molecular weight ladder, broad range (New England Biolabs, USA). Note: The lanes of the SDS-PAGE gel have been separated in the above image to enable clear definition of each fraction. The above image is the result of a single experimental run.

4.2.3 Determination of the Kinetic Parameters of Enzyme Activity

Purified recombinant proteins expressed from each of the putative candidate sequences were analysed for their enzymatic activity to further support their inclusion in each respective biosynthetic pathway. A summary of the proteins successfully purified (as detailed in Section 4.2.2) for enzymatic analysis are listed in Table 4.1.

Table 4.1: Summary of the purified recombinantly expressed protein used for analysis of enzymatic activity in this study. Samples of purified L-IdnDH.2 were provided by M Hayes (University of Adelaide).

Candidate	Figure Number	Purified Sample Obtained	Fraction Analysed for Enzymatic Activity
2-Ketogluconate Reductase			
TC61548	4.1	No	N/A
TC59682	4.2	Yes	7
TC55752	4.3	Yes	1
Gluconate 5-dehydrogenase			
TC58004	4.4	Yes	4
TC55097	4.5	Yes	5

The conditions under which each recombinant enzyme was most reactive were investigated including temperature, buffer and pH. The activity of each enzyme against various substrates in the presence of NAD(P)H was also investigated. Purified samples of recombinant TC58004, TC55097 and L-IdnDH.2 were tested under multiple substrate and coenzyme combinations. No detectable activity was observed (data not shown) suggesting the extracted proteins were inactive in the conditions tested.

4.2.4 Optimal pH of Enzyme Activity

The pH range and buffer type at which the purified recombinant proteins TC59682 were most reactive was determined as described in Section 2.16. No detectable activity was observed against purified samples of recombinant TC58004, TC55097 and L-IdnDH.2 under all pH's tested (data not shown) indicating the extracted proteins were inactive under these conditions. Activity was observed against samples of both recombinant proteins TC55752 and TC59682; however, due to the limited sample of purified TC55752 protein optimisation of assay conditions was performed on recombinant protein TC59682 only.

4.2.5 Favourable pH of TC59682 Catalytic Activity

The pH range and buffer type at which recombinant protein TC59682 was most reactive were determined (Figure 4.6) as described in Section 2.16. An aliquot of fraction 7 of purified recombinant TC59682 (Figure 4.2) was diluted to 0.1mg/mL with fresh protein extraction buffer (MEB, Section 2.15.2) and used in the analysis. Activity was monitored spectrophotometrically at 340nm via the oxidation of coenzyme NADH in the presence of substrate 2-keto-L-gulonate (2KGA), the expected primary substrate based upon the *V. vinifera* TA pathway. Although activity was detected at all pH concentrations tested, the activity of TC59682 was observed to be most reactive at pH 7.5 in 100mM HEPES (4-(2-Hydroxyethyl)piperazine-1-ethanesulfonic acid). A no enzyme control was also tested under all pH conditions with minimal activity observed (Figure 4.6). All assay constituents including substrate and coenzyme were used in excess to ensure the reaction was not limited.

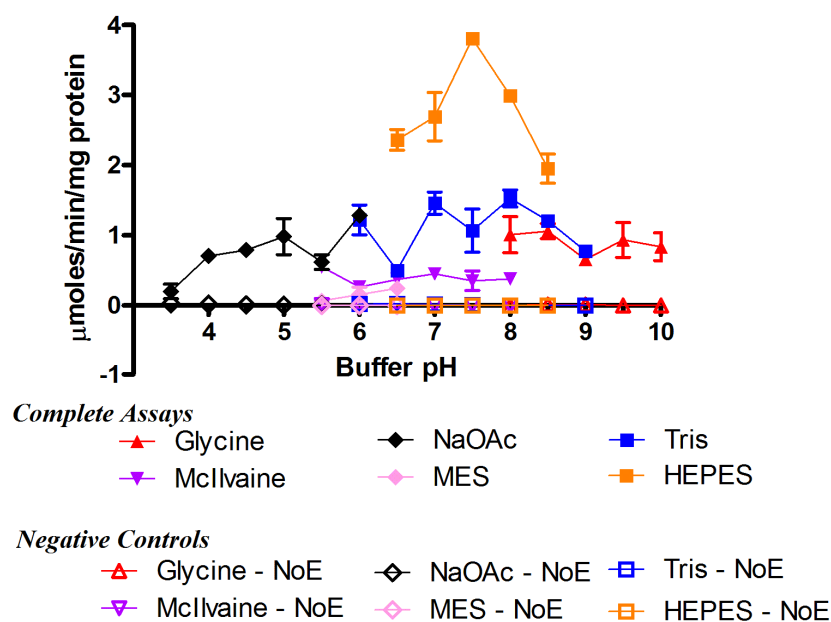


Figure 4.6: Activity of recombinant TC59682 at various pH and in a range of buffer types. Assays were performed with (200µL total reaction volume): 0.4µg purified recombinant enzyme, 40mM (final) 2-keto-L-gulonate (substrate) and 0.25mM (final) NADH (coenzyme) at 37°C. Plotted values represent the mean of triplicate assays with error bars representing standard deviation. Red closed triangle – 40mM Glycine-NaOH buffer pH 8.0-10.0 (De Ley, 1966), Red open triangle – No enzyme control in 40mM Glycine-NaOH buffer: Purple closed triangle – 100mM McIlvaine buffer pH 5.5-8.0, Purple open triangle - No enzyme control in 100mM McIlvaine buffer: Black closed diamond – 100mM NaOAc (sodium acetate) buffer pH 3.5-6.0, Black open diamond – No enzyme control in 100mM NaOAc buffer: Pink closed diamond – 100mM MES (2-[N-morpholino]ethanesulfonic acid) buffer pH 5.5-6.5, Pink open diamond – No enzyme control in 100mM MES buffer: Blue closed squares – 100mM Tris-HCl buffer pH 6.0-9.0, Blue open squares – No enzyme control in 100mM Tris-HCl buffer: Orange closed squares – 100mM HEPES (4-(2-Hydroxyethyl)piperazine-1-ethanesulfonic acid) buffer pH 6.5-8.5, Orange open squares – No enzyme control in 100mM HEPES

4.2.6 Activity of Recombinant TC59682 Protein Against 2-keto-L-gulonate

The protein encoded by *TC59682* is suggested to be responsible for the conversion of 2-keto-L-gulonate to L-idonate, step 2a of the primary-Asc biosynthetic pathway in *V. vinifera*. Therefore, the activity of putative TC59682 was analysed against 2-keto-L-gulonate (2KGA) as described in Section 2.16. An aliquot of fraction 7 of purified recombinant TC59682 (Figure 4.2) was diluted to 0.1mg/mL with fresh protein extraction buffer (MEB, Section 2.15.2) and used in the analysis. Multiple negative controls were tested including: no enzyme (NoE), no substrate (NoS), no coenzyme (NoC) and protein extraction buffer substituted for purified enzyme (PEB, see Section 2.16). No activity was observed in all of the aforementioned negative controls (Figure 4.7) suggesting that enzyme TC59682 was responsible for the observed activity and not an artefact of the assay protocol. Oxidation of NADH was observed after the addition of 2KGA (indicated by arrows on Figure 4.7) suggesting the observed oxidation of NADH is due to TC59682 activity. This is also supported by the no substrate control.

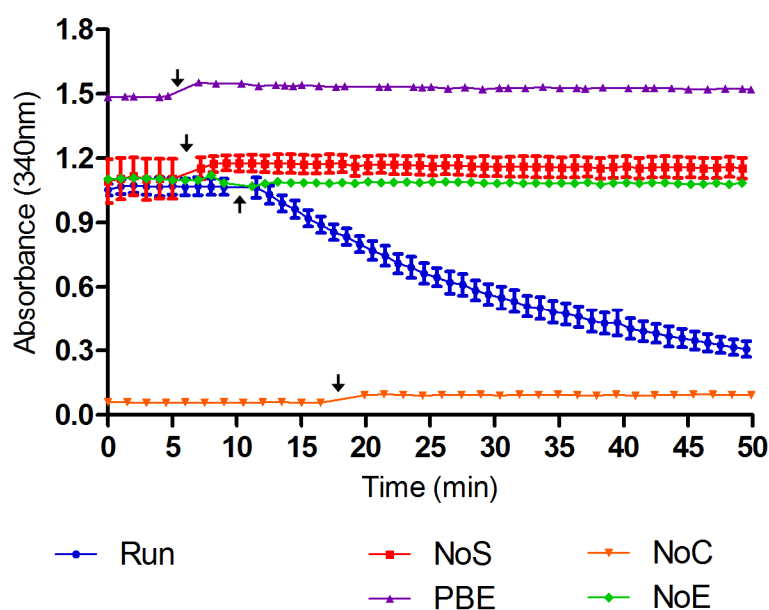


Figure 4.7: Representation of the TC59682 activity assays conducted including negative controls. Assays were performed using (200 μ L total reaction volume): 0.4 μ g purified recombinant enzyme, 40mM 2-keto-L-gulonate (substrate) and 0.25mM (final) NADH (coenzyme) in 100mM HEPES buffer pH 7.5 at 37°C. Plot represents the mean of triplicate assays with error bars representing standard deviation. Arrows indicate the addition of substrate. Blue solid square – Run, assay with all components; Red solid square – NoS, no substrate added; Purple solid triangle – PEB, protein extraction buffer substituted for purified enzyme, no purified TC59682 enzyme added; Orange solid triangle – NoC, no coenzyme added; Greens solid diamond – NoE, no enzyme added.

The initial rate of TC59682 activity was calculated against various concentrations of 2KGA as described in Section 2.17 and fitted to the hyperbolic saturation curve and thus displayed Michaelis-Menten kinetics (Figure 4.8).

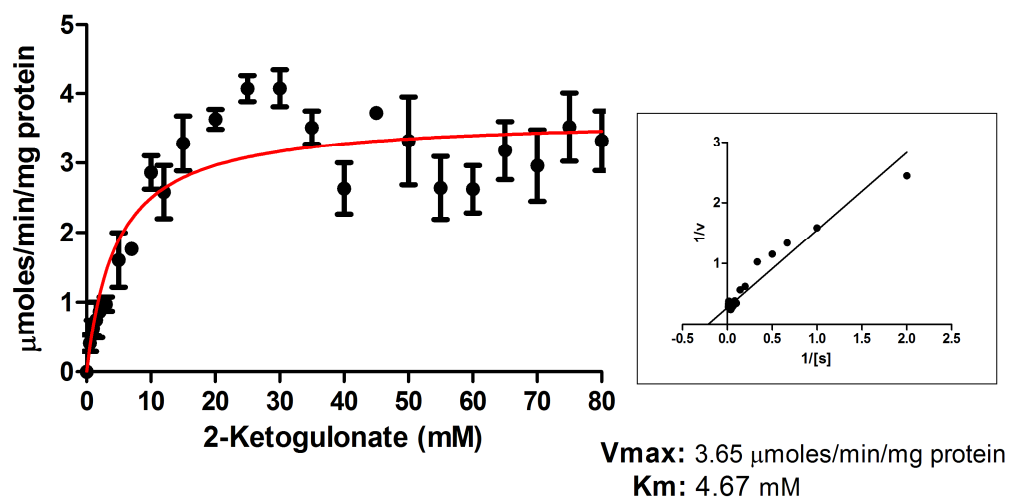


Figure 4.8: Activity of TC59682 against various concentrations of substrate 2-keto-L-gulonate. Assays were performed using (200 μL total reaction volume): 0.4 μg purified recombinant enzyme, 0.25mM (final) NADH (coenzyme) in 100mM HEPES buffer pH 7.5 at 37°C. Plot represents the mean of triplicate assays with error bars representing standard deviation. The red bar represents the hyperbolic curve of Michaelis-Menten kinetic analysis fitted using GraphPad Prism version 5.03. Inset: Linear transformation of the data in a double-reciprocal Lineweaver-Burk plot.

A V_{max} of 3.65 $\mu\text{mol/min/mg protein}$ and K_{m} of 4.67mM against 2KGA were calculated using Michaelis-Menten kinetics. The fitted Michaelis-Menten hyperbolic curve had a calculated R^2 of 0.85. As the K_{m} against 2KGA is calculated as 4.67mM, further kinetic analysis was conducted in the presence of 40mM (final) substrate to ensure the reaction was not substrate limited.

4.2.7 Coenzyme Affinity of TC59682

The affinity of recombinant TC59682 for the common coenzyme NADH was also investigated. The oxidation of NADH was monitored spectrophotometrically at 340nm as previously described in Section 2.16. A diluted aliquot of fraction 7 of

purified recombinant TC59682 (Figure 4.2) was used in the analysis. No activity was observed in all negative controls (Figure 4.9) suggesting that enzyme TC59682 was responsible for the observed oxidation of NADH. This is supported by the no enzyme (NoE) control.

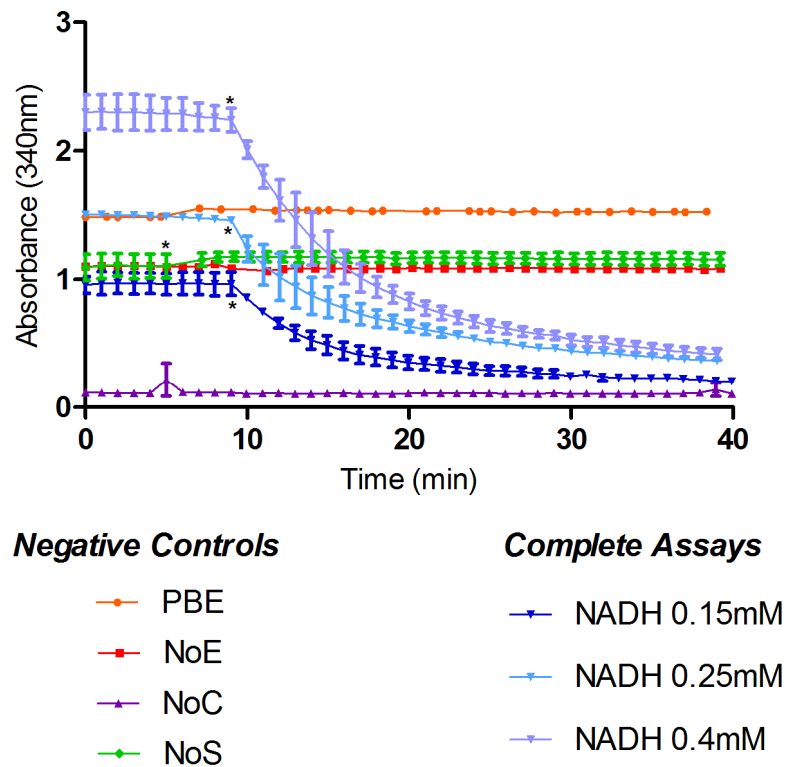


Figure 4.9: Representation of the TC59682 activity assays conducted with differing concentrations of the coenzyme NADH. Assays were performed using (200 μ L total reaction volume): 1 μ g purified recombinant enzyme, 40mM 2-keto-L-gulonate (substrate) and in 100mM HEPES buffer pH 7.5 at 37°C. Plot represents the mean of triplicate assays with error bars representing the standard deviation. Asterisk indicates the addition of substrate. Dark Blue solid triangle – assay with all components including: 0.15mM (final) NADH; Light Blue solid triangle – assay with all components including 0.25mM (final) NADH; Teal solid triangle – assay with all components including 0.4mM (final) NADH; Orange solid circle – PEB, protein extraction buffer added substituted for purified enzyme, no purified TC59682 enzyme added; Red solid square – NoE, no enzyme added; Purple solid triangle –NoC, no coenzyme added; Greens solid diamond – NoS, no substrate added.

The initial rate of TC59682 activity was calculated against various concentrations of NADH as described in Section 2.17 and fitted to the hyperbolic saturation curve, displaying Michaelis-Menten kinetics (Figure 4.10).

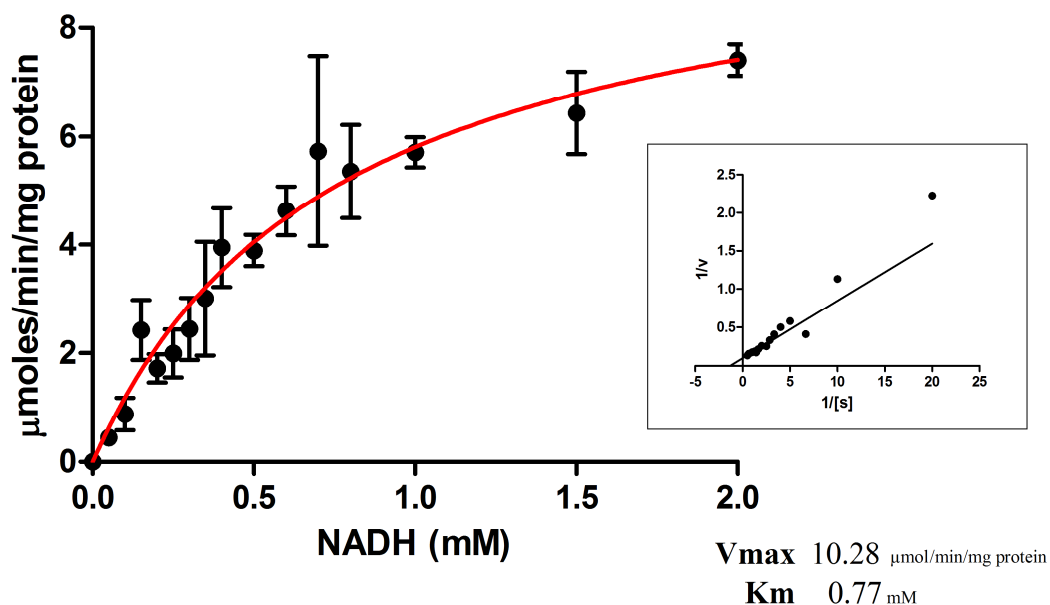


Figure 4.10: Activity of TC59682 against various concentrations of coenzyme NADH. Assays were performed using (200 μL total reaction volume): 1 μg purified recombinant enzyme, 40 mM (final) 2-keto-L-gulonate (substrate) in 100 mM HEPES buffer pH 7.5 at 37 $^{\circ}\text{C}$. Plot represents the mean of triplicate assays with error bars representing standard deviation. The red bar represents the Michaelis-Menten kinetic analysis fitted using GraphPad Prism version 5.03. Inset: Linear transformation of the data in a double-reciprocal Lineweaver-Burk plot.

A V_{max} of 10.28 $\mu\text{mol/min/mg protein}$ and K_m of 0.77 mM against NADH were calculated using Michaelis-Menten kinetics. The fitted Michaelis-Menten hyperbolic curve was shown to be a close fit with the calculated data with a resultant R^2 of 0.96. Transformation of the values in a double-reciprocal plot (Lineweaver-Burk plot, Figure 4.10 Inset) indicates the lower concentrations tested were less accurate, suggesting the sensitivity of the equipment used not appropriate at this lower level. Further analysis of TC59682 activity showed

TC59682 was also capable of utilising NADPH (see Section 4.2.6.5). The Kinetic parameters of this activity were not investigated further in this study.

Based upon the calculated K_m of 0.77mM against NADH, further kinetic analysis was conducted in the presence of 1mM (final) coenzyme. General convention states a concentration of 10 times the K_m value should be used to ensure saturation (Campbell and Farrell, 2007); however, coenzyme concentrations were not increased beyond 1mM to ensure spectrophotometric readings remained within the range of the equipment used.

4.2.8 Optimal Temperature of TC59682 Activity

The optimal temperature for the reaction of the putative 2-ketogluconate reductase encoded by *TC59682* in the presence of substrate 2KGA and coenzyme NADH was tested over a range of 20°C at 5°C increments (Figure 4.11). Activity was monitored spectrophotometrically at 340nm under conditions previously determined optimal (100mM HEPES pH 7.5, 40mM 2KGA, 1mM NADH).

The initial rate of recombinant TC59682 activity across the tested range was calculated as previously described in Section 2.17 with 35°C and 45°C showing the greatest activity (Figure 4.11). No significant difference was identified between these temperatures; therefore 35°C was selected.

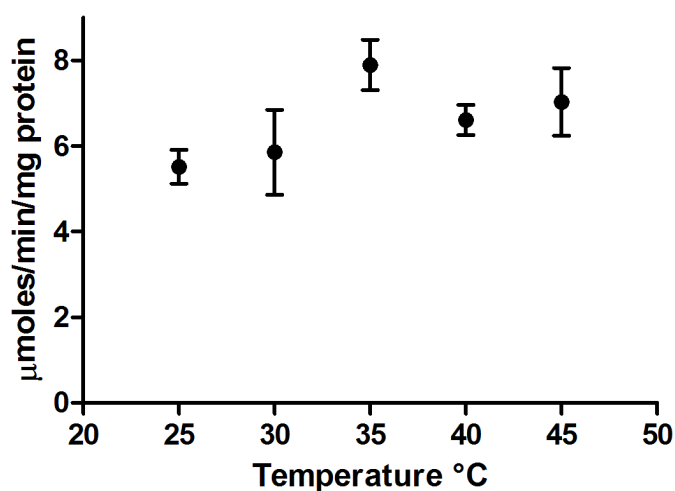


Figure 4.11: Temperature of optimal TC59682 activity measured over a range of 20°C. Assays were performed using (200μL total reaction volume): 1μg purified recombinant enzyme, 40mM (final) 2-keto-L-gulonate (substrate) and 1mM (final) NADH (coenzyme) in 100mM HEPES buffer pH 7.5. Plot represents the mean of triplicate assays with error bars representing standard deviation.

4.2.9 Substrate Range of Putative Recombinantly Expressed *Vitis vinifera* Enzymes

The activity of the candidate 2-ketogluconate reductases TC59682 and TC55752 (step 2a of the primary-Asc pathway in *V. vinifera*), candidate gluconate 5-dehydrogenases TC58004 and TC55097 (step 2b of the secondary glucose pathway in *V. vinifera*) and L-IdnDH.2 (putative homologue of L-IdnDH.1) was tested against a broad range of substrates. The substrates tested were selected due to their presence in either the *V. vinifera* or bacterial pathway's, or due to tentative annotations of candidates during bioinformatic analysis.

Activity of purified recombinant TC59682 was tested under conditions previously determined (200μL total reaction volume: 1mM coenzyme, 40mM substrate, 100mM HEPES pH 7.5, 35°C).

Putative 2KGR TC59682 displayed a broad substrate range with activity against 6 of the 9 substrates tested (Figure 4.12). The highest activity detected was against 2KGA in the presence of coenzyme NADPH, suggesting a preference for NADPH binding. Activity was also detected against L-idonate in the presence of coenzyme NAD⁺ and NADP⁺, indicating the potential reversibility of the enzyme. This observed activity was at a decreased rate, 37-fold and 26-fold lower than compared to 2KGA respectively. Activity was also observed against D-gluconate and 5-keto-D-gluconate, at a rate 30-fold and 125-fold lower than 2KGA respectively. Interestingly, TC59682 was found to be active against L-ascorbate, the precursor to 2KGA in the primary-Asc *V. vinifera* pathway. L-Ascorbate was shown to be the second-most active substrate tested, at a rate 8.9-fold (with coenzyme NADH) and 14.7-fold (with coenzyme NADPH) lower than observed with 2KGA. Control assays were also run including NoE (no enzyme) and NoC (no coenzyme). All control assays showed no observed activity except those against L-ascorbate (data not shown). These values were subtracted from the L-ascorbate values displayed. The observed activity suggests 2KGA is the preferred substrate of TC59682. The utilisation of both NAD(P)⁺ and NAD(P)H suggests TC59682 is not coenzyme specific.

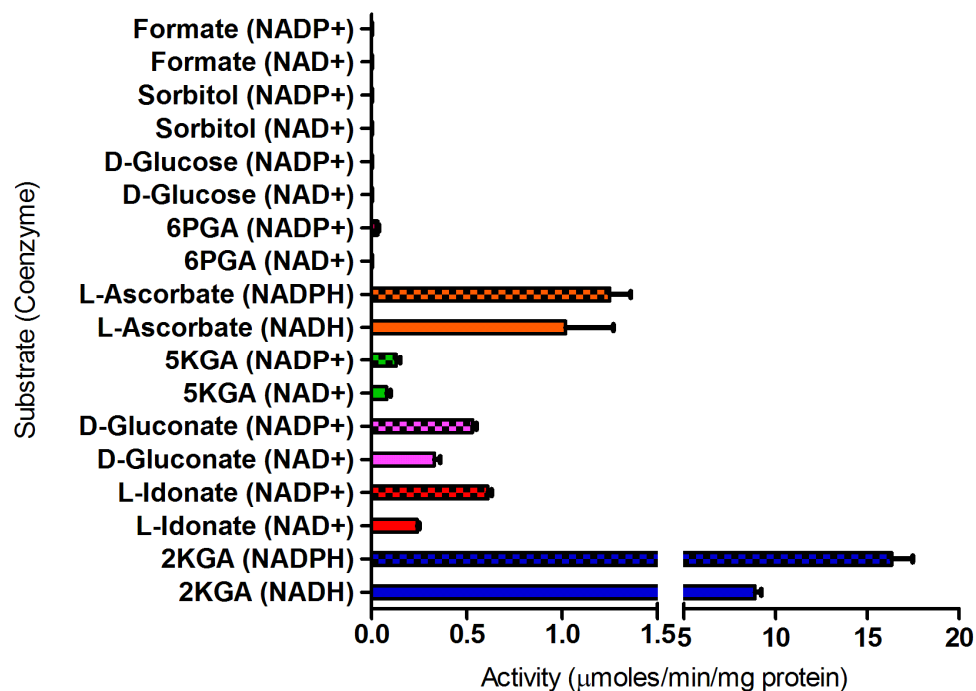


Figure 4.12: Substrate activity of purified heterologously expressed TC59682. Assays were performed using (200μL total reaction volume): 1μg purified enzyme, 40mM (final) substrate and 1mM (final) NADH (coenzyme) in 100mM HEPES buffer pH 7.5 at 35°C. The bars represent the mean of triplicate assays with error bars representing standard deviation. 2KGA: 2-keto-L-gulonate. 5KGA: 5-keto-D-gluconate. 6PGA: 6-phosphogluconate

TC55752, a putative 2KGR, was tested under conditions previously determined optimal for TC59682. TC55752 exhibited a narrow substrate range. Activity was observed against L-Asc and 2KGA in the presence of coenzyme NADH and NADPH (Figure 4.13). A low level of activity was also observed against D-gluconate and L-idonate in the presence of NADP⁺ only. This suggests TC55752 is capable of utilising both coenzyme NAD(P)⁺ and NAD(P)H dependent upon the substrate involved.

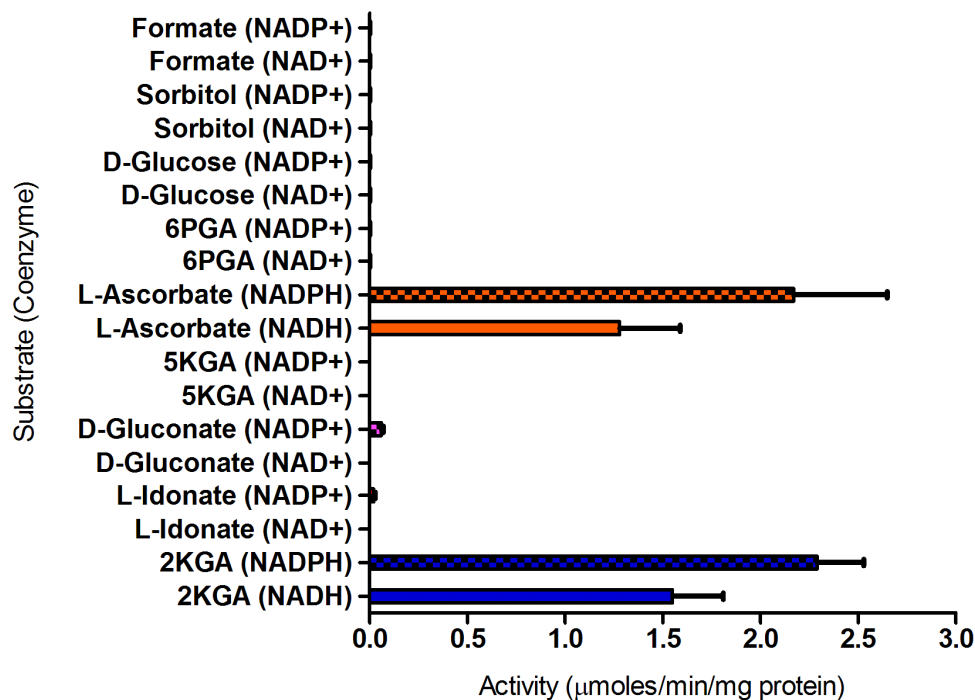


Figure 4.13: Substrate activity of purified heterologously expressed TC55752. Assays were performed using (200μL total reaction volume): 1μg purified enzyme, 40mM (final) substrate and 1mM (final) NADH (coenzyme) in 100mM HEPES buffer pH 7.5 at 35°C. The bars represent the mean of triplicate assays with error bars representing standard deviation. 2KGA: 2-keto-L-gulonate. 5KGA: 5-keto-D-gluconate. 6PGA: 6-phosphogluconate

Activities of recombinant TC58004 and TC55097 were tested under conditions described by Ameyama and Adachi (1982a, 0.15mM coenzyme, 20mM substrate, 1.7mM MgCl₂, 20mM Glycine pH 10, 30°C). L-IdnDH.2 was tested under conditions identified optimal for L-IdnDH.1 (DeBolt, 2006, 0.25mM coenzyme, 20mM substrate, 100mM Tris-HCl pH 8, 30°C).

Table 4.2: Summary of substrate activity of purified heterologously expressed TC58004, TC55097 and L-IdnDH.2. All assay combinations described were performed in triplicate

Candidate	TC58004	TC55097	L-IdnDH.2
Substrate - Coenzyme	Activity ($\mu\text{mol}/\text{min}/\text{mg}$ protein)		
2-Keto-L-gulonate			
NADPH	0	0	0
NADH	0	0	0
5-Keto-D-gluconate			
NADP ⁺	0	0	0
NAD ⁺	0	0	0
D-Glucose			
NADP ⁺	0	0	0
NAD ⁺	0	0	0
L-Ascorbate			
NADPH	0	0	0
NADH	0	0	0
D-Gluconate			
NADP ⁺	0	0	0
NAD ⁺	0	0	0
L-Idonate			
NADP ⁺	0	0	0
NAD ⁺	0	0	0
6-Phosphogluconate			
NADP ⁺	0	0	0
NAD ⁺	0	0	0
Sorbitol			
NADP ⁺	0	0	0
NAD ⁺	0	0	0
Formate			
NADP ⁺	0	0	0
NAD ⁺	0	0	0

No detectable activity was observed with TC58004, TC55097 and L-IdnDH.2 against the substrate/coenzyme combinations tested (Table 4.2) suggesting the extracted recombinant proteins were inactive under the conditions tested.

4.2.10 Identification of Product Obtained from Candidate TC59682's Primary Reaction

Samples of an endpoint assay of recombinant TC59682 (performed as described in Section 2.16) conducted in the presence of 2KGA and NADH were processed by Flinders Analytical Services (Section 2.18) to confirm the reaction product. L-Idonate is the expected product of this reaction. Unfortunately, both the 2KGA standard (Figure 4.14 A) and L-idonate standard (Figure 4.14 B) have identical

retention times. Due to this, 2KGA and L-idonate were unable to be separated in mixed-standard samples. Modification to the separation procedures was unable to separate the compounds with an effective HPLC separation method unable to be designed in the required timeframe of this project. Spectrophotometric monitoring of the assay (as described in Section 2.16) showed the substrate-dependent oxidation of NADH (Figure 4.7). This suggests 2KGA underwent catabolism, forming a product. The chromatogram of the assay performed (Figure 4.14 C) shows a single peak with a retention time of 5.88 minutes. One could conclude that this singular peak is representative of both the reaction product and un-catabolised substrate, which would suggest L-idonate as the reaction product. This however, is not enough evidence to conclusively state that L-idonate is the product of this reaction. The development of a HPLC method enabling the separation of the un-catabolised substrate from the product prior to mass spectrometry or nuclear magnetic resonance spectroscopy is required to enable conclusive identification of the assay product.

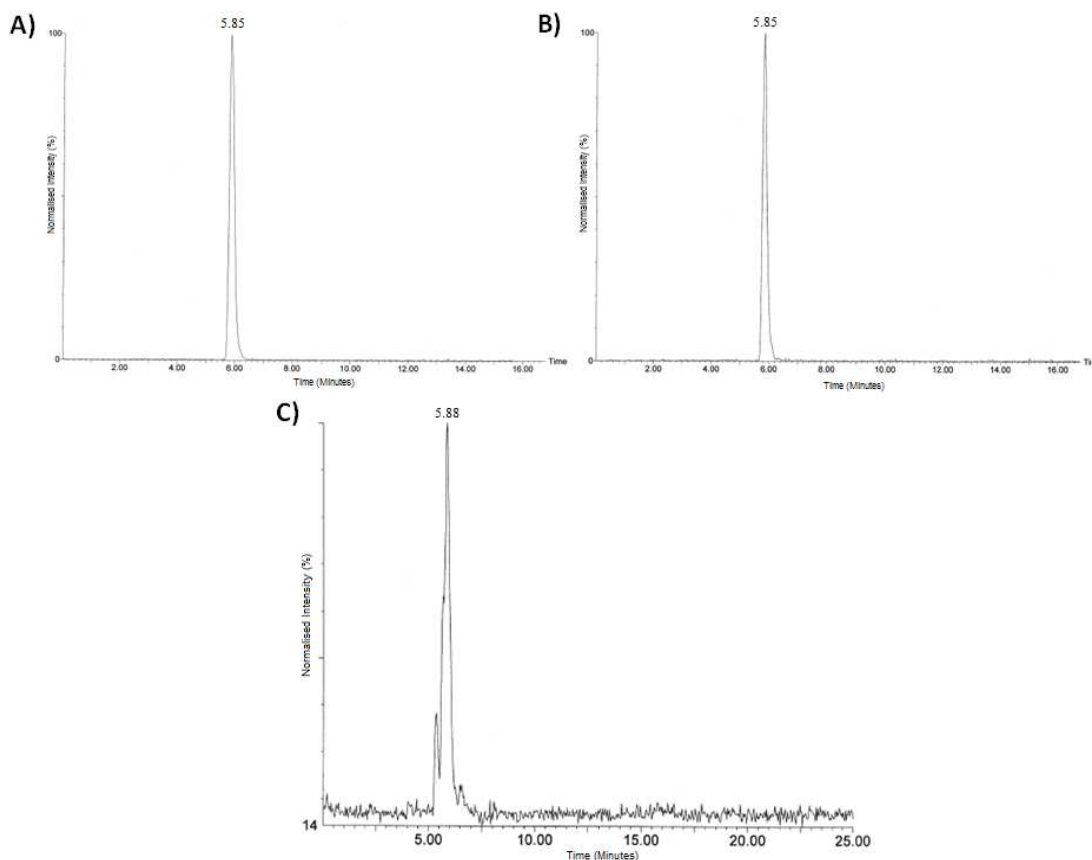


Figure 4.14: Trace of MS detection of HPLC separated samples; A) 2-keto-L-gulonate standard, eluting 5.85 minutes. B) L-idonate standard, eluting 5.85 minutes and C) TC59682 end-point assay, major peak eluting 5.88 minutes. Performed by Flinders Analytical Services (<http://www.flinders.edu.au/research/flinders-laboratories/flinders-analytical/>).

To provide further evidence supporting L-idonate as the assay product, a 2-step assay was designed under the conditions deemed optimal for TC59682. It has been previously determined that L-IdnDH.1 is specific to L-idonate and is not reactive against 2KGA (DeBolt, 2006). Should L-idonate be the product of the TC59682 reaction, the addition of L-IdnDH.1 to a completed assay would result in the generation of 5KGA, reducing the NAD^+ present (Figure 4.15). The oxidation of NADH by TC59682 and subsequent reduction of NAD^+ by L-IdnDH.1 was monitored spectrophotometrically (Figure 4.16).

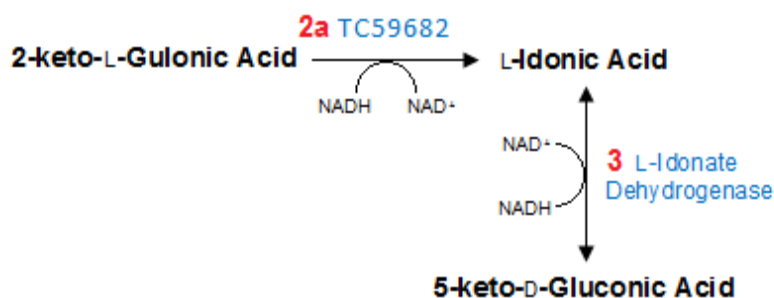


Figure 4.15: Summary of the reaction expected by the 2-step assay. Enzymes are shown in blue with the steps of the pathway labelled in red. TC59682 is suggested to be responsible for step 2a of the primary (Asc-C4/C5) pathway of TA synthesis identified in Vitaceae. L-Idonate dehydrogenase (L-IdnDH.1) has been confirmed as responsible for step 3.

The first step of the assay, the activity of TC59682 against 2KGA, was conducted as previously described (Section 2.16). The ceasing of NADH oxidation, as indicated by a flat-line in decreased absorbance was deemed the completion of TC59682 activity (Figure 4.16). Purified recombinant L-IdnDH.1 was then added to the assay. The expected increase in absorbance was observed post-L-IdnDH.1 addition, supporting L-idonate as the product of TC59682 catalytic activity against 2KGA (Figure 4.16). Controls of NoE (no enzyme) and TC59682 activity with no added L-IdnDH.1 were performed to ensure the observed increase in absorbance was attributed solely to the addition of recombinant L-IdnDH.1 (Figure 4.16).

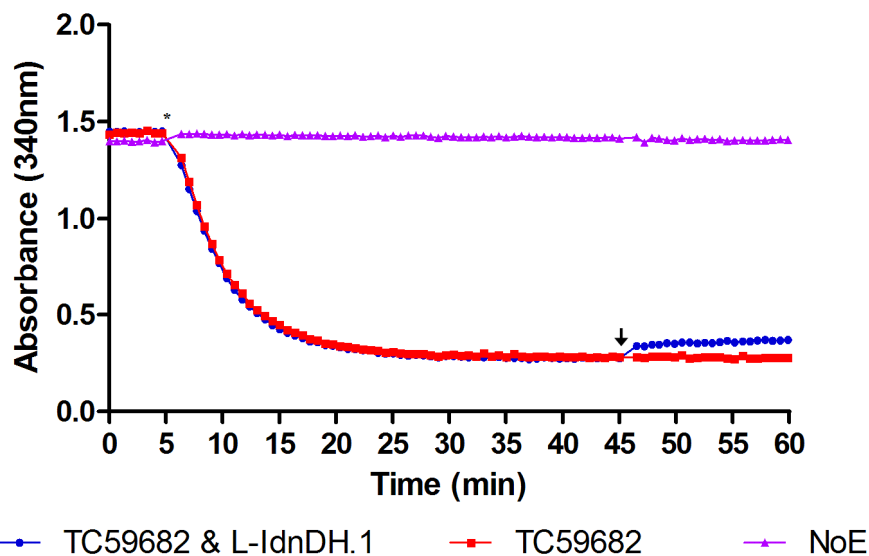


Figure 4.16: 2-step assay using purified heterologously expressed TC59682 and L-IdnDH.1. * Indicates the addition of substrate 2-keto-L-gulonate; the Arrow indicates the addition of L-IdnDH.1. Assays were performed using 1 μ g purified TC59682 and 1.2 μ g purified L-IdnDH.1, 40mM (final) 2-keto-L-gulonate (substrate) and 1mM (final) NADH (coenzyme) in 100mM HEPES buffer pH 7.5 at 35°C. Blue solid circles – Assay of TC59682 with added L-IdnDH.1; Red solid squares – Assay of TC59682, no L-IdnDH.1 added; Purple solid triangle – NoE, no enzyme added, negative control.

4.3 Discussion

Tartaric (TA) and malic (MA) acids account for 69-90% of total acid in the grape berry (Kliewer, 1966, Lamikanra *et al.*, 1995). Although the acids are structurally similar, the pathway's involved in the biosynthesis of TA (reviewed by Loewus, 1999) and MA (reviewed by Sweetman *et al.*, 2009) are vastly different. To date, a single enzyme, L-idonate dehydrogenase 1, has been identified in the TA biosynthetic pathway (DeBolt *et al.*, 2006). Chapter 3 described the identification of three candidate enzymes for steps 2a of the primary-Asc and 2b of the secondary glucose pathway. These candidates, a 2-ketogluconate reductase and

gluconate 5-dehydrogenase respectively, were identified in the *V. vinifera* genome based on the high level of sequence similarity to known bacterial enzymes.

TC61548, *TC59682* and *TC55752*, each encoding a putative 2-ketogluconate reductase were successfully amplified from pre-véraison berry cDNA and cloned into pET-14b.

TC59682 was purified in high yields enabling characterisation from a single fraction. Visualisation of the purified protein via SDS-PAGE identified an additional band, approximately 29 kDa co-eluting with the HisTag bound *TC59682*. Extended wash periods prior to elution and purification at 4°C did not remove this band. This unidentified band may be a breakdown product or partially expressed *TC59682*, or a protein that has interacted with *TC59682* during the purification process.

The activity of *TC59682* against the substrates tested was monitored spectrophotometrically at 340nm. Activity was not observed until the addition of substrate to the assay, suggesting in all tested cases, the observed oxidation of NAD(P)H was due to *TC59682* activity. Analysis of the initial rate data of *TC59682* against 2KGA using a sigmoidal model shows a closer fit (Figure 4.8) with an R^2 of 0.87 as compared to 0.85 of Michaelis-Menten kinetics. This suggests a cooperative or allosteric mechanism may be operating. The kinetic values for the allosteric model were not substantially different to the Michaelis-Menten model, suggesting if allosteric, any cooperation is minimal. Further investigations into the mode of the *TC59682*'s activity are required to determine if an allosteric mechanism of substrate binding is operational. Regulation at an intermediate position may suggest the intermediate involved was a component of multiple pathway's. Intermediate regulation may also be used to alter cellular metabolism under stress conditions.

A K_m of 4.67mM was determined for *TC59682* against 2KGA. This low K_m value suggests *TC59682* has a high binding affinity to 2KGA. Determination of kinetic parameters in the reverse direction (defined as the conversion of L-idonate to 2-keto-L-gulonate) could not be calculated due to the limited availability of L-

Idonate. A K_m of 0.77mM for NADH against TC59682 was also determined. The concentration of free NADH in potato tuber mitochondria was detected at 100-150 μ M (Kasimova *et al.*, 2006) whereas cytosolic NADH was measured at <5 μ M in spinach leaf cells (Heineke *et al.*, 1991). These values are a fraction of the determined K_m for TC59682 against NADH. This suggests the majority of TC59682 is in its free state, suggesting TC59682's binding of NADH is inefficient. The K_{cat} (turn over number) of TC59682 activity against 2KGA was also calculated. The number of active sites TC59682 possesses has yet to be determined; however, the UniProt database (<http://www.uniprot.org/>) lists 2 putative (*Dictyostelium discoideum*, UniProt #Q54DP1 and *Bacillus subtilis*, UniProt #O32264) and 1 identified (*E. coli* K12 #P37666) 2-ketogluconate reductase enzymes with three active sites, based upon sequence similarity. Therefore, it was assumed TC59682 possesses three active sites. With this assumption, K_{cat} was calculated as 17497.6 sec⁻¹. Recombinant TC59682 therefore has a calculated K_{cat}/K_m value, based on the assumption of three active sites, of $3.742 \times 10^6 \text{ M}^{-1} \text{ S}^{-1}$. A K_{cat}/K_m value of between 10^8 and 10^9 suggests near-perfect efficiency (Rogers and Gibon, 2009), suggesting TC59682 is a moderate to highly efficient enzyme in respect to the binding of 2KGA. It is important to note that this calculation was performed with the assumption of three substrate binding active sites on a monomeric protein. The identification of active sites and protein interactions *in situ* are required.

The true parameters of an enzyme's activity need to be calculated under biologically relevant conditions (Cornish-Bowden, 1984). *In situ* analysis of protein activity is required to confirm the aforementioned values in TC59682's native environment. The aforementioned kinetic values relate to the activity of recombinant TC59682 in the forward direction (defined as the conversion of 2KGA to L-idonate) of the TA biosynthetic pathway in *V. vinifera*. A 6x HisTag was fused to the recombinant protein, later used in the purification process and was not cleaved prior to kinetic analysis. Investigations by Carson *et al* (2007) showed the addition of these purification tags did not result in a conformational change of the proteins native structure. Chant *et al* (2005) investigated the addition of a HisTag on the activity of the gene regulatory protein AreA in *Aspergillus nidulans* and showed function was not altered. Therefore, it is

unlikely that the presence of the HisTag during the characterisation of enzymatic activity resulted in altered calculated values. System specific investigations however are required to confirm this.

The pH range and buffer type at which recombinant protein TC59682 was most reactive was investigated (Figure 4.6). Activity was detected at all pH concentrations tested, with pH 7.5 in 100mM HEPES observed to be most reactive. Although activity was detected at pH 7.5 utilising buffers Tris-HCl, Glycine and McIlvaine, this activity was lower under the same conditions as HEPES pH 7.5. This suggests that the alternative buffers may be affecting the enzyme activity. Due to the higher level of activity observed utilising HEPES pH 7.5, this buffer was utilised throughout all enzyme testing.

The activity of the purified TC59682 was analysed against a number of substrates selected due to their presence in the bacterial or *V. vinifera* pathway's, or due to annotation suggesting specified activity. The V_{max} and K_m of TC59682 against 2KGA were calculated as 3.65 $\mu\text{mol}/\text{min}/\text{mg}$ protein and 4.67mM respectively (Figure 4.8) and against the coenzyme NADH as 10.28 $\mu\text{mol}/\text{min}/\text{mg}$ protein and 0.77mM respectively (Figure 4.10). A native 2-ketogluconate reductase purified from a cell free extract of *Acetobacter rancens* was calculated to have a K_m of 91mM against 2KGA and a K_m of 0.1mM against NADPH (NADH was not tested), with an optimum pH of 7.0 at 50°C (Chiyonobu *et al.*, 1976). These values, although highly specific to the enzyme and organism the enzyme originates, indicate TC59682 has a higher affinity to 2KGA.

The high level of activity observed against substrate 2KGA suggests 2KGA is the preferred substrate of TC59682, supporting TC59682 role the TA biosynthetic pathway. TC59682 showed activity against six of the nine compounds tested (Figure 4.13). Although active against multiple substrates, Asc, the second active substrate, was 8.9-fold (with coenzyme NADH) and 14.7-fold (with coenzyme NADPH) lower than observed with 2KGA. Activity was also detected against L-idonate, suggesting the potential reversibility of TC59682. The activity against L-idonate was 37-fold (with coenzyme NAD^+) and 26-fold (with coenzyme NADP^+) lower than observed with 2KGA, suggesting this is not the preferred direction of

the enzyme. The potential reversibility of TC59682 is of interest and warrants further investigation. A detailed thermodynamic analysis of this reaction will enable the ΔG of the reaction to be defined supporting the reversibility of this reaction *in vivo*. The observed activity of TC59682 against Asc suggests the possibility of a single enzyme catalysing the first two steps on the primary TA biosynthetic pathway. Activity against 2KGA was shown to be greater than Asc suggesting this as the preferred reaction. Melino *et al* (2009a) showed that in early berry development the metabolism of Asc to products TA and oxalate more active than Asc recycling suggesting TA biosynthesis is a gradual process with the synthesised Asc in immature berries predominantly catabolised, and predominantly recycled in mature berries without a significant change in genetic regulation. The ability for TC59682 to metabolise Asc may be utilised in mature berry tissue when Asc is predominantly recycled. Confirmation of this activity *in planta* is required.

To confirm the role of TC59682 in TA biosynthesis, the product of TC59682 catalysed oxidation of NADH in the presence of 2KGA requires identification. Unfortunately, the purification of 2KGA from its product was unsuccessful. The retention time of the expected product, L-idonate, was identical to the substrate 2KGA. Analysis of an endpoint assay shows a single peak at the retention time of 2KGA and L-idonate, suggesting L-idonate as the product of the reaction. This evidence is not conclusive, therefore a 2-step assay was designed utilising the specificity of L-IdnDH.1 to L-idonate. L-IdnDH.1, the only confirmed enzyme of the TA biosynthetic pathway, was shown to be highly substrate specific. L-IdnDH.1 is not reactive against 2KGA but has been shown to catalyse the reduction of NAD^+ while converting L-idonate to 5KGA (DeBolt, 2006). L-IdnDH.1 was added to a completed assay of TC59682 against 2KGA and NADH. The increase in absorbance observed suggests the reduction of NAD^+ present, suggesting L-idonate as the product of the reaction (Figure 4.16). The increase in absorbance observed attributed to L-IdnDH.1 activity was not large with a recorded activity of 0.22 $\mu\text{mol}/\text{min}/\text{mg}$ protein, compared to 5.2 $\mu\text{mol}/\text{min}/\text{mg}$ protein of TC59682. This may be attributed to the L-IdnDH.1 assay not conducted under optimal conditions or the produced L-idonate from the first stage of the assay being in low quantities, limiting L-IdnDH.1 activity (Figure 4.16).

Additionally, the initial reaction may yield lower than expected quantities of L-Idonate and NAD^+ , resulting in the low levels of activity observed. Further degradation and loss of NADH in the initial reaction is also a possible factor requiring further investigation. Additional NAD^+ was not added to the reaction as the oxidised NADH from the first reaction was thought to be adequate. The collective addition of NAD^+ and L-IdnDH.1 to the reaction may result in increased activity of L-IdnDH.1. Additionally, assuming the UV absorbance spectra of the product and substrate of this reaction is distinguishable, spectral analysis may be useful in the identification of the product. Determination of the product of TC59682's primary reaction and the quantities produced from the known substrates is therefore a priority.

Low quantities of soluble TC55752 (Figure 4.3) were successfully purified from a small batch-culture (100mL) expression system using a high detergent extraction buffer. A scale-up of the culture system (1L) did not result in a purified protein suggesting interactions in the larger cell volume decreased the stability of the protein or in such a large culture volume the protein became insoluble. Additional purification of the inclusion bodies with strong denaturing agents may have yielded greater quantities soluble TC55752 (Thatcher and Hitchcock, 1994, Widersten, 1998). Due to the limited quantity of TC55752 protein obtained, a complete kinetic investigation was not conducted. Tests to determine TC55752 substrate and cofactor specificity were performed. The substrate specificity of recombinant TC55752 was determined under conditions determined optimal for TC59682 activity.

TC55752 had a narrower substrate range than TC59682 with activity observed against 4 of the 9 substrates tested (Figure 4.13). Although the highest activity of TC55752 was detected against 2KGA in the presence of NADPH, the observed activity was 5.7-fold (with coenzyme NADH) and 7.1-fold (with coenzyme NADPH) lower than that observed with TC59682. This suggests TC55752 is capable only of low-level reactions or its primary substrate was not tested. The observed activity of TC55752 against L-ascorbate in the presence of NADPH was not significantly different (2-way ANOVA; $p = 0.6564$) to that of 2KGA. Activity was observed against D-gluconate and L-Idonate in the presence of NADP^+ at a

rate 38-fold and 114.5-fold less than 2KGA in the presence of NADPH. These results suggest TC55752 is not effective in catalysing the reverse reaction of L-idonate to 2KGA. The observed activity of TC55752 against 2KGA was 5.7-fold (with coenzyme NADH) and 7.1-fold (with coenzyme NADPH) lower than observed with TC59682. This difference may be attributed to the assay conditions optimised to TC59682 activity and not TC55752. Due to this, the substrate concentration used may not have been adequate and so limited the reaction, resulting in the low rates observed. Optimisation of assay conditions specific to TC55752 activity may result in increased activity. Optimisation specific to TC55752 activity was not performed due to the limited availability of stable purified protein. Addition of an agent to aid in stabilising the purified heterologously expressed sample would enable further testing without loss of activity. Bioinformatic analysis tentatively annotated TC55752 as a formate dehydrogenase based on sequence similarity (Table 3.1). This was investigated with activity of TC55752 tested against formate as described by Nanba *et al* (2003). No activity was observed suggesting TC55752 is not an NAD-dependent formate dehydrogenase (Figure 4.13).

Increased activity of TC59682 and TC55752 was consistently observed against all tested substrates with the coenzyme NADPH suggesting NADPH as the preferred coenzyme. Affinity studies are required to confirm this; however, TC59682 and TC55752 have been confirmed as capable of utilising both NADH and NADPH (Figure 4.12 and 4.13 respectively). Aldo-keto reductase family members generally catalyse reversible reactions that are NADPH dependent, although some members display dual NADH/NADPH activity with only one aldo-keto reductase member identified as NADH specific. AKR members capable of dual NADH/NADPH activity have been shown to have a higher affinity to NADPH than NADH (Di Luccio *et al.*, 2006). NADH and NADPH have several specific roles within the cell. NADH has been implicated in multiple roles including protein modification, modulating cellular energy metabolism, gene expression and cell death (reviewed by Berger *et al.*, 2004, Ying, 2008). NADPH has been proven to be key in the regulatory control of fundamental cellular processes including synthesis of fatty acids, steroids, and DNA as well as a key component in cellular antioxidation (reviewed by Berger *et al.*, 2004, Ying, 2008). The high

activities observed of TC59682 and TC55752 against both NADH and NADPH suggest the enzymes are not specific to either coenzyme. The capacity to utilise whichever molecule is available adds to the flexibility of the enzyme to catalyse reactions involving multiple substrates under various cellular conditions. Structural studies have shown AKR members to possess an α/β -barrel binding region. The flexibility of this region enables the catalysis of multiple substrates (Jez *et al.*, 1997). 2-Ketogluconate reductases in *Corynebacterium* sp (Truesdell *et al.*, 1991), *Erwinia* sp (Sonoyama *et al.*, 1987), *E. coli* (Jeudy *et al.*, 2006, Yum *et al.*, 1998a) and multiple acetic acid bacteria (Adachi *et al.*, 1978, Chiyonobu *et al.*, 1974, Chiyonobu *et al.*, 1976) have been identified as responsible for catalysing multiple reactions, aiding in the enzymes role of cellular detoxification. This suggests TC59682 and TC55752 may have additional roles within the cell. Cellular localisation of TC59682 and TC55752 is also important in understanding their enzymatic role within the cell. Currently, 21 genes with the AKR signature have been identified throughout the Arabidopsis genome, yet very little is known of their catalytic function (Simpson *et al.*, 2009a). Arabidopsis is a non-tartrate accumulating higher plant. Although characterisation of these identified genes within Arabidopsis would be beneficial, identification of these biosynthetic genes native to *V. vinifera* is required.

TC55752 was shown to catalyse the oxidation of NAD(P)H in the presence of Asc as efficiently as 2KGA, the proposed primary substrate of step 2a of the primary-Asc TA biosynthetic pathway. TC59682 was also observed catalysing the oxidation of NAD(P)H in the presence of Asc although at a much lower rate to that of 2KGA. The ability of these candidate enzymes to catalyse reactions involving Asc suggests the possibility of a single enzyme catalysing the first two steps of the primary-Asc TA biosynthetic pathway of *V. vinifera* (Figure 1.8). Speculation as to the involvement of dehydroascorbate (DHA) in the primary pathway is apparent with DHA proposed to be an intermediate compound (Green and Fry, 2005, Hancock and Viola, 2005). Investigation into the capacity of TC59682 and TC55752 to metabolise DHA would aid in increasing the understanding of this initial step, and the possible involvement of DHA within the pathway. The broad range of substrates identified against TC59682 and TC55752 suggests step 2a is not a regulatory step in TA biosynthesis or is a branch-point in

the biosynthetic pathway feeding alternative unassociated pathway's. No evidence for the latter has been found.

Purification of soluble TC61548 was not successful. Optimisation of expression conditions including induction temperature, duration, extraction buffer and IPTG concentration did not result in a purified soluble protein. Visualisation via SDS-PAGE shows a darkened band of the expected size in the insoluble fraction of the protein extract. Observation of the soluble fraction at the expected size shows a band visually similar to the pre-induction fraction. This suggests that TC61548 is expressed under these conditions; however, the protein is insoluble. Mehlin *et al* (2006) observed a correlation of high PI (isoelectric point) with protein insolubility in heterologously expressed *Plasmodium falciparum* proteins. Mehlin *et al* (2006) showed a PI of >6.0 had reduced success of solubility. TC61548 predicted PI is above this range (7.23, Table 3.5) suggesting it may be a contributing factor to its insolubility. Due to the insoluble nature of TC61548, alternative methods were tested to obtain a purified soluble sample. The high detergent buffer BugBuster™ (Novagen, Germany) was not successful in the purification of TC61548. As TC61548 was expressed under the tested conditions, extraction of the protein from the insoluble fraction under denaturing conditions and *in vitro* refolding under a decreasing urea gradient or via a protein refolding kit is the next course of action. Refolding into an active tertiary structure, however, is inefficient and requires additional optimisation (Novagen, 2006). Alternatively, the use of a vector with an associated solubility factor would be beneficial. The vector pET-32a(+) acts by fusing the expressed protein with the *E. coli* protein thioredoxin. Thioredoxin is a soluble thermo-stable protein which, in effect, pulls the recombinant protein into the soluble fraction (Novy *et al.*, 1995). This method enables *in vitro* protein folding with reduced error.

TC52437, TC58004 and TC55097 are candidate gluconate 5-dehydrogenases suggested responsible for step 2b of the secondary glucose-precursor TA biosynthetic pathway (Figure 1.8). TC58004 and TC55097, putative gluconate 5-dehydrogenases were successfully amplified from pre-véraison berry cDNA. The expected sequence of TC52437, the third selected gluconate 5-dehydrogenase was not successfully amplified. Predictive translation of the amplified sequence to

amino acids generated multiple stop codons throughout the putative protein sequence. This suggests TC52437 is not present in berry cDNA tissue as annotated in the Gene Index Project: Gene Indices: Grape database (www.compbio.dfc.harvard.edu/tgi) used. This database was constructed through the alignment of shotgun sequences of the *V. vinifera* cv Pinot Noir whereas the cDNA used in this study was *V. vinifera* cv Shiraz (Quackenbush *et al.*, 2000, Velasco *et al.*, 2007). Cultivar difference or a misalignment of 2 similar sequences may explain this discrepancy. Analysis of TC52437 was not pursued further.

High-yield TC55097 was successfully purified from large-scale culture (2L). TC58004 was successfully purified at a low-yield from a small culture (100mL) expression system. Scale-up of this protocol (1L) did not increase the yield of purified protein. The low-yield of TC58004 obtained suggests TC58004 may be unstable or toxic to the cell limiting expression or the purification procedure used was not sufficient. Extraction of the inclusion bodies or modifications to the purification protocol may yield higher quantities of soluble TC58004. Activity analysis performed using these purified samples and L-IdnDH.2 (samples obtained from M Hayes, University of Adelaide), the putative homologue of L-IdnDH.1, was unsuccessful with no activity observed. Although tested against 10 substrates, these proteins may be highly specific to a singular substrate, rendering the tests performed here negative. Post-translational modification is often used to regulate the activation of protein activity in eukaryotic systems. Predictive analysis of L-IdnDH.2, TC58004 and TC55097 identified multiple residues predicted to undergo phosphorylation (Table 3.5, L-IdnDH.2 results not shown). Expression in a eukaryote system capable of post-translational modifications such as *Saccharomyces cerevisiae* or baculovirus will eliminate this as a factor in protein inactivity. Di Luccio *et al* (2006) observed no catalytic activity of a candidate aldo-keto reductases. Further investigations showed it was still capable of binding both NADH and NADPH with similar affinities of other aldo-keto reductase members (Di Luccio *et al.*, 2006). Therefore, the binding activity of L-IdnDH.2, TC58004 and TC55097 to NAD(P)H was investigated. Predictive analysis of each candidates deduced amino acid sequence indicated the presence of an NAD(P)-binding domain (Table 3.4, L-IdnDH.2 results not shown). A wavelength scan of L-IdnDH.2, TC58004 and TC55097 was performed in the presence of NAD(P)⁺

and NAD(P)H without additional enzyme to enable calculation of each enzyme's dissociation constant (data not shown, method modified from Di Luccio *et al.*, 2006, Fromm, 1963). Preliminary experiments suggest NAD(P)H binding was not successful, indicating the lack of activity observed is enzymatic and not due to the appropriate substrate being analysed.

The activity of gluconate 5-dehydrogenase has been identified as highly unstable, with over 75% of activity lost within 3 days from samples purified from cell-free extracts of *Gluconobacter suboxydans* (Adachi *et al.*, 1979, Ameyama and Adachi, 1982a). Stability was increased via the addition of compounds gluconate or 5KGA. The observed inactivity of TC58004 and TC55097 may be a result of purification or extended storage times without a stabilising compound present in the buffer. Modifications to the purification protocol or analysis of activity immediately following purification may result in active protein samples.

TC59682 and TC55752 were successfully cloned, recombinantly expressed and purified. Substrate analysis of TC55752 indicates it is capable of catalysing step 2b of the primary-Asc TA biosynthetic pathway, although only at a low rate (as compared to TC59682). This low rate suggests TC55752 is not involved in TA biosynthesis and is expected to have a high affinity to a compound not tested in this study. Kinetic analysis of TC59682 showed high affinity to 2KGA, the forward substrate of the reaction. Preliminary identification indicates L-idonate as the reaction product. Reversibility of TC59682 was also confirmed with activity observed against L-idonate. Activity analysis of TC59682 supports its involvement in step 2a of the primary-Asc pathway. Correlation of gene expression data with the accumulation of TA over development (Chapter 5) will provide further support to TC59682 involvement in TA biosynthesis. Characterisation *in vitro* determines the capabilities of the enzyme; however, biological constraints may alter the efficiency of the enzyme *in vivo*. Due to this, comparison of *in vitro* and *in vivo* activity is required to obtain a definitive kinetic analysis. Enzyme activity has been shown to differ between species (Chiyonobu *et al.*, 1975b, Shinagawa *et al.*, 1976, Shinagawa *et al.*, 1978). Therefore *in situ* analysis is also a requirement in the tissue specific characterisation of enzyme activity (Chapter 5).

Chapter 5:

Characterisation of Various Physiological and Molecular Parameters of Tartaric Acid Biosynthesis in *Vitis vinifera* cv Shiraz over the 2007/2008 Season

5.1 Introduction

Grape berry development is a 3 phase process during which distinctive physiological and metabolic events occur. The first phase, berry formation, occurs immediately post-anthesis and is characterised by rapid cell growth and the accumulation of malic and tartaric acids (Ruffner and Hawker, 1977). Tartrate accumulation is exclusive to this developmental stage of berry formation during which the appearance of the immature berry tissue remains green and hard. During the second phase of development, denoted lag phase, cell division is minimal with change in berry size, colour and deformation minimal (Coombe and Iland, 2004, Skene and Hale, 1971). Berry ripening is the third phase of development characterised by rapid growth of berry tissue, the onset of anthocyanin and hexose accumulation (rise in °Brix) and the metabolism of malate causing an associated pH change. The initiation of berry ripening is termed véraison, observed visually by the acquisition of colour (in red fruit varieties) and a swelling and softening of the berry tissue due to water intake (Coombe, 1960, Coombe and Bishop, 1980). Véraison is a significant time in berry development as it sees a metabolic shift in which TA and MA accumulation ceases and MA undergoes catabolism. The monitoring of the progression of berry ripening, enables optimal harvesting of the berries for consumer purpose as either food-stuffs or in winemaking.

Qualitative real time polymerase chain reaction (QRT-PCR) is the touchstone for gene expression quantification (Bustin *et al.*, 2009) enabling the detection and measurement of minute amounts of RNA transcripts from numerous samples across a variety of sources (Bustin, 2000, Kubista *et al.*, 2006). The expression of individual genes of interest can therefore be analysed in specific tissues. This approach has been used successfully in a number of studies in berry tissue over development analysing the expression of genes including those involved in abscisic acid regulation (Wheeler, 2006), berry size (Davies *et al.*, 2006), cell wall metabolism and water transport (Schlosser *et al.*, 2008). QRT-PCR was used to identify L-idonate dehydrogenase 1 expression exclusively in green immature berry tissue (DeBolt, 2006). This expression pattern coincided with the period of TA synthesis, indicating specificity of the enzyme to the TA pathway and not

general metabolism. In this chapter the expression of the proposed TA biosynthetic genes will be analysed via QRT-PCR techniques.

The corresponding metabolic changes associated with the biosynthesis of TA during berry formation and its cessation at véraison is of significant interest in this study. In this chapter the defined stages of berry development will be determined via the analysis of the physiological changes previously described including berry weight, colour, hexose and organic acid accumulation. Definition of these developmental stages will enable the correlation of the accumulation of TA with the expression levels of the proposed TA biosynthetic genes. *In vivo* activity analysis has been used to support the developmental function of proteins in grape berry tissue for enzymes such as phosphoenolpyruvate carboxykinase (Ruffner and Kliewer, 1975), phosphoenolpyruvate carboxylase and malic enzyme (Lakso and Kliewer, 1975). The activity of the candidate enzymes for steps 2a and 2b of the primary Asc-C4/C5 and secondary glucose pathway respectively were tested *in vitro* (see Chapter 4). The activity of these enzymes extracted from berry tissue will also be described in this chapter and correlated with TA accumulation.

5.2 Results

5.2.1 Fresh Weight and °Brix

V. vinifera cv Shiraz (clone BVRC12 on Schwarzmann rootstock) were sampled every 3-4 days throughout development from the University of Adelaide Coombe vineyard, Waite Campus, Urrbrae, South Australia (elevation 123m, latitude 34°58'S). A randomized complete block design was employed to ensure a random selection across the vineyard was obtained. Samples collected across multiple vines were pooled and snap frozen until required. Allocation of the sampled berries into two sets enabled molecular and physiological characterisation to occur on the same berry sample.

Colour acquisition of berry tissue over development was observed visually (Figure 5.1). This observation enabled a non-destructive approximation of the phases of berry development infield. Onset of the developmental stage véraison was deemed the stage at which individual berries began to acquire colour.

Véraison was denoted as the time at which approximately 50% of the berries per bunch acquired colour.



Figure 5.1: Development of *V. vinifera* cv Shiraz berries sampled over the 2007/2008 season. Véraison occurred 60 days post-anthesis as indicated by the acquisition of colour by approximately 50% of the berries per bunch.

Physiological parameters including berry fresh weight (FW) and total soluble solids ($^{\circ}$ Brix) was analysed for each replicate (Figure 5.2). Based on this data set, the phases of berry development were determined to be berry formation 0-35 days, lag phase 35-60 days and berry ripening 60-110 days post-anthesis. The onset of hexose accumulation (rise in total soluble solids, $^{\circ}$ Brix), in conjunction with visual observations, enabled refinement of the date at which véraison occurred. These measurements indicate véraison occurred 60 days post-anthesis (January 1st 2008). Variation across replicates was minimal as indicated by the tight error bars. Harvest occurred at 105 days post-anthesis (February 15th 2008).

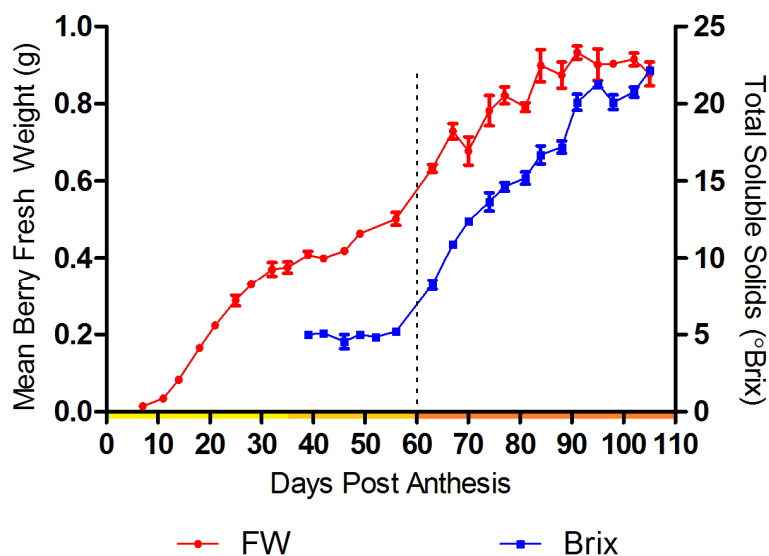


Figure 5.2: Accumulation of fresh weight (FW, closed red circles) and total soluble solids (°Brix, closed blue squares) over development of *V. vinifera* cv Shiraz berries sampled in quadruplicate over the 2007/2008 season. Error bars represent the standard error of the mean. Developmental stages are indicated by the coloured bar incorporated into the x-axis with berry formation, lag phase and berry ripening indicated in yellow, gold and orange respectively. Véraison occurred 60 days post-anthesis, indicated by the dotted line. This data has also been represented in Melino (2009) and Sweetman (2011).

5.2.2 Organic Acids Accumulation

Organic acid (OA) levels were determined from the same sample sets of berries as described in section 5.2.1. The accumulation of tartaric (TA) and malic acid (MA) occurred rapidly during stage 1 of berry development (Figure 5.3). TA accumulation occurred rapidly 0-20 days post-anthesis, with accumulation occurring at a slower rate with levels peaking 46 days post-anthesis. The quantity of TA remained constant throughout the remainder of berry development. MA also experienced accelerated accumulation 0-20 days post-anthesis, peaking 52 days post-anthesis. MA underwent catabolism post-véraison resulting in a decline in the acid level. Asc is known to exist in both a reduced and oxidised state within

the cell (reviewed by Buettner and Schafer, 2004). All Asc was reduced during analysis to enable total Asc quantification. Asc accumulation was sigmoidal with production in both stage 1 and stage 3 of berry development. Variation among replicates was minimal as indicated by tight error bars validating the sampling technique used.

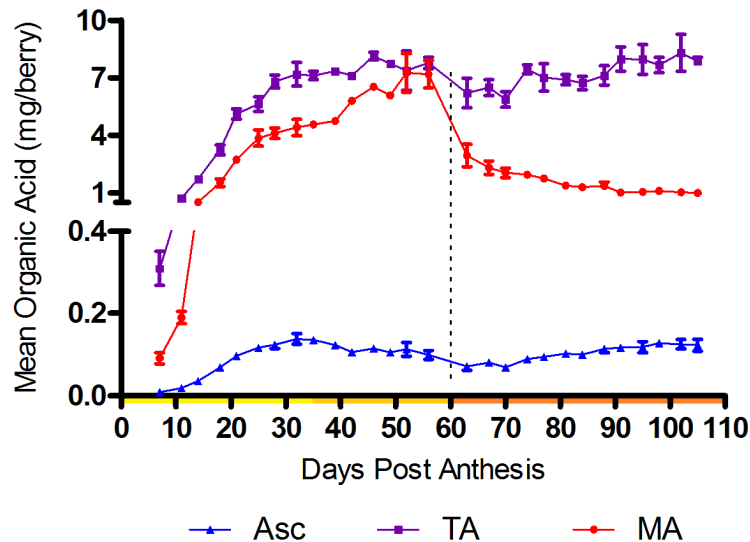


Figure 5.3: Accumulation of the organic acids ascorbate (Asc, blue closed triangles), tartrate (TA, purple closed squares) and malate (MA, red closed circles) over berry development. Berries were sampled in quadruplicate over the 2007/2008 season. Error bars represent the standard error of the mean. Developmental stages are indicated by the coloured bar incorporated into the x-axis with berry formation, lag phase and berry ripening indicated in yellow, gold and orange respectively. Véraison occurred 60 days post-anthesis indicated by the dotted line. This data has also been represented in Melino (2009) and Sweetman (2011).

5.2.3 Gene Expression Analysis utilising Qualitative Real Time PCR

The berries used for qualitative real time PCR (QRT-PCR) analysis were a subsample of the sampled *V. vinifera* cv Shiraz berries analysed for FW, °Brix

and OA accumulation (Sections 5.2.1 and 5.2.2). This enables a direct comparison of results without vine-to-vine or seasonal variation.

The expression of potential reference genes *Ankyrin*, *Ubiquitin* and *Actin* was analysed prior to the experiment using the PleX Grape database (www.plexdb.org). Sequences that showed steady expression levels across development under conditions described in the various experimental conditions were selected. *VvActin* was shown to be too variable across development and was not selected. *VvAnkyrin* (*Ank*) and *VvUbiquitin* (*Ubq*) were stably expressed and selected to normalise the data. Candidate gene expression was normalised against both *Ank* and *Ubq* with no difference between each house-keeping gene expression pattern observed. Data presented here show candidate expression patterns normalised against *Ank*. Four replicates were obtained for each timepoint; however, extractions did not obtain high quality RNA for all replicates. Therefore the three replicates with the highest quality of RNA were analysed.

Candidates *TC61548*, *TC59682* and *TC55752* are enzymes proposed to be involved in step 2a of the primary Asc-precursor TA biosynthetic pathway (Figure 1.8). *TC61548* expression (Figure 5.4 A) oscillates during berry formation. Although the expression was not constant throughout this stage, it was the stage with average peak *TC61548* expression. Expression decreased during lag phase and remained low throughout berry ripening. This pattern indicated that *TC61548* expression was associated with pre-véraison development. *TC59682* expression (Figure 5.4 B) peaked at anthesis and decreased 4-fold within 10 days of berry development. Expression increased at the initiation of berry ripening to a level half that of its peak during berry formation. This expression pattern suggests that, *TC59682* is strongly associated with the initial stages of berry development. Expression of *TC55752* (Figure 5.4 C) increased throughout berry formation. The level of expression steadied during lag phase with a slight decrease during berry ripening. This pattern of expression suggests that *TC55752* is associated with the latter stages of berry development, not during TA biosynthesis.

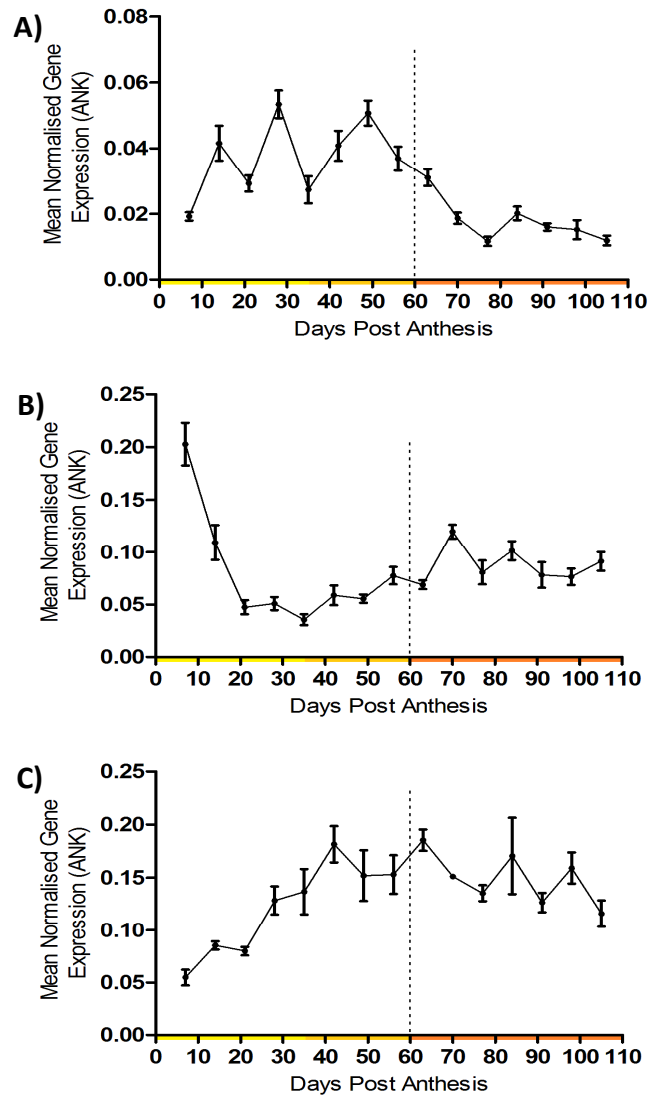


Figure 5.4: Analysis of gene expression of the candidates for step 2a of the primary Asc-precursor pathway (Figure 1.8). Berries were analysed in triplicate over the 2007/2008 season and normalised against the housekeeper *V. vinifera* Ankyrin. Error bars represent the standard error of the mean. Developmental stages are indicated by the coloured bar incorporated into the x-axis with berry formation, lag phase and berry ripening indicated in yellow, gold and orange respectively. Véraison occurred 60 days post-anthesis indicated by the dotted line. A) Candidate *TC61548*; B) Candidate *TC59682*; C) Candidate *TC55752*

TC58004 and *TC55097* are candidates for step 2b of the secondary glucose-precursor TA biosynthetic pathway (Figure 1.8). *TC58004* (Figure 5.5 A) showed minimal expression throughout berry formation, increasing in the lag phase and remaining high throughout berry ripening. Variability of *TC58004* expression in the post-véraison berry was higher as compared to the pre-véraison berry. *TC55097* (Figure 5.5 B) shows steady expression throughout each stage of development. This indicates that this gene's expression is not linked to a specific developmental phase. The level of expression was the lowest of all the candidates tested.

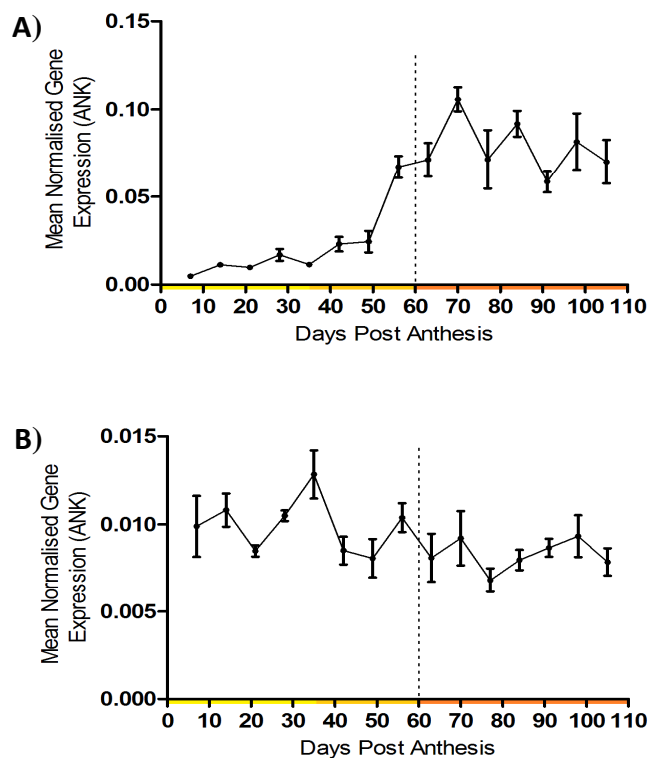


Figure 5.5: Analysis of gene expression of the candidates for step 2b of the secondary glucose-precursor pathway (Figure 1.8). Berries were analysed in triplicate over the 2007/2008 season and normalised against the housekeeper *V. vinifera* Ankyrin. Error bars represent the standard error of the mean. Developmental stages are indicated by the coloured bar incorporated into the x-axis with berry formation, lag phase and berry ripening indicated in yellow, gold and orange respectively. Véraison occurred 60 days post-anthesis indicated by the dotted line. A) Candidate *TC58004*, B) Candidate *TC55097*

L-IdnDH.1 is to date the only confirmed enzyme involved in TA biosynthesis (DeBolt *et al.*, 2006), responsible for step 3 of the Primary Asc-precursor pathway (Figure 1.8). *L-IdnDH.2* has been identified as a possible homologue to *L-IdnDH.1* based on a 70% nucleic acid and 77.59% amino acid identity (Hayes, DeBolt, Cook and Ford, manuscript in preparation). *L-IdnDH.1* expression (Figure 5.6 A) was strongly associated with the initial stage of berry development. Expression levels decreased 4-fold within 30 days of berry development. Expression levels remained minimal throughout the remainder of development with a slight increase

3 weeks pre-harvest. *L-IdnDH.2* expression (Figure 5.6 B) increased throughout berry development spiking at the transition of each stage between berry formation-lag phase, lag phase-berry ripening, and harvest. This expression pattern suggests that *L-IdnDH.2* is associated with the lag phase and berry ripening and not berry formation, the phase associated with TA biosynthesis.

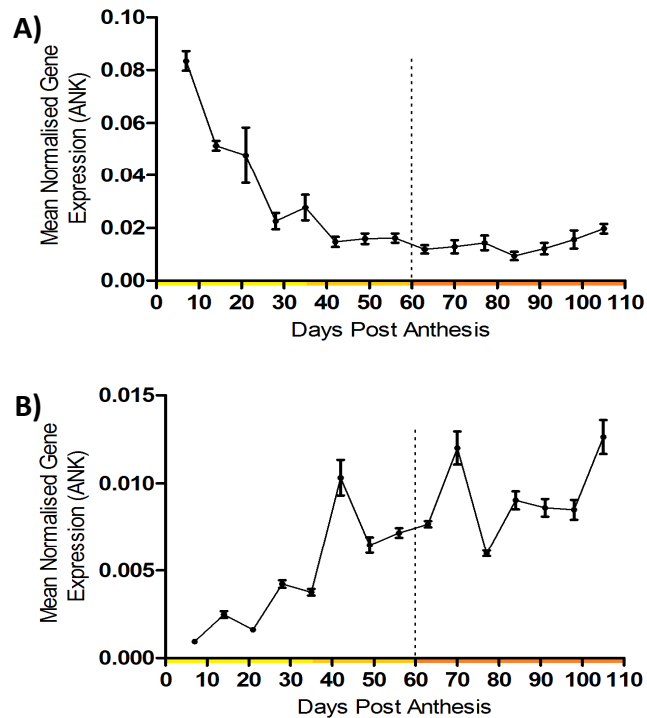


Figure 5.6: Analysis of gene expression of the enzyme *L-IdnDH.1* and possible homologue *L-IdnDH.2* for step 3 of the primary ascorbate-precursor pathway (Figure 1.8). Berries were analysed in triplicate over the 2007/2008 season and normalised against the housekeeper *V. vinifera* Ankyrin. Error bars represent the standard error of the mean. Developmental stages are indicated by the coloured bar incorporated into the x-axis with berry formation, lag phase and berry ripening indicated in yellow, gold and orange respectively. Véraison occurred 60 days post-anthesis indicated by the dotted line. A) Enzyme *L-IdnDH.1*; B) Candidate *L-IdnDH.2*

5.2.4 Enzyme Extractions

Soluble protein was extracted from the same set of sampled *V. vinifera* cv Shiraz berries analysed for FW, °Brix, OA accumulation and gene expression (Sections 5.2.1, 5.2.2 and 5.2.3) enabling a direct comparison between gene expression and protein activity. Enzyme extracts were used in spectrophotometric assays based on conditions determined in Chapter 4. Potassium cyanide (KCN) and octyl gallate (OG) were added to the assay buffer to inhibit the activity of the metabolic enzymes cytochrome oxidase (Baker *et al.*, 1987) and alternative oxidase (Albury *et al.*, 1996) respectively, preventing the oxidation of any NAD(P)H by these metabolic enzymes during the assay.

The concentration of protein extracts was measured to determine the amount of protein extracted from each timepoint throughout development (Figure 5.7). Analysis shows the level of protein extracted was consistent over development.

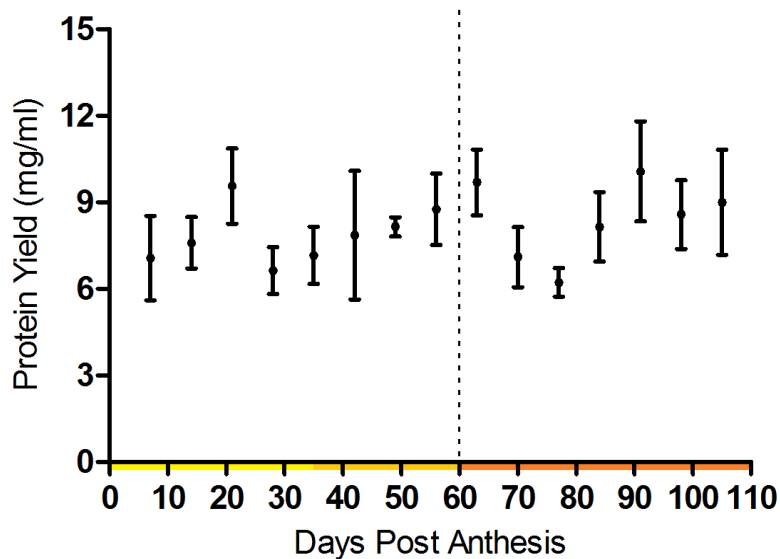


Figure 5.7: Quantity of protein extracted from *V. vinifera* cv Shiraz berry tissue following a 65% (w/v) PEG precipitation. Measurements were performed in triplicate with mean values shown. Error bars represent the standard error of the mean. Developmental stages are indicated by the coloured bar incorporated into the x-axis with berry formation, lag phase and berry ripening indicated in yellow, gold and orange respectively. Véraison is indicated by the dotted line.

Malate dehydrogenase (MDH) is a ubiquitous enzyme crucial in cellular metabolism involved in the citric acid cycle. The enzyme is responsible for catalysing the reversible reaction of oxaloacetate to malate in the presence of NADH/NAD⁺ (reviewed by Minárik *et al.*, 2002). Due to the enzyme's ubiquitous nature within the cell and the high content of malate within the berry, MDH was chosen as a positive control of protein extraction due to its high likelihood of being present in the extract.

Activity of the enzymes in the extract was observed spectrophotometrically in the presence of a specific cofactor and substrate. MDH activity was observed, in the presence of NADH and the substrate oxaloacetate, and monitored overdevelopment (Figure 5.8). MDH activity increased over berry development, with the greatest amount of activity in the post-véraison tissue. The greatest

amount of variation was also seen in this tissue. MDH activity showed that active protein was extracted at each timepoint over development. A negative control of added NADH without substrate was performed which showed no activity at all timepoints, indicating that the observed oxidation of NADH was due to enzymatic activity in the presence of the substrate.

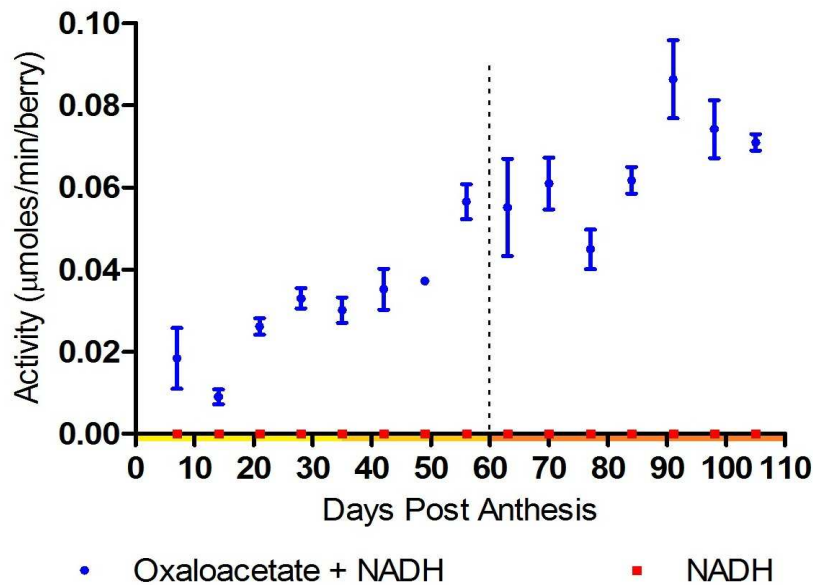


Figure 5.8: Activity of Malate Dehydrogenase (MDH) observed spectrophotometrically via the consumption of NADH in the presence of oxaloacetate (blue closed circles). A negative control of NADH without added substrate was also measured (red closed squares). Triplicate samples were extracted at each timepoint with mean values shown. Error bars represent the standard error of the mean. Soluble protein was extracted from *V. vinifera* cv Shiraz berry tissue over development. Developmental stages are indicated by the coloured bar incorporated into the x-axis with berry formation, lag phase and berry ripening indicated in yellow, gold and orange respectively. Véraison is indicated by the dotted line.

The enzyme responsible for catalysing step 2a of the Asc-precursor pathway (Figure 1.8) is a putative 2-ketogluconate reductase. This enzyme would be responsible for the reduction of 2KGA in the presence of NADH to L-idonate.

TC61548, TC59682 and TC55752 are candidates for this step. Enzyme extracts of each timepoint were observed spectrophotometrically for the oxidation of NADH in the presence of 2KGA (Figure 5.9). OG and KCN were also present to prevent metabolic oxidation of NADH. Activity against 2KGA was shown to increase over development, with the greatest activity in the post-véraison tissue. A high degree of variability was also detected in this tissue. A no substrate negative control was also performed, which showed no NADH oxidation at all timepoints.

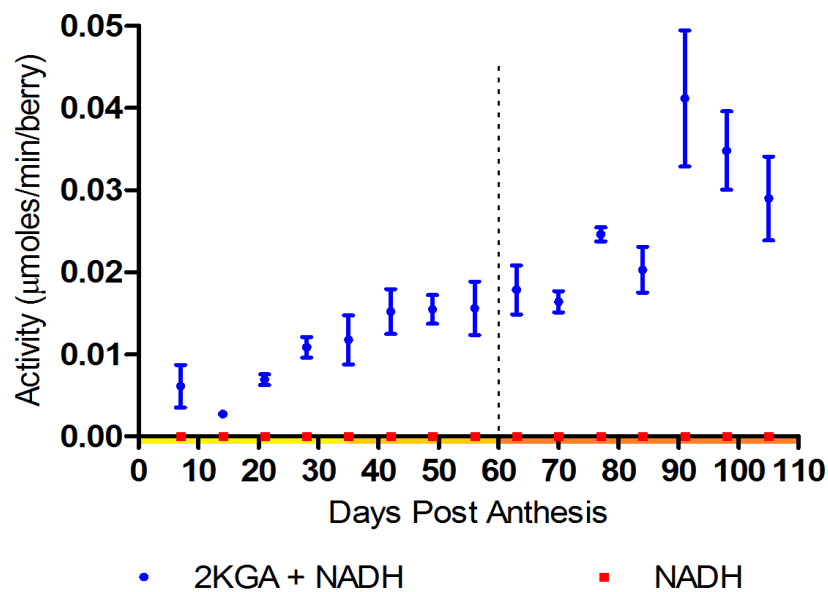


Figure 5.9: Activity of putative 2-ketogluconate reductase's observed spectrophotometrically via the oxidation of NADH in the presence of 2KGA (blue closed circles). A negative control of NADH without added substrate was also measured (red closed squares). Soluble enzyme was extracted from *V. vinifera* cv Shiraz berry tissue over development. Triplicate samples were extracted at each timepoint with mean values shown. Error bars represent the standard error of the mean. Developmental stages are indicated by the coloured bar incorporated into the x-axis with berry formation, lag phase and berry ripening indicated in yellow, gold and orange respectively. Véraison is indicated by the dotted line.

The enzyme responsible for catalysing step 3 of the Asc-precursor pathway (Figure 1.8) is L-idonate dehydrogenase (DeBolt *et al.*, 2006). This step involves the interconversion of L-idonate to 5KGA in the presence of NAD⁺/NADH. L-Idonate is not commercially available and so this activity was not tested, however, it was assayed in the reverse direction, i.e. with 5KGA as the substrate in the presence of NADH. Under these conditions no activity was detected at any timepoint throughout development (data not shown).

The step of the pathway whereby the secondary glucose-precursor and primary Asc-precursor pathway intersect is step 2b, catalysed by a putative gluconate 5-dehydrogenase. TC58004 and TC55097 are both candidates for this step (Figure 1.8). Activity was tested in the presence of NAD⁺ and gluconate. Activity was not detected consistently throughout development (data not shown). Activity was also tested in the presence of NAD⁺ and 5KGA (Figure 5.10), the theoretical reverse direction of this enzyme. Activity was detected throughout development, most active in the post-véraison berry. There was a high amount of variation between samples throughout development. A no substrate negative control was also performed which showed no NAD⁺ reduction at all timepoints.

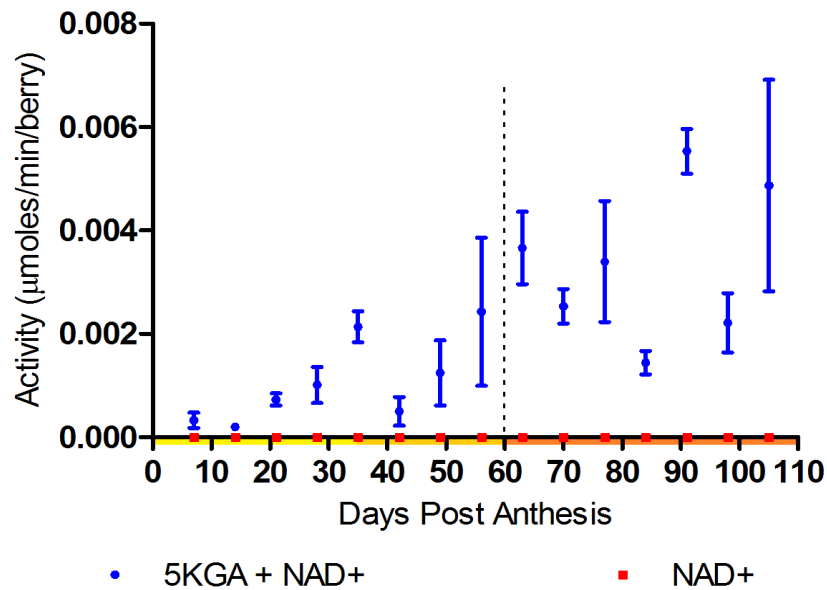


Figure 5.10: Activity of a putative gluconate 5-dehydrogenase's observed spectrophotometrically via the consumption of NAD^+ in the presence of 5KGA (blue closed circles), the theoretical reverse direction of the enzyme. A negative control of NAD^+ without added substrate was also measured (red closed squares). Soluble enzyme was extracted from *V. vinifera* cv Shiraz berry tissue over development. Triplicate samples were extracted at each timepoint with mean values shown. Error bars represent the standard error of the mean. Developmental stages are indicated by the coloured bar incorporated into the x-axis with berry formation, lag phase and berry ripening indicated in yellow, gold and orange respectively. *Véraison* is indicated by the dotted line.

5.3 Discussion

The development of *V. vinifera* cv Shiraz berries over the 2007/2008 season was followed using numerous physiological parameters including FW and °Brix (Figure 5.1), colour acquisition (Figure 5.2) and organic acid accumulation (Figure 5.3). All parameters were consistent with previously described developmental patterns (Coombe, 1980, Coombe and Bishop, 1980, Terrier and Romieu, 2001). The phases of berry development based on these parameters were

determined to be: berry formation 0-35 days, lag phase 35-60 days and berry ripening 60-110 days post-anthesis. The developmental stage véraison occurred 60 days post-anthesis.

TA was determined to be the dominant acid throughout development. TA accumulation was consistently higher than MA at each sampled timepoint throughout development. MA has been reported as the dominant acid in pre-véraison tissue (Terrier and Romieu, 2001). Varietal difference and environmental effects may account for this discrepancy. With the accumulation of FW, °Brix and organic acid as reported throughout the literature we have a high degree of confidence that the molecular parameters are indicative of standard growth and not a response to any biotic or abiotic stress the vine may have experienced throughout the season.

QRT-PCR analysis was used to determine the developmental stage at which the candidate genes were highly expressed. TA accumulation occurred during pre-véraison (Figure 5.3), therefore, the genes associated with TA biosynthesis would be expected to be highly expressed during this phase. Genetic expression of the only known TA biosynthetic enzyme L-IdnDH.1 was shown previously to be expressed predominantly in pre-véraison tissue (DeBolt, 2006) confirming this hypothesis.

TC61548, TC59682 and TC55752 were identified as candidates (Chapter 3) for a putative 2-ketogluconate reductase responsible for catalysing step 2a (Figure 1.8) of the primary Asc-precursor pathway. *TC61548* showed expression predominantly in the pre-véraison tissue (Figure 5.4 A). Although this expression showed large variation between timepoints, véraison triggered a consistent decrease in expression. This suggests *TC61548* is involved in pre-véraison activity and is regulated by a véraison switch. Unfortunately, no soluble protein of TC61548 was obtained preventing activity analysis from being conducted (see Figure 4.1). *TC59682* expression pattern indicates it is strongly associated with pre-véraison development (Figure 5.4 B). Expression of *TC59682* peaked 7 days post-anthesis, decreasing 4-fold within 20 days of development. This period of development correlates with the majority of TA biosynthesis (Figure 5.3). The

expression of *TC55752* steadily increased in pre-véraison tissue, remaining steady throughout post-véraison development (Figure 5.4 C). This pattern suggests *TC55752* is associated with post-véraison development and not in TA biosynthesis. Of the three candidates for a putative 2-ketogluconate reductase, data analysed supports *TC59682* as responsible for this role in TA biosynthesis especially in conjunction with enzymatic analyses of recombinant forms of the enzyme (see Chapter 4).

TC58004 and *TC55097* were identified as candidates (Chapter 3) for a putative gluconate 5-dehydrogenase responsible for catalysing step 2b (Figure 1.8) of the secondary glucose-precursor pathway. Expression of candidate *TC58004* showed a low level of expression in pre-véraison tissue, doubling in the post-véraison tissue (Figure 5.5 A). This expression pattern indicates that expression is responsive to a véraison switch, suggesting the gene maybe involved in post-véraison development. This does not support a role in net TA biosynthesis but may suggest a role in the maintenance of TA levels in later development. Candidate *TC55097* was shown to have the lowest expression level of all genes tested (Figure 5.5 B). Expression was steady throughout all stages of development, indicating it was not required during a specific developmental stage. The low level of gene expression suggested that the gene is either not required in berry tissue, or is a background gene required in low levels for cellular function. This does not support a role in TA biosynthesis.

L-IdnDH.1 has been confirmed as a TA biosynthetic enzyme (DeBolt *et al.*, 2006). The pattern of *L-IdnDH.1* expression matches that previously described in the literature (DeBolt, 2006, Melino *et al.*, 2009a) with one slight variation. DeBolt (2006) found expression exclusive to 8 weeks post-anthesis with peak activity 4 weeks post-anthesis. This variation in peak activity could be due to varietal difference with *V. vinifera* cv Cabernet Sauvignon being analysed by DeBolt whereas *V. vinifera* cv Shiraz was used in this study.

L-IdnDH.2 was selected as a possible homologue to *L-IdnDH.1* due to a 70% nucleic and 77.59% amino acid identity identified via the grapevine EST database (Hayes, DeBolt, Cook and Ford, manuscript in preparation). Expression patterns of *L-IdnDH.2* increased throughout development (Figure 5.6 B). This pattern was

not consistent with a TA biosynthetic gene. The expression of *L-IdnDH.2* opposes that of *L-IdnDH.1*. This suggests that should *L-IdnDH.2* be confirmed as a TA biosynthetic gene, they are working cooperatively throughout development ensuring continual TA biosynthesis. TA biosynthesis has not been shown to occur during the latter stages of berry development, however, a double knockdown of each gene in *V. vinifera* cv Thompson Seedless showed active TA production (Appendix A.1). *L-IdnDH.1* is a member of the sorbitol dehydrogenase family (DeBolt, 2006). The expression of *L-IdnDH.2* detected in this study correlates with the activity of sorbitol dehydrogenase in developing apple fruit (Teo *et al.*, 2006) and seed (Nosarzewski and Archbold, 2007) and expression in developing loquat fruit (Bantog *et al.*, 2000). This suggests that *L-IdnDH.2* may be a sorbitol dehydrogenase and not an *L-IdnDH.1* homologue.

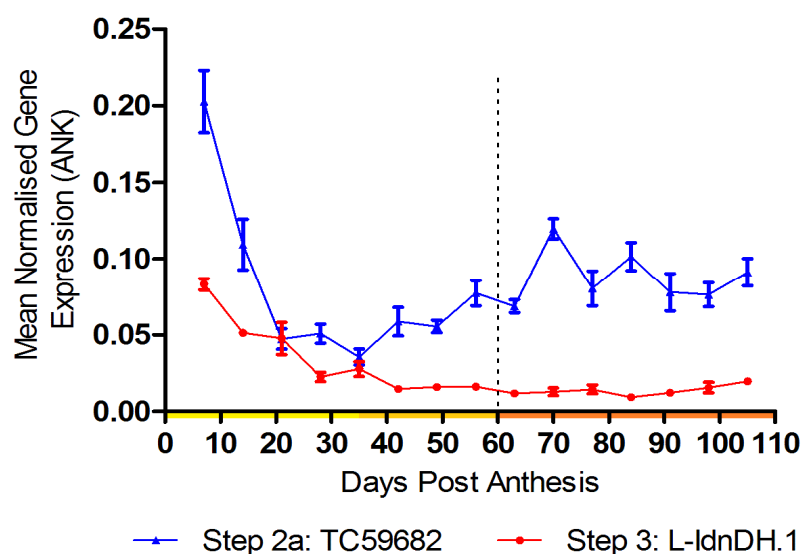


Figure 5.11: Composite of figures 5.6 A and 5.4 B comparing the expression of the known TA biosynthetic gene *L-IdnDH.1* (red solid circle) and the candidate for the preceding step in the pathway, candidate *TC59682* (blue closed triangle) respectively. Developmental stages are indicated by the coloured bar incorporated into the x-axis with berry formation, lag phase and berry ripening indicated in yellow, gold and orange respectively. Véraison is indicated by the dotted line. Error bars represent the standard error of the mean.

Candidate *TC59682* and *L-IdnDH.1* encode enzymes responsible for consecutive steps in the Asc-precursor pathway. *TC59682* displayed a higher level of expression compared to *L-IdnDH.1* with an additional accumulation phase (Figure 5.11). This suggests that *TC59682* may have an additional role in later berry development. The accumulation pattern of TA over development shows a slight decrease in TA levels at véraison, increasing to the previous peak at approximately 70 days post anthesis (Figure 5.3). This secondary peak in expression *TC59682* correlates with this secondary increase in TA levels. This secondary increase in TA levels was not substantial and no increase in L-idonate expression correlates with this timepoint. Wen *et al* (2010) identified L-idonate in mature berry tissue. This suggests that the TA biosynthetic pathway is present in mature berry tissue however not active. A secondary biosynthetic phase in late

berry development (when required) may suggest the maintenance of TA levels crucial in berry development. A correlation between rapid cell division and TA biosynthesis has been proposed (Hale, 1962). Melino *et al* (2009a) showed that in early berry development the metabolism of Asc to products TA and oxalate more active than Asc recycling. This suggests TA biosynthesis requires an initial trigger driving the Asc to TA biosynthesis in early berry development, whereas in later stages of development the key enzymes (L-ascorbylase) are already present with the intermediary enzymes synthesised (TC59682) to enable biosynthesis, depending on which intermediary compound is present.

Confirmation of enzymatic activity *in planta* was also conducted. Total protein was extracted from sampled berry tissue and activity analysed throughout development. The concentration of total protein was also measured throughout development (Figure 5.7). Analysis showed that the level of extracted protein was consistent over development. This finding is supported by Sweetman (2011) using a subset of the same berry samples. Ghisi *et al* (1984) measured total protein over development in *V. vinifera* cv. Merlot and showed immature berries had a higher protein level than mature tissue on a mg/g dry matter basis. This was later supported in *V. vinifera* cv. Nebbiolo Lampia berries on a mg/g fresh weight basis (Giribaldi *et al.*, 2007). This discrepancy in protein levels of the mature tissue is expected with the values obtained in this study presented on a mg/ml basis. Over development, berry FW increased due to the uptake of solutes (Figure 5.2, Coombe, 1976) accounting for the decreased protein concentration in mature tissue reported by Ghisi *et al* (1984) and Giribaldi *et al* (2007).

MDH was used as a positive indicator of active protein extraction from tissue. MDH activity in *V. vinifera* has been previously shown to increase over development (Sweetman, 2011). This developmental pattern was confirmed in this study, although the activity levels detected were at a reduced rate. The reduced rate of activity in this study may be resultant from the difference in absolute protein levels extracted from the berry tissue. De Souza *et al* (2005) extracted and assayed MDH using a modified protocol to the one in this study without the addition of OG or KCN and attributed activity in the extracts to MDH. The addition of KCN and OG to the assay buffer ensured the inhibition of

cytochrome oxidase (Baker *et al.*, 1987) and alternative oxidase (Hoefnagel *et al.*, 1995). Neither metabolic enzymes involve the metabolism of NAD(H); however, both are involved in the mitochondrial electron transport chain (mETC). NADH:coenzyme Q reductase precedes both enzymes in the mETC and involves NAD(P)H metabolism. Rotenone inhibits NADH coenzyme Q reductase (Darrouzet *et al.*, 1998, Okun *et al.*, 1999); however, this was not added to the assay buffer. Plant mitochondria possess an alternative mETC which can bypass NADH coenzyme Q reductase (Soole and Menz, 1995). The simultaneous inhibition of cytochrome oxidase and alternative oxidase inhibits the flow of electrons through both pathways of the mETC, inhibiting NADH coenzyme Q reductase and so NADH metabolism in the process.

Enzymatic activity of NAD⁺ in the presence of gluconic acid showed a limited number of timepoints with detectable activity (data not shown). Step 2b of the secondary glucose-precursor pathway is the step at which gluconic acid (GA) is committed to TA biosynthesis. Studies using dual-labelled [³H, ¹⁴C]GA indicate this to be a single step involving one enzyme (Saito, 1994). Observations of the process occurring at this step indicate gluconate undergoes hydrolysis due to the loss of a hydroxyl group. This indicates NADH to be the likely cofactor involved, and possibly the requirement of an ATP molecule. Enzyme activity analysis should have been conducted observing NADH oxidation in the presence of GA. The reverse of this step, the reduction of NAD⁺ in the presence of 5KGA showed an increase in activity over development (Figure 5.10). The levels of activity were the lowest detected for all tested activities. The greatest level of activity occurred in the post-véraison tissue, with a high level of variability observed. No reduction of NAD⁺ was observed in the absence of 5KGA indicating this activity was substrate dependent. TC58004, a candidate for this step was shown to have peak expression in the post-véraison berry (Figure 5.4). This may account for the increased activity observed over development. The lack of active protein *in vitro* prevents the confirmation of this protein's activity (Chapter 4). Kinetic analysis on an active protein sample is required.

Due to the limitations of L-idonate availability, the reduction of NAD⁺ in the presence of L-idonate was not conducted. This would have provided evidence for

the operation of L-IdnDH.1 and L-IdnDH.2 in the forward direction (producing 5KGA), and the putative 2-ketogluconate reductase in the reverse direction (producing 2KGA). Putative 2-ketogluconate reductase was tested in the forward direction with the oxidation of NADH in the presence 2KGA (Figure 5.9). Activity was shown to increase over development, peaking in post-véraison tissue. TC59682 and TC61548 are candidate enzymes for this activity. Both candidates show peak expression in the pre-véraison tissue (Figure 5.5 A, B), suggesting peak activity would be observed in this tissue also. TC59682 had been shown *in vitro* to possess catalytic activity specific to this reaction, suggesting TC59682 as the stronger candidate. The lack of peak activity in pre-véraison tissue may be due to the extraction process used. The quantity of total protein extracted was consistent over development (Figure 5.7). 2KGR are known to be unstable (Adachi *et al.*, 1979, Ameyama and Adachi, 1982b). Modifications to the extraction protocol may enable a higher yield of soluble stable protein from green hard pre-véraison berry tissue. The half-life or stability in a bound substrate-protein complex of TC59682 may account for this extended activity, and so investigations into TC59682 stability and half-life would be warranted. Protein-protein interactions may also be a factor in the high protein extract. A western blot with a TC59682 protein-specific antibody against the protein extract would indicate the presence of this protein in tissues where expression was low. An antibody specific to TC59682 has yet to be manufactured. Although prominent respiratory enzymes were inhibited other cellular enzymes that are capable of metabolising NADH in the presence of 2KGA may be present in the extract and responsible for the activity detected in the late seasonal timepoints. Although this activity cannot be attributed solely to TC59682, the negative control and inhibition of other known enzymes gives strong evidence that the oxidation of NADH observed is due to enzymatic activity specific to 2KGA.

Identification of the genes involved in TA biosynthesis will enable application of forward and reverse genetic tools in the manipulation of the pathway for further study. The developmental stage of gene expression and protein activity correlating with the accumulation of TA provides strong evidence for the association with the acids biosynthesis. Developmental and *in vitro* kinetic analysis of TC59682 suggests it is involved in TA biosynthesis. *TC61548* expression patterns show

activity exclusive to pre-véraison tissue, indicative of TA biosynthesis, warranting further investigation into a possible biosynthetic role.

Chapter 6:

Using Complementation Strategies to Characterise Candidates Genes Encoding Putative Members of Tartaric Acid Biosynthetic Pathway

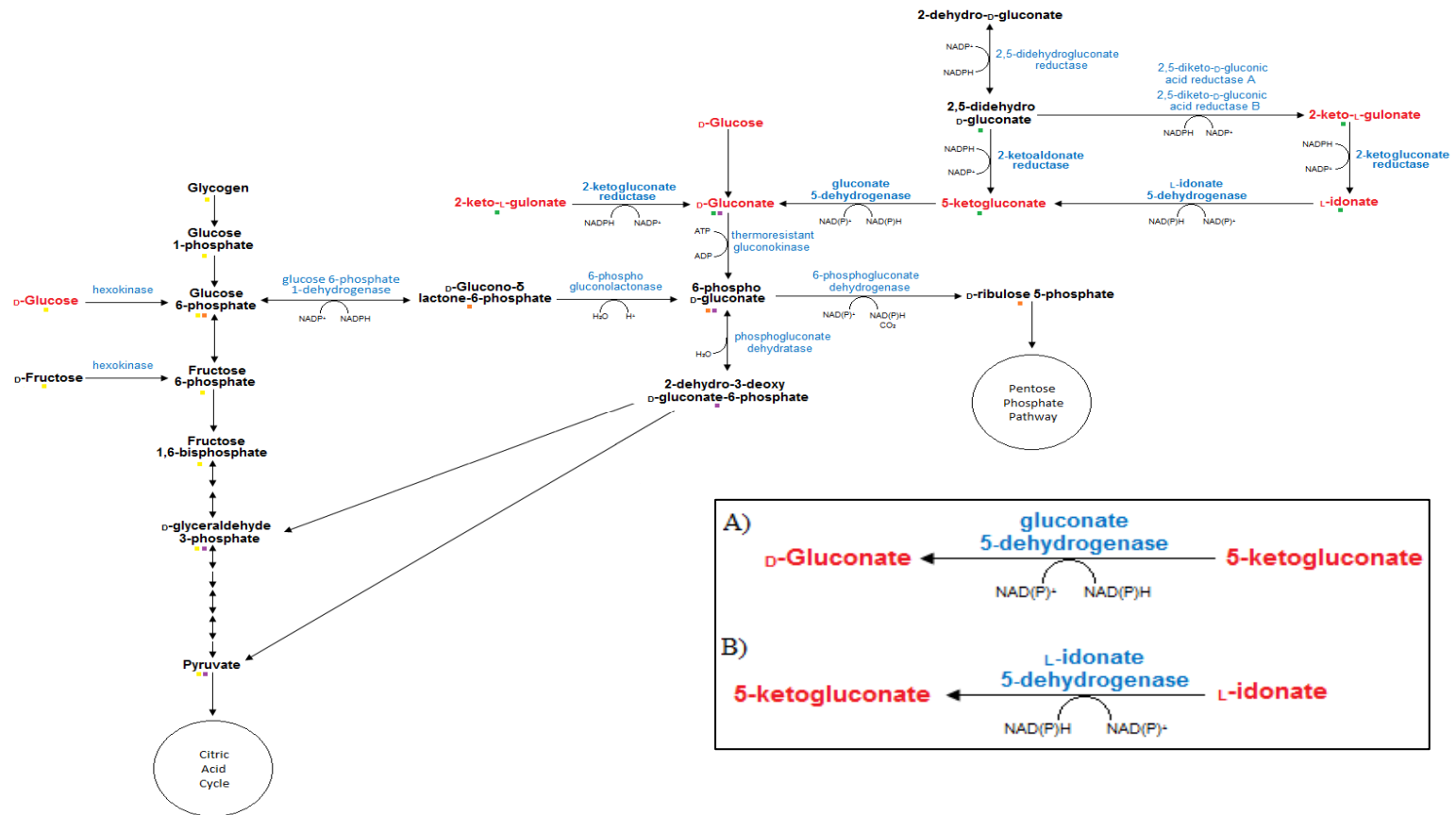
6.1 Introduction

The work described in this chapter involves the use of genetically altered tartaric acid accumulating and non-accumulating systems for the *in vivo* testing of the putative tartaric acid (TA) biosynthetic enzyme gene sequences. *In vivo* characterisation of enzyme activity is vital in the confirmation of the enzymes role under physiologically relevant conditions (Cornish-Bowden, 1984). Unfortunately, constraints including the long generation time of *V. vinifera* have hampered investigations into enzymes in *V. vinifera* (Chaïb *et al.*, 2010), including the biosynthetic enzymes of tartaric acid (TA). In recent years, forward and reverse genetic strategies for gene discovery have been performed using *Arabidopsis thaliana*, the model plant species, due to its small genome, its rapid generation time and the plethora of mutants publically available for use. However, in this study, the use of *A. thaliana* was limited due to the inability of *Arabidopsis* to naturally accumulate TA (Caldwell *et al.*, 2004). The development of microvine technology in 2010 by Chaïb *et al.* promises to be a useful tool in the understanding *V. vinifera* biology (Chaïb *et al.*, 2010). Although the use of microvine technology was not feasible in this study, three reverse genetic systems were employed to investigate the *in vivo* function of the candidate TA biosynthetic pathway enzymes identified in Chapter 3.

The first technique used involved the model bacterial species *Escherichia coli*. *E. coli* possesses a number of enzymes identified to catalyse reactions identical to those responsible for TA synthesis in plants. Figure 6.1 shows that the steps common to TA biosynthesis in *V. vinifera* feed major metabolic pathway's including glycolysis, Entner-Doudoroff and pentose phosphate pathway's. *E. coli* K-12 is one of the most characterised organisms (Baba *et al.*, 2007) with readily available collections of transformed lines. One such collection, the Keio collection (National BioResources Project, NIG, Japan), consists of single-gene deletion lines covering 92.4% of the *E. coli* genome (Baba *et al.*, 2006). Highly-specific deletions to 3985 nonessential genes were successfully obtained in the *E. coli* K-12 strain BW25113. Of interest in this study are the lines JW4223, with a disruption to the *IdnO* gene encoding a gluconate-5 dehydrogenase (Figure 6.1 inset A) and JW4224, with a disruption to the *IdnD* gene encoding a L-idonate-5-

dehydrogenase (Figure 6.1 inset B). It is predicted that the deletion of these genes will have detrimental effects to these lines, which will be manifested by their differential utilisation of carbon sources. Complementation studies of these lines via the incorporation of the respective putative *V. vinifera* candidates (Chapter 3) will provide additional support for the candidates' *in vivo* activity.

Figure 6.1: Composite bacterial pathway constructed from data obtained from the EcoCyc database (<http://ecocyc.org/>) (Keseler, 2005). Compounds listed in red are those common to the primary-Asc and secondary glucose precursor pathway's, with enzymes listed in blue. The coloured squares indicate the bacterial metabolic pathway the substrate is associated with: yellow: glycolysis, purple: Entner-Doudoroff pathway, green: ketogluconate metabolism, orange: pentose phosphate pathway. Inset A: the inhibited reaction in mutant bacterial strain JW4223. Inset B: The inhibited reaction in mutant bacterial strain JW4224.



The second approach utilised in this chapter involved the identification of putative TA biosynthetic genes in previously identified TA accumulating and non-accumulating members of the family, Vitaceae. *Ampelopsis aconitifolia* has previously been identified as a natural variant, lacking *L-IdnDH.1*, the only identified TA biosynthetic gene (DeBolt, 2006, DeBolt *et al.*, 2006). The absence of *L-IdnDH.1* is suggested to be the reason *A. aconitifolia* is incapable of TA accumulation (DeBolt, 2006, DeBolt *et al.*, 2006). Additionally, significant amounts of ascorbate, the primary precursor of TA have been detected within this species (DeBolt, 2006). Another member of the Vitaceae family, *A. aconitifolia* is an ornamental grape variety not used in commercial wine production, it is closely related to *V. vinifera* residing within the same clade (Wen *et al.*, 2007). *L-IdnDH.1* was identified in related ornamental varieties *A. brevipedunculata* and *Parthenocissus henryana* (DeBolt *et al.*, 2006) along with the accumulation of TA (Figure 1.2). Should the candidate genes, identified in this study, be involved in TA biosynthesis, then their presence within the TA-accumulating species genomes would be expected.

The third strategy that was explored was the analysis of the candidate enzymes in tissue from a previously engineered RNAi L-idonate dehydrogenase knockdown line (Hayes, DeBolt, Cook and Ford, manuscript in preparation). The *V. vinifera* L-idonate dehydrogenase enzyme (denoted L-IdnDH.1 in this study) was identified by DeBolt *et al.* (2006) as responsible for the catalysis of the perceived rate limiting step (Malipiero *et al.*, 1987) of the primary Asc-precursor TA biosynthetic pathway. Construction of recombinant *V. vinifera* cv Thompson Seedless vines, where RNAi knockdown was used to suppress expression of L-idonate dehydrogenase in a previous study (Hayes, DeBolt, Cook and Ford, manuscript in preparation), have been used to investigate what the subsequent effects of L-idonate dehydrogenase suppression are on TA biosynthesis. Malipiero *et al* (1987) showed that the cessation of TA biosynthesis in mature leaves *Vitis vinifera* L cv Riesling x Silvaner occurred at the level of L-idonic acid oxidation which subsequently accumulated. The knockdown of L-IdnDH.1 activity was expected to significantly decrease TA biosynthesis through the primary-Asc pathway leading to an accumulation in L-idonate and a possible rise in ascorbate

levels. Significant TA accumulation was still observed in the leaf tissue of all lines tested (Appendix 1, Hayes, DeBolt, Cook and Ford, manuscript in preparation). Due to the timeframe of fruit production from immature seedling vines, berry tissue was not available for analysis. The biosynthesis of TA observed in these lines is expected to be occurring through the secondary glucose pathway, which may be up-regulated due to the expected inhibition of the primary-Asc pathway (Hayes, DeBolt, Cook and Ford, manuscript in preparation).

The detection of the putative TA biosynthetic genes in expected TA accumulating lines (Section 6.2.2) and the observation of complementary activity in genetically modified bacteria (Section 6.2.1) in conjunction with an expected altered expression due to a genetically altered TA biosynthetic pathway (Section 6.2.3) would support the candidate genes role in TA biosynthesis. Thus, these strategies were explored in this study to provide further evidence of their function in grape berries.

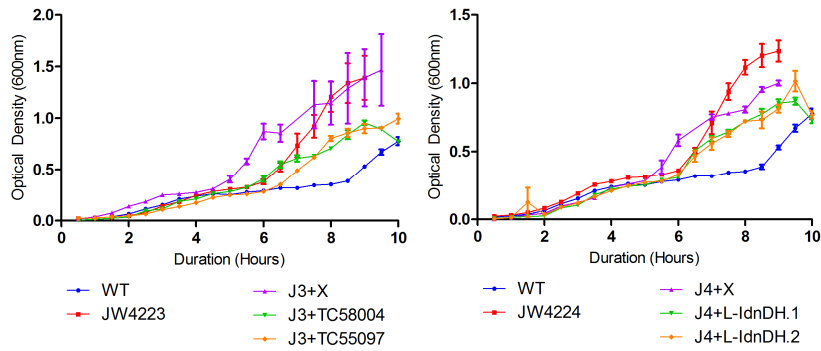
6.2 Results

6.2.1 Complementation Studies using Mutant *Escherichia coli* Strains Growing on Various Carbon Sources

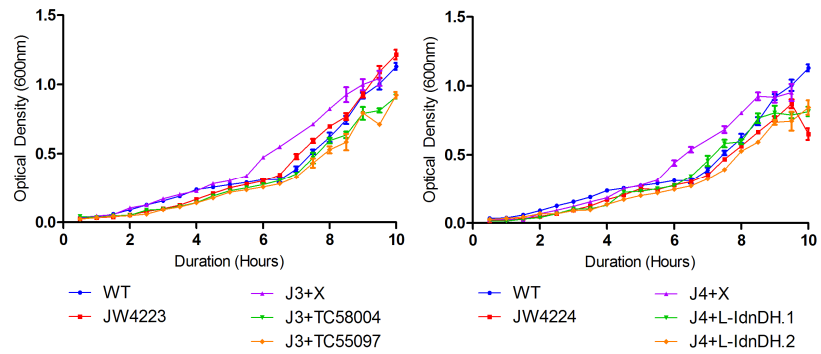
Mutant *E. coli* K-12 lines JW4223 and JW4224 from the Keio collection were transformed with the respective *V. vinifera* candidate gene identified in Chapter 3 as described in Section 2.12.3, using bacterial expression vectors. Gluconate-5 dehydrogenase (G5Dh) mutant bacterial strain JW4223 was transformed with the expression vector of putative *V. vinifera* enzymes TC55097 and TC58004, candidate G5Dh for step 2b of the secondary glucose pathway (Figure 1.8). The L-Idonate-5-dehydrogenase mutant bacterial strain JW4224 was transformed with the expression vector of L-idonate dehydrogenase 1 (L-IdnDH.1) and its putative homologue L-idonate dehydrogenase 2 (L-IdnDH.1). No mutant 2-ketogluconate reductase line was obtained from the Keio collection. Shaking cultures of each line were grown as described in Section 2.14. The carbon sources selected (glucose, fructose, gluconate, 2-keto-L-gulonate, 5-keto-D-gluconate) enter the

pathway at different stages (Figure 6.1). Glucose and fructose were used as standard carbon sources for normal growth of each bacterial strain.

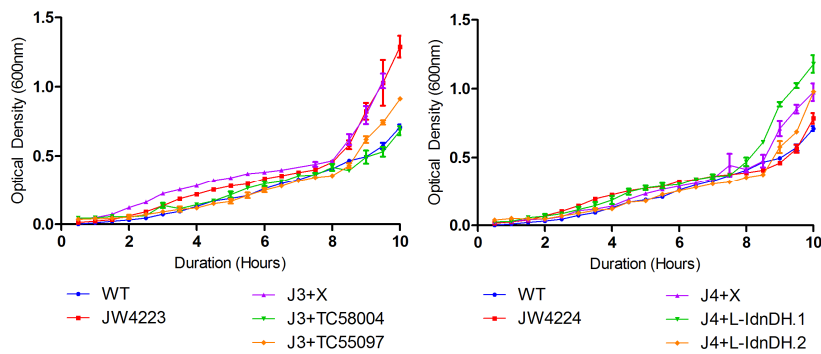
A) Glucose



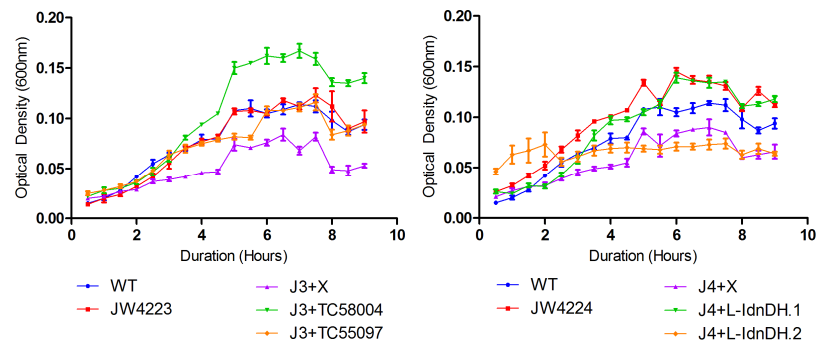
B) Fructose



C) Gluconate



D) 2-Keto-L-Gulonate



E) 5-Keto-D-Gluconate

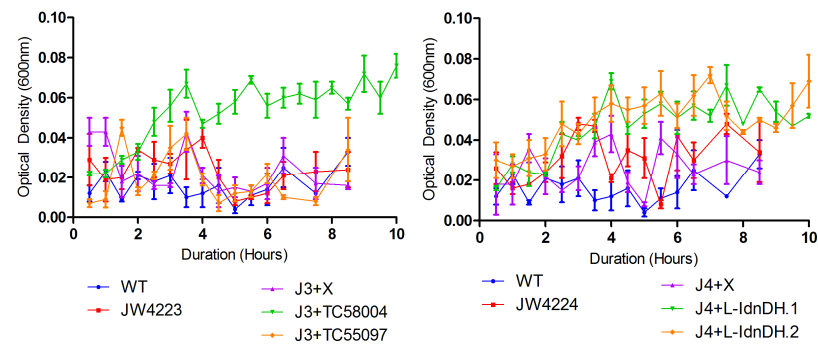


Figure 6.2: Growth studies of transformed and transformed mutant *E. coli* K-12 bacterial strains in M9 minimal media with a selected carbon source. Plotted values represent the mean of triplicate cultures with error bars representing the standard error of the mean. Bacterial strains used include WT: wild type bacterial strain *E. coli* K-12; JW4223: gluconate 5-dehydrogenase mutant bacterial strain; JW4224: L-idonate-5-dehydrogenase mutant bacterial strain; J3+X: JW4223 transformed with an empty pET-14b vector; J4+X: JW4224 transformed with an empty pET-14b vector; J3+TC58004: JW4223 transformed with TC58004 expression vector; J3+TC55097: JW4223 transformed with TC55097 expression vector; J4+L-IdnDH.1: JW4224 transformed with L-IdnDH.1 expression vector; J4+L-IdnDH.2: JW4224 transformed with L-IdnDH.2 expression vector. Carbon sources used include **A)** Glucose, **B)** Fructose, **C)** Gluconate, **D)** 2-Keto-L-Gulonate and **E)** 5-Keto-D-Gluconate.

Growth was observed in all bacterial strains utilising the carbon sources glucose (Figure 6.2 A), fructose (Figure 6.2 B) and gluconate (Figure 6.2 C). Growth of the WT (wild type, *E. coli* K-12) cells was the slowest in the presence of glucose compared to the other lines tested (Figure 6.2 A). This may be a result of a non-optimal starter culture used for this line. Strains WT, JW4223, JW4224, J4+L-IdnDH.1 (JW4224 transformed with L-IdnDH.1 expression vector) and J4+L-IdnDH.2 (JW4224 transformed with L-IdnDH.2 expression vector) reached exponential growth phase in the presence of glucose. Steady growth was observed by strains: J3+X (JW4223 transformed with an empty pET-14b vector (control)), J4+X (JW4224 transformed with an empty pET-14b vector (control)), J3+TC58004 (JW4223 transformed with TC58004 expression vector) and J3+TC55097 (JW4223 transformed with TC55097 expression vector). Exponential growth phase was observed by all bacterial strains in the presence of fructose and gluconate with comparable growth patterns across each line observed (Figure 6.2 B, C). The initial lag phase of growth in the presence of gluconate was the longest measured with exponential growth not observed until late in the 10 hour incubation period (Figure 6.2 C).

Growth was also monitored in the presence of 2-keto-L-gulonate (Figure 6.2 D) and 5-keto-D-gluconate (Figure 6.2 E). Metabolism of 5-keto-D-gluconate should be directly affected by the mutation of the JW4223 bacterial strain. 2-Keto-L-Gulonate metabolism is affected downstream by the mutation of both JW4223 and JW4224 bacterial strains, or 2-Keto-L-Gulonate can enter the pathway at a different stage bypassing the mutation (Figure 6.1). L-Idonate metabolism is directly affected by the mutation of the JW4224 bacterial strain; however, as it is not commercially available this carbon source could not be tested. No growth was observed by the WT or transformed bacterial strains in the presence of 5-keto-D-gluconate (Figure 6.2 E). The lack of growth by the WT strain suggests *E. coli* K-12 is incapable of using 5-keto-D-gluconate as its sole carbon source. Minimal growth, as indicated by the nominal increase in optical density, was observed by the WT and transformed bacterial strains in the presence of 2-keto-L-gulonate (Figure 6.2 D). This negligible

growth suggests partial metabolism of 2-keto-L-gulonate enabling slight growth, but not enough to reach exponential growth phase.

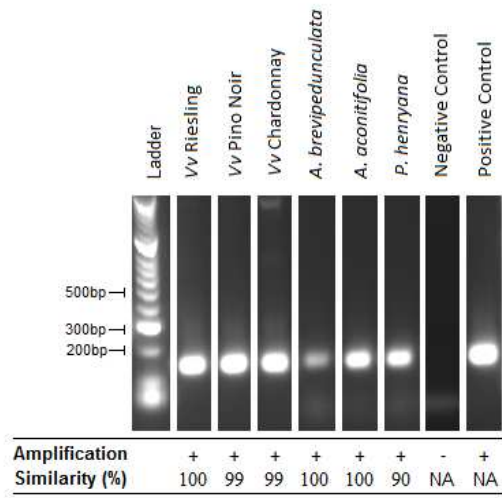
No difference in growth was observed in the transformed strains compared to the WT line in the presence of the carbon sources tested. Altered growth patterns were not observed by the complementation of the transformed bacterial strain with the putative *V. vinifera* protein.

6.2.2 Identification of Putative Tartaric Acid Biosynthetic Enzymes in Members of the Vitaceae Family.

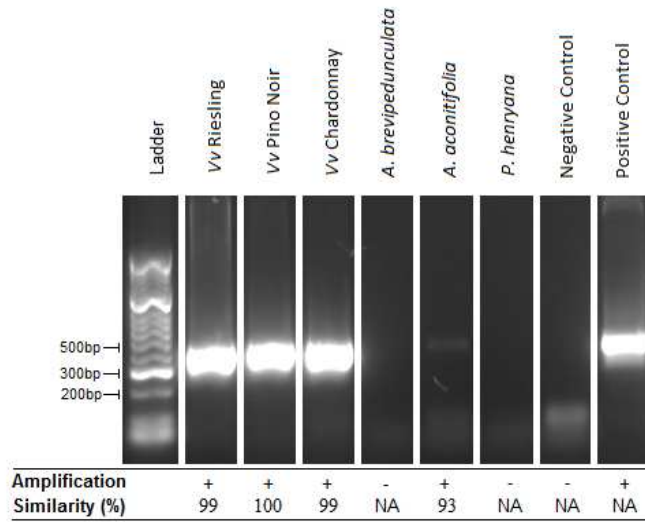
The presence of the putative tartaric acid (TA) biosynthetic genes was investigated in the ornamental species *Ampelopsis aconitifolia*, *A. brevipedunculata* and *Parthenocissus henryana*, and *V. vinifera* cvs Riesling, Pinot Noir and Chardonnay. *V. vinifera* cv Shiraz has previously been identified as possessing these genes (Chapter 4). *A. aconitifolia* is a non-TA accumulating line previously identified as a natural mutant, lacking the tartaric acid biosynthetic enzyme L-idonate dehydrogenase 1 (DeBolt, 2006, DeBolt *et al.*, 2006). All other Vitaceae members tested have previously been identified as TA-accumulators (Figure 1.2). Primers were designed to amplify a segment of each candidate gene within a single exon based upon the obtained *V. vinifera* cv Shiraz nucleotide sequence. The nucleotide sequence of the amplified segment was purified and sequenced to confirm its similarity to the *V. vinifera* cv Shiraz sequence.

Figure 6.3: Amplification of candidate 2-ketogluconate reductase genes from genomic DNA extracted from leaf tissue of various Vitaceae family members. DNA visualisation via GelRed™ Nucleic Acid staining of a 1% agarose gel electrophoresis under ultraviolet light. +: positive PCR amplification. -: negative PCR amplification. NA: PCR product sequence not required to be determined. *: sequence of amplified PCR product not determined. Ladder: DNA marker Hyperladder 2 (Bioline, Australia). Similarity of amplified sequence calculated as a percentage at the nucleotide level as compared to the *V. vinifera* cv Shiraz sequence obtained in Chapter 3. A) TC61548, B) TC59682, C) TC55752

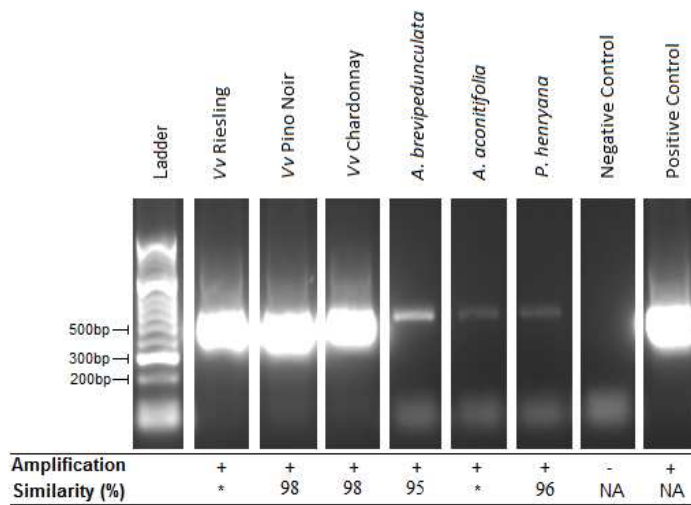
A) TC61548



B) TC59682



C) TC55752



Putative 2-ketogluconate reductases TC61548, TC59682 and TC55752 are candidates for step 2a of the primary-Asc biosynthetic pathway (Figure 1.8). Candidate TC61548 was identified in each of the 6 Vitaceae members tested. The sequence obtained was determined via sequencing (see Section 2.11.1) and found to be highly similar to the *V. vinifera* cv Shiraz sequence with *P. henryana* the least identical (Figure 6.3 A). Candidate TC59682 was identified in each of the *V. vinifera* cultivars and *A. aconitifolia*; however, was absent from both the *A. brevipedunculata* and *P. henryana* genomes. High similarity of the amplified segments against the *V. vinifera* cv Shiraz sequence of those Vitaceae members with positive amplification (Figure 6.3 B). Positive PCR amplification of candidate TC55752 was identified in each of the 6 Vitaceae members tested. Although PCR resulted in a band of expected size, cloning of the PCR product from Vitaceae members *V. vinifera* cv Riesling and *A. aconitifolia* into a vector for sequencing was unsuccessful. Sequencing directly from the PCR fragment was not attempted due to the small size of the resultant amplicon. As a result, the sequence of the PCR products of these Vitaceae members was not confirmed. The sequence obtained from the remaining varieties was highly similar to the *V. vinifera* cv Shiraz sequence (Figure 6.3 C).

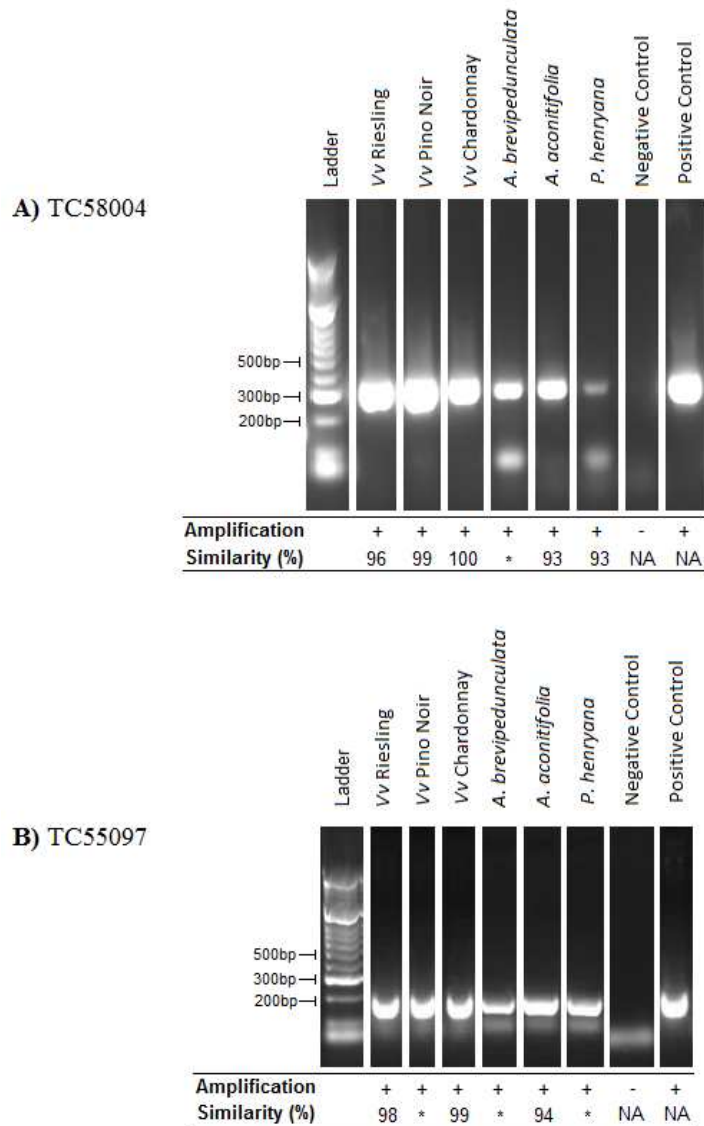


Figure 6.4: Amplification of candidate gluconate 5-dehydrogenase genes from genomic DNA extracted from leaf tissue of various Vitaceae family members. DNA visualisation via GelRed™ Nucleic Acid staining of a 1% agarose gel electrophoresis under ultraviolet light. +: positive PCR amplification. -: negative PCR amplification. NA: PCR product sequence not required to be determined. *: sequence of amplified PCR product not determined. Ladder: DNA marker Hyperladder 2 (Bioline, Australia). Similarity of amplified sequence calculated as a percentage at the nucleotide level as compared to the *V. vinifera* cv Shiraz sequence obtained in Chapter 3. A) TC58004, B) TC55097

Putative gluconate 5-dehydrogenases TC58004 and TC55097 are candidates for step 2b of the secondary glucose biosynthetic pathway (Figure 1.8). PCR amplification of candidates TC58004 and TC55097 was successful against each of the 6 Vitaceae members tested (Figure 6.4 A and B respectively). Although PCR resulted in a band of expected size, cloning of the PCR product of TC58004 from *A. aconitifolia* and TC55097 from *V. vinifera* cv Pinot Noir, *A. brevipedunculata* and *P. henryana* into a vector for sequencing was unsuccessful. As a result, the sequence of the PCR products of these varieties was not confirmed. Greater than 93% similarity was calculated from the sequence obtained for TC58004 within *V. vinifera* cvs Riesling, Pinot Noir and Chardonnay, *A. brevipedunculata* and *P. henryana*, and for TC55097 within *V. vinifera* cvs Riesling and Chardonnay and *A. aconitifolia* as compared to the *V. vinifera* cv Shiraz sequence.

6.2.3 Gene Expression Analysis utilising Qualitative Real Time PCR in RNAi Thompson Seedless Lines

Qualitative real time PCR (QRT-PCR) was performed on leaf tissue from a transformed *V. vinifera* cv Thompson Seedless L-idonate dehydrogenase RNAi knockdown line engineered in a previous study (Hayes, DeBolt, Cook and Ford, manuscript in preparation). Each knockdown line was grouped based on its observed phenotype as mild, moderate or severe. The labels of each line correspond to Appendix 1. The transformed Thompson seedless lines were immature with only leaf tissue available for analysis. The tartaric acid (TA) levels and the RNA used for the QRT-PCR (Figure 6.5) were extracted by Dr M Hayes (University of Adelaide). QRT-PCR was performed as described in Section 2.7.

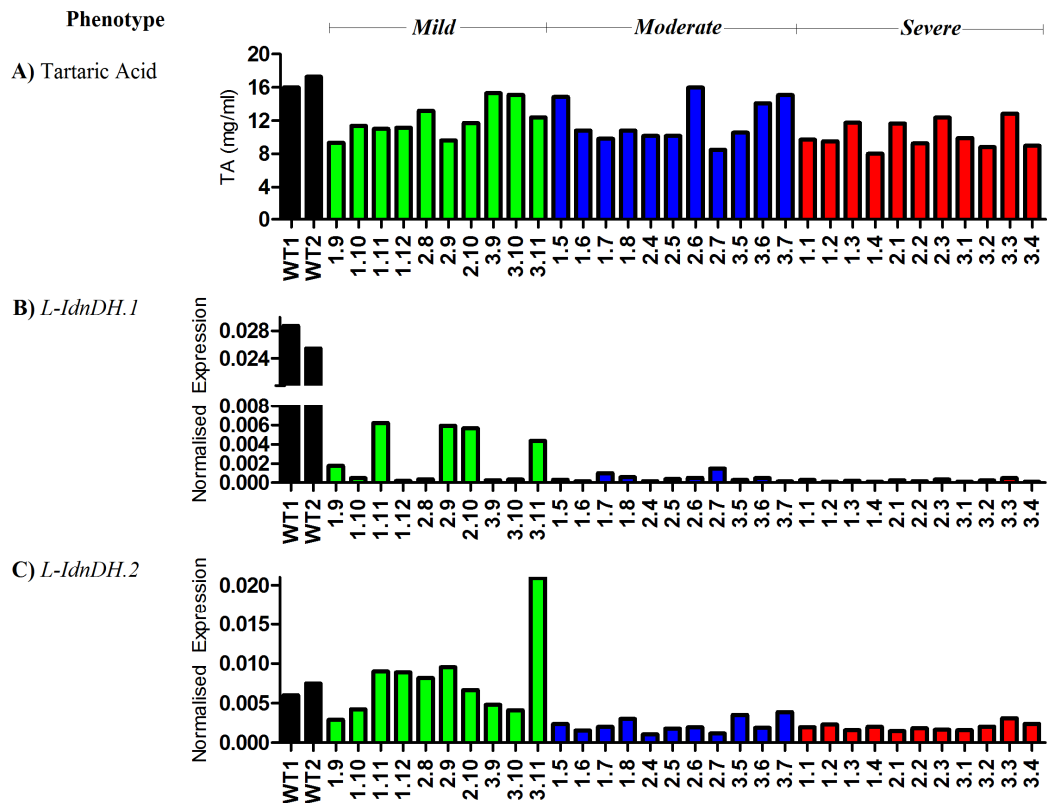


Figure 6.5: Analysis of gene expression of *L-IdnDH.1* and the putative homologue *L-IdnDH.2*. Young leaf tissue of RNAi knockdown *V. vinifera* Thompson seedless lines and normalised against the reference gene Ankyrin. Lines are grouped into phenotype with WT: wild type Thompson Seedless – solid black; mild phenotype – solid green; moderate phenotype – solid blue; severe phenotype – solid red. Tartrate (TA) levels and phenotype allocation was determined by Dr M. Hayes (University of Adelaide), QRT-PCR was conducted as part of this study. The labels of each recombinant line correspond to Appendix 1. A) Tartaric acid levels, B) Expression of *L-IdnDH.1*, C) Expression of *L-IdnDH.2*

All RNAi knockdown lines showed a decrease in *L-IdnDH.1* expression compared to the wild type (WT, Figure 6.5 B). Due to the high sequence similarity of *L-IdnDH.1* to its putative homologue *L-IdnDH.2*, the expression of *L-IdnDH.2* was also knocked-down (Figure 6.5 C). The knockdown of both *L-IdnDH.1* and *L-IdnDH.2* was predominantly greatest in the moderate and severe phenotypes. With the knockdown of *L-IdnDH.1* it was expected the levels of accumulated TA in

these lines would be minimal. Although the measured levels of TA were lower in the RNAi lines than the WT, the quantities of accumulated TA were higher than expected (Figure 6.5 A).

Candidates *TC61548*, *TC59682* and *TC55752* are putative homologues for step 2a of the primary-Asc pathway. Expression of candidate *TC61548* was the highest of the 3 candidates for this step (Figure 6.6 A). The levels of expression detected across the RNAi knockdown lines varied with higher and lower levels detected compared to the WT. Expression of *TC59682* was the lowest observed of the 3 candidates for this step (Figure 6.6 B). Expression of *TC59682* was decreased in all RNAi knockdown lines compared to the WT. Expression of *TC55752* varied across all recombinant lines, with the majority equal to, or greater than that observed in the WT (Figure 6.6 C). A general trend of decreased expression of *TC59682* was observed across all RNAi lines; however, expression levels suggest *TC61548* and *TC55752* were not affected by the knockdown of *L-IdnDH.1* or its putative homologue *L-IdnDH.2*.

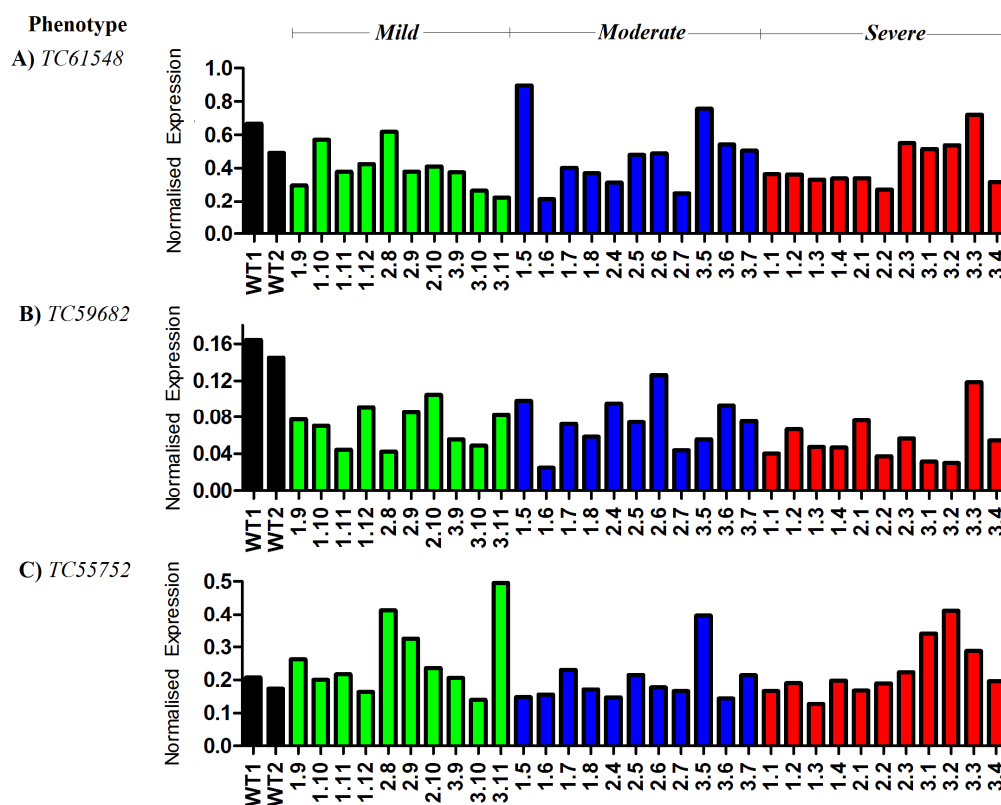


Figure 6.6: Analysis of gene expression of the putative 2-ketogluconate reductase candidates for step 2a of the primary Asc-precursor pathway (Figure 1.8). Young leaf tissue of RNAi knockdown *V. vinifera* Thompson seedless lines and normalised against the reference gene Ankyrin. Lines are grouped into phenotype with WT: wild type Thompson Seedless – solid black; mild phenotype – solid green; moderate phenotype – solid blue; severe phenotype – solid red. Phenotype allocation was determined by Dr MA Hayes (University of Adelaide), QRT-PCR was conducted as part of this study. The labels of each recombinant line correspond to Appendix 1. A) Expression of *TC61548*, B) Expression of *TC59682*, C) Expression of *TC55752*.

Candidates *TC58004* and *TC55097* are putative homologues for step 2b of the secondary glucose pathway. Expression levels of candidate *TC58004* was minimal across all lines tested (Figure 6.7 A). A trend of decreased expression in the RNAi

lines tested was observed, with higher expression observed in 3 of the 32 recombinant lines, as compared to the WT. Expression of *TC55097* varied across all tested lines, with a 2 fold difference observed between the WT lines (Figure 6.7 B). This difference resulted in no apparent trend across the recombinant lines. A general trend of decreased expression of *TC58004* was observed across the recombinant lines; however, expression levels suggest *TC55097* was not affected by the knockdown of *L-IdnDH.1* or *L-IdnDH.2*.

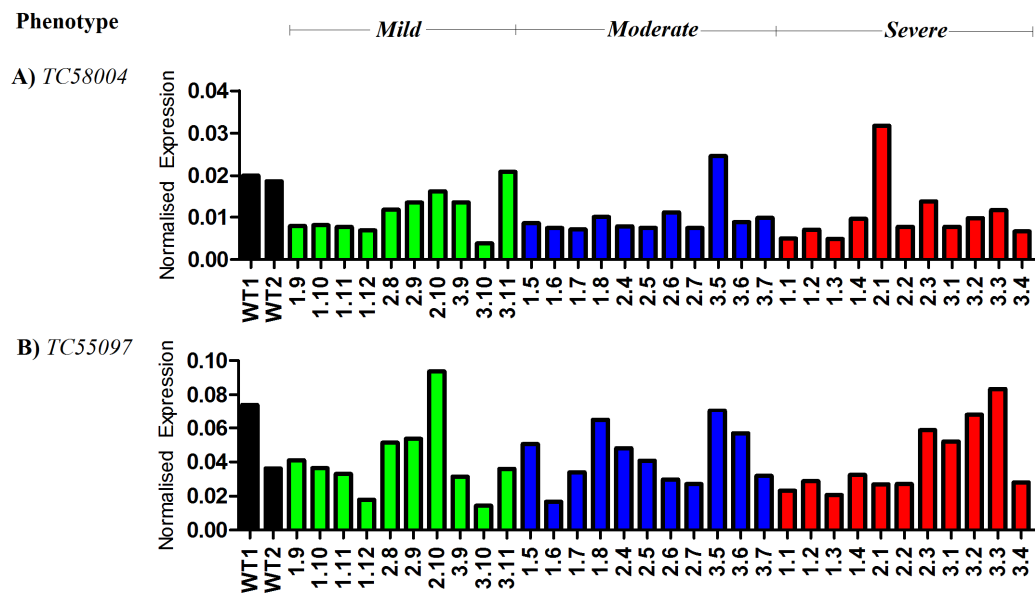


Figure 6.7: Analysis of gene expression of the putative gluconate-5 dehydrogenase candidates for step 2b of the secondary glucose pathway (Figure 1.8). Young leaf tissue of RNAi knockdown *V. vinifera* Thompson seedless lines and normalised against the reference gene Ankyrin. Lines are grouped into phenotype with WT: wild type Thompson Seedless – solid black; mild phenotype – solid green; moderate phenotype – solid blue; severe phenotype – solid red. Phenotype allocation was determined by Dr MA Hayes (University of Adelaide), QRT-PCR was conducted as part of this study. The labels of each recombinant line correspond to Appendix 1. A) Expression of *TC58004*, B) Expression of *TC55097*

6.3 Discussion

Reverse genetics is a molecular technique enabling the characterisation of a specific enzyme activity as a consequence of the loss of the genes function on the whole organism (Baba *et al.*, 2007). This chapter has investigated the characterisation of each candidate through three different reverse genetic strategies.

The first approach involved the use of commercially available genetically modified *E. coli* K-12 from the Keio collection. The strains obtained, JW4223 and JW4224, had a single-gene deletion inhibiting the expression of gluconate-5 dehydrogenase and L-idonate-5-dehydrogenase respectively. The deletion of these genes was expected to have a detrimental effect to these strains, when grown on different carbon sources. Complementation of the bacterial strains with the putative *V. vinifera* cDNA was expected to restore the deleted genes function, re-establishing the mutant line's growth pattern under a limiting carbon source, providing support for the genes function *in vivo*. Growth was analysed against carbon sources glucose, fructose, gluconate, 5-keto-D-gluconate and 2-keto-L-gulonate (Figure 6.2). The mutant bacterial strains grew at a comparable rate to the WT strain on carbon sources glucose (Figure 6.2 A), fructose (Figure 6.2 B) and gluconate (Figure 6.2 C) suggesting the respective mutations was not detrimental to the growth of the strain. This growth pattern was not conducive to the hypothesis of an altered ability to utilise carbon sources resultant from the absence of specific genes. Cellular growth on carbon sources 5-keto-D-gluconate and L-idonate was expected to be hindered the greatest due to the inhibition of the metabolism of the compounds catalysed by the genetically deleted enzymes gluconate-5 dehydrogenase and L-idonate-5-dehydrogenase respectively.

No growth was observed for the WT or mutant strains tested against the carbon source, 5-keto-D-gluconate. Further investigation into the literature regarding the catabolism of sugars by *E. coli* identified multiple genes responsible for the transport of nutrients across the membrane (reviewed by Peekhaus and Conway, 1998). Of specific interest to this study, *gntT* and *idnT* are responsible for the transport of gluconate and L-idonate respectively. A gene enabling the cellular uptake of 5-keto-D-gluconate was not identified in *E. coli*. This suggests that the

lack of growth observed by the *E. coli* strains tested was due to the cells inability to uptake the compound. Minute levels of growth were observed by lines grown on 2-keto-L-gulonate (Figure 6.2 D). 2-Keto-L-Gulonate can be broken down to gluconate (Figure 6.1) which can then be transported into the cell. Although a transporter was identified for the cellular uptake of L-idonate and it is directly metabolised by the deleted enzyme of line JW4224, L-idonate is not commercially available. Synthesis of L-idonate was investigated; however, this was not a feasible option within the financial constraints of this project. Therefore, growth on L-idonate was unable to be tested.

Analysis of the quantity of compounds downstream of the deleted biosynthetic steps in the transformed strains compared to the WT would provide a deeper understanding of the reactions of interest. Although 5-keto-D-gluconate and D-gluconate are the products of multiple steps within the pathway (Figure 6.1), an increase in these intermediate compounds is expected in the mutant lines due to the deletion of gluconate-5 dehydrogenase and L-idonate-5-dehydrogenase. Should transformation of these lines with the putative *V. vinifera* enzymes re-establish the pathway's function, and in turn the metabolism of these compounds, this will provide support for the candidates role *in vivo*.

The second strategy explored for the identification of the putative TA biosynthetic genes in TA accumulating and non-accumulating species, involved an assessment of the presence of the genes of interest in the genomes of members of Vitaceae family that vary in their production of TA. Previous work (DeBolt, 2006, DeBolt *et al.*, 2006) has shown an ornamental species of grape, *Ampelopsis aconitifolia* as a natural mutant lacking the L-idonate dehydrogenase gene. As a result, *A. aconitifolia*, a relative of *V. vinifera*, is unable to accumulate TA. The presence of the candidate TA biosynthetic genes (identified in chapter 3) was investigated in additional members of Vitaceae family using a genomic PCR strategy in leaf tissue of cultivars including *V. vinifera* cv Riesling, *V. vinifera* cv Pinot Noir, *V. vinifera* cv Cabernet, *A. brevipedunculata*, *Parthenocissus henryana* and *A. aconitifolia*. Primers were based on the known *V. vinifera* cv Shiraz sequence for a resulting amplicon within a single exon.

The presence of the genes for the TA biosynthetic enzymes are expected in TA accumulating species. Putative *V. vinifera* 2-ketogluconate reductase *TC59682*, identified as capable of catalysing step 2a of the primary-Asc pathway, was identified in all Vitaceae members except *A. brevipedunculata* and *P. henryana*. *A. brevipedunculata* and *P. henryana* are both TA accumulating species (Figure 1.2). This suggests either TA biosynthesis occurs via an alternative pathway in non-*Vitis* species, or *TC59682* is not a gene for a TA biosynthetic enzyme. Alternatively, *A. brevipedunculata* and *P. henryana* may still possess *TC59682*; however, its coding at the nucleic acid level may be different to that of Shiraz; the cultivar the primers were designed against. Putative *V. vinifera* 2-ketogluconate reductases *TC61548* and *TC55752* and putative *V. vinifera* gluconate 5 dehydrogenases *TC58004* and *TC55097* were identified in all Vitaceae members tested. All candidate TA biosynthetic genes were identified in *A. aconitifolia* supporting DeBolt's (2006) hypothesis that the lack of TA accumulation is solely due to the absence of *L-IdnDH.1*. The genes successfully identified and sequenced show a high identity with >90% identity as compared to the Shiraz sequence. This suggests the candidates are highly similar across the cultivars supporting the implication of the negative PCR result.

The third strategy used involved QRT-PCR analysis of the candidate enzymes in tissue from previously engineered *V. vinifera* cv Thompson Seedless L-idonate dehydrogenase knockdown vines (Hayes, DeBolt, Cook and Ford, manuscript in preparation). These vines were immature and therefore yet to produce berry tissue. Due to this limitation, leaf tissue was used in the analysis of candidate gene expression. Of the 34 lines tested, 2 were unmodified *V. vinifera* cv Thompson Seedless lines (wildtype, WT). The engineered lines were allocated into groups based upon the resultant phenotype observed, with 10 displaying mild phenotypic effects, 11 displaying moderate and 11 displaying severe effects. The phenotype effects observed included stunted growth and browning upturned leaves (Appendix 1).

Analysis of the expression of *L-IdnDH.1* in young leaf tissue (Figure 6.5 B) shows *L-IdnDH.1* was successfully knocked-down in all engineered lines. The severe phenotype lines showed the highest level of *L-IdnDH.1* knockdown. Due to the

high sequence similarity of *L-IdnDH.1* to its putative homologue *L-IdnDH.2*, the expression of *L-IdnDH.2* was also knocked-down (Figure 6.5 C) with the moderate and severe phenotypes showing the highest levels of knockdown. With the successful knockdown of *L-IdnDH.1* the accumulation of TA was expected to be inhibited. Tartaric acid (TA) levels of young leaf tissue were analysed with all lines showing reduced quantities of TA (Figure 6.5 A). Although reduced, the levels detected were less than 2 fold lower than the WT. This suggests the recombinant *V. vinifera* cv Thompson Seedless L-idonate dehydrogenase knockdown vines are still capable of substantial TA accumulation. The results obtained from the RNAi vines suggest an alternative pathway, the secondary glucose precursor pathway, may be up-regulated to compensate, or the minimal quantities of *L-IdnDH.1* observed are capable of significant TA biosynthesis. Candidates *TC58004* and *TC55097* are putative homologues for step 2b of the secondary glucose pathway. QRT-PCR analysis showed a general trend of decreased expression levels of candidate *TC58004* across the recombinant lines, with higher expression observed in 3 of the 32 recombinant lines compared to the WT (Figure 6.7 A). No general trend in expression of candidate *TC55097* was observed, with both increased and decreased levels detected compared to the WT (Figure 6.7 B). Neither candidate was up-regulated suggesting either *TC58004* and *TC55097* are not responsible for catalysing step 2b, or step 2b is not up-regulated due to *L-IdnDH.1* knockdown.

Candidates *TC61548*, *TC59682* and *TC55752* are putative homologues for step 2a of the primary-Asc pathway, preceding *L-IdnDH.1*. Expression of *TC59682* was decreased in all recombinant knockdown lines compared to the WT (Figure 6.6 B). The decreased levels detected varied greatly across the lines. No general trend for candidates *TC61548* and *TC55752* (Figure 6.7 A and B respectively) was observed across the recombinant lines. Expression levels varied across the candidates with increased and decreased levels detected compared to the WT. Further investigation into these RNAi lines of both leaf and berry tissue is required. The QRT-PCR analysis performed was conducted on a single sample of young leaf tissue. Additional replication and a greater number of time-points are required. A complete physiological and genetic characterisation of each recombinant line is required to investigate the changes resultant from the

knockdown of *L-IdnDH.1*. Investigations utilising microarray techniques would enable a complete transcriptome approach. With the successful knockdown of *L-IdnDH.1*, these lines will be a valuable tool in future research into the TA biosynthetic pathway.

Three independent approaches utilising reverse genetic strategies were designed to support the role of the putative TA biosynthetic genes in TA biosynthesis. Firstly, the restoration of enzymatic function to the genetically modified Keio lines JW4223 and JW4224 would have supported the enzymatic function of the *V. vinifera* genes *in vivo*. The observed growth of the mutant lines compared to the wild type on the tested carbon sources was not altered rendering complementation invalid. Secondly, the presence of the genes for TA biosynthetic enzymes are required in TA accumulating Vitaceae species. Therefore the presence of these genes was investigated in multiple TA accumulating and non-accumulating lines. Enzyme TC59682 was identified as capable of catalysing step 2b of the primary-Asc pathway (Chapter 4); however, was not present in all tested TA accumulating members. Thirdly, gene expression was investigated in leaf tissue of a previously engineered RNAi L-idonate dehydrogenase knockdown vine. Expression of *TC59682* was decreased in all RNAi knockdown lines. Due to the high quantities of TA detected, the secondary-glucose pathway was expected to be up-regulated to compensate for the loss of the primary-Asc pathway. No uniform changes in expression of the candidate genes for the secondary pathway were identified in the engineered lines.

Unfortunately the results obtained from these experiments do not contribute conclusively to support or dismiss these candidates as putative TA biosynthetic enzymes in *V. vinifera*.

Chapter 7:
Discussion and Future Work

7.1 Introduction

The accumulation of tartaric acid (TA) in higher plants is a curious occurrence limited to the Vitaceae, Geraniaceae and Leguminosae higher plant families (Stafford, 1959, Vickery and Palmer, 1954). Two TA biosynthetic pathway's have been identified in *Vitis vinifera*, using various radiolabelled and inhibitor studies (Loewus and Stafford, 1958, Saito, 1992, Saito and Kasai, 1982, 1984, Saito and Loewus, 1989a, Saito *et al.*, 1984, Wagner and Loewus, 1974, Wagner *et al.*, 1975). The primary pathway catabolises ascorbate (Asc), whereas the secondary pathway catabolises glucose, a primary fuel source (Xavier *et al.*, 2000). Work by Saito and Loewus (1989b) showed the secondary pathway is responsible for a minor proportion (<5%) of TA synthesis in Vitaceae.

To date, there is no evidence linking TA with the wider metabolic activities of the berry, adding to the curious nature of its accumulation. TA however, is important in commercial winemaking, responsible for a number of factors including the lowering of pH to prevent discolouration and spoilage due to microorganisms (Cirami, 1973, Es-Safi *et al.*, 2000, Toit *et al.*, 2006, Zoecklein *et al.*, 1995). TA is also important in the palatability of wine with the content and composition of organic acids in conjunction with the sugars present greatly affecting the organoleptic quality of the resultant wine (Liu *et al.*, 2007, Plane *et al.*, 1980).

Since the elucidation of the biosynthetic pathway's, predominantly by Saito, Loewus and Kasai in the 1960's to 1980's, work into TA has been limited. Investigations into the enzymes involved in the biosynthesis of TA by DeBolt (2006) identified L-idonate dehydrogenase (denoted L-idonate dehydrogenase 1 in this study) responsible for catalysing the perceived 'rate-limiting' step of the primary Asc precursor pathway (Malipiero *et al.*, 1987). The expression pattern of *L-IdnDH.1* showed high levels of expression in the green immature berry, ceasing 14 weeks post-flowering, coinciding with TA biosynthesis. The detection of L-IdnDH.1 in mature berry tissue when *L-IdnDH.1* expression has ceased by Wen *et al* (2010) suggested an extended half life of the protein. A natural variant of TA metabolism was identified in the species *Ampelopsis aconitifolia*, which accumulated high levels of Asc and no TA (DeBolt *et al.*, 2006). *A. aconitifolia*

was shown to lack *L-IdnDH.1*, the perceived reason for its inability to accumulate TA.

The present investigation has sought to increase the understanding of TA biosynthesis in *Vitis vinifera* through the identification of additional biosynthetic enzymes, and the genes that encode them. The identification of putative *V. vinifera* homologues to enzymes responsible for the catalysis of reactions within *E. coli* identical to those involved in TA biosynthesis resulted in the identification multiple candidate genes which were investigated for a possible role in TA biosynthesis.

7.2 Future Research

The results presented in this study demonstrate that TC59682 and TC55752 have the ability to catabolise multiple substrates. Bacterial 2-ketogluconate reductases have a broad substrate range (Adachi *et al.*, 1978, Ameyama and Adachi, 1982b, Chiyonobu *et al.*, 1976) leading to the suggestion that 2-ketogluconate reductases are responsible for the regeneration of NADP⁺ (Adachi *et al.*, 1979). The ability to catabolise multiple substrates may be exploited in mature berry tissue under stress where the biosynthesis of TA has ceased. The detection of protein in mature tissue through western blot analysis is required. Recently, western blot analysis using an L-IdnDH.1 specific antibody detected L-IdnDH.1 in mature berry tissue when gene expression was minimal (Wen *et al.*, 2010). In this study, analysis of enzyme activity extracted from mature berry tissue showed high levels of activity upon the addition of intermediate TA biosynthetic compounds (Figure 5.9 and 5.10). This suggests enzymes responsible for TA biosynthesis may still be present in berry tissue in which expression is minimal. This indicates that the cessation of TA biosynthesis may be due to the unavailability of substrates (due to compartmentalisation or protein-protein interactions) and not enzymatic activity. This suggests the primary Asc precursor pathway is subject to regulation upstream of the proposed rate-limiting step catalysed by L-IdnDH.1, with the fate of Asc the defining factor of TA biosynthesis. Determination of protein half-life in conjunction with a detailed thermodynamic analysis of the flux through pathway is required to propose the most probable rate-limiting steps of this pathway.

The development of a technique to measure the quantity of the pathway's intermediate compounds in developing berry tissue is crucial to the understanding of TA biosynthesis on a biochemical level. These intermediate compounds are expected to be present in low quantities, requiring the refinement of techniques including LC or GC/MS enabling the detection of minute concentrations with a high level of confidence. Detection of intermediate compounds will provide a greater understanding towards the rate of TA biosynthesis through the pathway as a whole and provide support to the hypothesis of the pathway regulation being, in part, substrate limitation. Analysis of intermediate levels in genetic studies utilising forward and reverse genetic techniques will provide further support to the enzymes involved due to an increase in these intermediate compounds and their regulation.

The development of the *V. vinifera* cv Thompson Seedless RNAi knockdown line (Hayes, DeBolt, Cook, and Ford, manuscript in preparation) will be a valuable tool in future investigations of the primary Asc precursor pathway. TA biosynthesis in *V. vinifera* occurs through two pathway's, thus inhibition of the primary Asc pathway through the knockdown of *L-IdnDH.1* may have resulted in over-expression of the secondary glucose precursor pathway to compensate. Analysis of the levels of metabolites, specifically the TA intermediates would be highly beneficial in understanding the changes resulting from the knockdown of *L-IdnDH.1*. The dual knockdown of both *L-IdnDH.1* and *L-IdnDH.2* increases the complexity of determining which gene is responsible for the observed physiological and metabolic changes. A complete physiological investigation of these lines is required to understand the impact of the knockdown on the plant system. Use of microarrays will enable efficient and rapid analysis of altered gene expression compared to the wild type lines (Schena *et al.*, 1995). Currently the Thompson Seedless knockdown lines are immature and not yet producing berries. Analysis of TA accumulation, intermediate levels and expression of TA biosynthetic genes over development in berry tissue obtained from these lines will greatly increase the understanding of TA biosynthesis. Recently, Melino *et al* (2009a) showed the Asc biosynthetic, recycling and catabolic genes in grape

berries are under developmental regulation. Changes to the expression of these genes due to the knockdown of *L-IdnDH.1* should be investigated.

This study has investigated candidate TC59682 as responsible for the conversion of 2-keto-L-gulonate to L-idonate in the primary Asc pathway. *In vitro* characterisation of recombinant protein and *in planta* expression analysis supports the involvement of TC59682 in TA biosynthesis. Forward and reverse genetic techniques *in situ* would provide further evidence supporting TC59682's role in TA biosynthesis. The development of microvine technology (Chaïb *et al.*, 2010) will be a powerful and effective tool for rapid forward and reverse genetic techniques previously unavailable in grapevine tissue. Knockdown of TC59682 in a microvine system would enable investigations into the primary Asc precursor pathway upstream of L-IdnDH.1.

TA biosynthetic enzymes are expected to be localised in the cytoplasm. Localisation studies of TC59682 utilising GFP-labelled probes will support its involvement in the pathway. Confirmation of VvALMT9 (Patel, 2008, Rongala, 2008) affinity to transport TA across the tonoplast is required to understand the transport systems of TA throughout the cell. Recently, Wen *et al* (2010) determined that L-IdnDH.1 is localised predominantly in the cytoplasm of immature berries whereas mature berry tissue showed localisation to the cytoplasm and vacuole. Transport systems must be identified to understand the relocation of this protein in mature tissue in relation to the regulation of TA biosynthesis.

In this study, a preliminary investigation into *L-IdnDH.1* putative homologue *L-IdnDH.2* was undertaken. L-IdnDH.2 was identified due to the high sequence similarity with L-IdnDH.1. Expression of the two genes over development was contradictory, with *L-IdnDH.1* expression high in developmental stages when *L-IdnDH.2* was low. Characterisation of kinetic activity was not performed due to the lack of active recombinant protein, therefore confirmation of *L-IdnDH.2* as an *L-IdnDH.1* putative homologue was not obtained. Greater investigation into L-IdnDH.2 is required prior to annotation as a homologue of L-IdnDH.1.

Effective and inexpensive production of L-idonate is an important requirement for studies on the TA biosynthetic pathway. L-Idonate is the primary substrate for the rate-limiting enzyme L-idonate dehydrogenase. The lack of commercial availability of this compound is a limiting factor in the investigations of TA biosynthesis.

Active recombinant protein of both TC55097 and TC58004, candidates for the secondary pathway, was not obtained. Based upon the expression patterns alone, a role in TA biosynthesis is not expected. The expressed open reading frame did encode a soluble protein. The lack of active recombinant protein hinders the annotation of each gene. Expression of these candidates in a eukaryote system such as *Saccharomyces cerevisiae* or baculovirus may result in an active purified sample, enabling protein characterisation and gene annotation.

7.3 Conclusion

Much work is still required to understand the enzymes involved in TA biosynthesis and their regulation. The work presented in this thesis supports the annotation of the *V. vinifera* gene TC59682 as a 2-keto-L-gulonate reductase. Gene expression patterns, in combination with *in vitro* recombinant kinetic activity supports TC59682 inclusion in the primary Asc precursor TA biosynthetic pathway. Future research supporting this enzyme *in planta* is required.

This study has also identified genes which warrant further investigation. Expression pattern of gene TC58004 shows expression increasing at the developmental stage of véraison. TC55752 expression increases until the developmental stage of véraison then steadies for the remainder of development. Both expression patterns suggest regulation with a 'véraison switch' influencing expression. This study has also utilised the natural and engineered *L-IdnDH* reverse genetic lines, *A. aconitifolia* and RNAi knockdown Thompson Seedless lines respectively. A greater understanding of these lines would enhance the knowledge of the TA biosynthetic pathway. An alternative technique for the identification of TA biosynthetic enzymes was also employed which may prove useful in future investigations in *Vitis vinifera*.

A greater understanding of the TA biosynthetic pathway will provide viticulturalists with a greater understanding of organic acids accumulation prior to vinification. Genetic manipulation of grapevines for commercial purposes is banned in Australia (Winemakers Federation of Australia, 2003). Cross-breeding of high-acid varieties shown to have a high activity of the TA biosynthetic enzymes with a low acid variety may increase the acid level of subsequent generations while still being suitable for wine production. Alternatively, cross-breeding of varieties low in TA biosynthetic enzyme activity would yield higher levels of Asc, an antioxidant crucial in the human diet (reviewed by Davies *et al.*, 1991), in the berry and resultant wine increasing the benefits of consumption. An increase in Asc would increase the nutritional value of the plant, and may also improve resistance to abiotic stresses (Smirnoff *et al.*, 2004). This would have significant implications on the table grape and wine industry. Any changes in organic acid level due to the manipulation of this pathway must be approached with caution as not only does TA levels affect the organoleptic properties of the resultant wines, the malate:tartrate ratio also impacts on wine quality (Liu *et al.*, 2007).

Appendix

A.1 Analysis of the RNAi *L-IdnDH* knockdown Thompson Seedless

Lines

Organic acids were analysed by Dr MA Hayes (University of Adelaide). DHA was not analysed therefore ascorbate values listed are not total ascorbate. Each mutant line had multiple labels dependent upon the experiment conducted; the labels displayed throughout this thesis are corrected to each line. Graphic representation of each lines phenotype are displayed where possible (images taken by Dr MA Hayes, University of Adelaide). Each line was grouped based on the resultant phenotype observed by Dr MA Hayes (University of Adelaide). When compared to control lines, RNAi *L-IdnDH* lines showed stunted growth and leaves displayed irregular morphology in terms of shape, size and leaf blade patterning (Hayes, DeBolt, Cook and Ford, manuscript in preparation). This appendix corresponds to Chapter 6.

* CAU = Corrected Area Units. This value represents the ascorbate peak on the HPLC chromatogram. This value is not a concentration.

Phenotype	Line	Tartrate (mg/g FW)	Ascorbate (CAU)*	Image
Control	WT1	17.033	11346.26	
	WT2	17.533	11891.81	
Mild	1.9	9.347	11379.48	
	1.10	11.368	11134.94	
	1.11	11.004	9627.89	

	1.12	11.140	9595.36	
	2.8	13.180	9277.99	
	2.9	9.611	10983.18	
	2.10	11.698	13479.84	
	3.9	15.295	10626.11	
	3.10	15.109	9849.13	
	3.11	12.395	9397.69	
Moderate	1.5	14.835	10250.9	
	1.6	10.799	11191.86	

1.7	9.822	5463.37	
1.8	10.814	13231.26	
2.4	10.153	8363.41	
2.5	10.161	7043.96	
2.6	15.986	8030.37	
2.7	8.490	8492.53	
3.5	10.538	11333.45	

3.6	14.091	12336.2	
-----	--------	---------	---

3.7	15.076	5548.46	
-----	--------	---------	---

Severe	1.1	9.702	8906.24
	1.2	9.505	11157.75
	1.3	11.724	8462.15
	1.4	8.011	11375.75

2.1	11.641	11872.8	
-----	--------	---------	---

2.2	9.261	10252.71	
-----	-------	----------	---

<p>2.3 12.366 9541.8</p>	
<p>3.1 9.914 10969.29</p>	
<p>3.2 8.786 14284.07</p>	
<p>3.3 12.851 9265.11</p>	
<p>3.4 8.978 9311.93</p>	

Bibliography

- Adachi, O., Chiyonobu, T., Shinagawa, E., Matsushita, K. & Ameyama, M.** (1978) Crystalline 2-Ketogluconate Reductase from *Acetobacter ascendens*, the Second Instance of Crystalline Enzyme in Genus *Acetobacter*, *Agricultural and Biological Chemistry*, 42(11): 2057-2062.
- Adachi, O., Shinagawa, E., Matsushita, K. & Ameyama, M.** (1979) Crystallization and Properties of 5-Keto-D-gluconate Reductase from *Gluconobacter suboxydans*, *Agricultural and Biological Chemistry*, 43(1): 75-83.
- Albury, M. S., Dudley, P., Watts, F. Z. & Moore, A. L.** (1996) Targeting the Plant Alternative Oxidase Protein to *Schizosaccharomyces pombe* Mitochondria Confers Cyanide-Insensitive Respiration, *The Journal of Biological Chemistry*, 271(29): 17062-17066.
- Altschul, S. F., Gish, W., Miller, W., Myers, E. W. & Lipman, D. J.** (1990) Basic Local Alignment Search Tool, *Journal of Molecular Biology*, 215: 403-410.
- Amerine, M. A.** (1956) The Maturation of Wine Grapes, *Wines and Vines*, 37(11): 53-55.
- Ameyama, M. & Adachi, O.** (1982a) [33] 5-Keto-D-gluconate Reductase from *Gluconobacter suboxydans*. In: **WOOD, W. A.** (ed.) *Methods in Enzymology*. New York: Academic Press.
- Ameyama, M. & Adachi, O.** (1982b) [34] 2-Keto-D-gluconate Reductase from Acetic Acid Bacteria. In: **WOOD, W. A.** (ed.) *Methods in Enzymology*. New York: Academic Press.
- Ameyama, M., Chiyonobu, T. & Adachi, O.** (1974) Purification and Properties of 5-Ketogluconate Reductase from *Gluconobacter liquefaciens*, *Agricultural and Biological Chemistry*, 38(7): 1377-1382.
- Anastassiadis, S., Aivasidis, A. & Wandrey, C.** (2003) Continuous gluconic acid production by isolated yeast-like mould strains of *Aureobasidium pullulans*, *Applied Microbiology and Biotechnology*, 61(2): 110-117.
- Audic, S. & Claverie, J.-M.** (1997) The Significance of Digital Gene Expression Profiles, *Genome Research*, 7: 986-995.
- Australian Bureau of Statistics** (2010) Value of Agricultural Commodities Produced 2008-2009. Canberra, Australia.
- Baba, T., Ara, T., Hasegawa, M., Takai, Y., Okumura, Y., Baba, M., Datsenko, K. A., Tomita, M., Wanner, B. L. & Mori, H.** (2006) Construction of *Escherichia coli* K-12 In-Frame, Single-Gene Knockout Mutants: The Keio Collection, *Molecular Systems Biology*, 2: 2006.0008.
- Baba, T., Huan, H.-C., Datsenko, K., Wanner, B. L. & Mori, H.** (2007) The Applications of Systematic In-Frame, Single-Gene Knockout Mutant Collection of *Escherichia coli* K-12, *Methods In Molecular Biology*, 416: 183-94.
- Baker, G. M., Noguchi, M. & Palmer, G.** (1987) The Reaction of Cytochrome Oxidase with Cyanide, *The Journal of Biological Chemistry*, 262(2): 595-604.
- Bánhegyi, G. & Loewus, F. A.** (2004) Ascorbic Acid Catabolism: Breakdown Pathways in Animals and Plants. In: **ASARD, H., MAY, J. M. & SMIRNOFF, N.** (eds.) *Vitamin C: Functions and Biochemistry in Animals and Plants*. Oxford: BIOS Scientific Publishers Ltd.

- Bantog, N. A., Yamada, K., Niwa, N., Shiratake, K. & Yamaki, S.** (2000) Gene Expression of NAD⁺ - Dependent Sorbitol Dehydrogenase and NADP⁺ - Dependent Sorbitol-6-Phosphate Dehydrogenase During Development of Loquat (*Eriobotrya japonica* Lindl.) Fruit, *Journal of the Japanese Society for Horticultural Science*, 69(3): 231-236.
- Beever, H.** (1969) Metabolic Sinks. In: **EASTIN, J. D., HASKINS, F. A., SULLIVAN, C. Y., BAVEL, C. H. M. V. & DINAUER, R. C.** (eds.) *Physiological Aspects of Crop Yield*. Nebraska, USA: American Society of Agronomy & Crop Science Society of America.
- Berger, F., Ramírez-Hernández, M. H. & Ziegler, M.** (2004) The New Life of a Centenarian: Signalling Functions of NAD(P), *Trends in Biochemical Sciences*, 29(3): 111-118.
- Blattner, F. R., Plunkett III, G., Bloch, C. A., Perna, N. T., Burland, V., Riley, M., Collado-Vides, J., Glasner, J. D., Rode, C. K., Mayhew, G. F., Gregor, J., Davis, N. W., Kirkpatrick, H. A., Goeden, M. A., Rose, D. J., Mau, B. & Shao, Y.** (1997) The Complete Genome Sequence of *Escherichia coli* K-12, *Science*, 277(5331): 1453-1462.
- Blom, N., Gammeltoft, S. & Brunak, S.** (1999) Sequence- and Structure-Based Prediction of Eukaryotic Protein Phosphorylation Sites, *Journal of Molecular Biology*, 294(5): 1351-1362.
- Buettner, G. R. & Schafer, F. Q.** (2004) Ascorbate as an Antioxidant. In: **ASARD, H., MAY, J. M. & SMIRNOFF, N.** (eds.) *Vitamin C: Functions and Biochemistry in Animals and Plants*. Oxford: BIOS Scientific Publishers Ltd.
- Bustin, S. A.** (2000) Absolute Quantification of mRNA Using Real-Time Reverse Transcription Polymerase Chain Reaction Assays, *Journal of Molecular Endocrinology*, 25: 169-193.
- Bustin, S. A., Benes, V., Garson, J. A., Hellemans, J., Huggett, J., Kubista, M., Mueller, R., Nolan, T., Pfaffl, M. W., Shipley, G. L., Vandesompele, J. & Wittwer, C. T.** (2009) The MIQE Guidelines: Minimum Information for Publication of Quantitative Real-Time PCR Experiments, *Clinical Chemistry*, 55(4): 611-622.
- Buttrose, M. S., Hale, C. R. & Kliever, W. M.** (1971) Effect of Temperature on the Composition of 'Cabernet Sauvignon' Berries, *American Journal of Enology and Viticulture*, 22(2): 71-75.
- Caldwell, D. G., McCallum, N., Shaw, P., Muehlbauer, G. J., Marshall, D. F. & Waugh, R.** (2004) A Structured Mutant Population for Forward and Reverse Genetics in Barley (*Hordeum vulgare* L.), *The Plant Journal*, 40: 143-150.
- Campbell, M. K. & Farrell, S. O.** (2007) *Biochemistry*, USA, Brooks/Cole.
- Carson, M., Johnson, D. H., McDonald, H., Brouillette, C. & DeLucas, L. J.** (2007) His-Tag Impact on Structure, *Acta Crystallographica Section D Biological Crystallography*, D63: 295-301.
- Chandrashekar, K., Felse, P. A. & Panda, T.** (1999) Optimization of Temperature and Initial pH and Kinetic Analysis of Tartaric Acid Production by *Gluconobacter suboxydans*, *Bioprocess Engineering*, 20: 203-207.
- Chant, A., Kraemer-Pecore, C. M., Watkin, R. & Kneale, G. G.** (2005) Attachment of a Histidine Tag to the Minimal Zinc Finger Protein of the *Aspergillus nidulans* Gene Regulatory Protein AreA Causes a

Conformational Change at the DNA-Binding Site, *Protein Expression and Purification*, 39(2): 152-159.

- Chaïb, J., Torregrosa, L., Mackenzie, D., Corena, P., Bouquet, A. & Thomas, M. R.** (2010) The Grape Microvine – A Model System for Rapid Forward and Reverse Genetics of Grapevines, *The Plant Journal*, 62: 1083-1092.
- Chiyonobu, T., Adachi, O. & Ameyama, M.** (1974) Substrate Specificity of 2-Ketogluconate Reductase from *Gluconobacter liquefaciens*, *Agricultural and Biological Chemistry*, 38(9): 1743-1744.
- Chiyonobu, T., Shinagawa, E., Adachi, O. & Ameyama, M.** (1975a) Crystallization of 2-Ketogluconate Reductase from *Gluconobacter liquefaciens*, *Agricultural and Biological Chemistry*, 39(11): 2263-2264.
- Chiyonobu, T., Shinagawa, E., Adachi, O. & Ameyama, M.** (1975b) Distribution of 2-Ketogluconate Reductase and 5-Ketogluconate Reductase in Acetic Acid Bacteria, *Agricultural and Biological Chemistry*, 39(12): 2425-2427.
- Chiyonobu, T., Shinagawa, E., Adachi, O. & Ameyama, M.** (1976) Purification, Crystallization and Properties of 2-Ketogluconate Reductase from *Acetobacter rancens*, *Agricultural and Biological Chemistry*, 40(1): 175-184.
- Cirami, R. M.** (1973) Changes in the Composition of Ripening Grapes in a Warm Climate, *Australian Journal of Experimental Agriculture and Animal Husbandry*, 13: 319-323.
- Coombe, B. G.** (1960) Relationship of Growth and Development to Changes in Sugars, Auxins and Gibberellins in Fruit of Seeded and Seedless Varieties of *Vitis vinifera*, *Plant Physiology*, 35(2): 241-250.
- Coombe, B. G.** (1976) The Development of Fleshy Fruits, *Annual Review of Plant Physiology*, 27: 507-528.
- Coombe, B. G.** (1980) Development of the Grape Berry I: Effects of Time of Flowering and Competition, *Australian Journal of Agricultural Research*, 31(1): 125-131.
- Coombe, B. G.** (1992) Research on Development and Ripening of the Grape Berry, *American Journal of Enology and Viticulture*, 43(1): 101-110.
- Coombe, B. G. & Bishop, G. R.** (1980) Development of the Grape Berry II: Changes in Diameter and Deformability During Veraison, *Australian Journal of Agricultural Research*, 31(3): 499-509.
- Coombe, B. G. & Iland, P. G.** (2004) Grape Berry Development and Winegrape Quality. In: **DRY, P. R. & COOMBE, B. G.** (eds.) *Viticulture*. Adelaide: Winetitles.
- Cornish-Bowden, A.** (1984) Enzyme Specificity: Its Meaning in the General Case, *Journal of Theoretical Biology*, 108(3): 451-457.
- Cornish-Bowden, A.** (2001) Detection of Errors of Interpretation in Experiments in Enzyme Kinetics, *Methods*, 24: 181-190.
- Cramer, G., Ergül, A., Grimplet, J., Tillett, R., Tattersall, E., Bohlman, M., Vincent, D., Sonderegger, J., Evans, J., Osborne, C., Quilici, D., Schlauch, K., Schooley, D. & Cushman, J.** (2007) Water and Salinity Stress in Grapevines: Early and Late Changes in Transcript and Metabolite Profiles, *Functional Integrated Genomics*, 7(2): 111-134.
- Crouzet, P. & Otten, L.** (1995) Sequence and Mutational Analysis of a Tartrate Utilization Operon from *Agrobacterium vitis*, *Journal of Bacteriology*, 177(22): 6518-6526.

- Dagley, S. & Trudgill, P. W.** (1963) The Metabolism of Tartaric Acid by a *Pseudomonas*: A NEW PATHWAY, *Biochemical Journal*, 89: 22-31.
- Darrouzet, E., Issartel, J.-P., Lunardi, J. & Dupuis, A.** (1998) The 49-kDa Subunit of NADH-Ubiquinone Oxidoreductase (Complex I) is Involved in the Binding of Piericidin and Rotenone, Two Quinone-Related Inhibitors, *FEBS Letters*, 431: 34-38.
- Davies, C. & Robinson, S. P.** (1996) Sugar Accumulation in Grape Berries: Cloning of Two Putative Vacuolar Invertase cDNAs and Their Expression in Grapevine Tissues, *Plant Physiology*, 111(1): 275-283.
- Davies, C., Shin, R., Liu, W., Thomas, M. R. & Schachtman, D. P.** (2006) Transporters Expressed During Grape Berry (*Vitis vinifera* L.) Development are Associated with an Increase in Berry Size and Berry Potassium Accumulation, *Journal of Experimental Botany*, 57(12): 3209-3216.
- Davies, M. B., Austin, J. & Partridge, D. A.** (1991) Medical Aspects of Vitamin C. In: **DAVIES, M. B., AUSTIN, J. & PARTRIDGE, D. A.** (eds.) *Vitamin C: Its Chemistry and Biochemistry*. The Royal Society of Chemistry: Cambridge.
- de Castro, E., Sigrist, C. J. A., Gattiker, A., Bulliard, V., Langendijk-Genevaux, P. S., Gasteiger, E., Bairoch, A. & Hulo, N.** (2006) ScanProsite: Detection of PROSITE Signature Matches and ProRule-Associated Functional and Structural Residues in Proteins, *Nucleic Acids Research*, 34: W362-W365.
- De Ley, J.** (1966) [40] 5-Ketogluconic Acid Reductase. In: **WILLIS, A. W.** (ed.) *Methods in Enzymology*. New York: Academic Press.
- De Ley, J. & Stouthamer, J.** (1959) The Mechanism and Localization of Hexonate Metabolism in *Acetobacter suboxydans* and *Acetobacter melanogenum*, *Biochim. Biophys. Acta*, 34: 171-183.
- De Souza, C. R., Maroco, J. P., Dos Santos, T. P., Rodrigues, M. L., Lopes, C. M., Pereira, J. S. & Chaves, M. M.** (2005) Grape Berry Metabolism in Field-Grown Grapevines Exposed to Different Irrigation Strategies, *Vitis*, 44(3): 103-109.
- DeBolt, S.** (2006) *Tartaric Acid Biosynthesis in Plants*, PhD Thesis, The University of Adelaide.
- DeBolt, S., Cook, D. R. & Ford, C. M.** (2006) L-Tartaric Acid Synthesis from Vitamin C in Higher Plants, *Proceedings of the National Academy of Sciences*, 103(14): 5608-5613.
- DeBolt, S., Melino, V. & Ford, C. M.** (2007) Ascorbate as a Biosynthetic Precursor in Plants, *Annals of Botany*, 99(1): 3-8.
- DeBolt, S., Ristic, R., Iland, P. G. & Ford, C. M.** (2008) Altered Light Interception Reduces Grape Berry Weight and Modulates Organic Acid Biosynthesis During Development, *HortScience*, 43(3): 957-961.
- Deluc, L. G., Grimplet, J., Wheatley, M. D., Tillett, R. L., Quilici, D. R., Osborne, C., Schooley, D. A., Schlauch, K. A., Cushman, J. C. & Cramer, G. R.** (2007) Transcriptomic and Metabolite Analyses of Cabernet Sauvignon Grape Berry Development, *BMC Genomics*, 8: 429.
- Di Luccio, E., Elling, R. A. & Wilson, D. K.** (2006) Identification of a Novel NADH-Specific Aldo-Keto Reductase Using Sequence and Structural Homologies, *Biochemical Journal*, 400: 105-114.

- Dokoozlian, N. K. & Kliewer, W. M.** (1996) Influence of Light on Grape Berry Growth and Composition Varies During Fruit Development, *Journal of the American Society for Horticultural Science*, 121(5): 869-874.
- Ebbighausen, H. & Giffhorn, F.** (1984) A Novel Mechanism Involved in the Metabolism of the Tartaric Acid Stereoisomers in *Rhodopseudomonas sphaeroides*: Enzymatic Conversion of *meso*-Tartaric Acid to D(-)-Glyceric Acid and CO₂, *Archives of Microbiology*, 138: 338-344.
- Elfari, M., Ha, S.-W., Bermus, C., Merfort, M., Khodaverdi, V., Herrmann, U., Sahn, H. & Görisch, H.** (2005) A *Gluconobacter oxydans* Mutant Converting Glucose Almost Quantitatively to 5-Keto-D-Gluconic Acid, *Applied Microbiology and Biotechnology*, 66(6): 668-674.
- Emanuelsson, O., Nielsen, H., Brunak, S. & von Heijne, G.** (2000) Predicting Subcellular Localization of Proteins Based on their N-Terminal Amino Acid Sequence, *Journal of Molecular Biology*, 300: 1005-1016.
- Emmerlich, V., Linka, N., Reinhold, T., Hurth, M. A., Traub, M., Martinoia, E. & Neuhaus, H. E.** (2003) The Plant Homolog to the Human Sodium/Dicarboxylic Cotransporter is the Vacuolar Malate Carrier, *Proceedings of the National Academy of Sciences of the United States of America*, 100(19): 11122-11126.
- Es-Safi, N.-E., Guernevé, C. L., Cheynier, V. & Moutounet, M.** (2000) New Phenolic Compounds Formed by Evolution of (+)-Catechin and Glyoxylic Acid in Hydroalcoholic Solution and Their Implication in Color Changes of Grape-Derived Foods, *Journal of Agricultural and Food Chemistry*, 48: 4233-4240.
- Fedorova, M., van de Mortel, J., Matsumoto, P. A., Cho, J., Town, C. D., VandenBosch, K. A., Gantt, J. S. & Vance, C. P.** (2002) Genome-Wide Identification of Nodule-Specific Transcripts in the Model Legume *Medicago truncatula*, *Plant Physiology*, 130(2): 519-537.
- Fernández, M. J. & Ruíz-Amil, M.** (1965) Tartaric Acid Metabolism in *Rhodotorula glutinis*, *Biochimica et Biophysica Acta*, 107: 383-385.
- Foyer, C. H.** (2004) The Role of Ascorbic Acid in Defence Networks and Signalling in Plants. In: **ASARD, H., MAY, J. M. & SMIRNOFF, N.** (eds.) *Vitamin C: Functions and Biochemistry in Animals and Plants*. Oxford: BIOS Scientific Publishers Ltd.
- Fromm, H. J.** (1963) Determination of Dissociation Constants of Coenzymes and Abortive Ternary Complexes with Rabbit Muscle Lactate Dehydrogenase from Fluorescence Measurements, *The Journal of Biological Chemistry*, 238(9): 2938-2944.
- Furuyoshi, S., Tanaka, H. & Soda, K.** (1987) Occurrence of a New Enzyme, *meso*-Tartrate Dehydratase of *Pseudomonas putida*, *Agricultural and Biological Chemistry*, 51(6): 1495-1499.
- Ghisi, R., Iannini, B. & Passera, C.** (1984) Changes in the Activities of Enzymes Involved in the Nitrogen and Sulphur Assimilation During Leaf and Berry Development of *Vitis vinifera*, *Vitis*, 23: 257-267.
- Giffhorn, F. & Kuhn, A.** (1983) Purification and Characterization of a Bifunctional L-(+)-Tartrate Dehydrogenase-D-(+)-Malate Dehydrogenase (Decarboxylating) From *Rhodopseudomonas sphaeroides* Y, *Journal of Bacteriology*, 155(1): 281-290.

- Giribaldi, M., Perugini, I., Sauvage, F.-X. & Schubert, A.** (2007) Analysis of Protein Changes During Grape Berry Ripening by 2-DE and MALDI-TOF, *Proteomics*, 7(17): 3154-3170.
- Gish, W. & States, D. J.** (1993) Identification of Protein Coding Regions by Database Similarity Search, *Nature Genetics*, 3: 266-72.
- Goes da Silva, F., Iandolino, A., Al-Kayal, F., Bohlmann, M. C., Cushman, M. A., Lim, H., Ergul, A., Figueroa, R., Kabuloglu, E. K., Osborne, C., Rowe, J., Tattersall, E., Leslie, A., Xu, J., Baek, J., Cramer, G. R., Cushman, J. C. & Cook, D. R.** (2005) Characterizing the Grape Transcriptome. Analysis of Expressed Sequence Tags from Multiple *Vitis* Species and Development of a Compendium of Gene Expression During Berry Development, *Plant Physiology*, 139(2): 574-597.
- Green, M. A. & Fry, S. C.** (2005) Vitamin C Degradation in Plant Cells via Enzymatic Hydrolysis of 4-*O*-Oxalyl-L-Threonate, *Nature*, 433(7021): 83-87.
- Grimplet, J., Deluc, L. G., Tillett, R. L., Wheatley, M. D., Schlauch, K. A., Cramer, G. R. & Cushman, J. C.** (2007) Tissue-Specific mRNA Expression Profiling in Grape Berry Tissues, *BMC Genomics*, 8: 187.
- Grimshaw, C.** (1992) Aldose Reductase: Model for a New Paradigm of Enzymic Perfection in Detoxification Catalysts, *Biochemistry*, 31(42): 10139-10145.
- Hale, C. R.** (1962) Synthesis of Organic Acids in the Fruit of the Grape, *Nature*, 195(4844): 917-918.
- Hale, C. R.** (1968) Growth and Senescence of the Grape Berry, *Australian Journal of Agricultural Research*, 19: 939-945.
- Hancock, R. D. & Viola, R.** (2005) Biosynthesis and Catabolism of L-Ascorbic Acid in Plants, *Critical Reviews in Plant Sciences*, 24(3): 167-188.
- Hardy, P. J.** (1968) Metabolism of Sugars and Organic Acids in Immature Grape Berries, *Plant Physiology*, 43(2): 224-228.
- Heineke, D., Riens, B., Grosse, H., Hoferichter, P., Peter, U., Flügge, U.-I. & Heldt, H. W.** (1991) Redox Transfer across the Inner Chloroplast Envelope Membrane, *Plant Physiology*, 95(4): 1131-1137.
- Helsper, J. P. & Loewus, F. A.** (1982) Metabolism of L-Threonic Acid in *Rumex x acutus* L. and *Pelargonium crispum* (L.) L'Hér, *Plant Physiology*, 69(6): 1365-1368.
- Helsper, J. P. F. G., Saito, K. & Loewus, F. A.** (1981) Biosynthesis and Metabolism of L-Ascorbic Acid in Virginia Creeper (*Parthenocissus quinquefolia* L.), *Planta*, 152(2): 171-176.
- Herbert, R. W., Hirst, E. L., Percival, E. G. V., Reynolds, R. J. W. & Smith, F.** (1933) The Constitution of Ascorbic Acid, *Journal of the Chemical Society*: 1270-1290.
- Herrmann, U., Merfort, M., Jeude, M., Bringer-Meyer, S. & Sahm, H.** (2004) Biotransformation of Glucose to 5-Keto-D-Gluconic Acid by Recombinant *Gluconobacter oxydans* DSM 2343, *Applied Microbiology and Biotechnology*, 64(1): 86-90.
- Hoefnagel, M., Wiskich, J. T., Madgwick, S. A., Patterson, Z., Oettmeier, W. & Rich, P. R.** (1995) New Inhibitors of the Ubiquinol Oxidase of Higher Plant Mitochondria, *European Journal of Biochemistry*, 233: 531-537.

- Hough, L. & Jones, J. K. N.** (1956) The Biosynthesis of the Monosaccharides. In: **WOLFROM, M. L. & TIPSON, R. S.** (eds.) *Advances in Carbohydrate Chemistry*. New York: Academic Press.
- Hrazdina, G., Parsons, G. F. & Mattick, L. R.** (1984) Physiological and Biochemical Events During Development and Maturation of Grape Berries, *American Journal of Enology and Viticulture*, 35(4): 220-226.
- Hurlbert, R. E. & Jakoby, W. B.** (1965) Tartaric Acid Metabolism I. Subunits of $L(+)$ -Tartaric Acid Dehydrase, *The Journal of Biological Chemistry*, 240(7): 2772-2777.
- Hurth, M. A., Suh, S. J., Kretzschmar, T., Geis, T., Bregante, M., Gambale, F., Martinoia, E. & Neuhaus, H. E.** (2005) Impaired pH Homeostasis in Arabidopsis Lacking the Vacuolar Dicarboxylate Transporter and Analysis of Carboxylic Acid Transport Across the Tonoplast, *Plant Physiology*, 137(3): 901-910.
- Hyndman, D., Bauman, D. R., Heredia, V. V. & Penning, T. M.** (2003) The Aldo-Keto Reductase Superfamily Homepage, *Chemico-Biological Interactions*, 143-144: 621-631.
- Iandolino, A., Nobuta, K., da Silva, F., Cook, D. & Meyers, B.** (2008) Comparative Expression Profiling in Grape (*Vitis vinifera*) Berries Derived from Frequency Analysis of ESTs and MPSS Signatures, *BMC Plant Biology*, 8(1): 53.
- Iandolino, A. B., da Silva, F. G., Lim, H., Choi, H., Williams, L. E. & Cook, D. R.** (2004) High-Quality RNA, cDNA, and Derived EST Libraries from Grapevine (*Vitis vinifera* L.), *Plant Molecular Biology Reporter*, 22(3): 269-278.
- Inoue, H., Nojima, H. & Okayama, H.** (1990) High Efficiency Transformation of *Escherichia coli* with Plasmids, *Gene*, 96(1): 23-28.
- Jeady, S., Monchois, V., Maza, C., Claverie, J.-M. & Abergel, C.** (2006) Crystal Structure of *Escherichia coli* DkgA, a Broad-Specificity Aldo-Keto Reductase, *PROTEINS: Structure, Function, and Bioinformatics*, 62: 302-307.
- Jez, J. M., Bennett, M. J., Schlegel, B. P., Lewis, M. & Penning, T. M.** (1997) Comparative Anatomy of the Aldo-Keto Reductase Superfamily, *Biochemical Journal*, 329: 625-636.
- Joubert, O., Nehmé, R., Bidet, M. & Mus-Veteau, I.** (2010) Heterologous Expression of Human Membrane Receptors in the Yeast *Saccharomyces cerevisiae*, *Methods in Molecular Biology*, 601: 87-103.
- Kamlet, J.** (1943) *Preparation of D-Tartaric Acid by Fermentation*. United States patent application 2,314,831.
- Kanehisa, M. & Goto, S.** (2000) KEGG: Kyoto Encyclopedia of Genes and Genomes, *Nucleic Acids Research*, 28: 27-30.
- Kasimova, M. R., Grigiene, J., Krab, K., Hagedorn, P. H., Flyvbjerg, H., Andersen, P. E. & Moller, I. M.** (2006) The Free NADH Concentration Is Kept Constant in Plant Mitochondria under Different Metabolic Conditions, *Plant Cell*, 18(3): 688-698.
- Keseler, I. M.** (2005) Eco-Cyc: A Comprehensive Database Resource for *Escherichia coli*, *Nucleic Acids Research*, 33: D334-D337.
- Kim, C. S., Lee, C. H., Shin, J. S., Chung, Y. S. & Hyung, N. I.** (1997) A Simple and Rapid Method for Isolation of High Quality Genomic DNA

from Fruit Trees and Conifers Using PVP, *Nucleic Acids Research*, 25(5): 1085-1086.

- Kim, O., Lux, S. & Uden, G.** (2007) Anaerobic Growth of *Escherichia coli* on d-tartrate Depends on the Fumarate Carrier DcuB and Fumarase, Rather than the L-Tartrate carrier TtdT and L-Tartrate Dehydratase, *Archives of Microbiology*, 188(6): 583-589.
- Kim, O. B. & Uden, G.** (2007) The L-Tartrate/Succinate Antiporter TtdT (YgjE) of L-Tartrate Fermentation in *Escherichia coli*, *Journal of Bacteriology*, 189(5): 1597-1603.
- Klasen, R., Bringer-Meyer, S. & Sahm, H.** (1992a) Incapability of *Gluconobacter oxydans* to Produce Tartaric Acid, *Biotechnology and Bioengineering*, 40(1): 183-186.
- Klasen, R., Bringer-Meyer, S. & Sahm, H.** (1992b) Investigation of 5-Ketogluconate Formation by *Gluconobacter oxydans*. In: **KREYSA, G. & DRIESEL, A. J.**, eds. DECHEMA Biotechnology Conference, 1992b Karlsruhe. 109-112.
- Klasen, R., Bringer-Meyer, S. & Sahm, H.** (1995) Biochemical Characterization and Sequence Analysis of the Gluconate:NADP 5-Oxidoreductase Gene from *Gluconobacter oxydans*, *Journal of Bacteriology*, 177(10): 2637-2643.
- Kliwer, W. M.** (1964) Influence of Environment on Metabolism of Organic Acids and Carbohydrates in *Vitis vinifera*. I. Temperature, *Plant Physiology*, 39(6): 869-880.
- Kliwer, W. M.** (1966) Sugars and Organic Acids of *Vitis vinifera*, *Plant Physiology*, 41: 923-931.
- Kliwer, W. M.** (1968) Effect of Temperature on the Composition of Grapes Grown Under Field and Controlled Conditions, *Journal of the American Society for Horticultural Science*, 93: 797-806.
- Kliwer, W. M.** (1971) Effect of Day Temperature and Light Intensity on Concentration of Malic and Tartaric Acid in *Vitis vinifera* Grapes, *Journal of the American Society for Horticultural Science*, 96(3): 372-377.
- Kliwer, W. M. & Lider, L. A.** (1968) Influence of Cluster Exposure to the Sun on the Composition of Thompson Seedless Fruit, *American Journal of Enology and Viticulture*, 19(3): 175-184.
- Kliwer, W. M., Lider, L. A. & Schultz, H. B.** (1967) Influence of Artificial Shading of Vineyards on the Concentration of Sugar and Organic Acid in Grapes, *American Journal of Enology and Viticulture*, 18(2): 78-86.
- Kliwer, W. M. & Nassar, A. R.** (1966) Changes in Concentration of Organic Acids, Sugars, and Amino Acids in Grape Leaves, *American Journal of Enology and Viticulture*, 17(1): 48-57.
- Kliwer, W. M. & Schultz, H. B.** (1964) Influence of Environment on Metabolism of Organic Acids and Carbohydrates in *Vitis vinifera*. II. Light, *American Journal of Enology and Viticulture*, 15(3): 119-129.
- Kohn, L. D. & Jakoby, W. B.** (1968) Tartaric Acid Metabolism III: The Formation of Glyceric Acid, *The Journal of Biological Chemistry*, 243(10): 2464-2471.
- Kohn, L. D., Packman, P. M., Allen, R. H. & Jakoby, W. B.** (1968) Tartaric Acid Metabolism V: Crystalline Tartrate Dehydrogenase, *The Journal of Biological Chemistry*, 243(10): 2479-2485.

- Koichi, Y., Minoda, Y. & Kotera, U.** (1971) *Novel Process of Producing L(+)-Tartaric Acid*. United States patent application 3,585,109.
- Kotera, U., Kodama, T., Minoda, Y. & Yamada, K.** (1972) Isolation and Chemical Structure of New Oxidation Product of 5-Ketogluconic Acid, and a Hypothetical Pathway from Glucose to Tartaric Acid Through this New Compound, *Agricultural and Biological Chemistry*, 36(8): 1315-1325.
- Kovermann, P., Meyer, S., Hortensteiner, S., Picco, C., Scholz-Starke, J., Ravera, S., Lee, Y. & Martinoia, E.** (2007) The Arabidopsis Vacuolar Malate Channel is a Member of the ALMT Family, *Plant Journal*, 52(6): 1169-1180.
- Kriedemann, P. E.** (1968) Observations on Gas Exchange in the Developing Sultana Berry, *Australian Journal of Biological Sciences*, 21: 907-916.
- Krogh, A., Larsson, B., Von Heijne, G. & Sonnhammer, E. L. L.** (2001) Predicting Transmembrane Protein Topology with a Hidden Markov Model: Application to Complete Genomes, *Journal of Molecular Biology*, 305(3): 567-580.
- Kubista, M., Andrade, J., Bengtsson, M., Forootan, A., Jonak, J., Lind, K., Sindelka, R., Sjoback, R., Sjogreen, B., Strombom, L., Stahlberg, A. & Zoric, N.** (2006) The Real-Time Polymerase Chain Reaction, *Molecular Aspects of Medicine*, 27: 95-125.
- la Cour, T., Kiemer, L., Mølgaard, A., Gupta, R., Skriver, K. & Brunak, S.** (2004) Analysis and Prediction of Leucine-Rich Nuclear Export Signals, *Protein Engineering, Design & Selection*, 17(6): 527-536.
- La Rivière, J. W. M.** (1956) Specificity of Whole Cells and Cell-Free Extracts of *Pseudomonas putida* Towards (+), (-), and Meso-Tartrate, *Biochimica et Biophysica Acta*, 22(1): 206-207.
- Lakso, A. N. & Kliewer, W. M.** (1975) The Influence of Temperature on Malic Acid Metabolism in Grape Berries I. Enzyme Responses, *Plant Physiology*, 56(3): 370-372.
- Lamikanra, O., Inyang, I. D. & Leong, S.** (1995) Distribution and Effect of Grape Maturity on Organic Acid Content of Red Muscadine Grapes, *Journal of Agricultural and Food Chemistry*, 43(12): 3026-3028.
- Lance, C. & Rustin, P.** (1984) The Central Role of Malate in Plant Metabolism, *Physiologie végétale*, 22(5): 625-641.
- Lewis, Y. S. & Neelakanthan, S.** (1959) Synthesis of Tartaric Acid in Tamarind Leaves, *Current Science*, 28: 152-153.
- Lindsley, J. E. & Rutter, J.** (2006) Whence Cometh the Allosterome?, *Proceedings of the National Academy of Sciences*, 103(28): 10533-10535.
- Liu, H.-F., Wu, B.-H., Fan, P.-G., Xu, H.-Y. & Li, S.-H.** (2007) Inheritance of Sugars and Acids in Berries of Grape (*Vitis vinifera* L.), *Euphytica*, 153(1-2): 99-107.
- Lockwood, L. B. & Nelson, G. E. N.** (1951) *Preparation of D-Tartaric Acid*. United States patent application 2,559,650.
- Loewus, F. A.** (1999) Biosynthesis and Metabolism of Ascorbic Acid in Plants and of Analogs of Ascorbic Acid in Fungi, *Phytochemistry*, 52(2): 193-210.
- Loewus, F. A. & Stafford, H. A.** (1958) Observations on the Incorporation of C¹⁴ into Tartaric Acid and the Labeling Pattern of D-Glucose from an Excised

Grape Leaf Administered L-Ascorbic Acid-6-C¹⁴, *Plant Physiology*, 33(2): 155-156.

- Loewus, F. A., Wagner, G. & Yang, J. C.** (1975) Biosynthesis and Metabolism of Ascorbic Acid in Plants, *Annals of the New York Academy of Sciences*, 258(1): 7-23.
- Lund, S., Peng, F., Nayar, T., Reid, K. & Schlosser, J.** (2008) Gene Expression Analyses in Individual Grape (*Vitis vinifera* L.) Berries During Ripening Initiation Reveal that Pigmentation Intensity is a Valid Indicator of Developmental Staging Within the Cluster, *Plant Molecular Biology*, 68(3): 301-315.
- Malipiero, U., Ruffner, H. P. & Rast, D. M.** (1987) Ascorbic to Tartaric Acid Conversion in Grapevines, *Journal of Plant Physiology*, 129(1-2): 33-40.
- Maroc-Gyr, J.** (1965) The Metabolism of Glucose and Gluconate in the Leaves of *Pelargonium zonale* L., and its Relation to the Formation of Organic Acids, in Particular, Tartaric Acid, *Physiologie végétale*, 3: 167-180.
- Mehlin, C., Boni, E., Buckner, F. S., Engel, L., Feist, T., Gelb, M. H., Haji, L., Kim, D., Liu, C., Mueller, N., Myler, P. J., Reddy, J. T., Sampson, J. N., Subramanian, E., Van Voorhis, W. C., Worthey, E., Zucker, F. & Hol, W. G. J.** (2006) Heterologous Expression of Proteins from *Plasmodium falciparum*: Results from 1000 Genes, *Molecular & Biochemical Parasitology*, 148: 144-160.
- Melino, V.** (2009) *Ascorbate Metabolism in Grape Berries During Development*, PhD Thesis, The University of Adelaide.
- Melino, V., Soole, K. & Ford, C.** (2009a) Ascorbate Metabolism and the Developmental Demand for Tartaric and Oxalic Acids in Ripening Grape Berries, *BMC Plant Biology*, 9(1): 145.
- Melino, V., Soole, K. & Ford, C.** (2009b) A Method for Determination of Fruit-Derived Ascorbic, Tartaric, Oxalic and Malic Acids, and its Application to the Study of Ascorbic Acid Catabolism in Grapevines, *Australian Journal of Grape and Wine Research*, 15(3): 293-302.
- Melino, V. J., Hayes, M., Soole, K. L. & Ford, C. M.** (2011) The Role of Light in the Regulation of Ascorbate Metabolism During Berry Development in the Cultivated Grapevine *Vitis vinifera* L., *Journal of the Science of Food and Agriculture*, 91(8).
- Merfort, M., Herrmann, U., Bringer-Meyer, S. & Sahn, H.** (2006a) High-Yield 5-Keto-D-Gluconic Acid Formation is Mediated by Soluble and Membrane-Bound Gluconate-5-Dehydrogenases of *Gluconobacter oxydans*, *Applied Microbiology and Biotechnology*, 73(2): 443-451.
- Merfort, M., Herrmann, U., Ha, S.-W., Elfari, M., Bringer-Meyer, S., Görisch, H. & Sahn, H.** (2006b) Modification of the Membrane-Bound Glucose Oxidation System in *Gluconobacter oxydans* Significantly Increases Gluconate and 5-Keto-D-Gluconic Acid Accumulation, *Biotechnology Journal*, 1: 556-563.
- Minárik, P., Tomásková, N., Kollárová, M. & Antalík, M.** (2002) Malate Dehydrogenases-Structure and Function, *General Physiology and Biophysics*, 21(3): 257-265.
- Mulder, N. J. & Apweiler, R.** (2008) The InterPro Database and Tools for Protein Domain Analysis, *Current Protocols in Bioinformatics*, 2.7.1-2.7.18.

- Nanba, H., Takaoka, Y. & Hasegawa, J.** (2003) Purification and Characterization of an α -Haloketone-Resistant Formate Dehydrogenase from *Thiobacillus* sp. Strain KNK65MA, and Cloning of the Gene, *Bioscience, Biotechnology, and Biochemistry*, 67(10): 2145-2153.
- Nicholas, K. B. & Nicholas, H. B. J.** (1997) GeneDoc: A Tool for Editing and Annotating Multiple Sequence Alignments, *Distributed by the author*. <http://www.psc.edu/biomed/genedoc>.
- Nosarzewski, M. & Archbold, D. D.** (2007) Tissue-Specific Expression of SORBITOL DEHYDROGENASE in Apple Fruit During Early Development, *Journal of Experimental Botany*, 58(7): 1863-1872.
- Novagen** (2006) *pET System Manual 11th Edition*, Novagen.
- Novy, R., Berg, J., Yaeger, K. & Mierendorf, R.** (1995) pET TRX Fusion System for Increased Solubility of Target Proteins Expressed in *E. coli*, *InNovations*, 3: 7-9.
- Nuss, R. F. & Loewus, F. A.** (1978) Further Studies on Oxalic Acid Biosynthesis in Oxalate-Accumulating Plants, *Plant Physiology*, 61(4): 590-592.
- Okun, J. G., Lummen, P. & Brandt, U.** (1999) Three Classes of Inhibitors Share a Common Binding Domain in Mitochondrial Complex I (NADH:Ubiquinone Oxidoreductase), *The Journal of Biological Chemistry*, 274(5): 2625-2630.
- Papadopoulos, J. S. & Agarwala, R.** (2007) COBALT: Constraint-Based Alignment Tool for Multiple Protein Sequences, *Bioinformatics*, 23(9): 1073-1079.
- Pasteur, L.** (1860) *Recherches sur la dissymétrie moléculaire des produits organiques naturels*, Paris, Librairie de L. Hachette.
- Patel, J.** (2008) *Identification and Localization of AtALMT9-like Vacuolar Malate Transporters from Grapevine (Vitis vinifera L.)*, Masters Thesis, Flinders University.
- Peekhaus, N. & Conway, T.** (1998) What's for Dinner?: Entner-Doudoroff Metabolism in *Escherichia coli*, *Journal of Bacteriology*, 180(14): 3495–3502.
- Persson, B., Krook, M. & Jornvall, H.** (1991) Characteristics of Short-Chain Alcohol Dehydrogenases and Related Enzymes, *European Journal of Biochemistry*, 200: 537-543.
- Peynaud, E. & Maurié, A.** (1958) Synthesis of Tartaric and Malic Acids by Grape Vines, *American Journal of Enology and Viticulture*, 9(1): 32-36.
- Pignocchi, C., Fletcher, J. M., Wilkinson, J. E., Barnes, J. D. & Foyer, C. H.** (2003) The Function of Ascorbate Oxidase in Tobacco, *Plant Physiology*, 132(3): 1631-1641.
- Pilati, S., Perazzolli, M., Malossini, A., Cestaro, A., Dematte, L., Fontana, P., Dal Ri, A., Viola, R., Velasco, R. & Moser, C.** (2007) Genome-Wide Transcriptional Analysis of Grapevine Berry Ripening Reveals a Set of Genes Similarly Modulated During Three Seasons and the Occurrence of an Oxidative Burst at Veraison, *BioMed Central Genomics*, 8: 428.
- Pitt, D. & Mosley, M.** (1985) Enzymes of Gluconate Metabolism and Glycolysis in *Penicillium notatum*, *Antonie van Leeuwenhoek*, 51(4): 353-364.
- Plane, R. A., Mattick, L. R. & Weirs, L. D.** (1980) An Acidity Index for the Taste of Wines, *American Journal of Enology and Viticulture*, 31(3): 265-268.

- Prust, C., Hoffmeister, M., Liesegang, H., Wiezer, A., Fricke, W. F., Ehrenreich, A., Gottschalk, G. & Deppenmeier, U.** (2005) Complete Genome Sequence of the Acetic Acid Bacterium *Gluconobacter oxydans*, *Nature Biotechnology*, 23(2): 195-200.
- Quackenbush, J., Liang, F., Holt, I., Pertea, G. & Upton, J.** (2000) The TIGR Gene Indices: Reconstruction and Representation of Expressed Gene Sequences, *Nucleic Acids Research*, 28(1): 141-145.
- Rabate, J. & Gourevitch, A.** (1938) Analysis of Fruit and Leaves of *Bauhenia reticulata* D.C. on the Presence of Large Quantities of L-Tartrate, *Rev. Bot. Appl. Agric. Trop*, 18: 604-612.
- Reid, R., Piagentini, M., Rodriguez, E., Ashley, G., Viswanathan, N., Carne, J., Santi, D. V., Hutchinson, C. R. & McDaniel, R.** (2003) A Model of Structure and Catalysis for Ketoreductase Domains in Modular Polyketide Synthases, *Biochemistry*, 42(1): 72-79.
- Rezaian, M. A. & Krake, L. R.** (1987) Nucleic Acid Extraction and Virus Detection in Grapevine, *Journal of Virological Methods*, 17(3-4): 277-285.
- Ribéreau-Gayon, G.** (1968) A Study of the Mechanism of Synthesis and Conversion of Malic Acid, Tartaric Acid and Citric Acid in *Vitis vinifera* L., *Phytochemistry*, 7(9): 1471-1482.
- Rode, H. & Giffhorn, F.** (1982) D-(-)-Tartrate Dehydratase of *Rhodopseudomonas sphaeroides*: Purification, Characterization, and Application to Enzymatic Determination of D-(-)-Tartrate, *Journal of Bacteriology*, 150(3): 1061-1068.
- Rode, H. & Giffhorn, F.** (1983) Adaptation of *Rhodopseudomonas sphaeroides* to Growth on D-(-)-Tartrate and Large-Scale Production of a Constitutive D-(-)-Tartrate Dehydratase During Growth on DL-Malate, *Applied and Environmental Microbiology*, 45(2): 716-719.
- Rogers, A. & Gibon, Y.** (2009) Chapter 4 - Enzyme Kinetics: Theory and Practice. In: **SCHWENDER, J.** (ed.) *Plant Metabolic Networks*. Springer Science and Business Media.
- Rongala, J.** (2008) *Identification and Localization of Vacuolar Organic Acid Carriers in Grapevine Berries*, Masters Thesis, The University of Adelaide.
- Ruffner, H. P.** (1982) Metabolism of Tartaric and Malic Acids in *Vitis*: A Review-Part A, *Vitis*, 21: 247-259.
- Ruffner, H. P., Brem, S. & Malipiero, U.** (1983) The Physiology of Acid Metabolism in Grape Berry Ripening, *Acta Horticulturae*, 139: 123-128.
- Ruffner, H. P. & Hawker, J. S.** (1977) Control of Glycolysis in Ripening Berries of *Vitis vinifera*, *Phytochemistry*, 16(8): 1171-1175.
- Ruffner, H. P. & Kliewer, W. M.** (1975) Phosphoenolpyruvate Carboxykinase Activity in Grape Berries, *Plant Physiology*, 56(1): 67-71.
- Saichana, I., Ano, Y., Adachi, O., Matsushita, K. & Toyama, H.** (2007) Preparation of Enzymes Required for Enzymatic Quantification of 5-Keto-D-gluconate and 2-Keto-D-gluconate, *Bioscience, Biotechnology, and Biochemistry*, 71(10): 2478-2486.
- Saito, K.** (1992) Metabolism of L-Threotetruronic Acid by *Pelargonium crispum*, *Phytochemistry*, 31(4): 1219-1222.
- Saito, K.** (1994) Specific Transfer of ³H from D-[3-³H]Gluconic Acid into L-Tartaric Acid in Vitaceous Plants, *Phytochemistry*, 37(4): 1017-1022.

- Saito, K. & Kasai, Z.** (1968) Accumulation of Tartaric Acid in the Ripening Process of Grapes, *Plant And Cell Physiology*, 9: 529-537.
- Saito, K. & Kasai, Z.** (1969) Tartaric Acid Synthesis from L-Ascorbic Acid-1-¹⁴C in Grape Berries, *Phytochemistry*, 8(11): 2177-2182.
- Saito, K. & Kasai, Z.** (1978) Conversion of Labeled Substrates to Sugars, Cell Wall Polysaccharides, and Tartaric Acid in Grape Berries, *Plant Physiology*, 62(2): 215-219.
- Saito, K. & Kasai, Z.** (1982) Conversion of L-Ascorbic Acid to L-Idonic Acid, L-Idono- γ -Lactone and 2-Keto-L-Idonic Acid in Slices of Immature Grapes, *Plant And Cell Physiology*, 23(3): 499-507.
- Saito, K. & Kasai, Z.** (1984) Synthesis of L-(+)-Tartaric Acid from L-Ascorbic Acid via 5-Keto-D-Gluconic Acid in Grapes, *Plant Physiology*, 76(1): 170-174.
- Saito, K. & Loewus, F. A.** (1989a) Formation of L-(+)-Tartaric Acid in Leaves of the Bean, *Phaseolus vulgaris* L.: Radioisotopic Studies With Putative Precursors, *Plant Cell Physiology*, 30(5): 629-636.
- Saito, K. & Loewus, F. A.** (1989b) Formation of Tartaric Acid in Vitaceous Plants: Relative Contributions of L-Ascorbic Acid-Inclusive and Acid-Noninclusive Pathways, *Plant And Cell Physiology*, 30(6): 905-910.
- Saito, K. & Loewus, F. A.** (1989c) Occurrence of L-(+)-Tartaric Acid and its Formation from D-Gluconate or D-xylo-5-Hexulosonate in Bean Leaf (*Phaseolus vulgaris* L.), *Plant Science*, 62(2): 175-180.
- Saito, K., Morita, S.-i. & Kasai, Z.** (1984) Synthesis of L-(+)-Tartaric Acid from 5-Keto-D-Gluconic Acid in *Pelargonium*, *Plant Cell Physiology*, 25(7): 1223-1232.
- Saito, K., Ohmoto, J. & Kuriha, N.** (1997) Incorporation of ¹⁸O into Oxalic, L-Threonic and L-Tartaric Acids During Cleavage of L-Ascorbic and 5-Keto-D-Gluconic Acids in Plants, *Phytochemistry*, 44(5): 805-809.
- Salusjärvi, T., Povelainen, M., Hvorslev, N., Eneyskaya, E. V., Kulminskaya, A. A., Shabalin, K. A., Neustroev, K. N., Kalkkinen, N. & Miasnikov, A. N.** (2004) Cloning of a Gluconate/Polyol Dehydrogenase Gene from *Gluconobacter suboxydans* IFO 12528, Characterisation of the Enzyme and its use for the Production of 5-Ketogluconate in a Recombinant *Escherichia coli* Strain, *Applied Microbiology and Biotechnology*, 65(3): 306-314.
- Sambrook, J., Fritsch, E. F. & Maniatis, T.** (1989) *Molecular Cloning: A Laboratory Manual, Second Edition*, USA, Cold Spring Harbour Laboratory Press.
- Schena, M., Shalon, D., Davis, R. W. & Brown, P. O.** (1995) Quantitative Monitoring of Gene Expression Patterns with a Complementary DNA Microarray, *Science*, 270(5235): 467-470.
- Schlosser, J., Olsson, N., Weis, M., Reid, K., Peng, F., Lund, S. & Bowen, P.** (2008) Cellular Expansion and Gene Expression in the Developing Grape (*Vitis vinifera* L.), *Protoplasma*, 232: 255-265.
- Schnell, S. & Maini, P. K.** (2003) A Century of Enzyme Kinetics: Reliability of the K_M and v_{max} Estimates, *Comments on Theoretical Biology*, 8: 169-187.
- Schulze, J., Tesfaye, M., Litjens, R., Bucciarelli, B., Trepp, G., Miller, S., Samac, D., Allan, D. & Vance, C. P.** (2002) Malate Plays a Central Role in Plant Nutrition, *Plant and Soil*, 247(1): 133-139.

- Shilo, M.** (1957) The Enzymic Conversion of the Tartaric Acids to Oxaloacetic Acid, *The Journal of General Microbiology*, 16(2): 472-81.
- Shilo, M. & Stanier, R. Y.** (1957) The Utilization of the Tartaric Acids by *Pseudomonads*, *The Journal of General Microbiology*, 16(2): 482-490.
- Shinagawa, E., Chiyonobu, T., Adachi, O. & Ameyama, M.** (1976) Distribution and Solubilization of Particulate Gluconate Dehydrogenase and Particulate 2-Ketogluconate Dehydrogenase in Acetic Acid Bacteria, *Agricultural and Biological Chemistry*, 40(3): 475-483.
- Shinagawa, E., Chiyonobu, T., Matsushita, K., Adachi, O. & Ameyama, M.** (1978) Distribution of Gluconate Dehydrogenase and Ketogluconate Reductases in Aerobic Bacteria, *Agricultural and Biological Chemistry*, 42(5): 1055-1057.
- Simpson, P. J., Tantitadapitak, C., Reed, A. M., Mather, O. C., Bunce, C. M., White, S. A. & Ride, J. P.** (2009a) Characterization of Two Novel Aldo-Keto Reductases from Arabidopsis: Expression Patterns, Broad Substrate Specificity, and an Open Active-Site Structure Suggest a Role in Toxicant Metabolism Following Stress, *Journal of Molecular Biology*, 392(2): 465-480.
- Simpson, P. J., Tantitadapitak, C., Reed, A. M., Mather, O. C., Bunce, C. M., White, S. A. & Ride, J. P.** (2009b) Characterization of Two Novel Aldo-Keto Reductases from Arabidopsis: Expression Patterns, Broad Substrate Specificity, and an Open Active-Site Structure Suggest a Role in Toxicant Metabolism Following Stress, *Journal of Molecular Biology*, 392: 465-480.
- Skene, K. G. M. & Hale, C. R.** (1971) Organic Acid Synthesis by Grape Berries Cultured *in vitro*, *Phytochemistry*, 10(8): 1779-1781.
- Smirnoff, N.** (2000) Ascorbic Acid: Metabolism and Functions of a Multi-Faceted Molecule, *Current Opinion in Plant Biology*, 3(3): 229-235.
- Smirnoff, N., Running, J. A. & Gatzek, S.** (2004) Ascorbate Biosynthesis: A Diversity of Pathways. In: **ASARD, H., MAY, J. M. & SMIRNOFF, N.** (eds.) *Vitamin C: Functions and Biochemistry in Animals and Plants*. Oxford: BIOS Scientific Publishers Ltd.
- Sofia, H. J., Burland, V., Daniels, D. L., Plunkett, G., III & Blattner, F. R.** (1994) Analysis of the *Escherichia coli* Genome. V. DNA Sequence of the Region from 76.0 to 81.5 Minutes, *Nucleic Acids Research*, 22(13): 2576-2586.
- Sonoyama, T., Kageyama, B., Yagi, S. & Mitsushima, K.** (1987) Biochemical Aspects of 2-Keto-L-Gulonate Accumulation from 2,5-Diketo-D-gluconate by *Corynebacterium* sp. and Its Mutants, *Agricultural and Biological Chemistry*, 51(11): 3039-3047.
- Soole, K. L. & Menz, R. I.** (1995) Functional Molecular Aspects of the NADH Dehydrogenases of Plant Mitochondria, *Journal of Bioenergetics and Biomembranes*, 27(4): 397-406.
- Stafford, H. A.** (1959) Distribution of Tartaric Acid in the Leaves of Certain Angiosperms, *American Journal of Botany*, 46(5): 347-352.
- Stafford, H. A.** (1961) Distribution of Tartaric Acid in the Geraniaceae, *American Journal of Botany*, 48(8): 699-701.
- Stafford, H. A. & Loewus, F. A.** (1958) The Fixation of C¹⁴O₂ into Tartaric and Malic Acids of Excised Grape Leaves, *Plant Physiology*, 33(3): 194-199.

- Sweetman, C.** (2011) *An Examination of Malate Metabolism in Vitis vinifera During Fruit Ripening and in Response to Elevated Vineyard Temperature*, PhD Thesis, Flinders University of South Australia.
- Sweetman, C., Deluc, L. G., Cramer, G. R., Ford, C. M. & Soole, K. L.** (2009) Regulation of Malate Metabolism in Grape Berry and Other Developing Fruits, *Phytochemistry*, 70(11-12): 1329-1344.
- Tadera, K. & Mitstda, H.** (1971) Isolation and Chemical Structure of a New Fluorescent Compound in Spinach Leaves, *Agricultural and Biological Chemistry*, 35: 1431-1435.
- Takimoto, K., Saito, K. & Kasai, Z.** (1976) Diurnal Change of Tartrate Dissimilation During the Ripening of Grapes, *Phytochemistry*, 15(6): 927-930.
- Teo, G., Suzuki, Y., Uratsu, S. L., Lampinen, B., Ormonde, N., Hu, W. K., DeJong, T. M. & Dandekar, A. M.** (2006) Silencing Leaf Sorbitol Synthesis Alters Long-Distance Partitioning and Apple Fruit Quality, *Proceedings of the National Academy of Sciences of the United States of America*, 103(49): 18842-18847.
- Terrier, N., Ageorges, A., Abbal, P. & Romieu, C.** (2001) Generation of ESTs From Grape Berry at Various Developmental Stages, *Journal of Plant Physiology*, 158(12): 1575-1583.
- Terrier, N., Deguilloux, C., Sauvage, F.-X., Martinoia, E. & Romieu, C.** (1998) Proton Pumps and Anion Transport in *Vitis vinifera*: The Inorganic Pyrophosphatase Plays a Predominant Role in the Energization of the Tonoplast, *Plant Physiology and Biochemistry*, 36(5): 367-377.
- Terrier, N. & Romieu, C.** (2001) Grape Berry Acidity. In: **ROUBELAKIS-ANGELAKIS, K. A.** (ed.) *Molecular Biology and Biotechnology of the Grapevine*. Netherlands: Kluwer Academic.
- Thatcher, D. & Hitchcock, A.** (1994) Protein Folding in Biotechnology. In: **PAIN, R. H.** (ed.) *Mechanism of Protein Folding*. Oxford University Press.
- The French-Italian Public Consortium for Grapevine Genome Characterization** (2007) The Grapevine Genome Sequence Suggests Ancestral Hexaploidization in Major Angiosperm Phyla, *Nature*, Advanced Online Publication.
- Toit, W. J. d., Marais, J., Pretorius, I. S. & Toit, M. d.** (2006) Oxygen in Must and Wine: A Review, *South African Journal of Enology and Viticulture*, 27(1): 76-94.
- Tolia, N. H. & Joshua-Tor, L.** (2006) Strategies for Protein Coexpression in *Escherichia coli*, *Nature Methods*, 3(1): 55-64.
- Toyama, H., Furuya, N., Saichana, I., Ano, Y., Adachi, O. & Matsushita, K.** (2007) Membrane-Bound, 2-Keto-D-Gluconate-Yielding D-Gluconate Dehydrogenase from *Gluconobacter dioxyaceticus* IFO 3271: Molecular Properties and Gene Disruption, *Applied and Environmental Microbiology*, 73(20): 6551-6556.
- Troggio, M., Malacarne, G., Coppola, G., Segala, C., Cartwright, D. A., Pindo, M., Stefanini, M., Mank, R., Moroldo, M., Morgante, M., Grando, M. S. & Velasco, R.** (2007) A Dense Single-Nucleotide Polymorphism-Based Genetic Linkage Map of Grapevine (*Vitis vinifera* L.) Anchoring Pinot Noir Bacterial Artificial Chromosome Contigs, *Genetics*, 176: 2637-2650.

- Truesdell, S. J., Sims, J. C., Boerman, P. A., Seymour, J. L. & Lazarus, R. A.** (1991) Pathways for Metabolism of Ketoaldonic Acids in an *Erwinia* sp., *Journal of Bacteriology*, 173(21): 6651-6656.
- Velasco, R., Zharkikh, A., Troggio, M., Cartwright, D. A., Cestaro, A., Pruss, D., Pindo, M., Fitzgerald, L. M., Vezzulli, S., Reid, J., Malacarne, G., Iliev, D., Coppola, G., Wardell, B., Micheletti, D., Macalma, T., Facci, M., Mitchell, J. T., Perazzolli, M., Eldredge, G., Gatto, P., Oyzerski, R., Moretto, M., Gutin, N., Stefanini, M., Chen, Y., Segala, C., Davenport, C., Dematte, L., Mraz, A., Battilana, J., Stormo, K., Costa, F., Tao, Q., Si-Ammour, A., Harkins, T., Lackey, A., Perbost, C., Taillon, B., Stella, A., Solovyev, V., Fawcett, J. A., Sterck, L., Vandepoele, K., Grando, S. M., Toppo, S., Moser, C., Lanchbury, J., Bogden, R., Skolnick, M., Sgaramella, V., Bhatnagar, S. K., Fontana, P., Gutin, A., Peer, Y. V. d., Salamini, F. & Viola, R.** (2007) A High Quality Draft Consensus Sequence of the Genome of a Heterozygous Grapevine Variety, *PLoS ONE*, (12): e1326.
- Vickery, H. B. & Palmer, J. K.** (1954) The Metabolism of the Organic Acids of Tobacco Leaves VII: Effect of Culture of Excised Leaves in Solutions of (+)-Tartrate, *The Journal of Biological Chemistry*, 207(1): 275-285.
- Wagner, G. & Loewus, F.** (1973) The Biosynthesis of (+)-Tartaric Acid in *Pelargonium crispum*, *Plant Physiology*, 52(6): 651-654.
- Wagner, G. & Loewus, F. A.** (1974) L-Ascorbic Acid Metabolism in Vitaceae: Conversion to (+)-Tartaric Acid and Hexoses, *Plant Physiology*, 54(5): 784-787.
- Wagner, G., Yang, J. C. & Loewus, F. A.** (1975) Stereoisomeric Characterization of Tartaric Acid Produced During L-Ascorbic Acid Metabolism in Plants, *Plant Physiology*, 55(6): 1071-1073.
- Walon, R.** (1969) *Enzymatic Production of Gluconic Acid*. United States patent application 3,619,396.
- Wen, J., Nie, Z.-L., Soejima, A. & Meng, Y.** (2007) Phylogeny of Vitaceae Based on the Nuclear *GAI1* Gene Sequences, *Canadian Journal of Botany*, 85: 731-745.
- Wen, Y.-Q., Li, J.-M., Zhang, Z.-Z., Zhang, Y.-F. & Pan, Q.-H.** (2010) Antibody Preparation, Gene Expression and Subcellular Localization of L-Idonate Dehydrogenase in Grape Berry, *Bioscience, Biotechnology, and Biochemistry*, 74(12): 2413-2417.
- Wheeler, S. F.** (2006) *The Role of Abscisic Acid in Grape Berry Development*, PhD Thesis.
- Widersten, M.** (1998) Heterologous Expression in *Escherichia coli* of Soluble Active-Site Random Mutants of Haloalkane Dehalogenase from *Xanthobacter autotrophicus* GJ10 by Coexpression of Molecular Chaperonins GroEL/ES, *Protein Expression and Purification*, 13(3): 389-395.
- Williams, M. & Loewus, F. A.** (1978) Biosynthesis of (+)-Tartaric Acid From L-[4-¹⁴C] Ascorbic Acid in Grape and Geranium, *Plant Physiology*, 61(4): 672-674.
- Winemakers Federation of Australia** (2003) The Australian Wine Industry Position on Gene Technology.
- Wise, R., Caldo, R., Hong, L., Shen, L., Cannon, E. & Dickerson, J.** (2007) BarleyBase/PLEXdb: A Unified Expression Profiling Database for Plants

and Plant Pathogens. In: **EDWARDS, D.** (ed.) *In Methods in Molecular Biology Plant Bioinformatics - Methods and Protocols*. Humana Press, Totowa, NJ.

- Xavier, G. d. S., Leclerc, I., Salt, I. P., Doiron, B., Hardie, D. G., Kahn, A. & Rutter, G. A.** (2000) Role of AMP-Activated Protein Kinase in the Regulation by Glucose of Islet Beta Cell Gene Expression, *Proceedings of the National Academy of Sciences*, 97(8): 4023- 4028.
- Yamada, K., Kodama, T., Obata, T. & Takahashi, N.** (1971) Microbial Formation of Tartaric Acid from Glucose (I) Isolation and Identification of Tartaric Acid Producing Microorganisms, *Journal of Fermentation Technology*, 49(2): 85-92.
- Yang, J. C. & Loewus, F. A.** (1975) Metabolic Conversion of L-Ascorbic Acid to Oxalic Acid in Oxalate-Accumulating Plants, *Plant Physiology*, 56(2): 283-285.
- Ying, W.** (2008) NAD⁺/NADH and NADP⁺/NADPH in Cellular Functions and Cell Death: Regulation and Biological Consequences, *Antioxidants and Redox Signaling*, 10(2): 179-206.
- Yum, D.-Y., Lee, B.-Y., Hahm, D.-H. & Pan, J.-G.** (1998a) The *viaE* Gene, Located at 80.1 Minutes on the *Escherichia coli* Chromosome, Encodes a 2-Ketoaldonate Reductase, *Journal of Bacteriology*, 180(22): 5984-5988.
- Yum, D., Bae, S. & Pan, J.** (1998b) Purification and Characterization of the 2-Ketoaldonate Reductase from *Brevibacterium ketosoreductum* ATCC2191, *Bioscience, Biotechnology, and Biochemistry*, 62(1): 154-156.
- Zdobnov, E. M. & Apweiler, R.** (2001) InterProScan - An Integration Platform for the Signature-Recognition Methods in InterPro, *Bioinformatics*, 17(9): 847-848.
- Zimmermann, C.** (2005) *Cloning, Expression and Characterisation of a Semialdehyde Dehydrogenase Whose Expression Suggests a Potential Role in the Biosynthetic Pathway for L-Tartaric Acid in the Grapevine Vitis vinifera L. Cabernet Sauvignon cv.*, University of Adelaide.
- Zoecklein, B. W., Fugelsang, K. C., Gump, B. H. & Nury, F. S.** (1995) *Wine Analysis and Production*, Maryland, Aspen Publishers, Inc.